CR-183932

TWR-17649

SPACE SHUTTLE
Solid Rocket Motors
Thiokol Corporation

Technical Evaluation Motor No. 5 (TEM-5) Final Test Report

19 March 1990

Contract No.	NAS8-30490
DR No.	5-3
WBS No.	HQ601-20-10
ECS No.	SS1026

Thiokol CORPORATION

SPACE OPERATIONS

P.O. Box 707, Brigham City, UT 84302-0707 (801) 863-3511

Publications No. 90450

N115573-5

TEM-5 Static Test

Technical Evaluation Motor No. 5 (TEM-05)
Final Test Report

Prepared by:

M R Cook (20 March 90)
Test Planning and Reports
Systems Engineer

Approved by:

Requirements Manager

System Integration Engineer

Program Manager

Fred Quesada Jr 20 March 90
Reliability

System Safety

P C Tydeck 3-20-90
Data Management
ECS No. SS1026

Major contributors to this report were:

Instrumentation:	D. South
Case/Leak Check/Seals:	L. Nelsen, A. Carlisle, D. Gurney, J. Heman, S. Eden, R. Ash, G. Abawi, K. Baker
Insulation:	J. Passman
Nozzle:	D. Smith Jr.,
Joint Protection System:	C. Prokop, C. Greatwood
Ballistics/Mass Properties:	A. Drendel
Aero/Thermal:	E. Mathias
Nozzle-to-Case Joint:	M. Perry

ABSTRACT

Technical Evaluation Motor No. 5 (TEM-5) was static test fired on 23 Jan 1990 at the Thiokol Corporation Static Test Bay T-97. TEM-5 was a full-scale, full-duration static test fire of a high performance motor (HPM) configuration solid rocket motor (SRM). The primary purpose of TEM static tests is to recover SRM case and nozzle hardware for use in the redesigned solid rocket motor (RSRM) flight program.

Inspection and instrumentation data indicate that the TEM-5 static test firing was successful. The ambient temperature during the test was 41°F and the propellant mean bulk temperature (PMBT) was 72°F. Ballistics performance values were within the specified requirements. The overall performance of the TEM-5 components and test equipment was nominal. Dissembly inspection revealed that joint putty was in contact with the inner groove of the inner primary seal of the ignitor adapter-to-forward dome (inner) joint gasket; this condition had not occurred on any previous static test motor or flight RSRM.

While no qualification issues were addressed on TEM-5, two significant component changes were evaluated. Those changes were a new vented assembly process for the case-to-nozzle joint and the installation of two redesigned field joint protection systems. Performance of the vented case-to-nozzle joint assembly was successful, and the assembly/performance differences between the two field joint protection system (FJPS) configurations were compared.

CONTENTS

PAGE vi INTENTIONALLY BLANK

PRECEDING PAGE BLANK NOT FILMED

CONTENTS (Cont)

CONTENTS (Cont)

FIGURES

FIGURES (Cont)

TABLES

ACRONYMS AND ABBREVIATIONS

1-L	first longitudinal
2-L	second longitudinal
A-M	arming-monitor
ac	alternating current
AP	ammonium perchlorate
B-B	barrier-booster
B-KNO_3	boron-potassium nitrate
C/A	center aft
CCP	carbon-cloth phenolic
CEI	contract end item
CF	carbon fiber-filled
C/F	center forward
CO_2	carbon dioxide
CP	circular perforated
CTPB	carboxyl-terminated polybutadiene polymer
CV	coefficient of variation
deg	degree
DM	development motor
DWV	dielectric withstanding voltage
EPDM	ethylene-propylene-diene monomer
ET	external tank
ETM	evaluation test motor
FJPS	field joint protection system
ft	foot
FWC	filament wound case
GCP	glass-cloth phenolic
HPM	high performance motor
hr	hour
Hz	hertz
ID	inside diameter
in.	inch
ips	inches per second
I_{sp}	specific impulse
JPS	joint protection system
klb	thousand pound
KSC	Kennedy Space Center
ksi	thousand square inches
kW	kilowatt
lb	pound
lbm	pounds mass
LSC	linear shaped charge
Mlbf	million pounds force
MOP	maximum operating pressure
ms	millisecond
MSFC	Marshall Space Flight Center
NA	not applicable
NBR	acrylonitrile butadiene rubber

ACRONYMS AND ABBREVIATIONS (Cont)

OBR	outer boot ring
OD	outside diameter
OPT	operational pressure transducer
PBAN	polybutadiene acrylic acid acrylonitrile terpolymer
PMBT	propellant mean bulk temperature
P/N	part number
psi	pounds per square inch
psia	pounds per square inch absolute
psig	pounds per square inch gage
PVM	performance verification motor
QM	qualification motor
RSRM	redesigned solid rocket motor
RTD	resistance temperature device
RTV	room temperature vulcanization
S&A	safety and arming (device)
SBRE	surface burn rate error
sccs	standard cubic centimeters per second
sec	second
SII	standard ignition initiator
S/N	serial number
SRB	solid rocket booster
SRM	solid rocket motor
TEM	technical evaluation motor
TVC	thrust vector control
V	volts
Vdc	volts direct current
yr	year
°F	degree Fahrenheit

1

INTRODUCTION

This report documents the procedures, performance, and results from the TEM-5 full-scale, full-duration static test fire of a HPM configuration SRM. The static test fire occurred on 23 Jan 1990 at the Thiokol Corporation Static Test Bay T-97. This test report includes a presentation and discussion of the TEM-5 performance, anomalies, and test result concurrence with the objectives outlined in CTP-0105 Revision B, Space Shuttle Technical Evaluation Motor No. 5 (TEM-5) Static Fire Test Plan.

SRMs, used in pairs, are the primary propulsive element for the space shuttle; providing impulse and thrust vector control (TVC) from SRM ignition to solid rocket booster (SRB) separation. TEM-configuration SRMs have been replaced by RSRMs for use as flight motors. The primary purpose of TEM static tests is to recover SRM case and nozzle hardware for use in the RSRM flight program. TEM static tests also provide windows of opportunity to evaluate or certify various design and/or process issues for the RSRM flight program.

TEM-5 postfire inspection procedures followed Volumes I through IX, TWR-16474.

1.1 TEST ARRANGEMENT AND FACILITIES

The TEM-5 static test arrangement was assembled in accordance with Drawing 2U129760. T-97 was equipped with a water deluge system and a $C0_2$ quench. An aft skirt ring/actuator support ring assembly was installed in place of the aft skirt. The ring provided mounting provisions for the fixed links that were used in place of TVC actuators.

1.2 TEST ARTICLE DESCRIPTION

The TEM-5 test assembly was in accordance with Drawing 7U76879. TEM-5 consisted of HPM-configuration motor segments that were fabricated and loaded with propellant at least 3 yr before the static test fire on 23 Jan 1990. A listing of each segment, segment flight identification, cast date, and storage history is shown in Table 1-1.

Table 1-1. TEM-5 Segment History

Segment	HPM Segment Identification	Cast Date	Storage History
Forward	SRM-31A Forward	19 Dec 1985	Stored at Thiokol since casting
Forward Center	SRM-31A C/F	20 Jan 1986	Stored at Thiokol since casting
Aft Center	SRM-32A C/A	23 Jan 1986	Stored at Thiokol since casting
Aft	SRM-26B Aft	31 Jul 1985	Shipped to KSC in January 1986. Returned to Thiokol March 1988

The HPM static test motor consisted of: a lined, insulated, segmented rocket motor case loaded with solid propellant; an ignition system complete with an electromechanical safety and arming (S&A) device, initiators, and loaded igniter; movable nozzle with flexible bearing and exit cone; and an aft skirt/actuator support ring assembly in place of the aft skirt to provide mounting provisions for the fixed links that were used in place of the TVC actuators. The motor was instrumented to provide data to satisfy the test objectives. An overall view of the test article is shown in Figure 1-1. A TEM-5 drawing tree is included in Appendix A.

The test article was not configured to approximate RSRM flight motors.

1.2.1 Case/Seals

The case consisted of 11 individual segments: the forward dome, six cylinder segments, the external tank (ET) attach segment, two stiffener segments, and the aft dome. The 11 segments were preassembled into four subassemblies before propellant casting. These four subassemblies were: the forward segment assembly, the forward center and aft center segment assembly, and the aft segment assembly. These individual casting segments were joined by HPM tang and clevis field joints, held in place with pins. The case-to-nozzle joint was formed by bolting the nozzle fixed housing into the aft dome with 100 axial bolts. The assembled case was approximately 116 ft long and 12 ft in diameter (see Figure 1-1).

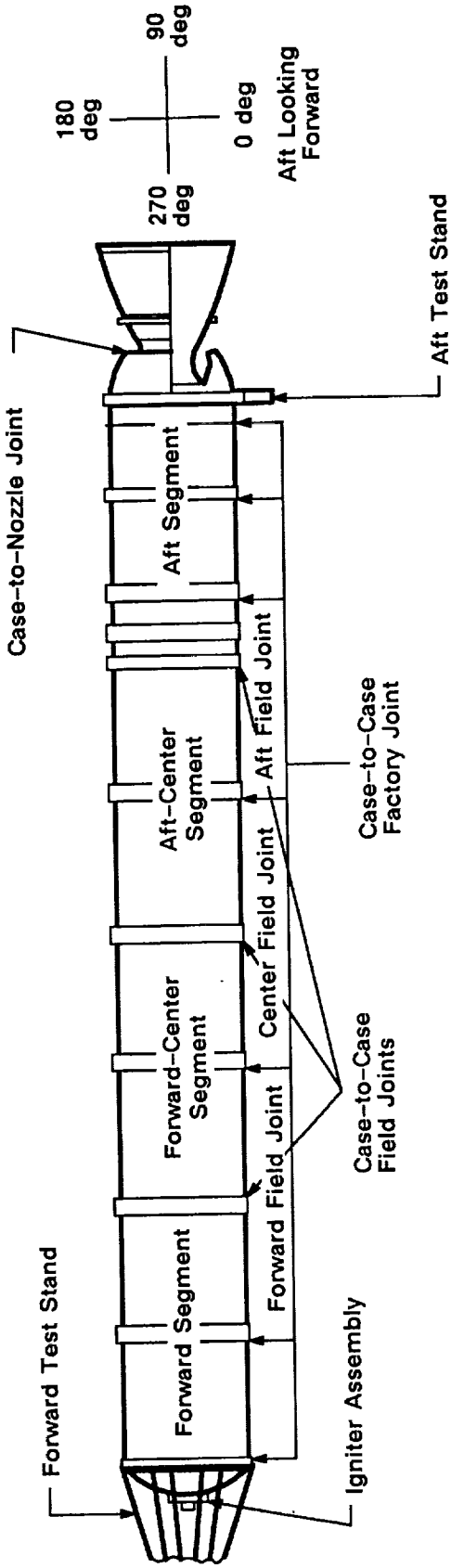

Figure 1-1. TEM-5 Test Article

The case-to-case factory joints were configured as follows:

a. HPM tang and clevis hardware design joint

b. Insulation overlaid and cured over interior of the joint (HPM configuration) (Figure 1-2)

c. HPM-type short pins and HPM-type pin retainer consisting of a steel band which is installed on each joint

d. Standard SRM shim clips

The case-to-case field joints were configured as follows:

a. RSRM-type long pins and RSRM-type hat band pin retainers

b. Standard-fit shims (custom-fit shim criteria)

c. Fluorocarbon O-rings were RSRM configuration 1U75150-11

d. O-ring squeeze was calculated for each assembly (minimum 15 percent squeeze for each seal)

e. Standard HPM internal insulation configuration with putty joint filler

f. Leak check port plugs

The case-to-nozzle joint was configured as follows:

a. Standard HPM case-to-nozzle joint internal insulation configuration with putty joint filler

b. Fluorocarbon O-rings (primary and secondary)

c. New 0.290-in. RSRM primary O-ring

d. HPM groove will accommodate larger diameter RSRM sizes

e. One hundred axial bolts installed and ultrasonically torqued to 120 ±9 klb

f. Four vent ports provided in fixed housing forward of primary O-ring; vents then plugged using adjustable vent port plugs (Figure 1-3) (additional description provided in Section 1.2.7)

The igniter-to-forward dome was configured as follows:

a. Fluorocarbon primary and secondary seals of the outer gasket

b. Putty joint filler

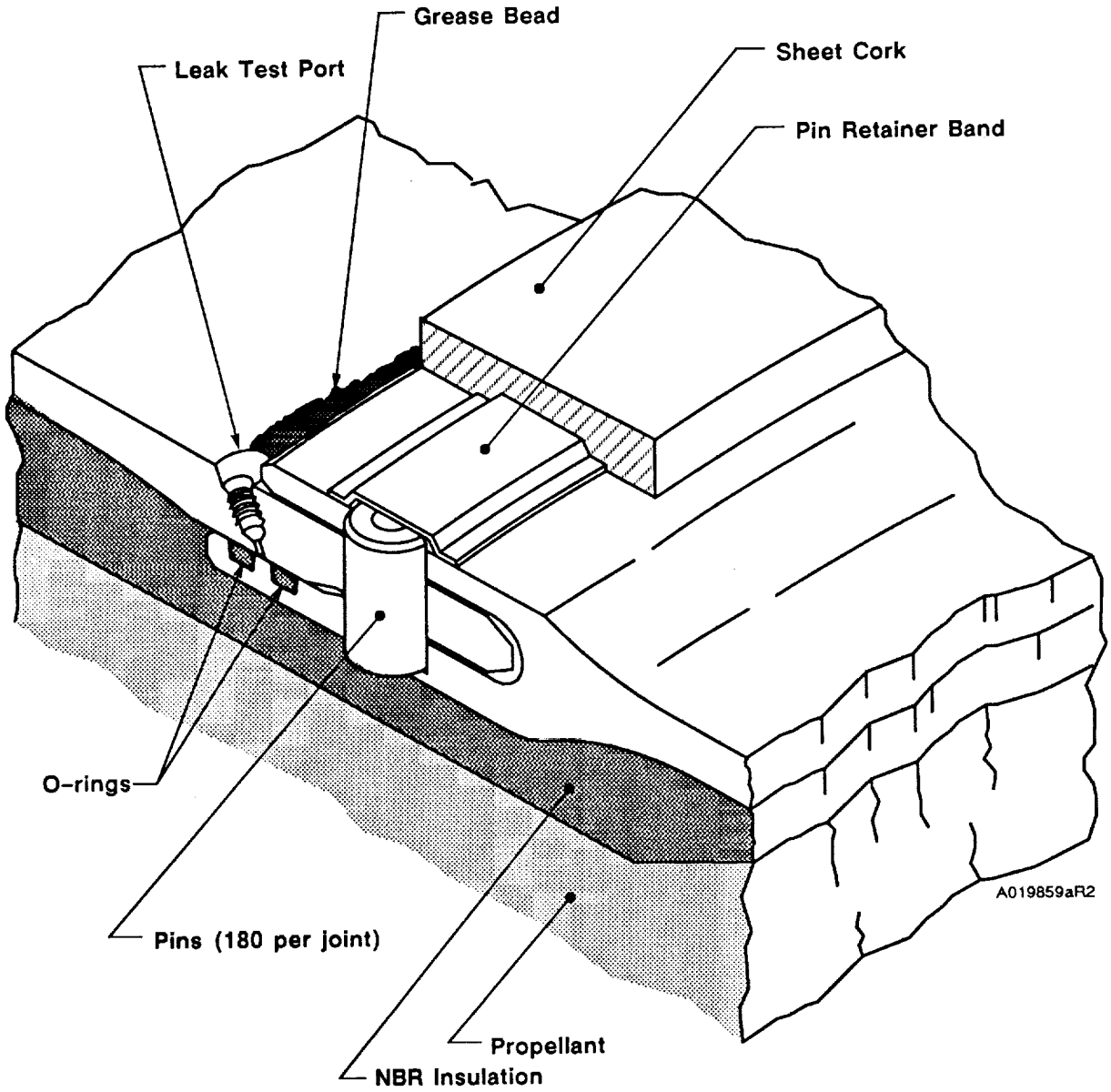

Figure 1-2. TEM Factory Joint Seal

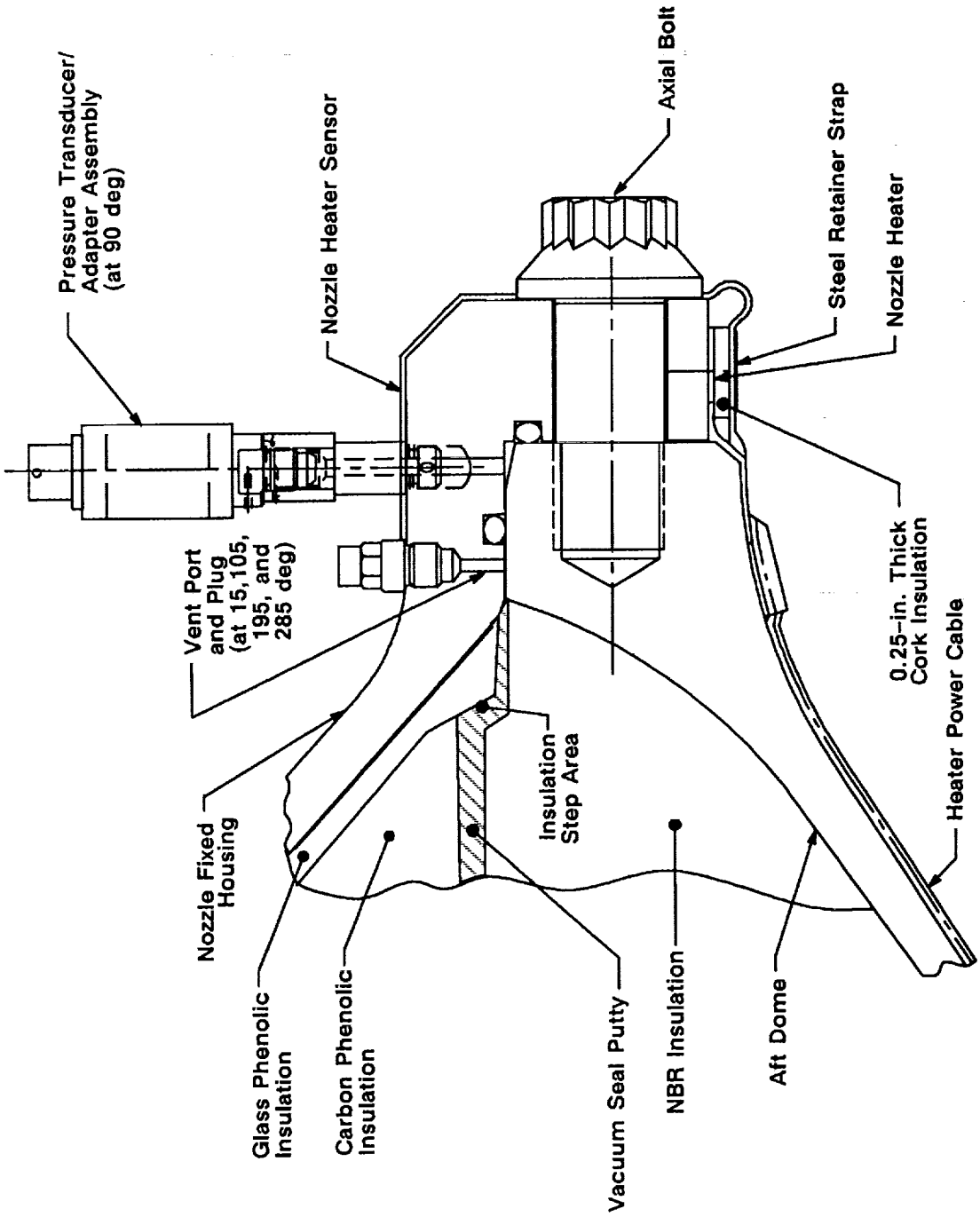

Figure 1-3. TEM-5 (HPM modified) Case-to-Nozzle Joint Configuration

Leak check port plugs with the Nylok® locking feature (1U100269-03) were installed in the leak check ports of all three field joints.

Corrosion protection consisted of full external paint and a thin film of grease (including O-rings, sealing surfaces, and pinholes).

1.2.2 Insulation/Liner/Inhibitor

The internal insulation system included case acreage insulation, joint insulation, and propellant stress relief flaps. The insulation material for these components was asbestos-silica-filled acrylonitrile butadiene rubber (NBR). Carbon fiber-filled ethylene-propylene-diene monomer (CF/EPDM) was bonded to the NBR insulation in a sandwich-type configuration under the propellant stress relief flap of both center segments. CF/EPDM was used in sandwich configuration in the aft dome. The CF/EPDM was also installed to reduce the erosion of the insulation near the submerged nozzle.

The liner material was an asbestos-filled carboxyl-terminated polybutadiene polymer (CTPB) which bonded the propellant to the case internal insulation.

The forward facing full web inhibitors, located on the forward end of the center and aft segments, were made of NBR. The aft facing partial web castable inhibitors, located on the aft end of the forward and center segments, were made of a material similar to the liner.

1.2.3 Propellant

The HPM propellant, TP-H1148, was a composite-type solid propellant, formulated from polybutadiene acrylic acid acrylonitrile terpolymer (PBAN) binder, epoxy curing agent, ammonium perchlorate (AP) oxidizer, and aluminum powder fuel. A small amount of burn rate catalyst (iron oxide) was added to achieve the targeted propellant burn rate of 0.368 ips at 625 psia and 60°F. TP-H1148 propellant is also used on RSRMs.

The propellant grain design consisted of an 11-point star with a smooth bore-to-fin cavity region that tapered into a circular perforated (CP) configuration in the forward segment. The two center segments were double-tapered CP configurations, and the aft segment was a triple-tapered CP configuration with a cutout for the partially submerged nozzle (Figure 1-4).

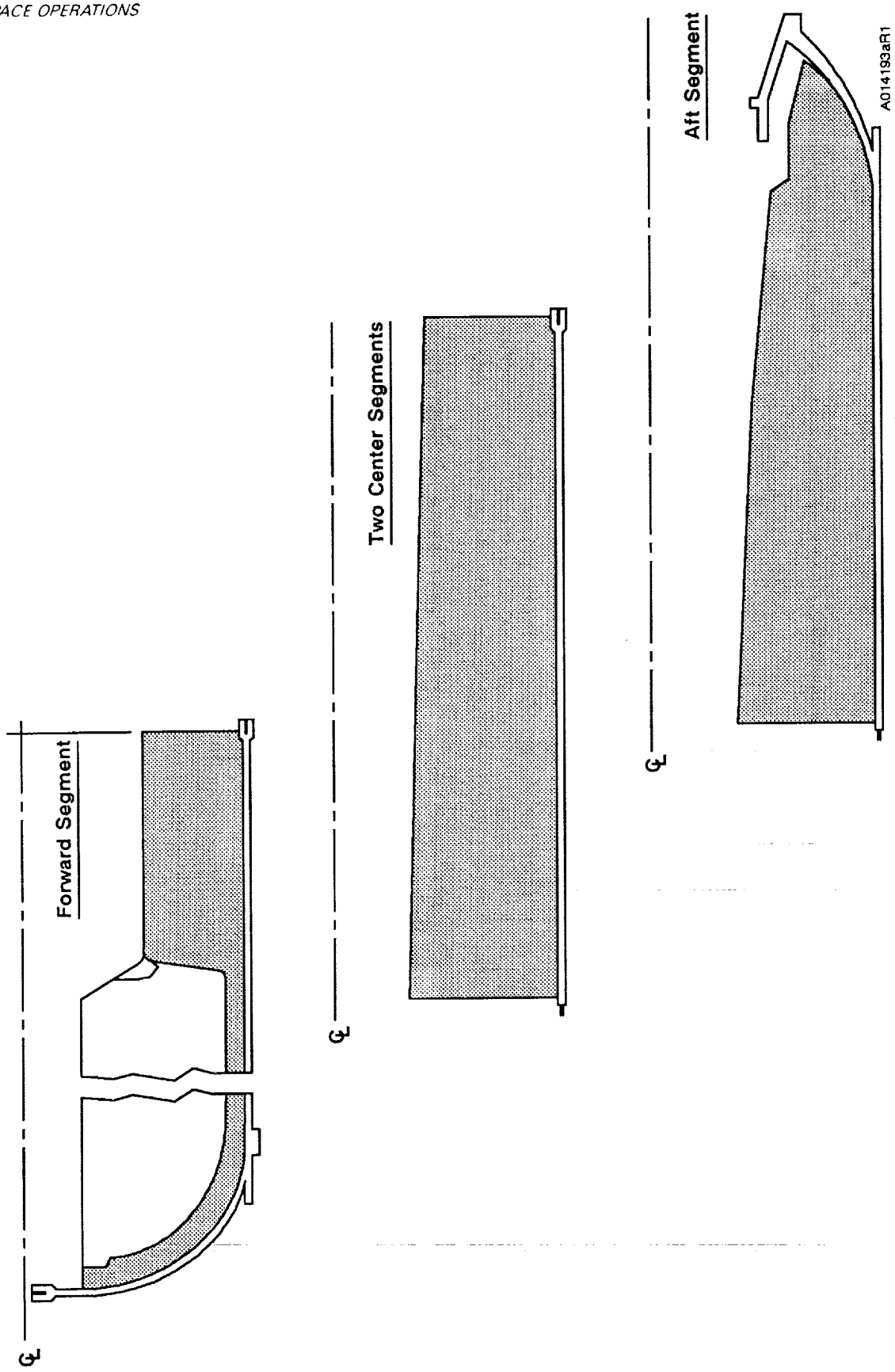

Figure 1-4. HPM Propellant Grain Design Configuration

1.2.4 Nozzle/TVC

The nozzle assembly was a partially submerged convergent/divergent movable configuration with an aft pivot point flexible bearing (Figure 1-5). An aft skirt/actuator support ring assembly was used instead of the aft skirt to provide mounting provisions for the fixed links that were used in place of the TVC actuators. The nozzle linear shaped charge (LSC) was removed from the aft exit cone assembly. The snubbers were removed from the forward exit cone. RSRM configuration O-rings were installed in the forward-to-aft exit cone joint.

1.2.5 Ignition System

The TEM-5 SRM ignition system consisted of a modified HPM igniter assembly (Figures 1-6 and 1-7). The igniter was modified with a CO_2 quench port. The ignition system contained a single nozzle, steel chamber, external and internal insulation, and solid propellant igniter containing a case-bonded 40-point star grain. This ignition system was configured to produce a short and predictable motor ignition that minimized thrust imbalance.

The 180 ksi bolts (A-286) used on both the igniter adapter-to-igniter chamber (inner) and the igniter adapter-to-forward dome (outer) joints were torqued to 275 to 295 ft (65 to 135 ksi stress).

New configuration igniter inner (1U51926-02) and outer (1U51927-02) joint gaskets were installed. The configuration change consisted of an inspection change, not a design change. The inspection was performed under STW7-2790 Rev D, and included a plexiglass compression inspection and a finger inspection.

An HPM configuration S&A device, using Krytox grease to lubricate the barrier-booster (B-B) rotor shaft O-rings, was installed on the igniter (Figure 1-8).

1.2.6 Joint Protection Systems (JPS)

FJPS--Each of the three TEM-5 field joints were protected by a different JPS configuration. The typical TEM JPS, consisting primarily of cork bands held in place with straps, was installed on the aft field joint (Figure 1-9).

The Concept 1 configuration of the redesigned FJPS was installed on the center field joint (Figure 1-10). The Concept 1 configuration consisted of two cork bands with K5NA ablation compound applied between them and to the bottom edge of the

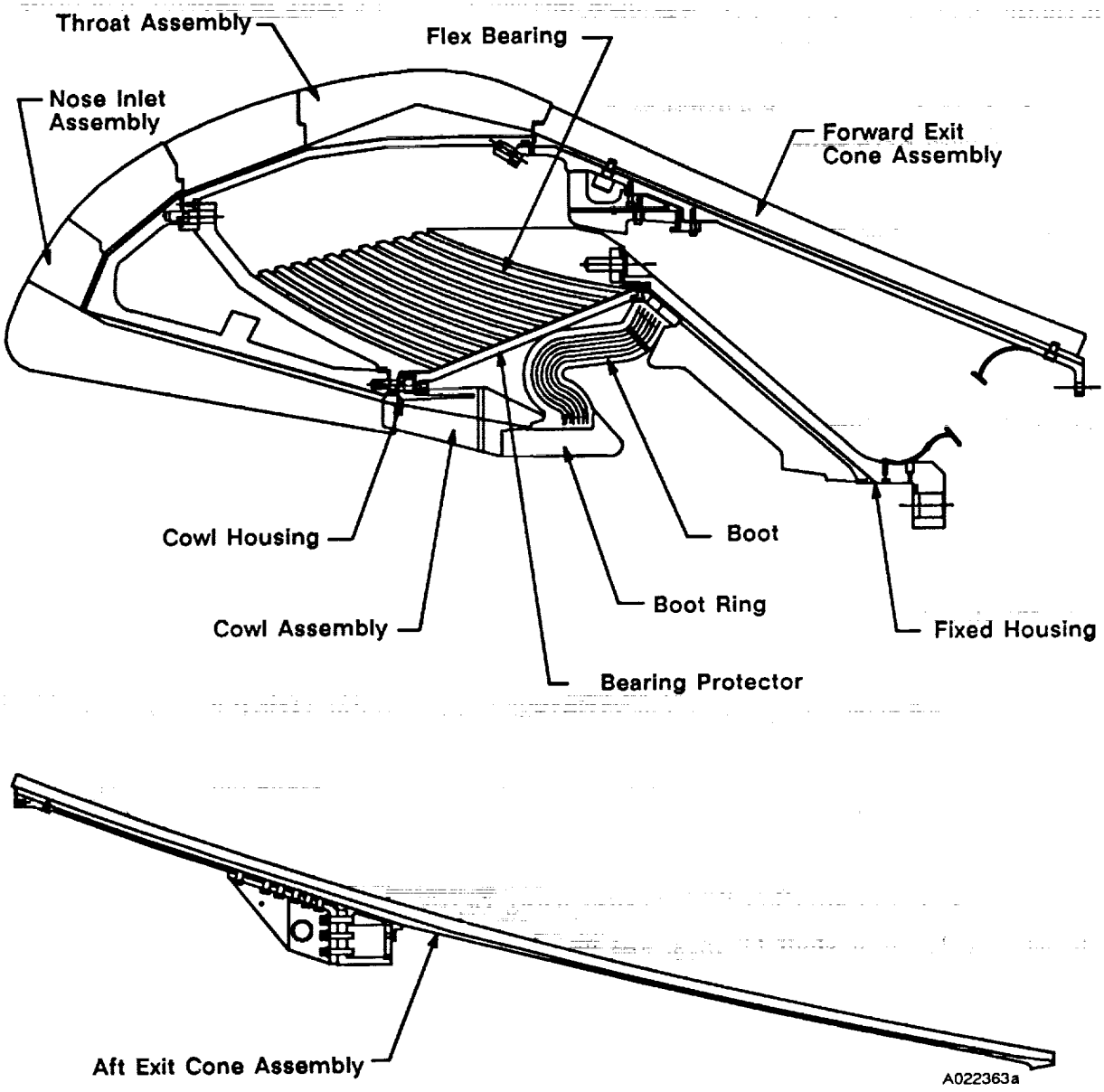

Figure 1-5. HPM Nozzle

A022491a

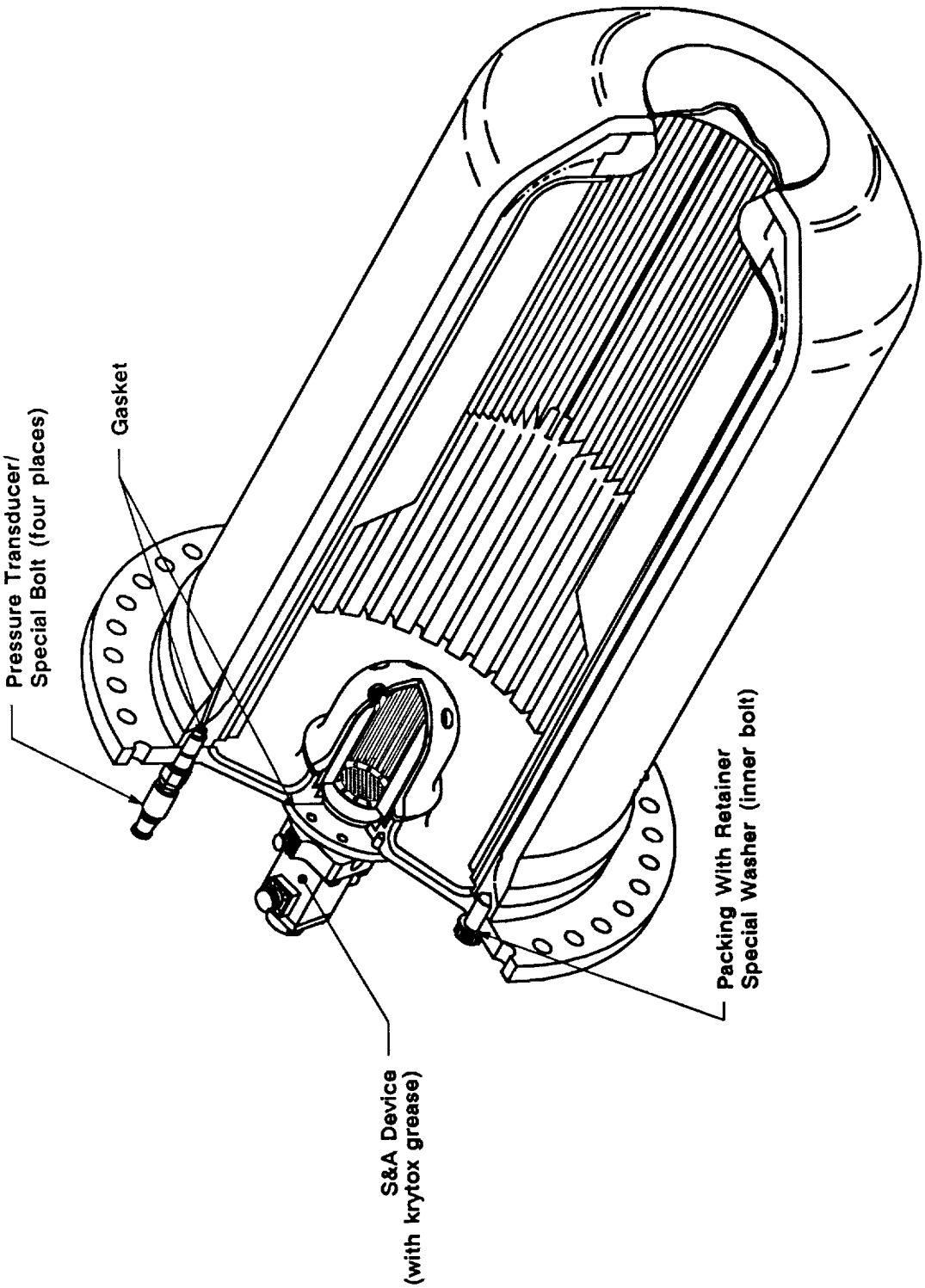

Figure 1-6. Standard HPM Igniter System

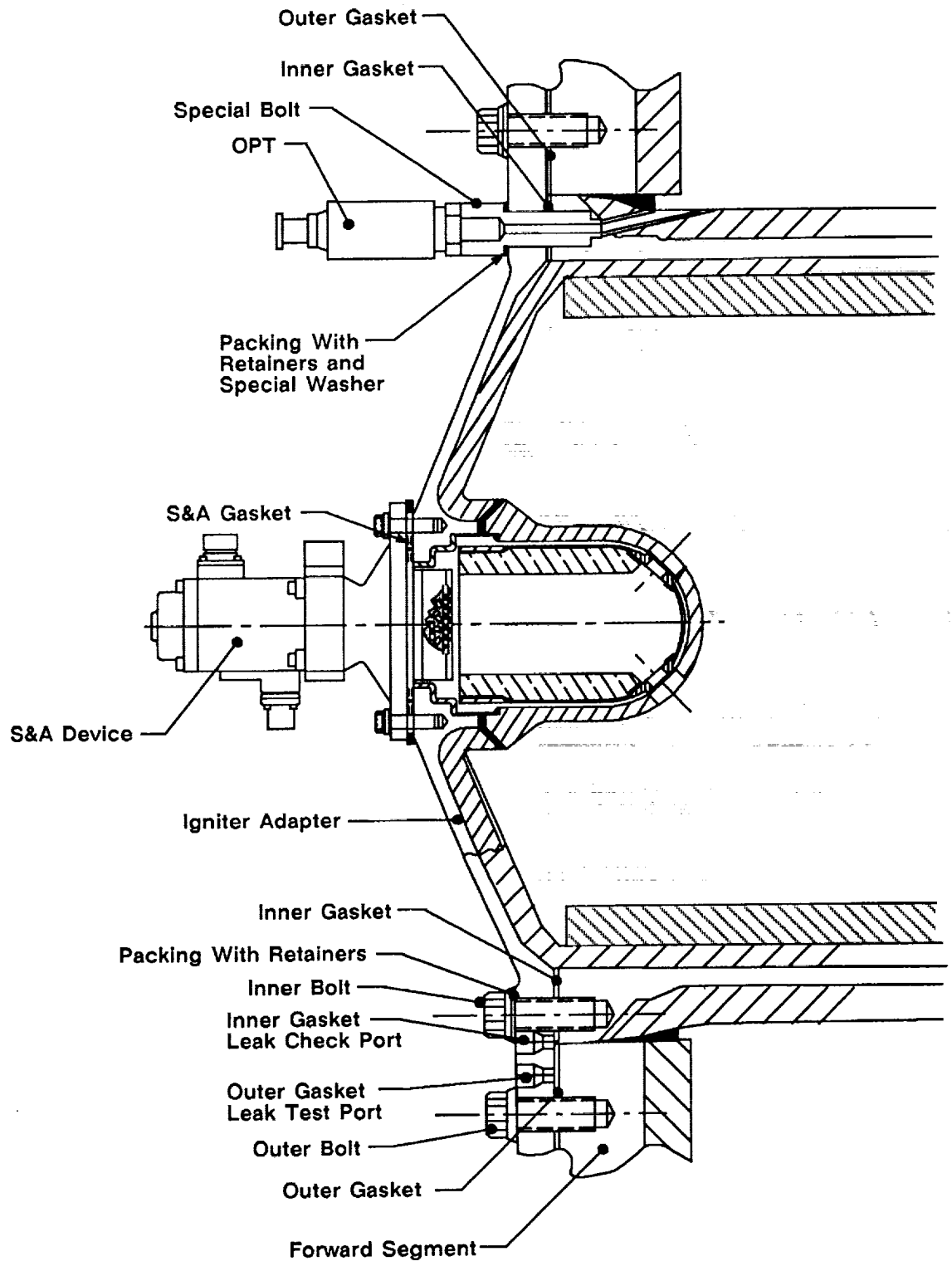

Figure 1-7. Ignition System Components and Seals

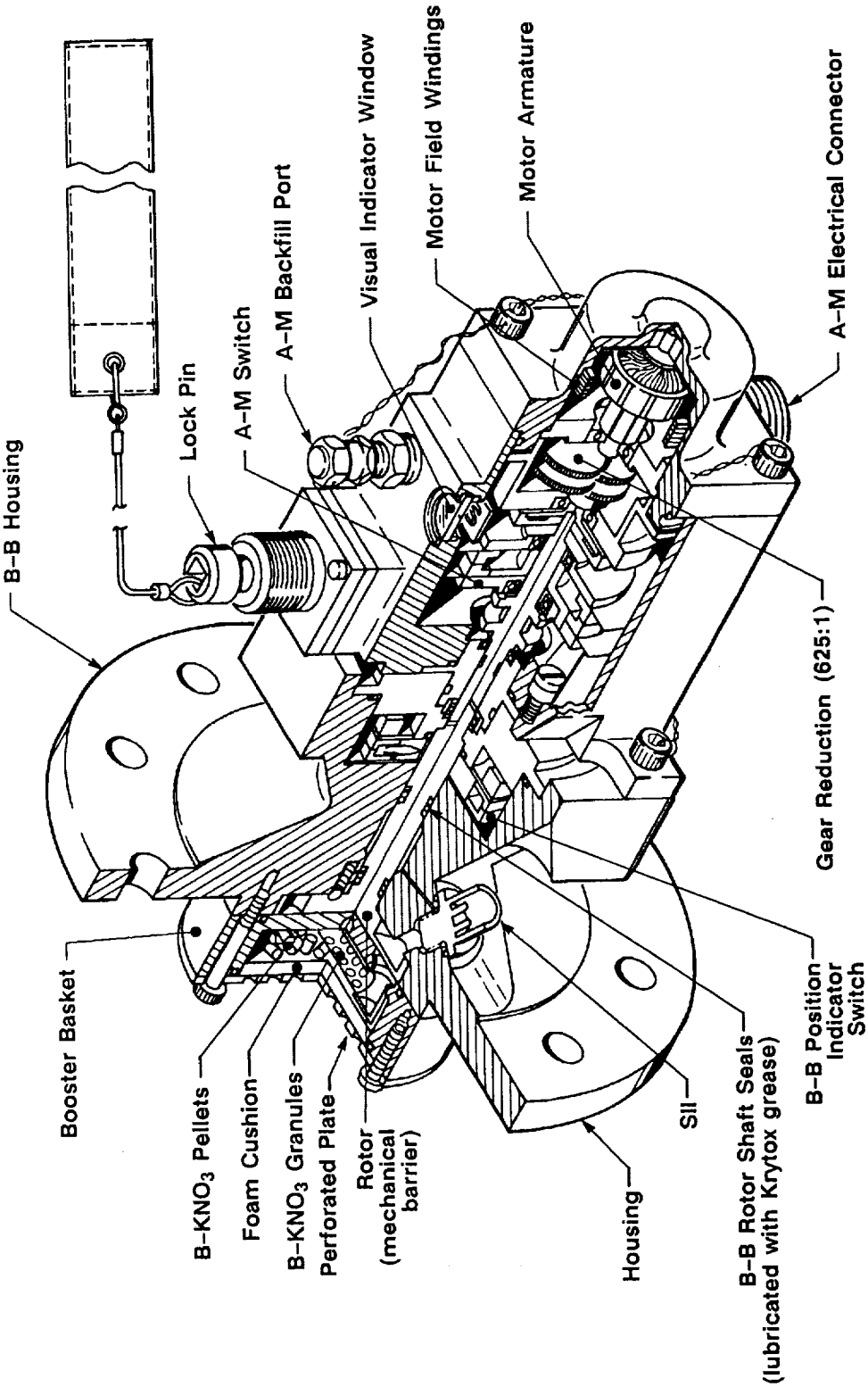

Figure 1-8. S&A Device Configuration

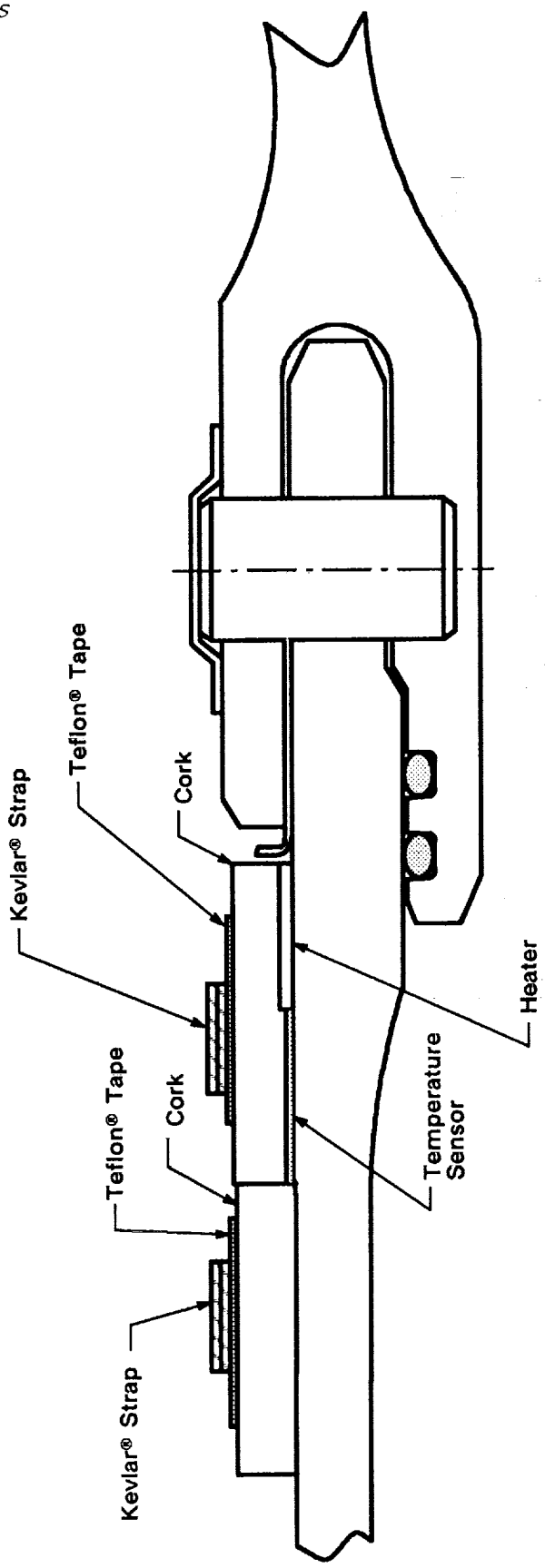

Figure 1-9. TEM-5 Aft Field Joint Heater/Cork Configuration (typical TEM)

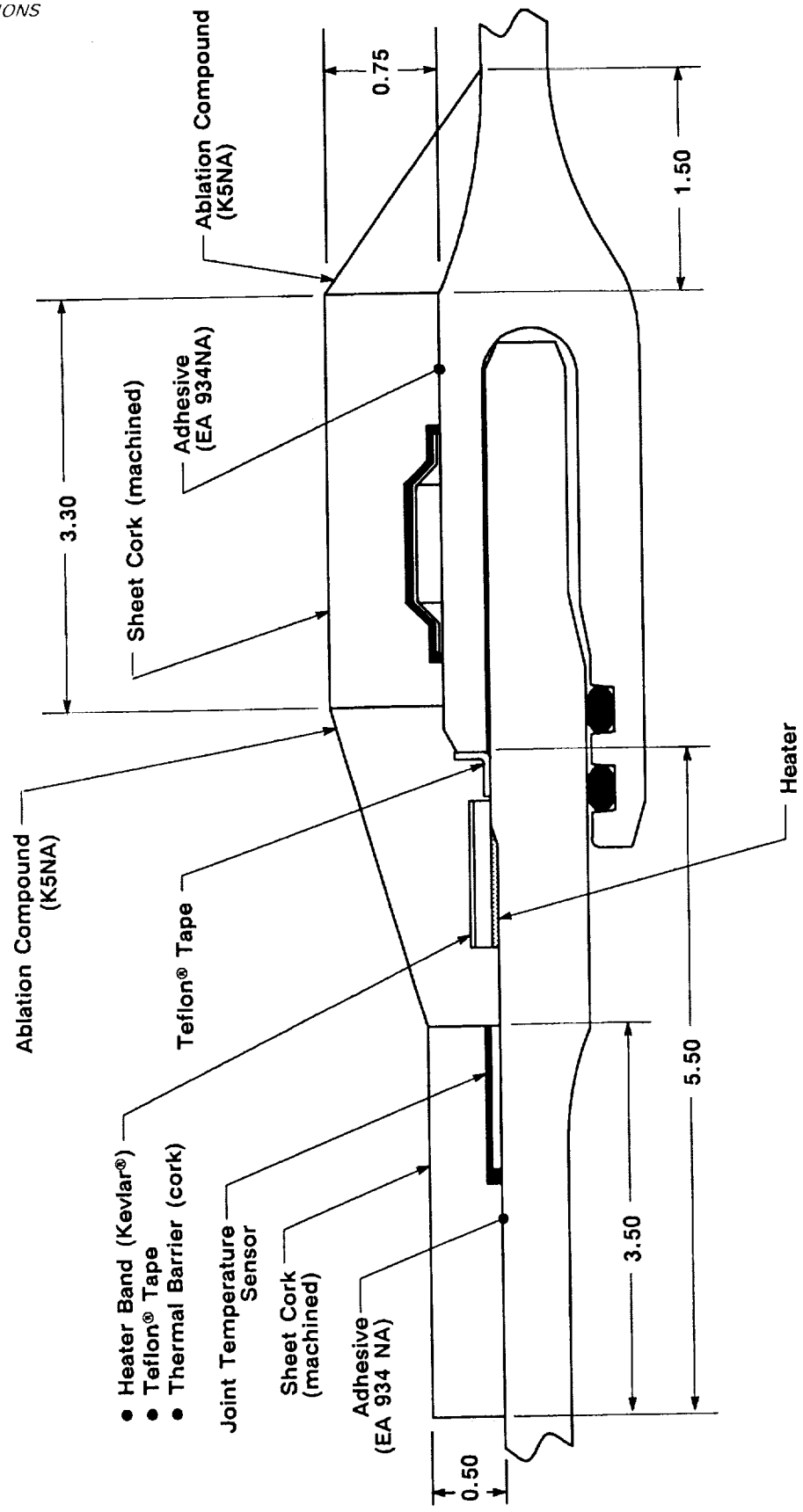

A026361a

Figure 1–10. TEM–5 Center Field Joint FJPS (Concept 1)

aft cork band. The aft cork band for the Concept 1 configuration was located over the joint pin retainer band.

The Concept 1C configuration of the redesigned FJPS was installed on the forward field joint (Figure 1-11). The Concept 1C configuration also consisted of two cork bands with ablation compound applied between them, with the aft cork band located over the outer clevis leg transition area.

Field Joint and Igniter-to-Case Joint Heaters--Redesigned field joint and igniter-to-case joint heaters were installed. The igniter-to-case joint heater configuration is shown in Figure 1-12. The changes incorporated in the redesigned heaters were intended to improve durability and reduce the possibility of damage due to handling. The redesigned heaters consisted of chemically etched, primary and redundant foil circuits which were superimposed upon one another, enclosed within a wire mesh grounding shield, and laminated in Kapton and FEP Teflon® insulation. Configuration of the heater circuits was not changed in the design of the redesigned heaters. The set point temperature of the field joint heaters was 121°F, with a minimum of 87°F at sensors. The set point of the igniter-to-case joint heater was 122°F, with a minimum of 87°F at sensors.

Case-to-Nozzle Joint Heater--A new 3.7 kW case-to-nozzle joint heater was installed on the case-to-nozzle joint (see Figure 1-3). The set point temperature of the heater was 76°F, with sensor readings to be between 71° and 81°F.

Heater Power Cables--Redesigned field joint heater and igniter-to-case joint heater power cables were used during TEM-5. The changes incorporated in the redesigned power cables were intended to improve durability and reduce the possibility of damage due to handling.

Systems Tunnel and LSC--The systems tunnel and systems tunnel LSC were not installed on TEM-5.

1.2.7 New Case-to-Nozzle Joint Assembly

A new case-to-nozzle joint assembly process, which incorporated four vent port holes on the nozzle fixed housing, was instituted on TEM-5 (see Figure 1-3).

Results from previous TEMs--The case-to-nozzle joints of TEM-1 through TEM-4 experienced putty blowholes and primary O-ring erosion. The diametrical primary O-ring erosion for these motors was 0.022-in. on TEM-1, 0.039-in. on TEM-2,

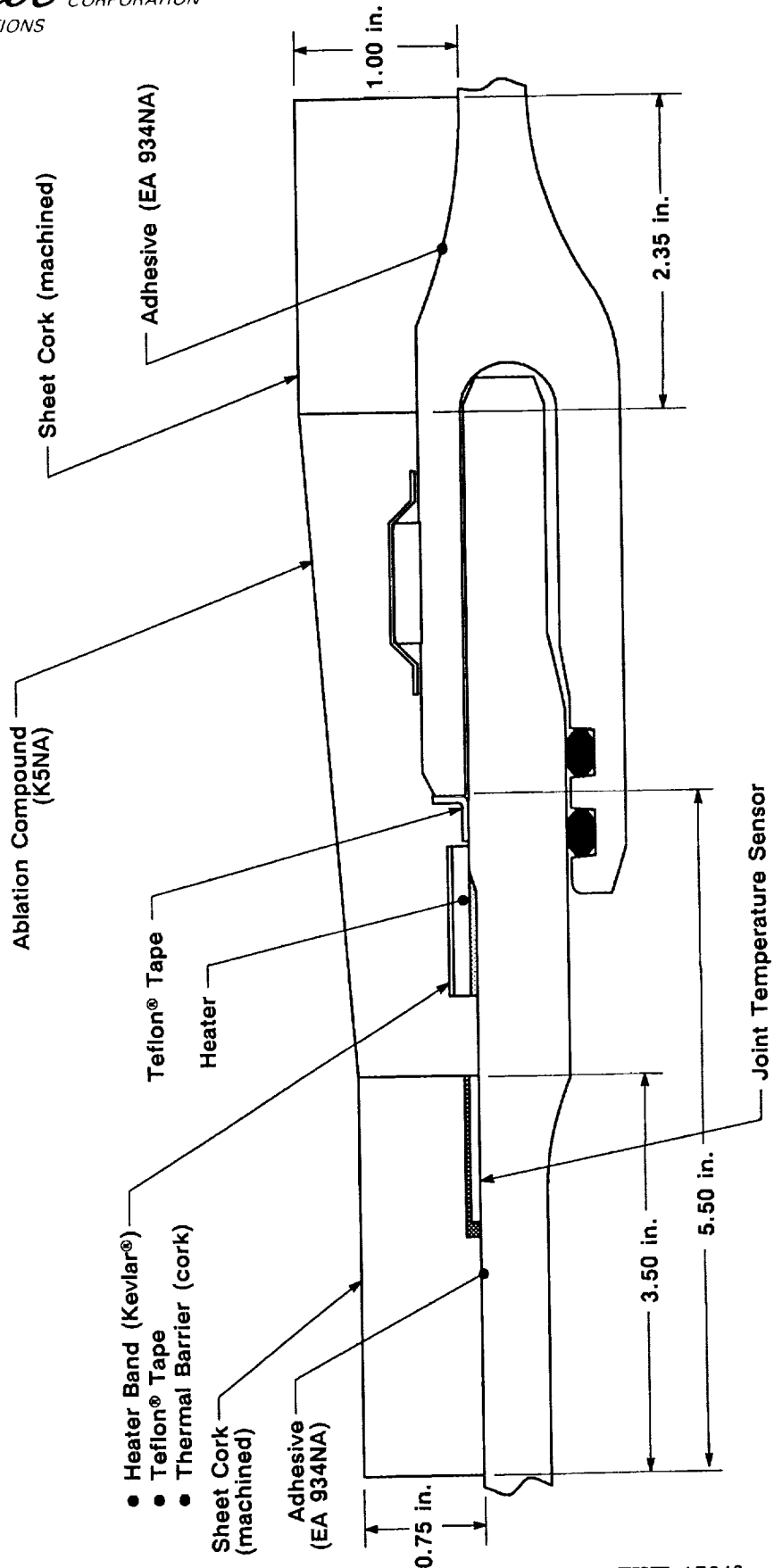

Figure 1-11. TEM-5 Forward Field Joint FJPS (Concept 1C)

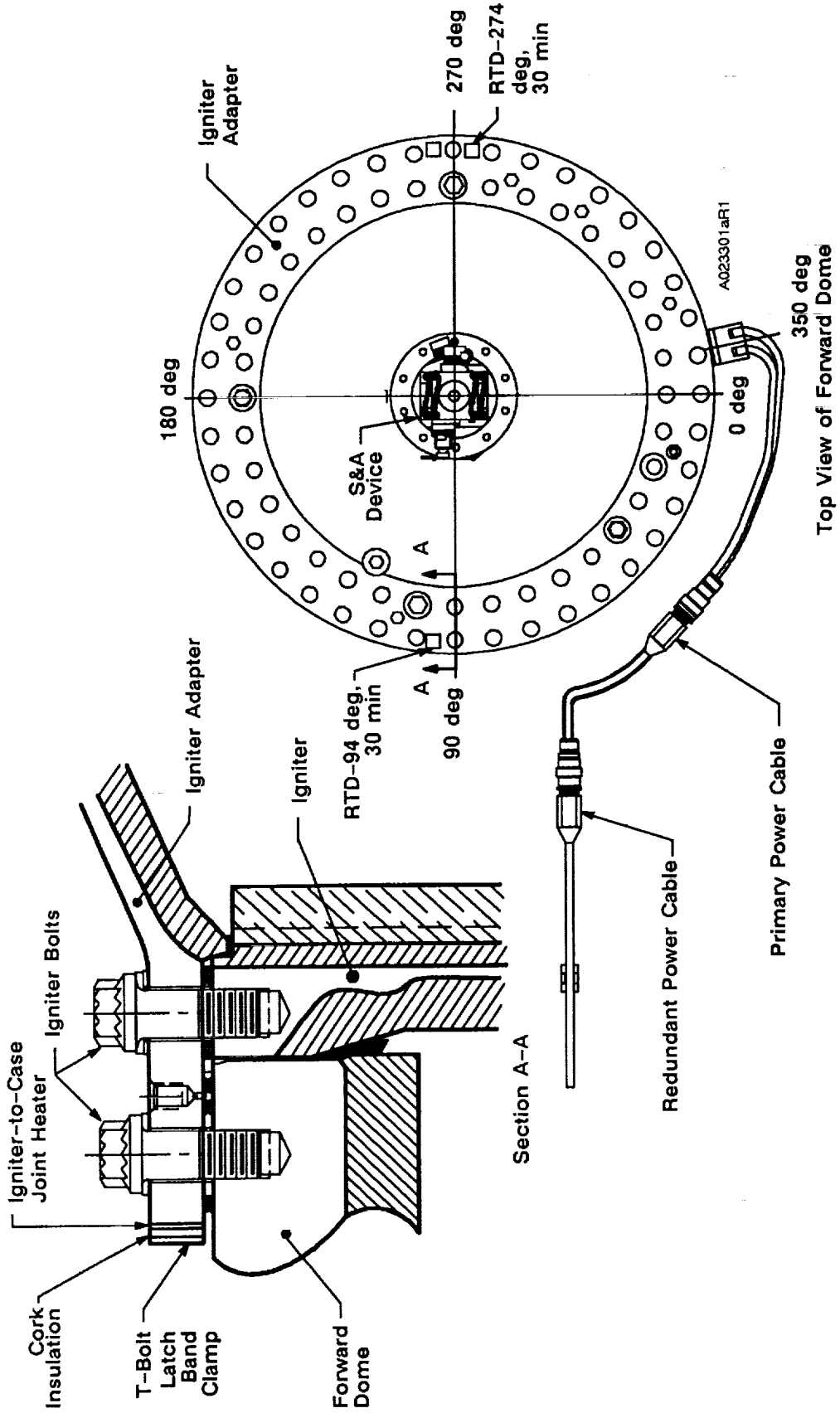

Figure 1-12. Igniter-to-Case Joint Heater Configuration

0.074-in. on TEM-3, and 0.112-in. on TEM-4. It was determined that a major cause of the blowholes was air entrapment within the putty (between the putty and the primary O-ring) during joint assembly.

On previous TEMs, the joint putty would be sheared and forced to flow by the verging insulation steps of the joint during the final stages of assembly. The aft flowing putty would pressurize the entrapped air. The entrapped air (which has a lower viscosity than putty) would escape through the weakest circumferential points in the putty, forming blowholes. The motor ignition pressure transient would rapidly force hot gas down blowhole paths and impinge on the primary O-ring.

After TEM-4, it was decided that a test hardware configuration change was necessary to eliminate the entrapped air during future TEM case-to-nozzle joint assemblies.

TEM-5 Configuration Case-to-Nozzle Joint--The design solution was to place four vent ports on the nozzle fixed housing, just forward of the primary O-ring groove. This configuration was similar to the single vent port design qualified for flight use on the RSRM. On TEM-5, the ports were located every 90 deg starting at 15 deg. These ports were installed to allow entrapped air to vent during the assembly process, and thus eliminate potential blowholes. Joint engagement speed was controlled to allow adequate time for venting. The four vent holes were plugged using flight configuration adjustable vent port plugs.

Prior to the final assembly of the joint for TEM-5, the design modification was verified in three tests using the TEM-5 nozzle and aft segment components. The tests consisted of assembling and disassembling the joint three times. Disassembly revealed that in each case there was no evidence of blowholes or unacceptable voids in the putty.

1.2.8 Static Test Support Equipment

The TEM-5 deluge system and related instrumentation was similar to previous TEMs except for two additional thermocouples and a pressure transducer on the end of the water deluge system plumbing.

2

OBJECTIVES

The TEM-5 test objectives of CTP-0105 were derived from the objectives of TWR-15723, Revision C, to satisfy the requirements of contract end item (CEI) Specification CPW1-3600A, dated 3 Aug 1987. The objectives of the test were:

A. Recover case, nozzle, and igniter hardware for RSRM flight and static test programs.

B. Obtain additional data on the effect of 3-yr storage of loaded SRM case segments upon motor ignition and performance.

C. Obtain data on the performance of the new flight configuration joint heaters on the igniter-to-case joint and field joints and the new higher output heater for the case-to-nozzle joint, which is used on static test motors only.

D. Obtain additional data on the low-frequency chamber pressure oscillations in the motor forward end.

E. Obtain additional breakaway and removal torque data for the leak check port plug Nylok® thread locking device.

F. Demonstrate the fit, operation, and similarity of the new JPS heater power cables to the old power cables.

G. Obtain additional data on the performance of Krytox grease on the B-B shaft O-rings.

H. Obtain additional data on nozzle axial deflection during motor pressurization.

I. Demonstrate and evaluate processing and installation of new FJPS designs.

J. Evaluate structural integrity of new FJPS designs through full-scale, full-duration static firing.

3

EXECUTIVE SUMMARY

3.1 SUMMARY

All of the test objectives have been met. All inspection and instrumentation data indicate that the TEM-5 static test firing was successful. Data was gathered at instrumented locations during pretest, test, and post-test operations. The information assembled from the test procedures has supplied valuable knowledge and understanding about the performance of the HPM and RSRM design components used in TEM-5.

3.1.1 Case Performance

No anomalies associated with case or joint hardware occurred in the TEM-5 static test. All case hardware was recovered for use on the RSRM flight program. Assembly procedures proved adequate. All field joint results were as expected, with no metal damage found during inspection. There was excessive amounts of grease on the sealing surfaces of the case-to-nozzle joint, but there was no evidence of damage or corrosion to the sealing surfaces. Refer to Section 6.1 for additional information about the case performance.

3.1.2 Case Internal Insulation Performance

A postfire internal walkthrough revealed no anomalous conditions. Case acreage insulation, NBR inhibitors, castable inhibitors, factory joint insulation, and igniter insulation were in normal condition. All three field joints were in excellent condition. No gas penetration into the field joint insulation or putty was observed. No edge separation growth from the noted prefire condition was detected.

The case-to-nozzle joint was also in excellent condition. The nozzle fixed housing vent ports were successful in eliminating joint putty blowholes and gas paths. No blowholes, terminated gas paths, or other anomalous conditions were found.

Final slag weight in the aft segment was determined to be 2,195 lb. Refer to Section 6.2 for additional information on the case internal insulation performance.

3.1.3 Seals/Leak Check Performance

Refer to Section 6.3 for additional seals/leak check performance information.

Leak Check--The leak tests performed on TEM-5 verified that the joints were properly assembled and that all O-rings sealed properly.

Field Joint Seals--The condition of the O-rings in each field joint was nominal. No hot gas or soot was observed past the putty.

Case-to-Nozzle Joint Seals--Seal performance was nominal. No hot gas or soot was observed past the putty.

Internal Nozzle Joint Seals--Disassembly/inspection of the internal joints revealed no anomalous conditions.

Igniter Joint Seals--No anomalous conditions were found on any of the igniter inner or outer joint seals. A blowhole occurred in the igniter outer joint putty at approximately 335 deg. Putty was in contact with the inner groove of the inner primary seal of the igniter inner gasket; this condition had not occurred on any previous static test motor or flight RSRM. Inspection of the three special bolts (for the chamber pressure and oscillation pressure transducers) revealed no anomalous conditions to the bolts or seals (packing with retainers).

Ignition System Seals--The performance of the S&A B-B rotor shaft O-rings with Krytox grease was nominal.

Inspection of the S&A-to-igniter adapter joint and gasket revealed no anomalous conditions. Inspection of the standard ignition initiators (SII), O-rings, and ports revealed no indication of soot to or blowby past the primary O-rings. The S&A SII sealing washer welds caused degradation (galling) on the land between the primary and secondary seal surfaces of both SII ports.

3.1.4 Nozzle Assembly Performance

The overall appearance of the TEM-5 nozzle phenolics was nominal, with no abnormal erosion characteristics observed. Refer to Section 6.4 for additional nozzle performance information.

3.1.5 Ignition System Performance

Igniter performance was as expected. S&A disassembly revealed no indications of blowby or erosion of any seal. Performance of the Krytox grease on the S&A B-B

shaft O-rings was nominal. Refer to Section 6.5 for additional information on the performance of the ignition system.

3.1.6 JPS

Refer to Section 6.6 for addition information on the TEM-5 JPS.

3.1.6.1 FJPS. No significant problems were encountered during the installation of each redesigned FJPS configuration, or to the standard TEM configuration JPS. No cracks, unbonds, or signs of overheating were detected on any of the JPS configurations after firing.

Upon disassembly of the Concept 1 FJPS, a significant amount of adhesive was found under approximately 95 percent of the pin retainer band. Upon joint demate, there was no evidence of adhesive in the joint. The adhesive migration did not impede removal of the joint pins.

3.1.6.2 Joint Heaters. The TEM-5 joint heaters maintained the joint temperatures within the required temperature range at the time of motor ignition.

Forward Field Joint Heater Dielectric Withstanding Voltage (DWV)--Prior to the static test fire, a DWV test failure occurred between the redundant forward field joint heater power line and shield. The primary heater circuit was subsequently used during the pretest countdown, and its performance was nominal. Evaluation of the heater after the test fire and heater removal identified the problem to be in the heater cold splice.

Heater Operation--The joint heaters were turned on 16 hr prior to the test firing to ensure that the joint O-ring temperatures were within the specified launch commit temperature at the time of ignition. During the motor fire, each field joint temperature sensor registered well over the minimum of 87°F, the igniter joint temperature sensors registered well over the minimum of 87°F, and the case-to-nozzle joint temperature sensors registered within the specified range of 71° to 81°F.

Post-test Heater Inspections--Each joint heater was inspected and no discolorations or any other anomalies, other than the forward field joint heater cold-splice short-circuit, were found.

3.1.6.3 Heater Power Cables. Operation of the new JPS heater power cables was nominal.

3.1.7 Ballistics/Mass Properties Performance

The TEM-5 ballistic performance was typical and within expected limits. The 3-yr open storage of loaded SRM case segments did not appear to affect motor performance. Ignition interval, pressure rise rate, and impulse gate limits were met. The TEM-5 ballistic performance compared closely with HPM historical data. Table 3-1 lists the predicted and reconstructed values for the performance of TEM-5 against the CPW1-3300 specification, Table 2 values. All the values were within the limits. Figure 3-1 shows the predicted pressure verses the measured headend pressure. Slag weight for TEM-5 was 2,195 lbm (aft segment only).

Table 3-1. TEM-5 Performance Summary* With CPW1-3300 CEI Specification Limits

	Vacuum Specification Limits (60°F)	TEM-5 Predicted (60°F)	TEM-5 Delivered (60°F)
Web Time (sec)	106.1 to 117.2	111.5	112.3
Action Time (sec)	115.4 to 131.4	122.9	124.0
MOP Headend (psia)	858.7 to 978.1	920.0	906.6
Maximum Sea Level Thrust (Mlbf)	2.87 to 3.25	3.07	3.02
Web Time Average Headend Pressure (psia)	625.8 to 695.8	663.9	658.7
Web Time Average Vacuum Thrust (Mlbf)	2.45 to 2.72	2.606	2.581
Web Time Total Impulse (Mlbf*sec)	286.1 to 291.8	290.6	289.8
Action Time Impulse (Mlbf*sec)	293.3 to 299.2	297.7	297.2
I_{sp} Average Delivered (lbf*sec/lbm)	265.3 to 269.0	268.4	267.9
Ignition Interval (sec), Time 563.5 psia	0.170 to 0.340	0.232	0.230
Maximum Pressure Rise Rate (psi/10 ms)	X < 109.0	90.5	87.1

Loaded Propellant Weight of 1,109,928 lb

*TEM-5 performance based on the following as-cast motor segments:

Forward:	SRM-31A FWD	Center Forward:	SRM-31A C/F
Center Aft:	SRM-32A C/A	Aft:	SRM-26B AFT

A026339a

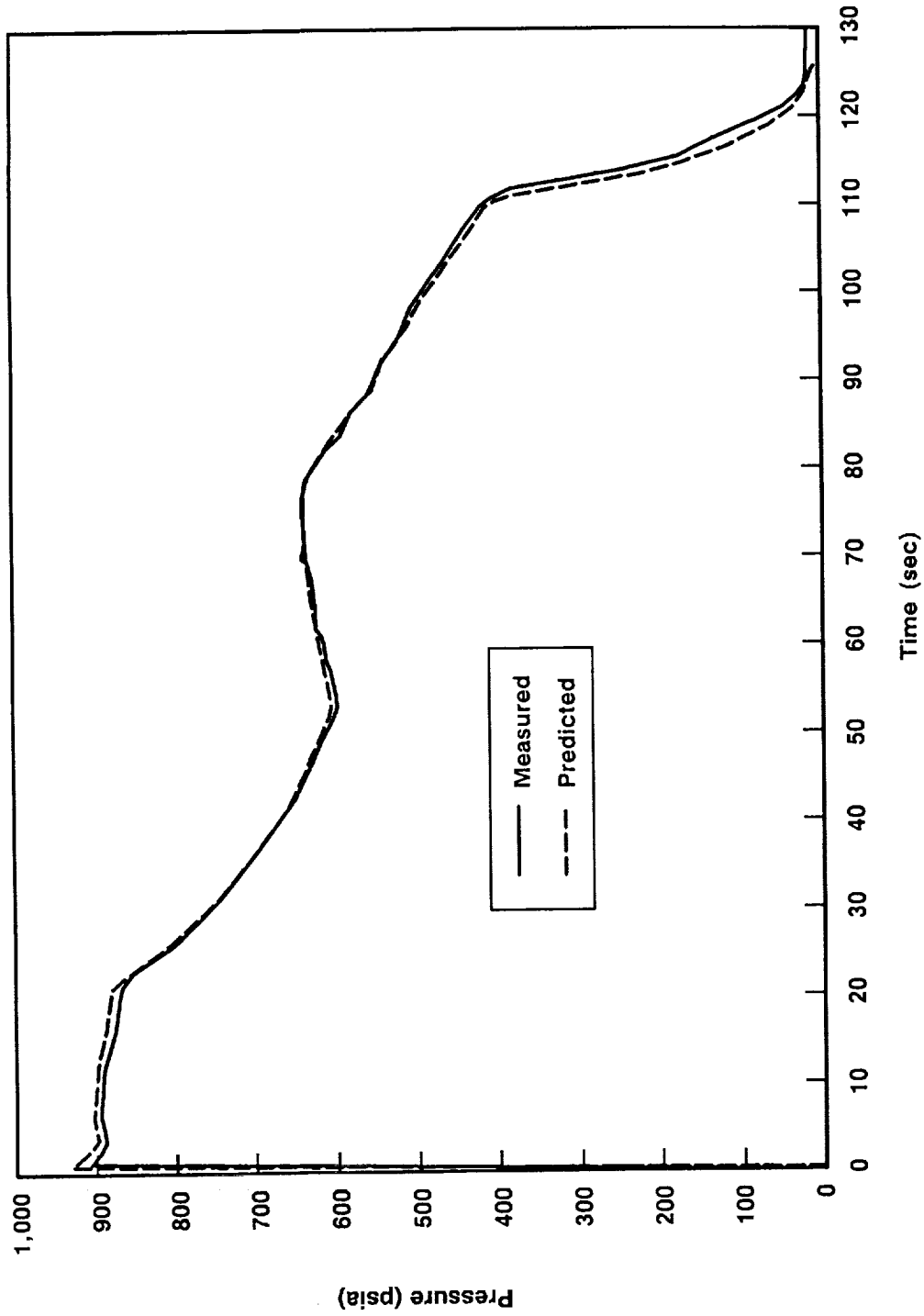

Figure 3-1. TEM-5 Predicted and Measured Pressure at 72°F

The TEM-5 motor exhibited chamber pressure oscillations similar to previously tested space shuttle HPMs. The first-longitudinal (1-L) mode oscillations were typical for an HPM. In general, HPM 1L mode amplitudes are lower than those for RSRMs. Much of the static test pressure oscillation data to date has been incorrect. Upon completion of the TEM-4 static test, several errors were found in the processing of the alternate current (ac) coupled data. This affected the data of past static tests as well. This report documents the latest information of data as supplied by test area. Refer to Section 6.7 for additional information about the ballistics/mass properties performance.

3.1.8 Static Test Support Equipment

The deluge system including the CO^2 quench performed adequately. Case temperatures were well below 500°F: the temperature at which the paint browns. Refer to Section 6.8 for additional information on the performance of the static test support equipment.

3.1.9 Instrumentation

TEM-5 instrumentation measurements consisted of chamber pressure, igniter chamber pressure, joint temperatures, nozzle axial deflections, case temperature for deluge control, and pressure between the O-rings on the case-to-nozzle joint. Fifty data channels were recorded during the motor firing, 46 of which were attached to the motor. The remaining four channels were timing and water deluge pressure channels. First time instrumentation measurements for TEMs consisted of two new thermocouples on the case stiffener segments (Stations 1735 and 1797) and an additional pressure transducer on the deluge spray plumbing.

A pressure transducer was installed in the leak check port of the case-to-nozzle joint to monitor pressure between the O-rings. During the motor fire, the case-to-nozzle joint expanded while the O-rings continued to seal. The increased volume between the O-rings resulted in a pressure decrease of 4 psi. The pressure reading provided early assurance that pressure did not reach the primary O-ring.

All instrumentation channels provided satisfactory data. Refer to Section 4 for additional instrumentation information.

3.1.10 Temperature Data

Temperature data were nominal. Ambient temperature at the time of ignition was 41°F and the PMBT was 72°F.

3.2 CONCLUSIONS

The following listing is the conclusions as they relate specifically to the objectives. Additional information about each conclusion can be found in the applicable referenced section.

Objective	Conclusion (section reference)
A. Recover case, nozzle, and igniter hardware for RSRM flight and static test programs.	Case, nozzle, and igniter hardware were recovered for use on the RSRM flight and static test programs (Sections 6.1, 6.4, and 6.5).
B. Obtain additional data on the effect of 3-yr storage of loaded SRM case segments upon motor ignition and performance.	Three-year storage did not appear to effect motor ignition and performance (Sections 4, 6.2, and 6.7).
C. Obtain data on the performance of the new flight configuration joint heaters on the igniter-to-case joint and field joints and the new higher output heater for the case-to-nozzle joint, which is used on static test motors only.	The performance of each joint heater was nominal throughout the TEM-5 countdown period (Sections 4 and 6.6).
D. Obtain additional data on the low-frequency chamber pressure oscillations in the motor forward end.	Operational pressure transducer (OPT) pressure oscillation measurements compared well with the baseline Minuteman pressure gage measurements. This test confirmed that satisfactory pressure oscillation data can be obtained from OPTs. TEM-5 exhibited chamber pressure oscillations similar to those measured on previous HPMs. The 1-L mode oscillations were typical for an HPM (Sections 4 and 6.7).
E. Obtain additional breakaway and removal torque data for the leak check port plug Nylok® thread locking device.	Breakaway and removal torque levels of the leak check port plug Nylok® thread locking device were recorded. The thread locking device was installed on the field joint leak check port plugs. Torque values were within the limits defined in NAS 1283 and MIL-F-18240. Torque values will be used in an evaluation on the holding power of Nylon (Section 6.3).

Demonstrate the fit, operation, and similarity of the new JPS heater power cables to the old power cables.	The fit and operation of the new JPS power cables was demonstrated to be similar in comparison to the old power cables (Section 6.6).
G. Obtain additional data on the performance of Krytox grease on the B-B shaft O-rings.	Performance of the Krytox grease on the B-B shaft O-rings was nominal. S&A cycle times were within the engineering requirements. All cycles were below 0.730 sec at 21.9 Vdc during checkout. Current engineering requirements are 2.0 sec or less at 24 Vdc (Sections 6.3 and 6.5).
H. Obtain additional data on nozzle axial deflection during motor pressurization.	Nozzle axial deflection was successfully measured by four extensometers during motor pressurization. Performance of the four extensometers was nominal. (Sections 4 and 6.4).
I. Demonstrate and evaluate processing and installation of new FJPS designs.	No significant problems were encountered during installation of the each FJPS configuration. Installation of both redesign Concepts 1 and 1C required approximately the same amount of skill and time.
J. Evaluate structural integrity of new FJPS designs through full-scale, full-duration static firing.	The nominal performance of both redesign FJPS Concepts 1 and 1C was the same. No cracks or unbonds were detected on either FJPS configuration after the motor fire. (Section 6.6). The TEM-5 FJPS demonstrations supported the choice of Concept 1 over Concept 1C (Section 6.6).

3.3 RECOMMENDATIONS

Based on the results of this test, the following recommendations have been made:

Instrumentation--Instrumentation should continue to be used on future TEMs to expand the database on pressure oscillation and joint performance.

New Case-to-Nozzle Design--Future TEM case-to-nozzle joints should be assembled with the same putty layup configuration and fixed housing vent port design as TEM-5.

Postfire Internal Insulation Inspection--On TEM-5, an internal walkthrough insulation inspection and slag evaluation were performed before the disassembly of the aft field joint. Because all pertinent engineering data could have been obtained after the joint was disassembled, this inspection presented an unnecessary confined space hazard. On future static test motors, this inspection should occur after the disassembly of the aft field joint, as has been the case for previous RSRM and TEM static test motors.

SII Sealing Washer Degradation--Because the S&A SII sealing washer welds caused degradation (galling) on the land between the primary and secondary seal surfaces of both SII ports, it is recommended that refurbishment criteria be established on the land of the SII ports.

FJPS Cork Adhesive--To reduce the occurrence of voids and the migration of adhesive under the pin retainer band during future Concept 1 FJPS installations, Cab-O-Sil (STW4-2679, microfine silicon dioxide) should be added to EA 934NA adhesive to increase its viscosity.

Water Deluge System Pressure--On future TEMs, it is recommended that a pressure transducer continue to be installed on the end of the water deluge system plumbing. This transducer can be used to verify the pressure during steady state conditions with the boost pump running. Results from this transducer can be used to determine if additional nozzles can be added to the system to further insure the proper cooling of the motor case aft end.

4

INSTRUMENTATION

4.1 INTRODUCTION

TEM-5 instrumentation measurements consisted of chamber and igniter chamber pressures, joint temperatures, case temperatures, nozzle axial deflections, and pressure between the O-rings of the case-to-nozzle joint. Normal test stand water deluge pressure and timing were also recorded. All of the data channels provided satisfactory data.

Appendix B contains the instrumentation list. A new instrumentation channel numbering system was started on TEM-5. The instrumentation list in Appendix B presents both the old and new instrumentation channel numbers. The text of this report will refer only to the new instrumentation channel numbers.

Appendix C contains the plots of the instrumentation channels. Refer to the instrumentation list (Appendix B) for a description of the data channel plots. The plots in Appendix C are presented in the order that they are listed in the instrumentation list.

4.2 OBJECTIVES

TEM-5 was instrumented to support the following objectives from Section 2:

B. Obtain additional data on the effect of 3-yr storage of loaded SRM case segments upon motor ignition and performance.

C. Obtain data on the performance of the new flight configuration joint heaters on the igniter-to-case joint and field joints and the new higher output heater for the case-to-nozzle joint, which is used on static test motors only.

D. Obtain additional data on the low-frequency chamber pressure oscillations in the motor forward end.

H. Obtain additional data on nozzle axial deflection during motor pressurization.

4.3 CONCLUSIONS/RECOMMENDATIONS

Overall, the TEM-5 instrumentation performed very well. Installation of the instrumentation was successfully completed and the instrumentation performed as expected.

Instrumentation was successfully used to obtain additional data on the effect of 3-yr storage of loaded SRM case segments upon motor ignition and performance.

Resistance temperature devices (RTD) were successfully used to control the temperatures of the field joint, igniter-to-case joint and case-to-nozzle joint heaters. The RTDs are inherent to the configuration of each joint heater.

OPT pressure oscillation measurements compared well with the baseline Minuteman pressure gage measurements. This test confirmed that satisfactory pressure oscillation data can be obtained from OPTs.

Nozzle axial deflection was successfully measured by four extensometers during motor pressurization. Performance of the four extensometers was nominal.

It is recommended that instrumentation continue to be used on future TEMs to expand the database on pressure oscillation and joint performance.

4.4 RESULTS/DISCUSSION

Forty-six channels of instrumentation were installed on TEM-5, including pressure, displacement, and temperature gages. Normal T-97 test stand measurements and countdown timing data were also recorded. All instrumentation channels operated nominally.

Chamber and Igniter Pressure--Five pressure transducers were installed to measure motor chamber and igniter pressure (data channels PNCAC001 through PNCAC005). Four gages measured chamber pressure and one gage measured igniter pressure. The performance of each gage was nominal.

Chamber Pressure Oscillations--The OPT data channel was AC coupled and processed through special signal conditioning systems for both headend chamber mean pressure (data channel PNCAC001) and headend chamber pressure oscillation measurements. A CEC (Minuteman) pressure gage (data channel PNCAC005) was installed for a pressure oscillation data comparison with the OPT. The Minuteman gage, used on all previous TEMs for pressure oscillation measurements, was used to

obtain baseline data to develop a database for replacing the CEC gage with the OPT. The Minuteman gage is considered obsolete and its use has been discontinued after TEM-5. The data from each pressure oscillation channel were sufficiently similar to indicate that the OPT can be used to measure satisfactory pressure oscillation data. Refer to Section 6.7 for additional information on chamber pressure oscillation.

Case-to-Nozzle Joint Pressure--A pressure transducer (data channel PNNAR001) was installed in the leak check port of the case-to-nozzle joint to monitor pressure between the O-rings (Figure 1-3). A pressure decrease of 4 psi was recorded, as compared to the 15 psi increase recorded on TEM-4. On TEM-4, hot gas reached the primary O-ring through blowholes and gas paths in the joint putty. The hot gas during the TEM-4 motor fire moved the primary O-ring toward the secondary O-ring, decreasing volume and increasing pressure between the O-rings. On TEM-5, the new case-to-nozzle joint assembly process resulted in no detectable blowholes or gas paths in the putty, and no hot gas reached the primary O-ring. During the TEM-5 motor fire, the case-to-nozzle joint expanded while the O-rings continued to seal. The increased volume between the O-rings resulted in the decrease in pressure. The decrease in pressure between the O-rings was also verified by analysis (Appendix D, TEM-5 Case-to-Nozzle Joint Pressure Measurement Analysis). It is worth noting that the range of the pressure transducer was 0 to 1,000 pisa, with an accuracy of ±20 psia. Refer to Sections 1.2.7, 6.2, and 6.3 for additional information about the case-to-nozzle joint performance.

Nozzle Axial Extension--Four extensometers were installed to measure nozzle deflections in the axial direction. Performance of each extensometer was nominal. Refer to Section 6.4.4.9 for additional nozzle deflection information.

Joint Temperature Measurements--RTDs were successfully used to control the temperatures of the field joint, igniter-to-case joint and case-to-nozzle joint heaters. The RTDs are inherent to the configuration of each joint heater. Refer to Section 7.6 for additional RTD information.

Twenty thermocouples were bonded on the bottom of the case to measure case temperature during motor cooldown and deluge water spray control. Two of these thermocouples, located at Stations 1735 and 1797, were first-time installations on a TEM.

Deluge System Pressure--A water pressure transducer was installed at the end of the deluge spray plumbing to gather data for possible expansion of the deluge system. This transducer gave data until T+175 sec, when the data channel became noisy and erratic. The most likely cause of the noisy and erratic data was moisture penetration into the electrical connector. Refer to Section 6.8 for additional deluge system information.

5

PHOTOGRAPHY

Photographic coverage was required to document the test, test configuration, instrumentation, and any anomalous conditions which may have occurred. The TEM-5 photographs and video tapes are available from the Thiokol's Photographic Services department.

5.1 STILL PHOTOGRAPHY

Still color photographs of the test configuration were taken before, during, and after the test. Photographs were taken of joints each 45 deg minimum and at anomalous conditions.

5.2 MOTION PICTURES

Color motion pictures of the test were taken with five video, three documentary, eight high-speed, and two still-sequence cameras. Documentary motion pictures are recorded on Roll 8154, high-speed motion pictures on Roll 8155, and videotape on 8154-V01. Cameras are listed in Table 5-1. The camera setup is shown in Figure 5-1.

Table 5-1. Photography and Video Coverage

Camera	Controller	Station	Start Time	Stop Time	Priority
1	19	7	T-5 sec	T+150 sec	M
2	1	1	T-5 sec	T+150 sec	M
3	NA	1	Manual	Manual	R
4	4	2	T-5 sec	T+150 sec	M
5	5	2	T-15 sec	T+180 sec	R
6	6	2	T-5 sec	T+150 sec	M
7	7	3	T-15 sec	T+180 sec	M
8	NA	3	Manual	Manual	R
9	NA	4	Manual	Manual	R
10	10	4	T-5 sec	T+150 sec	M
11	11	4	T-5 sec	T+150 sec	M
12	13	5	T-5 sec	T+150 sec	M
13	20	7	T-5 sec	T+150 sec	M
14	NA	7	Manual	Manual	R
15	20	7	T-5 sec	T+150 sec	M

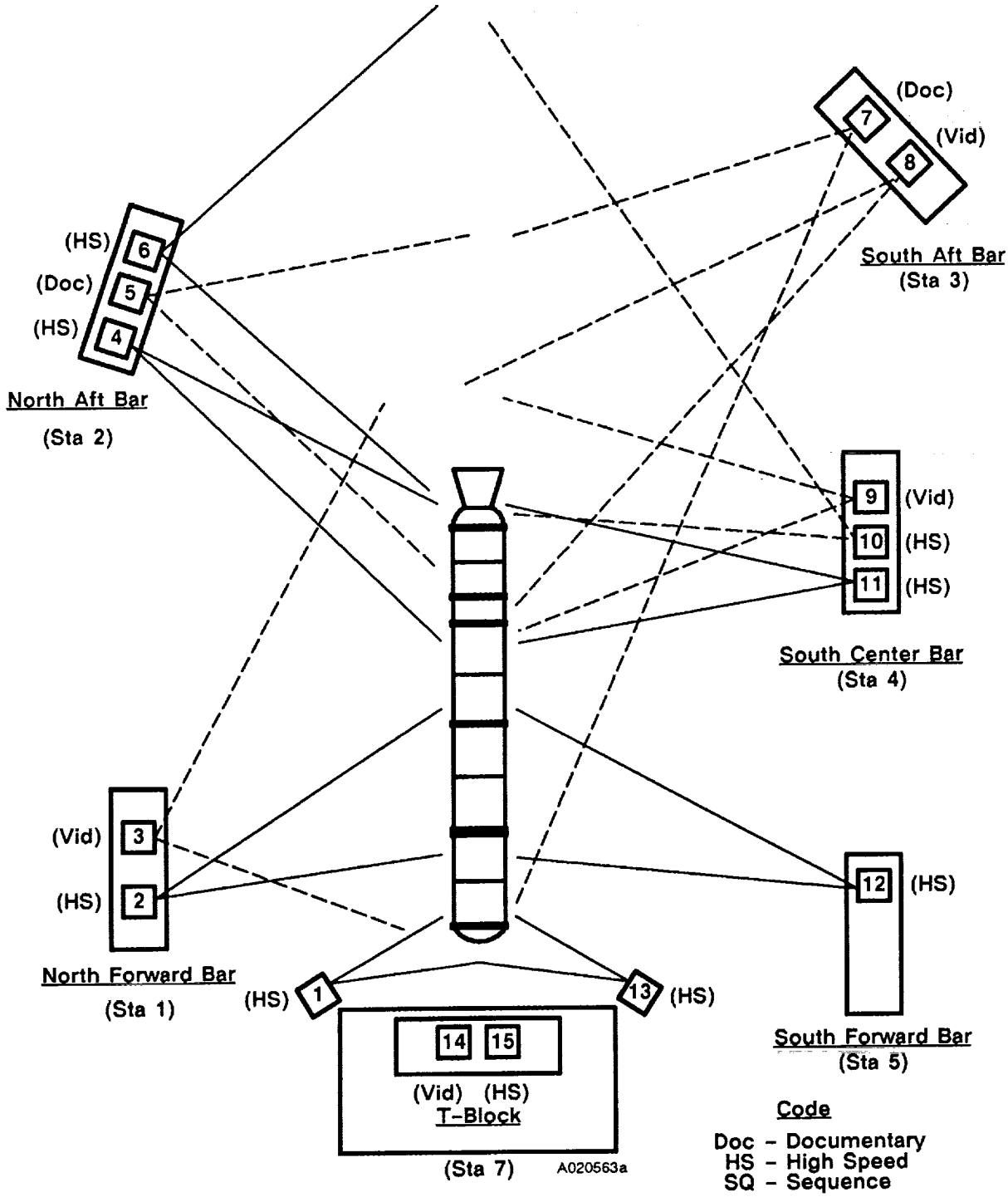

Figure 5-1. T-97 Photography Coverage—TEM-5

6

TEST RESULTS

6.1 CASE PERFORMANCE

6.1.1 Introduction

No anomalies associated with case or joint hardware occurred in the TEM-5 static test. All case hardware was recovered for use on the RSRM flight program. Assembly procedures proved adequate, and chamber pressure was contained. Remaining inspections include factory joint and internal nozzle joint demate and refurbishment. More information will become available as case refurbishment proceeds, and any anomalies will be documented according to refurbishment specification procedures.

6.1.2 Objectives

The objective from Section 2 regarding case performance was:

A. Recover case, nozzle, and igniter hardware for RSRM flight program.

6.1.3 Conclusions/Recommendations

All sealing surfaces were visually inspected and found to be in good condition with no evidence of damage, corrosion, or excess grease coverage. No apparent metal damage was found during the joint inspections.

All case hardware was recovered for use on the RSRM flight program.

A complete inspection will be performed as the segment undergoes refurbishment per STW7-2744, and any anomalies will be documented according to refurbishment specifications.

6.1.4 Results/Discussion

Case External Inspection--An external postfire walkaround was performed to assess the external condition of the case, field joints, and factory joints. No external case hot spots, sooting, gas paths, bubbles in the grease beads, or other anomalous conditions were found.

Forward Field Joint--There was no corrosion found on either the tang or clevis and no apparent metal damage was found on the clevis during the inspection. Several small scratches were found on the outside diameter (OD) of the tang. The grease on the O-ring and sealing areas was as prescribed in STW7-3688.

Center Field Joint--There was no corrosion found on either the tang or clevis. No apparent metal damage was found during the inspection. The grease on the O-ring and sealing areas was as prescribed in STW7-3688.

Aft Field Joint--The condition of the joint was nominal. There was no corrosion found on either the tang or clevis. Pinhole metal slivers were found at 52, 132, 146, 148, 206, and 336 deg. This is caused by installation of the pins at assembly. Otherwise, no apparent metal damage was found during the inspection. The grease on the O-ring and sealing areas was as prescribed in STW7-3688.

Case-to-Nozzle Joint--The sealing surfaces were visually inspected and no corrosion was observed on any of the joint areas and no metal damage was found on the sealing surfaces. Grease coverage on and around the joint sealing surfaces was excessive.

Igniter Inner and Outer Joints--The sealing surfaces were visually inspected and no corrosion was observed on any of the joint areas and no metal damage was found on the sealing surfaces.

6.2 CASE INTERNAL INSULATION PERFORMANCE

6.2.1 Introduction

The four TEM-5 segments had been insulated and cast with propellant at least 3 yr prior to TEM-5.

Field Joint Assembly--The case insulation of the three HPM-configuration field joints consisted of asbestos-silica filled NBR, as shown in Figure 6-1. Prior to mating, the joints were inspected per STW7-2831 Rev NC, the flight motor insulation criteria for the HPM joints. Putty was applied to the clevis joints per STW7-3746, as shown in Figure 6-2, and the joints were mated. After mate, each joint (Figure 6-3) was inspected from the bore for discontinuities and putty was tamped.

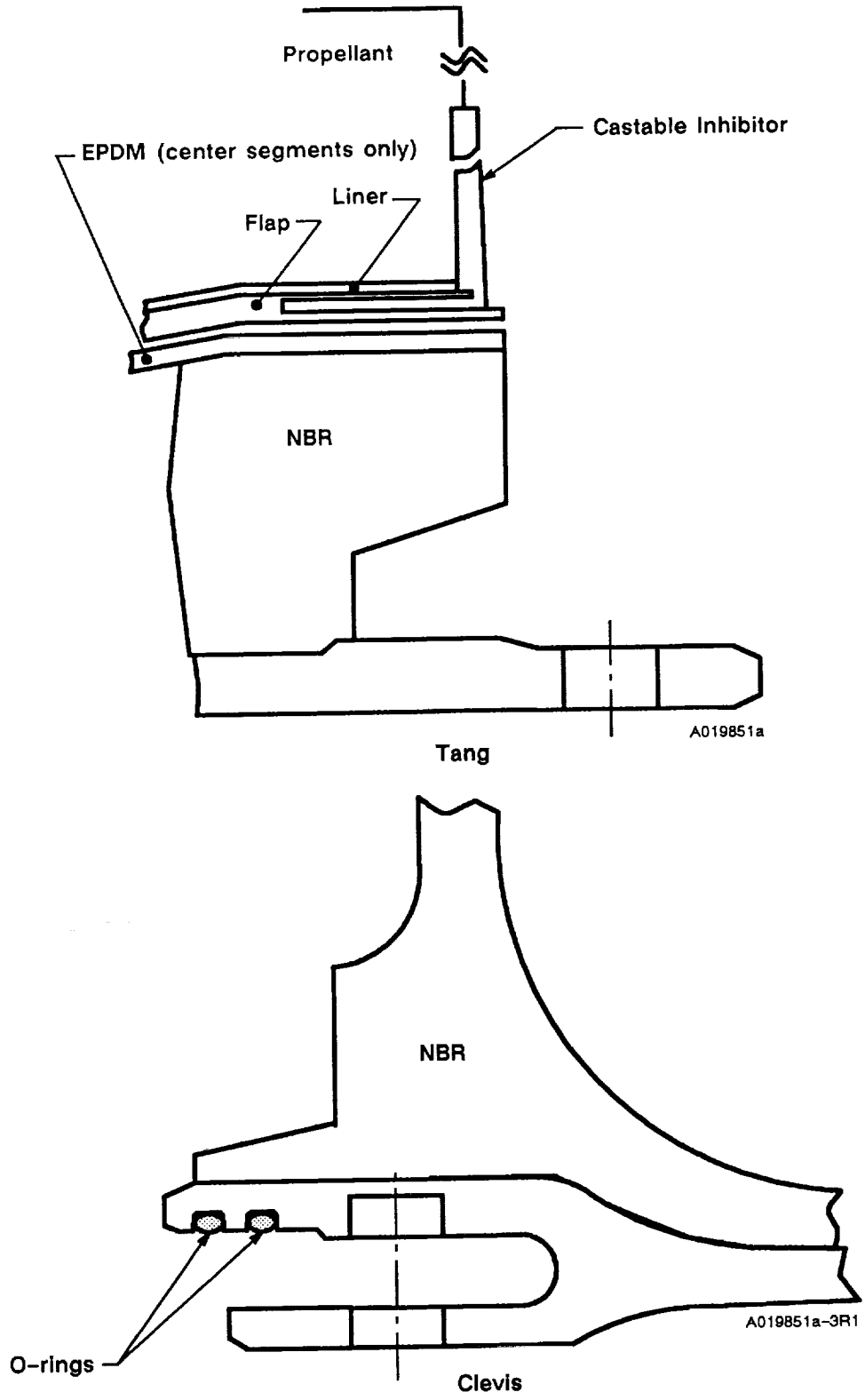

Figure 6-1. HPM Field Joint

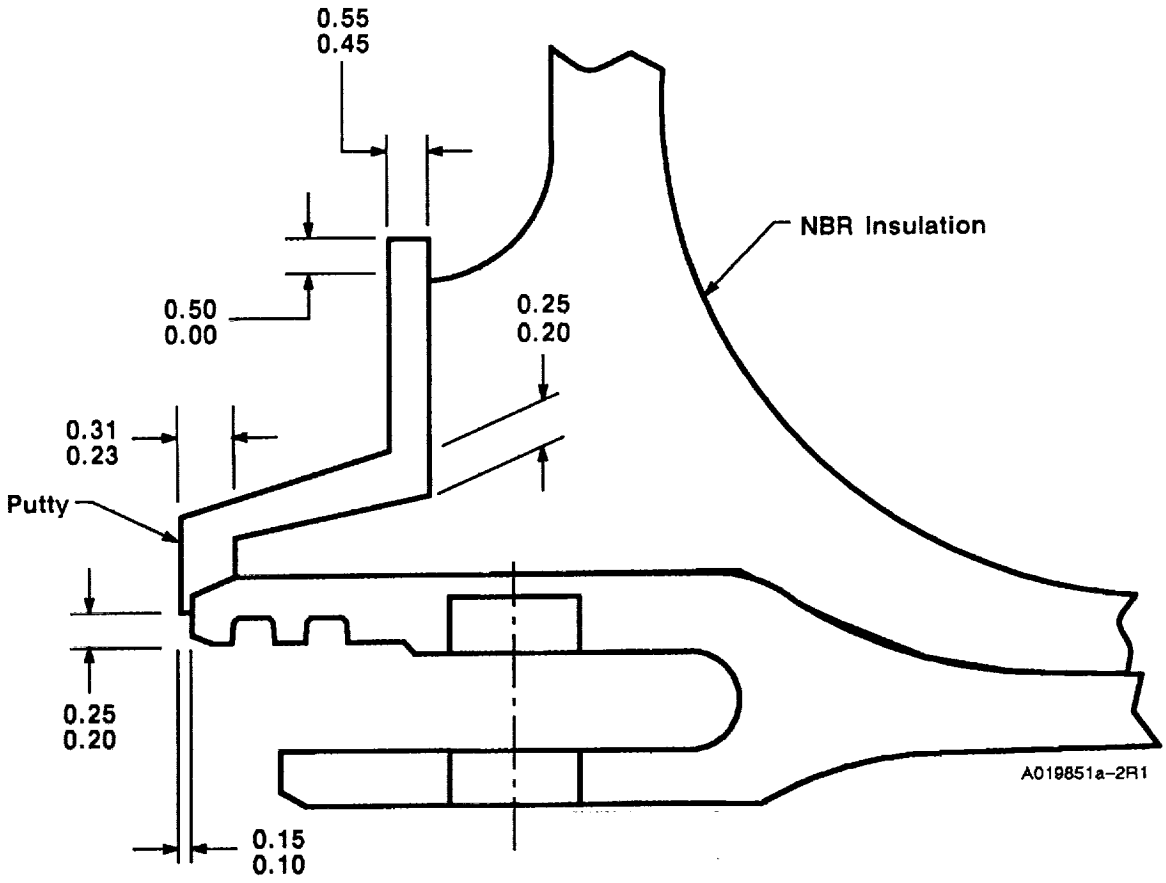

Figure 6-2. Clevis Joint Filler Putty Layup

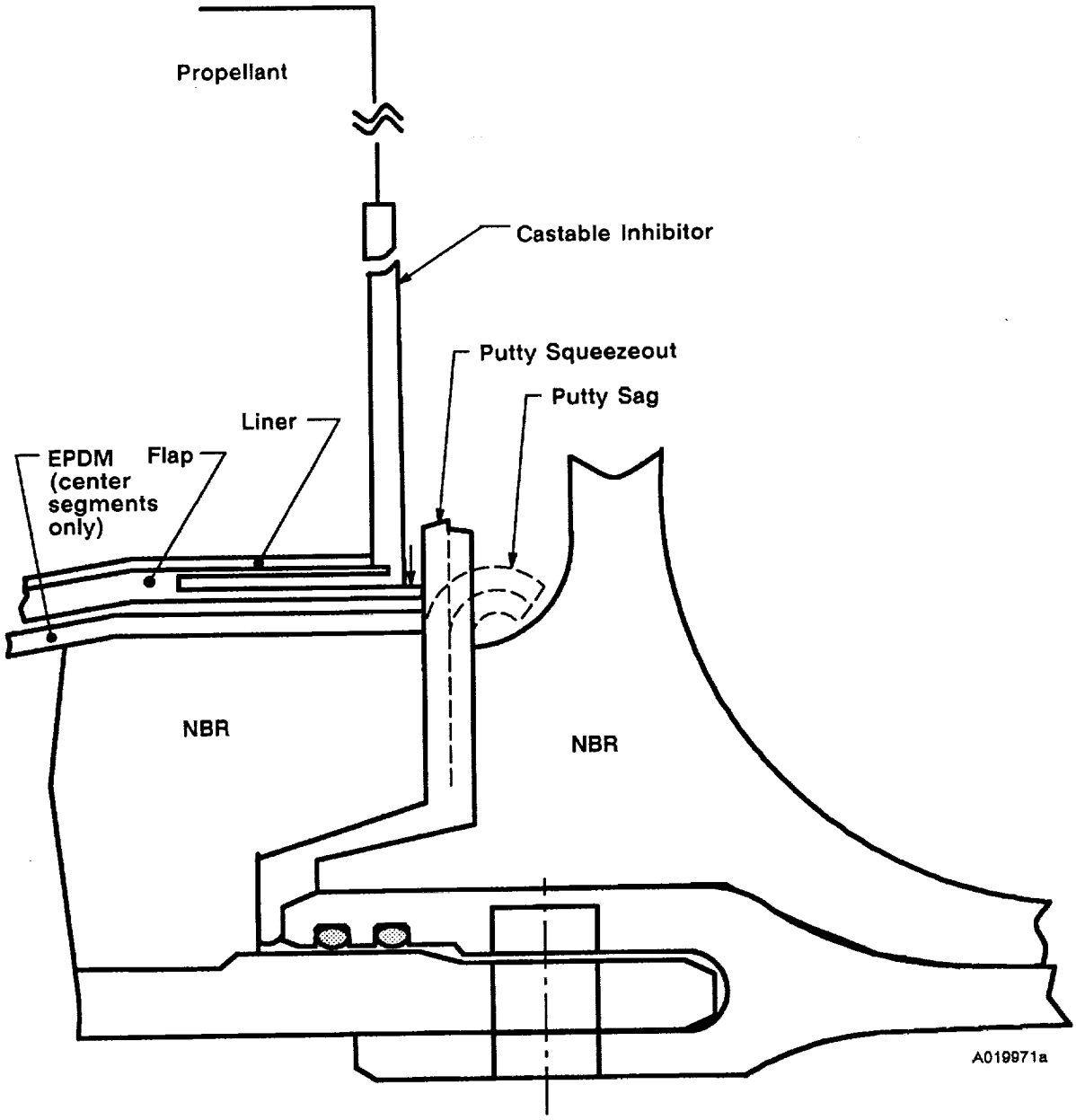

Figure 6-3. Assembled HPM Field Joint

Case-to-Nozzle Joint Assembly--The putty layup for the case-to-nozzle joint was performed to the pattern dimensions of STW7-3745, as were previous TEM motors (Figure 6-4). The amount of putty used was 28.99 lb, and this amount worked well with the new configuration joint assembly. The amount of putty used was within the lower and upper limits of 22 and 30 lb, which were established by the allowable putty dimensions. The TEM-5 nozzle was mated to the aft segment with no apparent anomalies. Because of inaccessibility, the case-to-nozzle joint was not inspected and tamped as were the field joints.

The case-to-nozzle joint incorporated four vent ports in the fixed housing (see Figure 1-3). The vent ports were left open during assembly to exhaust entrapped air from within the joint. This concept was designed to minimize O-ring damage from putty blowholes. Refer to Section 1.2.7 for additional information on the new case-to-nozzle joint design.

Prefire Inspection/Joint Putty Tamping--A prefire bore inspection was performed to assess the putty flow/layup of each field joint. The inspection occurred after the chocks were removed and the final leak check had been performed. This did not include the case-to-nozzle joint, which was inaccessible during this operation. The putty in the field joints was inspected for grease, discontinuities, bubbles, blowholes, etc.

Four to five small possible bubbles and two volcano areas (popped bubbles) were found in the forward field joint putty. Five to ten small possible bubbles, one large bubble, and one volcano were found in the center field joint. Four to six small possible bubbles were found in the aft field joint. All volcanos, bubbles, and possible bubbles were tamped closed with a putty tamping tool (2U132222-01). No grease contamination was found in any of the joint putty. The field joint putty condition was nominal. The overall prefire insulation condition of TEM-5 was similar to previous TEMs.

6.2.2 Objective

The test objective from Section 2 regarding insulation performance was:

B. Obtain additional data on the effect of 3-yr storage of loaded SRM case segments upon motor ignition and performance.

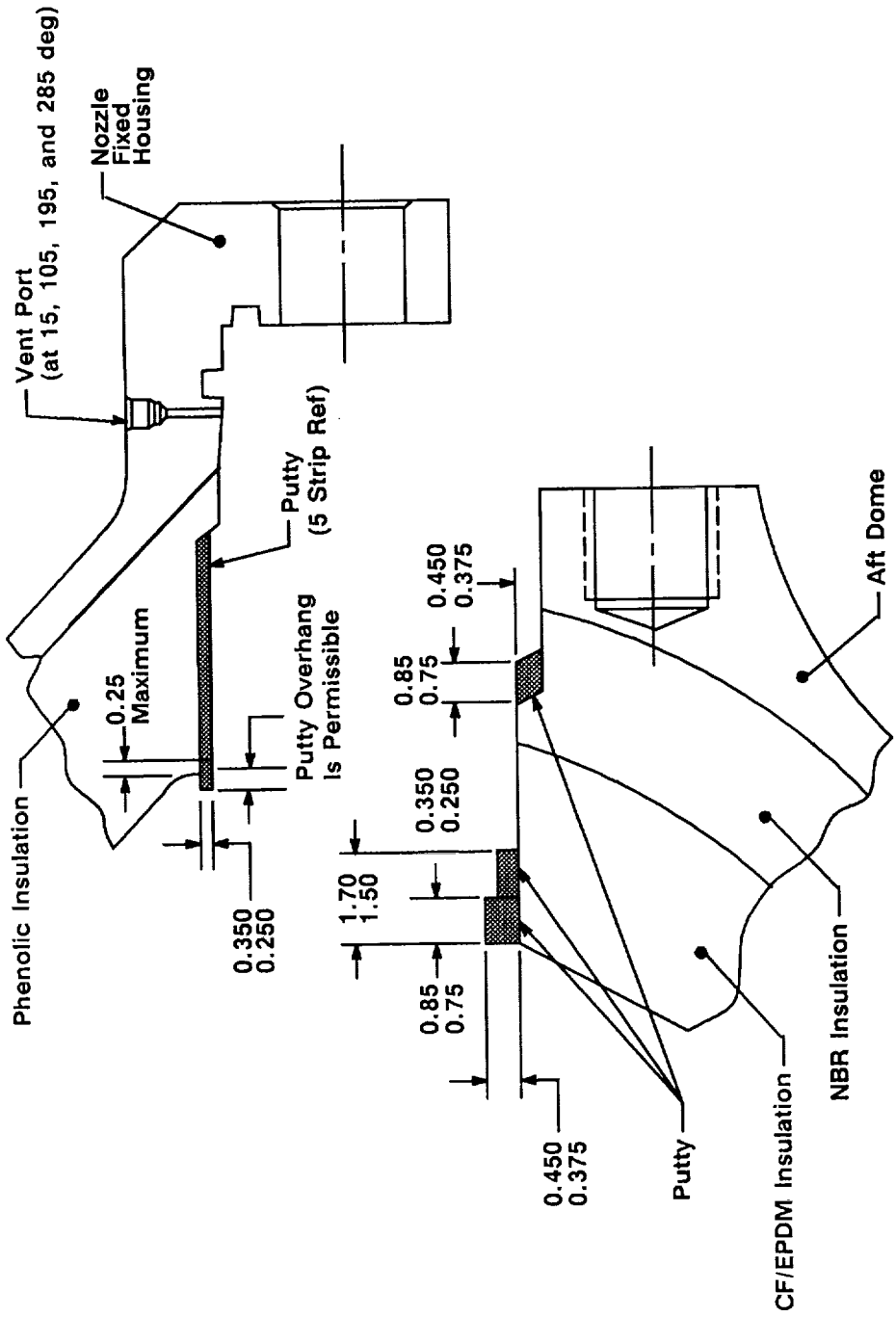

Figure 6-4. TEM-5 (HPM modified) Case-to-Nozzle Joint Configuration—Putty Layup

6.2.3 Conclusions/Recommendations

From an insulation standpoint, TEM-5 performed as expected. The performance of all three field joints and the case-to-nozzle joint was excellent; no gas penetration to the seals was observed. The joints functioned within the HPM experience. No adverse effects on the insulation performance was observed due to the 3-yr storage.

The fixed housing vent ports that were designed to minimize O-ring damage from putty blowholes were successful; no putty blowholes were detected, and no hot gas reached the primary O-ring. It is recommended that future TEM case-to-nozzle joints be assembled with the same putty layup configuration and fixed housing vent port design.

On TEM-5, an internal walkthrough insulation inspection and slag evaluation was performed before the disassembly of the aft field joint. Because all pertinent engineering data could have been obtained after the joint was disassembled, this inspection presented an unnecessary confined space hazard. On future static test motors, this inspection should occur after the disassembly of the aft field joint, as has been the case for previous RSRM and TEM static test motors.

6.2.4 Results/Discussion

Postfire Internal Insulation Inspection--A postfire internal walkthrough was performed to assess the postfire condition of the field joint and case-to-nozzle joint insulation and putty. Acreage insulation assessment and a slag evaluation were also performed. The inspection was accomplished before field joint disassembly. In the past, this inspection occurred after the aft field joint disassembly.

All field joint and case-to-nozzle joint insulation and putty appeared to be in normal condition during the postfire internal inspection. Joint insulation and putty were covered in soot and char and were not visible, as was expected. No evidence of gas penetration into any joint was observed at this time. Acreage insulation and NBR inhibitors showed normal charring and erosion.

The slag pool was approximately 54 in. wide, 2 to 3 in. deep, and extended the full length of the aft segment. A small amount of slag was present adjacent to the aft field joint in the aft center segment. Final slag weight in the aft segment was determined to be 2,195 lb, similar to most previous TEMs.

Forward Field Joint Insulation--The forward field joint insulation and putty were in good condition. The putty and NBR showed normal erosion and heat effects. No gas penetrated into the joint. The putty color was a consistent olive green and the putty had a moderate tack. Putty failure due to disassembly was mostly cohesive (85 percent) with areas of adhesive failure (15 percent) located on the tang. No tang or clevis insulation edge unbonds were detected. Clevis insulation flashing was found unbonded on the chamfer intermittently full circumference to a maximum depth of 0.150 inch.

Center Field Joint Insulation--The center field joint insulation and putty were in good condition. The putty and NBR showed normal erosion and heat effects. No gas penetrated into the joint. The putty exhibited cohesive failure with consistent olive green color and moderate tack. No edge unbonds were detected on the tang or clevis insulation bondline.

Aft Field Joint Insulation--The aft field joint insulation and putty were in good condition. The putty and NBR showed normal erosion and heat effects. No gas penetrated into the joint. The putty exhibited cohesive failure with consistent olive green color and good to moderate tack. Evaluation of the tang insulation bondline revealed four edge unbonds with a maximum depth of 0.100 inch. Prefire unbonds were documented in these locations. No growth occurred. No clevis edge unbonds were detected.

Case-to-Nozzle Joint Insulation--The nozzle boss NBR insulation was in good condition with a normal char- and heat-affected layer. The nozzle boss insulation bondline was also in good condition. No edge unbonds were detected.

Overall appearance of the case-to-nozzle joint putty was excellent, no gas penetration or blowholes were observed. The excellent condition of the putty was attributed to the new joint assembly procedure which used four vent ports to evacuate entrapped air. The putty that remained in the joint had an approximately 95 percent cohesive failure during disassembly. The putty had a consistent olive green color and moderate tack. Small void appearances were present at 70.4, 169.2, 225, 270, and 326 deg, adjacent to the O-ring groove, down to the fixed housing metal surface. No evidence of sooting or gas penetration was found within these possible voids; however, grease was found within and surrounding the possible voids.

It was determined that the voids were putty adhesive disassembly failures, caused by grease contamination. Grease was also found on the putty intermittently around the joint circumference.

Igniter Outer Joint Insulation--The igniter adapter-to-forward dome (outer) joint disassembly and inspection revealed that a blowhole occurred in the putty at approximately 335 deg.

Igniter Inner Joint Insulation--The igniter adapter-to-igniter chamber (inner) joint disassembly and inspection revealed that putty was in contact with the metal retainer of the inner gasket. No blowholes were found.

6.3 SEALS/LEAK CHECK PERFORMANCE

6.3.1 Introduction

Leak Check--After each pressure vessel joint is assembled, a leak test is performed to determine the integrity of the seals. The leak tests usually consist of a joint volume determination and a pressure decay test. The volume and pressure information is combined with temperature and time data, collected during the test, and used in the calculation of a leak rate, which is expressed in terms of standard cubic centimeters per second (sccs). Each leak test has a maximum leak rate allowed.

Some specifications require only a maximum pressure decay over time. This method has been determined as sufficient based on the small, constant volumes, and the equivalent leak rates, which are conservative when using all worst-case variables.

Table 6-1 lists all joints tested for TEM-5, the leak test specification, and the equipment used to test the joints. The case factory and nozzle internal joints were tested after the original assembly. This report does not discuss the results of those tests.

Seals--The three field joints used 1U75150-11 O-rings. The case-to-nozzle joint used a 1U75801-15 RSRM primary O-ring, and 1U75801-16 RSRM secondary O-ring. All internal nozzle joints, except the forward-to-aft exit cone, and all factory joints were assembled prior to 51-L. RSRM O-rings were used for the forward-to-aft exit cone.

The 180 ksi bolts (A-286) used on both the igniter adapter-to-igniter chamber (inner) and the igniter adapter-to-forward dome (outer) joints were torqued to 275 to 295 ft (65 to 135 ksi stress).

Table 6-1. Seal Leak Testing

Joint	Specification	Equipment
Case Field Joints	STW7-3682	8U75902
Case-to-Nozzle Joint	STW7-3682	2U129714
Ignition System		
Inner gasket	STW7-2787	2U129714
Outer gasket	STW7-2632	2U129714
Special bolt installation	STW7-2632	2U129714
S&A joint	STW7-3633	8U76500
Transducer assembly	STW7-2853	2U65686
Barrier-booster	STW7-2913	2U65848

New configuration igniter inner (1U51926-02) and outer (1U51927-02) joint gaskets were installed. The configuration change consisted of an inspection change, not a design change. The inspection was performed under STW7-2790 Rev D, and included a plexiglass compression inspection and a finger inspection.

The part and serial numbers of the S&A and B-B used were: S&A: P/N 1U52295-04, S/N 0000016; B-B: P/N 1U52293-03, S/N 0000053 R2. Krytox grease was applied to the S&A B-B shaft O-rings.

6.3.2 Objectives

The test objectives from Section 2 regarding seals/leak check were:

E. Obtain additional breakaway and removal torque data for the leak check port plug Nylok® thread locking device.

G. Obtain additional data on the performance of Krytox grease on the B-B shaft O-ring.

6.3.3 Conclusions/Recommendations

6.3.3.1 Leak Check. The leak tests performed on TEM-5 were not required to satisfy the objectives of the test plan. These tests were performed to verify that

the joints were properly assembled and that the O-rings would perform properly. As discussed in the following section, it was concluded the seals were acceptable for the TEM-5 joints.

Additional data were collected on the leak check port plug Nylok thread locking device. The device was installed on the field joint leak check port plugs. Torque values were within the limits defined in NAS 1283 and MIL-F-18240. Torque values will be used in an evaluation on the holding power of Nylon.

6.3.3.2 Seals. The performance of the TEM-5 seals was nominal. Future TEM motors should incorporate the same seal configuration as TEM-5.

Field Joint Seals--The condition of the seals of each field joint was nominal.

Case-to-Nozzle Joint Seals--The condition of the seals in the case-to-nozzle joint was nominal, and improved in comparison with previous TEMs due to the new vented assembly process.

Internal Nozzle Joint Seals--Disassembly/inspection of the internal joints revealed no anomalous conditions.

Igniter Joint Seals--No anomalous conditions were found on any of the igniter inner or outer joint seals. However, putty was in contact with the inner groove of the inner primary seal of the igniter inner gasket; this condition had not occurred on any previous static test motor or flight RSRM.

Ignition System Seals--The performance of the S&A B-B rotor shaft O-rings with Krytox grease was nominal.

Inspection of the S&A-to-igniter adapter joint and gasket revealed no anomalous conditions. Inspection of the SIIs, O-rings, and ports revealed no indication of soot to or blowby past the primary O-rings. Deformations were found in the sealing washer of both SIIs; this condition has been seen on previous SIIs.

Because the S&A SII sealing washer welds caused degradation (galling) on the land between the primary and secondary seal surfaces of both SII ports, it is recommended that refurbishment criteria be established on the land of the SII ports.

6.3.4 Results/Discussion

6.3.4.1 Leak Check. **Field Joints**--The case field joint leak test results are shown in Table 6-2. The TEM field joints were tested at lower pressures (185 psig) than RSRM field joints (1,000 psig) because of the HPM configuration. These joints were tested with and without the assembly stands in place. This was done since previous HPM motors showed the potential for leaking after the stands were removed. The results of the leak tests for the field joints were nominal.

Table 6-2. Case Field Joint Leak Test Results

Pressure (psig)	Maximum Leak Rate (sccs)	Actual Leak Rates (sccs), Prechock/Postchock		
		Forward	Center	Aft
185	0.072	0.0150/0.0124	0.0150/0.0099	0.0133/0.0123
30	0.0082	0.0006/-0.0001	0.0006/-0.0014	0.0004/-0.0005

The field tests were performed with a variation of the 8U75902 ground support equipment leak test system. For testing of the TEMs, the equipment was modified to include a pressure relief valve to preclude the possibility of over-pressurizing the joint.

Breakaway and removal torque levels of the leak check port plug Nylok® thread locking device are listed in Table 6-3. The thread locking device was installed on the field joint leak check port plugs. Torque values were within the limits defined in NAS 1283 and MIL-F-18240. Torque values will be used in an evaluation on the holding power of Nylon. Surfaces of the port plugs and port holes were covered with a light coat of grease.

Ignition System--The ignition system leak test results are shown in Table 6-4. The tests were performed with the new leak test equipment (as shown in Table 6-1). The equipment was identical to that used to test most of the RSRM joints. All results were within the limits.

The adapter plate of the igniter was of flight configuration and could not be used for a static test motor. Consequently, it was necessary to replace the adapter with one having a quench port. Because of this, the inner joint of the igniter was retested. Differing from previous TEMs, this test was performed to the RSRM leak

test requirements, which test the inner igniter seal at 1,000 and 30 psig and allow a maximum leak rate of 0.1 and 0.0082 sccs, respectively. The 2U129714 equipment was used to test the TEM-5 inner and outer igniter joints. This is the new equipment used to test all RSRM and TEM inner and outer joints starting with Flight 360L006A.

Table 6-3. Breakaway and Removal Torque Data for the Leak Check Port Plug Nylok® Thread Locking Device

Joint	Breakaway Torque (in.-lb)	Removal Torque (in.-lb)
Forward Field Joint	70	40
Center Field Joint	85	35
Aft Field Joint	75	30

Table 6-4. Igniter and S&A Leak Test Results

Joint Seal	Allowable Leak Rate (sccs), High/Low*	Actual Leak Rate (sccs), High/Low
Inner	0.10/0.0082	0.0033/0.0001
Outer	0.10/0.0082	0.0029/-0.0003
Transducer Installation	0.10/0.0082	0.0023/-0.0001
OPT**	10 psi/10 min/ 1 psi/10 min	3.0/0.0 3.0/0.0 2.0/0.0 4.0/0.0
B-B	1 psi/10 min	0.0
S&A	0.10/0.0082	0.0000/0.0003

*High = 1,000 psig, Low = 30 psig
**OPTs tested at 1,024 psig and 30 psig, leak rate units are psi/10 min

Case-to-Nozzle Joint--Table 6-5 lists the results of the case-to-nozzle joint leak test. This joint was tested at a maximum pressure of 185 psig. This differed from the RSRM case-to-nozzle joint leak tests which are performed at 920 psig. The

TEM-5 case-to-nozzle leak test was performed after the first torque sequence, when the axial bolts are torqued to 25 ft-lb. This procedure prevented the occurrence of a metal-to-metal seal between the fixed housing and the aft dome when the axial bolts were fully torqued. All leak test results were within the allowable limits.

Table 6-5. Case-to-Nozzle Leak Test Results

Pressure (psig)	Allowable Leak Rate (sccs)	Actual Leak Rate (sccs)
185	0.072	0.0141
30	0.0082	0.0003

The 2U129714 equipment was used to test the TEM-5 case-to-nozzle joint. This is the new equipment used to test all RSRM case-to-nozzle joints starting with Flight 360L006A.

6.3.4.2 Seals. **Forward Field Joint Seals**--The condition of the joint was nominal. No hot gas or soot was observed past the putty. There was no evidence of damage to the O-rings while in the groove. The grease on the O-rings and sealing areas was as prescribed in STW7-3688. No contamination was noted in the grease or seal areas which could be assessed as being introduced during assembly.

Center Field Joint Seals--The condition of the joint was nominal. No hot gas or soot was observed past the putty. There was no evidence of damage to the O-rings while in the groove. The grease on the O-rings and sealing areas was as prescribed in STW7-3688. No contamination was noted in the grease or seal areas which could be assessed as being introduced during assembly.

Aft Field Joint Seals--The condition of the joint was nominal. No hot gas or soot was observed past the putty. No soot or pressure reached the primary O-ring. The primary O-ring was damaged during joint separation at 198 deg. No damage was found on the secondary O-ring while in the groove. The grease on the O-rings and sealing areas was as prescribed in STW7-3688.

Case-to-Nozzle Joint Seals--No blowholes or evidence of gas paths were observed in the putty. The putty was in contact with the primary O-ring almost the full circumference of the joint. The putty was not across the O-ring or in the

O-ring groove. Heavy grease was observed on the primary and secondary O-rings and on the land between the O-ring grooves. Heavy grease was observed in the voids previously noted at 225 and 270 deg. A heavy grease build-up was noted on the associated aft dome surface at 270 deg. The sealing surfaces were visually inspected and found to be in good condition with no evidence of damage or corrosion. Inspec- tion revealed no erosion, heat effects, or damage on the O-rings.

A pressure transducer (data channel PNNAR001, plot included in the appendix) was installed in the leak check port of the case-to-nozzle joint to monitor pressure between the O-rings. During the TEM-5 motor fire, the case-to-nozzle joint expanded while the O-rings continued to seal. The increased volume between the O-rings resulted in a pressure decrease of 4 psi. The pressure decrease between the O-rings was also verified by analysis (Appendix D, TEM-5 Case-to-Nozzle Joint Pressure Measurement Analysis). The excellent condition of the joint putty and the performance of the seals was attributed to the new joint assembly procedure which used four vent ports to evacuate entrapped air. Refer to Sections 1.2.7, 4.4, and 6.2 for additional information about the case-to-nozzle assembly and results.

Internal Nozzle Joint Seals--Disassembly/inspection of the aft exit cone-to-forward exit cone joint revealed no pressure paths through the room temperature vulcanization (RTV) backfill. RTV was in contact with the primary O-ring intermittently throughout the circumference of the joint. No RTV was found past or on the sealing area of the primary O-ring. The sealing surfaces were in good condition with no evidence of damage, corrosion, or excess grease coverage. Preliminary assessment revealed no erosion, heat effects, or damage to the O-rings.

The overall condition of the remaining internal nozzle joints was nominal. On the forward end ring-to-nose joint, soot traveled between the EA 913 adhesive layer and the RTV layer interface and was deposited intermittently on the metal surface; however, no soot reached the primary O-ring. There were no RTV pressure paths on any other joint.

RTV was observed over and past the primary O-ring, and up to but not past the secondary O-ring, around the full circumference of the forward exit cone-to-throat joint, and intermittently on the nose inlet-to-throat joint. There was no RTV past the primary O-ring on any of the other joints. Inspection of the O-rings at the time

of each disassembly revealed no anomalous conditions except for some disassembly damage to the primary O-ring in the aft end ring-to-fixed housing joint.

The grease application on each O-ring and groove was very heavy, which was expected for the HPM design. The sealing surfaces and metal nonsealing surfaces were visually inspected and found to be in good condition with no evidence of damage or corrosion.

Special Bolt Seals--Inspection of the three special bolts (for the chamber pressure and oscillation pressure transducers) revealed no anomalous conditions to the bolts or seals (packing with retainers). Typical soot was found on the tips of each special bolt.

Igniter Outer Joint Seals--The igniter adapter-to-forward dome (outer) joint disassembly and inspection revealed no anomalous conditions associated with the outer gasket seals. A blowhole occurred in the outer joint putty at approximately 335 deg. Heavy soot was found on the aft face of the gasket from 95 to 265 deg. Soot was found up to, but not past, the primary seal.

Igniter Inner Joint Seals--The igniter adapter-to-igniter chamber (inner) joint disassembly and inspection revealed that putty was in contact with the metal retainer of the inner gasket. Putty was in contact with the inner groove of the inner primary seal (Figure 6-5). This condition had not occurred on any previous static test motor or flight RSRM. Putty was observed up to the seal crown aft face from 130 to 345 deg, and up to the seal crown forward face from 190 to 340 deg. No putty was found past the seal crown. No anomalous conditions were associated with the inner gasket seals. No blowholes or any evidence of pressure to the inner primary seal were found.

S&A Removal--Inspection of the S&A-to-igniter adapter joint and gasket revealed no anomalous conditions. Typical soot was found on the inside diameter (ID) of the gasket. The forward face of the gasket had soot half way to the primary seal across the full circumference. The aft face of the gasket had soot up to the primary seal across the full circumference. No damage to the gasket seals or the S&A sealing surfaces was found. Refer to Section 6.5.4 for information about the S&A disassembly.

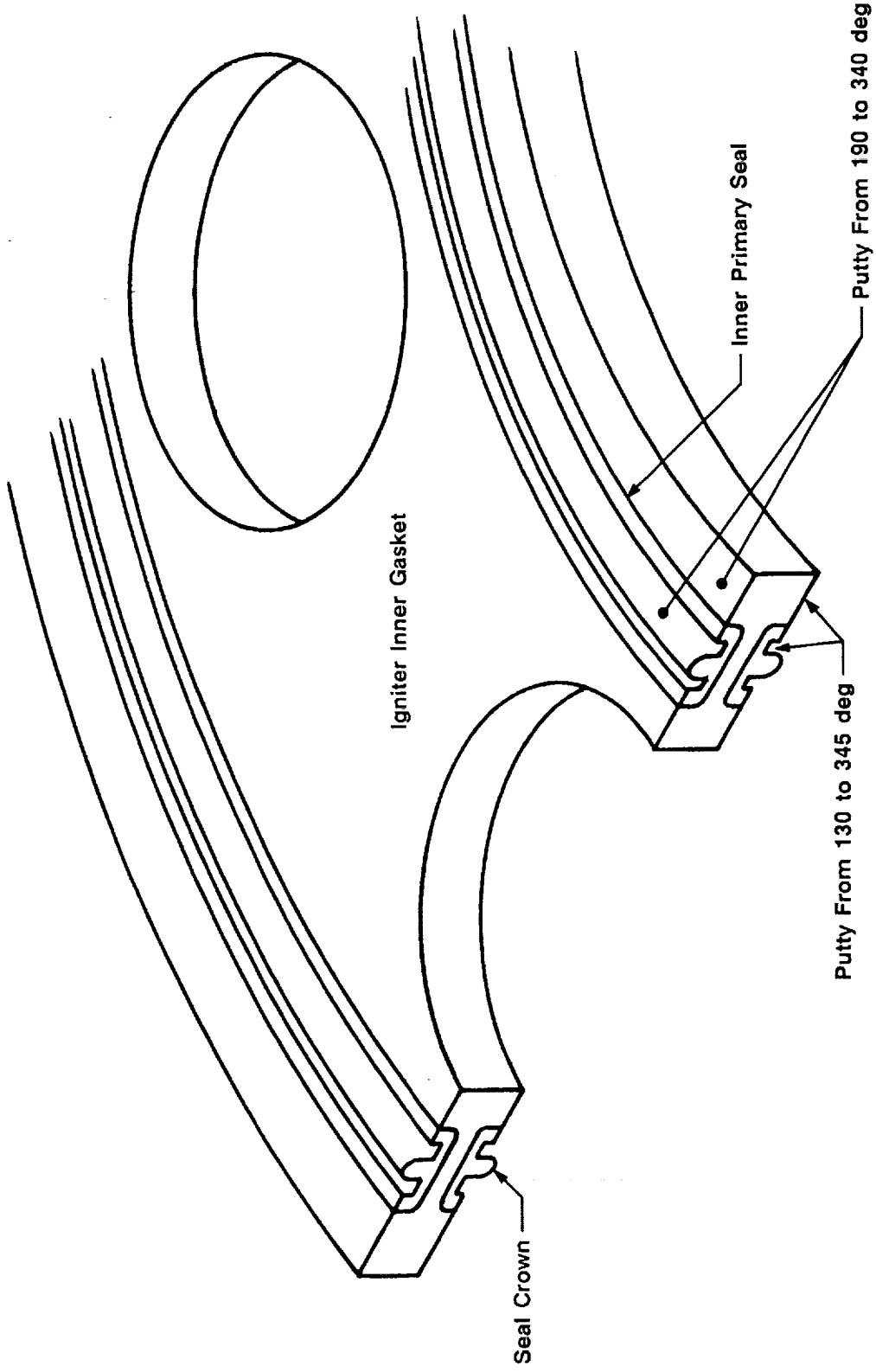

Figure 6-5. Location of Putty on TEM-5 Igniter Inner Joint Gasket

6.4 NOZZLE ASSEMBLY PERFORMANCE

6.4.1 Introduction

The TEM-5 nozzle assembly was a HPM-configured, partially-submerged, convergent/divergent movable design with an aft pivot point flexible bearing (see Figure 1-5). The nozzle incorporated the following features:

a. HPM forward exit cone

b. HPM fixed housing

c. HPM outer boot ring (OBR)

d. HPM cowl ring

e. HPM nose inlet assembly

f. HPM throat assembly

g. HPM aft exit cone assembly

h. RTV backfill in Joint No. 1

i. EA 913 (with asbestos) and EA 946 adhesives

j. Nozzle did not incorporate a nozzle plug

k. Nozzle was fixed linked (not vectored)

l. Four RSRM-type vent ports were machined into the nozzle fixed housing, forward of the primary O-ring. These vent ports were to facilitate venting of the cavity between the joint putty and the primary O-ring during the case-to-nozzle joint assembly.

m. The case-to-nozzle joint was assembled with RSRM axial bolts which had preload measuring capability. The assembly preload was a nominal 120,000 lb.

6.4.2 Objectives

The test objectives from Section 2 regarding nozzle performance were:

A. Recover case, nozzle, and igniter hardware for RSRM flight and static test programs.

H. Obtain additional data on nozzle axial deflection during motor pressurization.

6.4.3 Conclusions/Recommendations

The overall appearance of the TEM-5 nozzle phenolics was nominal, with no abnormal erosion characteristics observed.

Nozzle hardware will be dissembled and refurbished for use on the RSRM flight and static test programs.

Additional data on nozzle axial deflection during motor pressurization was obtained from four extensometers. Refer to Section 6.4.4.9 for additional information on nozzle axial deflection.

6.4.4 Results/Discussion

6.4.4.1 Nozzle. Overall erosion of the TEM-5 forward nozzle assembly and aft exit cone carbon-cloth phenolic (CCP) ablative liner was smooth and uniform.

6.4.4.2 Aft Exit Cone Assembly. The TEM-5 aft exit cone liner erosion appeared smooth and uniform. There were no wash areas, or surface ply lifting observed. There was a separation between charred carbon and virgin carbon on aft end of the aft exit cone 360 deg. A cohesive separation within the glass-cloth phenolic (GCP) was observed on the aft end of the aft exit cone centered at 45 deg and measured 14 in. circumferentially. The protective cork on the outside of the aft exit cone was in excellent condition, with small areas of unbonded cork and paint blistering. The aft 1 in. of the aft exit cone cork was charred 360 deg.

6.4.4.3 Forward Exit Cone Assembly. The TEM-5 forward exit cone liner erosion was nominal showing no major washing or pocketing, typical of the first four TEMs fired. Visual inspection of the forward exit cone showed a typical dimpled erosion pattern located circumferentially over the middle to aft end of the exit cone with a maximum radial depth of approximately 0.050 in.

6.4.4.4 Throat Assembly. Erosion of the throat and throat-inlet rings was smooth and uniform, and appeared typical of past motors. The throat postfired mean diameter was 56.121 in. (erosion rate of 9.21 mil/sec based on an action time of 122.7 sec). Nozzle postburn throat diameters have ranged from 55.787 to 56.380. This erosion is within the historical database. The throat ring showed typical rippled erosion near the center and was approximately 0.020 to 0.050 in. deep.

The throat/throat-inlet phenolics will be sectioned to establish char and erosion profiles for future reference and comparison to standard profiles.

6.4.4.5 Nose-Inlet Assembly. The forward nose ring eroded smoothly and flat along the 4 in. (expected due to the ply angle). Intermittent wash areas were found on the forward 3 in. approximately 0.25 in. deep on the aft inlet ring. The forward edge of the forward nose ring was raised above the nose cap 0.10 in. (postburn occurrence). Numerous minor wash areas were found along the length of the nose cap approximately 0.050 in. deep. Typical postburn popups and wedgeouts of the charred CCP were noted on the aft end of the nose cap. This has been noted on all previous post-test and postflight nozzles.

6.4.4.6 Cowl Ring. The cowl ring had typical erratic erosion with minor wash areas along the aft 4 in. extending onto the forward end of the OBR. Typical postburn popups and wedgeouts of charred CCP were noted on the aft end of the cowl ring. All cowl vent holes appeared to be plugged with slag on the OD of the ring. Typical postburn axial surface cracks between plug and vent hole locations were observed around the circumference. Cracked surfaces did not show any signs of erosion.

6.4.4.7 OBR. The OBR was intact and eroded smoothly and uniformly. Charred CCP material on the aft tip adjacent to the flex boot fractured and wedged out. The fractured edges of the OBR aft end were sharp and showed no signs of slag deposits. This indicates that the aft tip fractured off after motor operations. This is a typical observation found on post-test and postflight nozzles.

6.4.4.8 Fixed Housing Insulation. The fixed housing insulation erosion was smooth and uniform. Typical postburn fractures were found on the forward 2 in. intermittently around the circumference. No slag deposits were observed on the aft end of the CCP insulation around most of the circumference. No wedgeouts or popped-up material was observed.

6.4.4.9 Extensometers. Four extensometers were mounted in the axial direction between the nozzle fixed housing and the forward exit cone. The four extensometers were mounted around the nozzle 90 deg apart, starting at 0 deg.

The plots for extensometer data channels DANAU001 and DANAU003 (included in the appendix) present the data from the extensometers located at 0 deg and 180 deg, respectively (pitch plane). Analysis has shown that a vector angle of less

than 2 deg in the yaw plane has a negligible effect on the extensometer readings in the pitch plane. Since the vector angle of a fixed nozzle TEM is expected to be less than 2 deg, the pitch plane extensometers will give a direct reading for axial deflection. Therefore, the maximum axial deflection is -0.77 in. (forward direction) and occurs at T+124 sec, as shown in the plot for data channel DANAU003. The forward deflection was a result of the remaining boot cavity pressure.

The extensometer data at 90 and 270 deg (yaw plane) are shown in the plots for data channels DANAU002 and DANAU004, respectively. At T+124 sec, the maximum deflection measured by the extensometer at 90 deg was -0.193 in., while the extensometer at 270 deg measured a maximum deflection of -1.40 inches. These deflections indicate vectoring in the yaw plane due to flex bearing compression. The maximum vector angle at T+124 sec was calculated from the axial extensometer data in the yaw plane in conjunction with the pitch plane data and yielded a maximum vector angle of 0.81 deg.

6.5 IGNITION SYSTEM PERFORMANCE

6.5.1 Introduction

The SRM ignition system consisted of a modified HPM igniter assembly containing a single nozzle, steel chamber, external and internal insulation, and a solid propellant igniter containing a case-bonded 40-point star grain (see Figures 1-6 and 1-7). The ignition system was modified with a CO_2 quench port.

A S&A device using Krytox grease to lubricate the B-B shaft O-rings was installed on the igniter (see Figure 1-8).

6.5.2 Objectives

The objectives from Section 2 regarding the ignition system were:

A. Recover case, nozzle, and igniter hardware for RSRM flight and static test programs.

G. Obtain additional data on the performance of Krytox grease on the B-B shaft O-rings.

6.5.3 Conclusions/Recommendations

The TEM-5 igniter hardware will be recovered for use on the SRM static test program.

Performance of the Krytox grease on the B-B shaft O-rings was nominal. S&A cycle times were within the engineering requirements (Table 6-6). All cycles were below 0.730 sec at 21.9 Vdc during checkout. Current engineering requirements are 2.0 sec or less at 24 Vdc.

Table 6-6. Historical Data on S&A Cycle Times

Test Article	Off Motor Test Safe to Arm (sec)	On Motor Test Safe to Arm (sec)	Firing Safe to Arm (sec)	Off Motor Test Voltage to Arm (V)
QM-7	0.60			
PVM-1	0.73	0.79		
QM-8		0.90		
TEM-1	0.79	0.68		
TEM-2	0.67	0.65	0.66	
TEM-3	0.60	0.70	0.70	30.5
TEM-4	0.67	Test No. 1: 0.64 Test No. 2: 0.65	0.66	28.5
TEM-5	0.50	0.60	0.60	31.0

6.5.4 Results/Discussion

S&A Disassembly--Inspection of the SIIs, O-rings, and ports revealed no indication of soot to or blowby past the primary O-rings. Deformations were found in the sealing washer of both SIIs; this condition has been seen on previous SIIs.

The SII sealing washer welds caused degradation (galling) on the land between the primary and secondary seal surfaces of both SII ports. This condition has been seen before. The galled land was acceptable per the B-B refurbishment specification, STW7-3133, because the depth did not exceed 0.020 inch.

A visible radial scratch, similar to those found on sixth and seventh flight S&As, was found across the bottom of the 18-deg SII port secondary O-ring groove seal surface. The scratch could not be felt with a 5-mil shim and was acceptable per STW7-3133.

Light circumferential galling was found on the shoulder seal surface of both the B-B housing bore (126 deg) and S&A flange (306 deg) leak check plugs.

Inspection of the rotor shaft, housing bore, and rotor shaft O-rings showed soot to the first primary O-ring but no indication of blowby. There were no scratches found on the seal surfaces of the housing bore or rotor shaft O-ring grooves. No damage was found on the O-rings.

Igniter--Ballistics data and igniter disassembly showed that the igniter performed within the specified requirements.

6.6 JPS PERFORMANCE

6.6.1 Introduction

6.6.1.1 FJPS. Each of the three TEM-5 field joints were protected by a different JPS configuration. The aft field joint was protected by the typical TEM JPS, consisting primarily of cork bands held in place with straps (see Figure 1-9). Two redesigned FJPS configurations were installed on the center and forward field joints.

The FJPS is being redesigned to reduce installation timelines at KSC and to simplify or eliminate installation processing problems related to the present design of an EPDM moisture seal/extruded cork combination. Both FJPS redesign configurations eliminate the vent valves, the vacuum bagging process, and the need for a separate moisture seal. Both configurations use a single Kevlar® strap to hold the heater in place, as compared to the moisture seal/Kevlar® strap method of the current configuration. Previous development installations of both FJPS redesign concepts have been performed under ETP-0600 and ETP-0620, as reported in TWR-50138 and TWR-50290, respectively.

The two redesign configurations were installed on TEM-5 to develop and compare the installation procedures, identify problems, and to subject the designs to a full-scale, full-duration test firing.

Concept 1 FJPS--The Concept 1 configuration of the redesigned FJPS was installed on the center field joint (see Figure 1-10). This configuration used two cork bands with K5NA ablation compound (STW5-3183) applied between them and to the bottom edge of the aft cork band. The cork bands were bonded over the joint pin retainer band area and over the joint temperature sensor area. The aft cork band was machined to fit against the pin retainer band (nominal tolerance). The cork bands were bonded to the case with EA 934NA adhesive (STW4-3218).

The aft cork band was machined from 0.75-in.-thick sheet cork. The design specified 0.625-in.-thick cork, but this thickness was not available to support the test.

Teflon® tape was installed at the tang-to-clevis interface to provide stress relief for the FJPS from the 30-mil joint axial movement due to pin slop during the motor fire. Teflon® tape was also installed on the thermal barrier at the interface with the heater retention strap. The tape reduced the friction between the heater retention strap and thermal barrier during assembly, and ensured that a uniform radial force was applied to the heater.

The 1U82837-03 configuration Kevlar® strap that was installed for heater retention was the same type of strap that is used with the current FJPS design. The Concept 1 FJPS was designed to use a 1U77114-01 configuration Kevlar® strap which has a stainless steel coupling to eliminate strap contact with the vent port plug. The new configuration strap was not available, but its use on TEM-5 was not necessary because HPM field joints do not have a vent port plug.

Concept 1C FJPS--The concept 1C FJPS was installed on the forward field joint (see Figure 1-11). This configuration consisted of two cork bands with K5NA applied between them. The aft cork band location extended from the outer clevis leg transition area to just aft of the pin retainer band. The forward cork band was located over the joint temperature sensor. EA 934NA adhesive was used to bond the cork bands. Similar to the Concept 1 configuration installation, Teflon® tape was also installed at the tang-to-clevis interface and on the thermal barrier-to-heater retention strap interface. Also similar to the Concept 1 configuration installation, a 1U82837-03 configuration heater retention strap was installed.

6.6.1.2 Field Joint and Igniter-to-Case Joint Heaters. Redesigned field joint and igniter-to-case joint heaters were installed on TEM-5. The configuration of the igniter-to-case joint heater is shown in Figure 1-12. The changes incorporated in the redesigned heaters were intended to improve durability and reduce the possibility of damage due to handling. The redesigned heaters consisted of chemically etched, primary and redundant foil circuits which were superimposed upon one another, enclosed within a wire mesh grounding shield, and laminated in Kapton and FEP Teflon® insulation. Configuration of the heater circuits was not changed in the design of the redesigned heaters. The redesigned heaters were previously qualified under CTP-0138, and the test was documented in TWR-19899. Refer to TWR-19899 for a detailed description of the changes incorporated in the redesigned heaters.

The set point temperature of the field joint heaters was 121°F, with a minimum of 87°F at sensors. The set point of the igniter-to-case joint heater was 122°F, with a minimum of 87°F at sensors.

6.6.1.3 Case-to-Nozzle Joint Heater. A new 3.7 kW case-to-nozzle joint heater was installed on the case-to-nozzle joint (see Figure 1-3). The initial purpose of the new heater was to meet an elevated set point temperature requirement of 120°F. After the heater was designed, built, and delivered, the set point temperature was lowered to 76°F, with sensor readings to be between 71° and 81°F. The set point temperature was lowered as a result of postfire inspections that showed abnormally high erosion of the primary O-ring. The erosion was attributed to softening of the joint putty at the elevated heater set point temperature.

6.6.1.4 Heater Power Cables. Redesigned field joint heater and igniter-to-case joint heater power cables were used during TEM-5. The changes incorporated in the redesigned power cables were intended to improve durability and reduce the possibility of damage due to handling. The redesigned power cables were previously qualified under CTP-0153, and the test is documented in TWR-19941. Refer to TWR-19941 for a detailed description of the changes incorporated in the redesigned heaters.

6.6.1.5 Systems Tunnel and LSC. The systems tunnel and systems tunnel LSC were not installed on TEM-5.

6.6.2 Objectives

The objectives from Section 2 concerning the JPS were:

C. Obtain data on the performance of the new flight configuration joint heaters on the igniter-to-case joint and field joints and the new higher output heater for the case-to-nozzle joint, which is used on static test motors only.

F. Demonstrate the fit, operation, and similarity of the new JPS heater power cables to the old power cables.

I. Demonstrate and evaluate processing and installation of new FJPS designs.

J. Evaluate structural integrity of new FJPS designs through full-scale, full-duration static firing.

6.6.3 Conclusions/Recommendations

The TEM-5 JPS performed per specifications and maintained the joint temperatures within the required temperature range at the time of motor ignition.

FJPS--No significant problems were encountered during installation of the each JPS configuration. Installation of both redesign Concepts 1 and 1C required approximately the same amount of skill and time, and the performance of each configuration was the same. Personnel that performed the installations preferred Concept 1C over Concept 1 for ease of installation. It is worth noting that during previous development testing, installation personnel preferred Concept 1 to Concept 1C (TWR-50290). Each FJPS configuration performed as expected during the motor fire.

Prior to TEM-5, the Concept 1 configuration was determined to be the preferred configuration by KSC, MSFC, and Thiokol (TWR-50290).

To reduce the occurrence of voids and the migration of adhesive under the pin retainer band, Cab-O-Sil (STW4-2679, microfine silicon dioxide) should be added to EA 934NA adhesive to increase its viscosity.

On future installations, the aft piece of cork on Concept 1 configuration FJPS should be 0.625 in. thick instead of 0.75 inch. This lower thickness meets the thermal requirements and is easier to install.

Joint Heaters--The performance of each joint heater was nominal throughout the TEM-5 countdown period.

Heater Power Cables--The fit and operation of the new JPS power cables was demonstrated to be similar in comparison to the old power cables.

6.6.4 Results/Discussion

6.6.4.1 Field Joint Protection Systems. **FJPS Installations**--No significant problems were encountered during the installation of each redesigned JPS configuration, or to the standard TEM configuration JPS. The sheet cork installations conformed to requirements of STW4-2700.

Post-test Inspection--No cracks, unbonds, or heat effects were detected on any of the JPS configurations after the motor fire.

Cork Pull Tests--Post-test cork pull tests were performed on the Concept 1 FJPS. The results are presented in Table 6-7, and the condition of each pull test button is shown in Figure 6-6. Aft cork band test Specimen No. 3 was only partially bonded to the pin retainer band. Aft cork band test Specimen No. 14 had a 95 percent adhesive failure between the pin retainer band and the adhesive. These results were most likely a result of not having the pin retainer band abraded prior to bonding. Cohesive cork failures in the other pull tests indicate adequate adhesion for each adhesive.

Cork pull tests were not performed on the Concept 1C FJPS. Sufficient data had already been collected on the Concept 1C forward cork band (which is similar to the Concept 1 FJPS forward cork band) in previous tests to demonstrate that this is a strong bondline. The Concept 1C aft cork band could not be pull tested because it was on a contoured surface.

Adhesive Migration--Upon disassembly of the Concept 1 FJPS, a significant amount of adhesive was found under approximately 95 percent of the pin retainer band (Figure 6-7). Upon joint demate, there was no evidence of adhesive in the joint. The adhesive migration did not impede removal of the joint pins because each pin was coated with a film of grease.

6.6.4.2 Joint Heaters. The TEM-5 joint heaters maintained the joint temperatures within the required temperature range at the time of motor ignition.

Table 6-7. Concept 1 FJPS Cork Band Pull Test Results

Specimen No.	Location (deg)	Cork Band Tested	Ultimate Load (lb)	Ultimate Stress (psi)	Failure Mode		
					Cohesive Cork (%)	Adhesive Test Button (%)	Adhesive Hat Band (%)
1	57	Forward	50	42	60	40	
2	54	Forward	300	249	90	10	
3	61	Aft	0	0	30		70
4	56	Aft	200	166	95	5	
5	304	Forward	225	187	95	5	
6	306	Forward	150	131	95	5	
7	266	Forward	145	121	80	20	
8	270	Forward	200	166	90	5	
9	268	Aft	150	126	90	10	
10	274	Aft	150	126	100		
11	277	Aft	150	126	95	5	
12	280	Aft	175	145	90	5	
13	314	Aft	175	145	95	5	
14	317	Aft	175	145	5		95

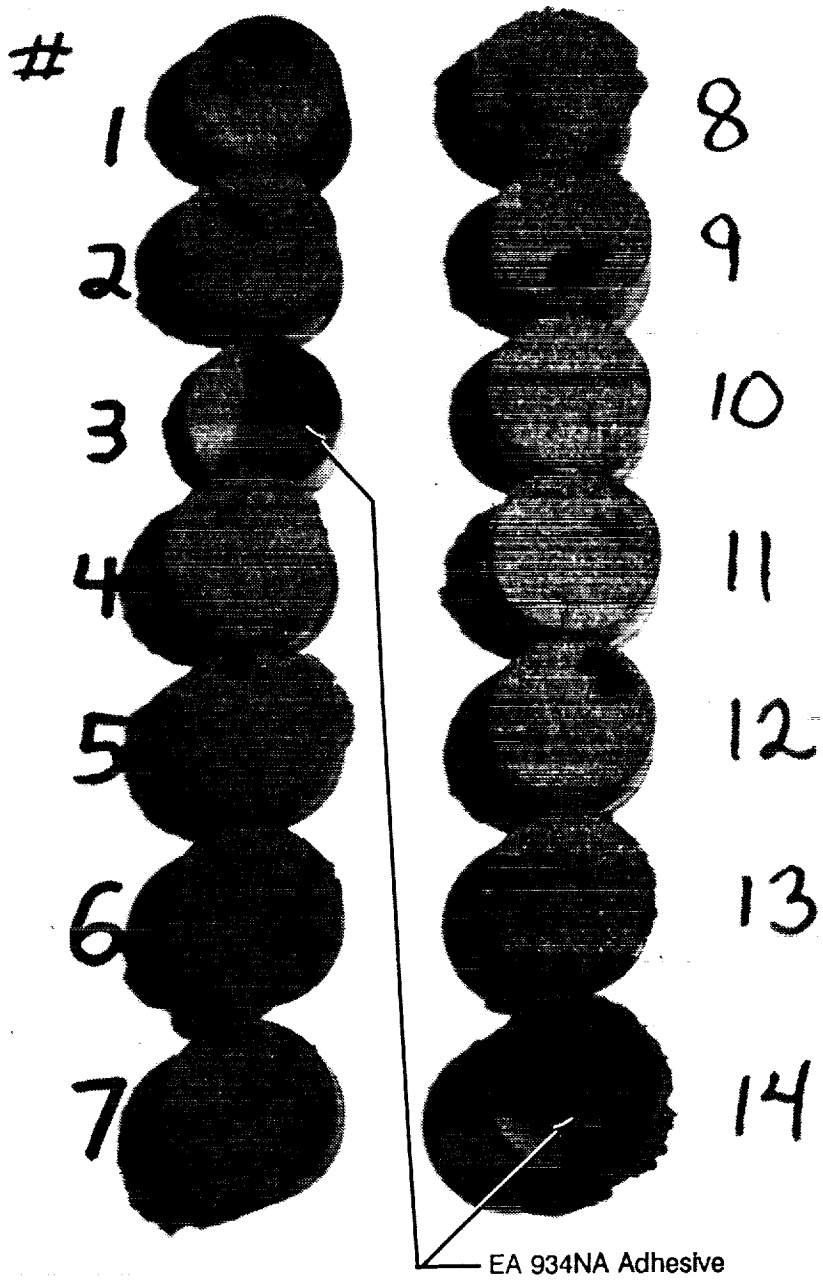

N115861-1

Figure 6-6. FJPS Concept 1--Cork Pull Test Buttons

ORIGINAL PAGE
BLACK AND WHITE PHOTOGRAPH

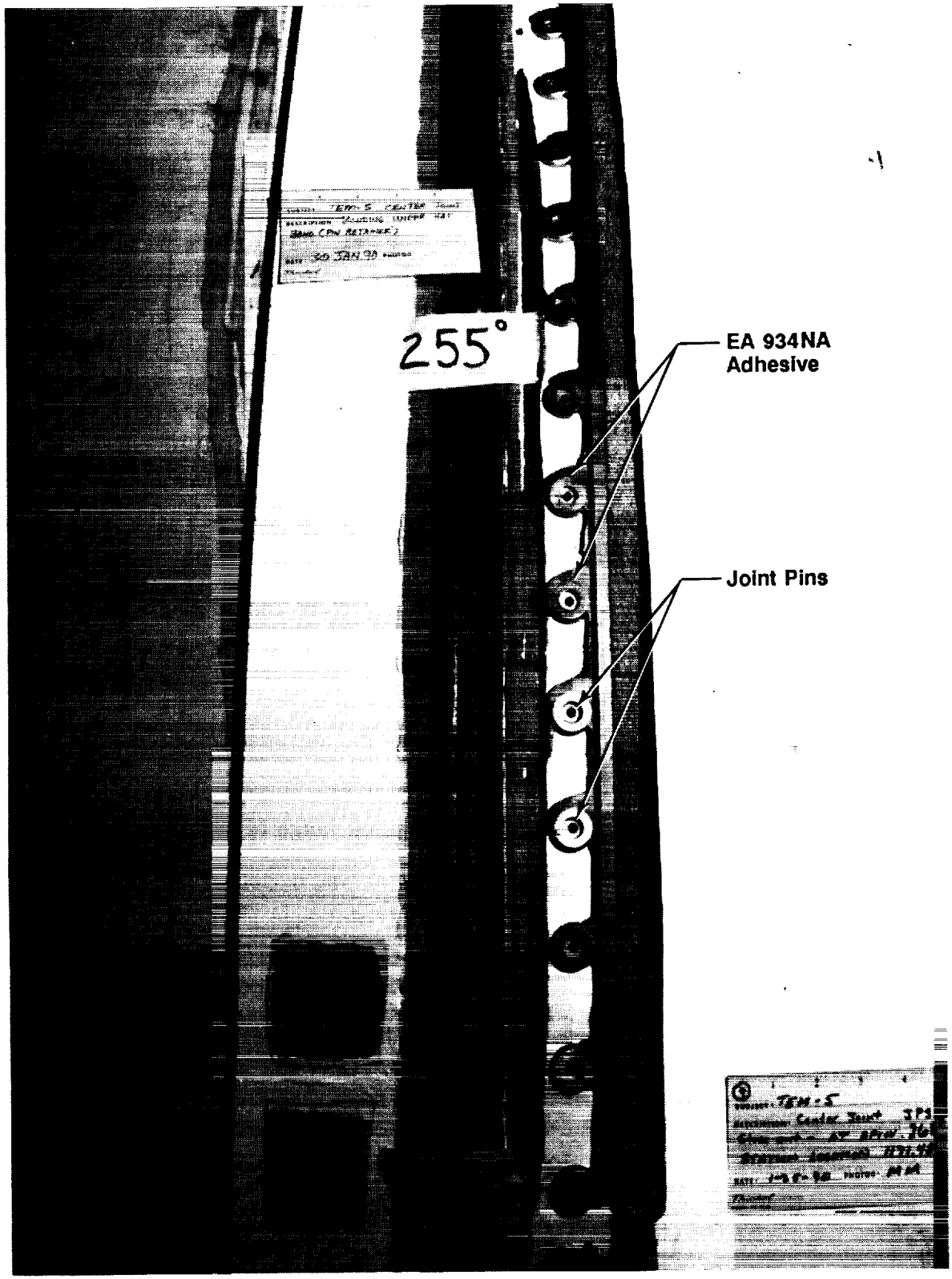

Figure 6-7. FJPS Concept 1--EA 934NA Adhesive Underneath the Pin Retainer Band

Forward Field Joint Heater DWV Test Failure--Prior to the static test fire, a 1,500 V DWV test was performed on each joint heater from the heater controller. During the test, a failure occurred between the redundant forward field joint heater power line and shield. Subsequent trouble shooting isolated the failure to the forward field joint heater. The primary heater circuit was subsequently used during the pretest countdown, and its performance was nominal. Evaluation of the heater after the test fire and heater removal identified the problem to be in the heater cold splice.

Heater Operation--The joint heaters were turned on 16 hr prior to the test firing to ensure that the joint O-ring temperatures were within the specified launch commit temperature at the time of ignition. The four temperature sensors at each field joint were continuously monitored and the hottest sensor was manually selected for temperature control. Plots of the RTD temperatures for each joint are included in Appendix D.

Field Joint Heaters--During the motor fire, each field joint temperature sensor registered well over the minimum of 87°F.

Igniter-to-Case Joint Heater--During the motor fire, the igniter joint temperature sensors registered well over the minimum of 87°F.

Case-to-Nozzle Joint Heater--During the motor fire, the case-to-nozzle joint temperature sensors registered within the specified range of 71° to 81°F.

Post-test Heater Inspections--Each joint heater was inspected and no discolorations or any other anomalies, other than the forward field joint heater cold-splice short-circuit, were found.

6.6.4.3 Heater Power Cables. Operation of the new JPS power cables was nominal.

6.7 BALLISTICS/MASS PROPERTIES PERFORMANCE

6.7.1 Introduction

The TEM-5 propellant, TP-H1148, was a composite type solid propellant, formulated from: PBAN, epoxy curing agent, AP oxidizer, and aluminum powder fuel. A small amount of burning rate catalyst (iron oxide) was added to achieve the desired propellant burn rate.

The forward segment propellant grain design consisted of an 11-point star that transitioned into a tapered CP configuration. The propellant grain design of the two center segments was a double-tapered CP configuration. The aft segment propellant grain design was a triple-tapered CP configuration with a cutout for the partially submerged nozzle.

6.7.2 Objectives

The primary test objectives from Section 2 regarding ballistics/mass properties were:

B. Obtain additional data on the effect of 3-yr open storage of loaded SRM case segments upon motor ignition and performance.

D. Obtain additional data on the low-frequency chamber pressure oscillations in the motor forward end.

6.7.3 Conclusions/Recommendations

The TEM-5 ballistic performance was within expected limits, and compared well with previous TEM performance and HPM historical data. The 3-yr open storage of loaded case segments did not appear to affect motor performance.

The TEM-5 motor exhibited chamber pressure oscillations similar to previously tested space shuttle HPMs. The 1-L mode oscillations were typical for an HPM. In general, HPM 1L mode amplitudes are lower than those for RSRMs.

Much of the static test pressure oscillation data measured to date have been incorrect. Upon completion of the TEM-4 static test, several errors were found in the processing of the ac coupled data (for additional information, refer to memo 5613-FY90-M82, TEM-4 Pressure Oscillation Study). This affected the data of past static tests as well. This report documents the latest data supplied by test area.

6.7.4 Results/Discussion

A comparison of TEM-5 performance with predicted values and with the nominal HPM performance revealed few differences. The predicted burn rate for TEM-5 was 0.368 ips at 625 psia and 60°F, the target burn rate was 0.368 ips and the delivered burn rate was 0.3654 ips. Predicted and measured performance compared well and was within the current HPM specifications.

Table 6-8 summarizes the measured ballistic and nozzle performance data. Figure 6-8 compares the measured and predicted pressure-time histories. Thrust was not measured for this static test, only reconstructed thrust based on nominal thrust-to-pressure ratios is available.

Figures 6-9 and 6-10 contain plots of the analytical reconstruction of the TEM-5 performance. The analytical model was used to calculate the motor burn rate and surface burn rate error (SBRE) factor. The calculated burn rate of 0.3654 ips at 625 psia and 60°F was approximately 0.7 percent below the predicted value of 0.368 ips, well within the burn rate variation. The calculated SBRE table compared well with the nominal HPM table as expected, since the propellant grain geometry was the same.

The motor average subscale burn rates, full-scale motor burn rates (determined from post-test curve matching), and resulting scale factors for SRM-15 to SRM-24, used to predict the TEM-5 burn rate, are listed in Table 6-9. The full-scale motor burn rates were determined from post-test curve matching in which the analytical model was forced to match the measured motor performance. The mean scale factor was 1.0175 with a sigma of 0.00440 and a coefficient of variation of 0.432 percent.

A plot of the measured data comparing the ignition transients of the TEM static tests is shown in Figure 6-11. The TEM-5 transient was very similar to previously measured motor ignition performance. The TEM-5 maximum pressure rise rate was 87.1 psi/10 ms. The historical three-point average pressure rise rate is 90.49 psi/10 ms with a variation of 7.07 psi/10 ms. TEM-5 was consistent with the nominal rise rates for the population. A summary table showing the historical pressure rise rates, thrust rise rates, and ignition intervals is shown in Table 6-10. A summary of the TEM-5 ignition events is shown in Table 6-11.

The TEM-5 igniter grain configuration was identical to the HPM flight and static test igniter design. The igniter was cast from propellant batch number D760010, using TP-H1178 propellant. The igniter maximum mass flow rate was 357.5 lbm/sec at 72°F. The TEM-5 igniter performance characteristics were within the expected ranges. A comparison of the TEM-5 igniter performance at 80°F with the igniter limits at 80°F is shown in Figure 6-12. The igniter was within the limits at 80°F.

Table 6-8. Summary of Measured Ballistic and Nozzle Performance Data

A. Ambient Conditions	
Date and time at fire pulse (hr) (23 Jan 1990)	14.50
Ambient temperature (°F)	41
Measured mean bulk temperature (°F)	72
Measured ambient pressure (psia)	12.29
B. Weight Data	
Total loaded propellant weight (lbf)	1,109,928
Total expended weight (lbf)	1,114,778
Unexpended propellant residue (slag) (lbf)	1,500
Expended inert weight	
1. Forward segment (lbf)	718.0
2. Forward center segment (lbf)	598.0
3. Aft center segment (lbf)	962.0
4. Aft segment (including nozzle less aft exit cone) (lbf)	4,072.0
5. Total expended inerts (lbf)	6,350.0
Total expended propellant weight (lbf)	1,108,428
C. Nozzle Data	
Initial throat area ($in.^2$)	2,278.2
Final throat area ($in.^2$)	2,457.3
Web time average throat area ($in.^2$)	2,371.3
Action time average throat area ($in.^2$)	2,379.3
Total time average throat area ($in.^2$)	2,379.6
Initial exit area ($in.^2$)	17,588
Final exit area ($in.^2$)	17,704
Total time average exit area ($in.^2$)	17,646
Web time average throat radial erosion rate (ips)	0.00906
Action time average throat radial erosion rate (ips)	0.00847
Total time average throat radial erosion rate (ips)	0.00842
Initial expansion ratio	7.7200
Web time average expansion ratio	7.4414
Action time average expansion ratio	7.4163
Action time average nozzle efficiency	0.97815
Total time average nozzle efficiency	0.97830

Table 6-8. Summary of Measured Ballistic and Nozzle Performance Data (Cont)

D. Time and Ballistic Data

Time at first indication of headend pressure (sec)	0.029
Ignition delay time (sec)	-0.025
Time at 90% maximum igniter pressure (sec)	0.054
Ignition interval time (sec)	0.230
Ignition rise time (sec)	0.201
Time when headend chamber pressure achieves 563.5 psia during ignition (sec)	0.230
Time at last indication of headend pressure (sec)	123.3
Time at web bisector (sec)	111.0
Web time (sec)	110.7
Action time (sec)	122.4
Total time (sec)	123.3
Tailoff thrust decay time (sec)	0.688
Maximum pressure rise rate (psi/10 ms)	87.1
Maximum thrust rise rate (lbf/10 ms)	253,894
Maximum igniter pressure (psia)	1996
Maximum measured headend pressure (psia)	921.5
Time at maximum headend pressure (sec)	0.616
Maximum thrust (lbf)	3,098,000
Time at maximum thrust (sec)	20.0
Maximum thrust corrected to vacuum (lbf)	3,315,000
Maximum thrust corrected to sea level (lbf)	3,056,000
Maximum nozzle stagnation pressure (psia)	843.2
Web time average headend chamber pressure (psia)	667.9
Action time average headend chamber pressure (psia)	619.7
Web time average nozzle stagnation pressure (psia)	650.6
Action time average nozzle stagnation pressure (psia)	603.9
Initial thrust (lbf)	2,889,000
Initial thrust corrected to vacuum (lbf)	3,105,000
Initial thrust corrected to sea level (lbf)	2,846,000
Web time average thrust (lbf)	2,397,000
Web time average thrust corrected to vacuum (lbf)	2,614,000
Action time average thrust (lbf)	2,214,000
Action time average thrust corrected to vacuum (lbf)	2,426,000
Characteristic exhaust velocity (ft/sec)	5047.75

Table 6-8. Summary of Measured Ballistic and Nozzle Performance Data (Cont)

E. Impulse Data

Measured total impulse (Mlbf-sec)	271.21
Total impulse corrected to vacuum (Mlbf-sec)	297.21
Measured impulse at 20 sec (Mlbf-sec)	60.12
20-sec impulse corrected to vacuum (Mlbf-sec)	64.44
Measured impulse at 60 sec (Mlbf-sec)	160.03
60-sec impulse corrected to vacuum (Mlbf-sec)	173.02
Web time impulse (Mlbf-sec)	265.39
Web time impulse corrected to vacuum (Mlbf-sec)	289.39
Action time impulse (Mlbf-sec)	271.07
Action time impulse corrected to vacuum (Mlbf-sec)	297.00
I_{sp} (sec)	243.29
I_{sp} corrected to vacuum (sec)	266.61
Web time specific impulse (sec)	244.76
Web time specific impulse corrected to vacuum (sec)	266.90
Action time I_{sp} (sec)	243.33
Action time I_{sp} corrected to vacuum (sec)	266.60
Propellant I_{sp} (sec)	244.68
Propellant I_{sp} corrected to vacuum (sec)	268.14

F. Pressure Integral Data

Total time pressure integral (psia-sec)	75,924
Web time pressure integral (psia-sec)	73,960
Action time pressure integral (psia-sec)	75,883

Table 6-8. Summary of Measured Ballistic and Nozzle Performance Data (Cont)

Corrected to 40°F

G. Time and Ballistic Data

Time and first indication of headend pressure (sec)	0.031
Time when headend chamber pressure achieves 563.5 psia during ignition (sec)	0.244
Time at last indication of headend pressure (sec)	127.7
Time at web bisector (sec)	115.1
Web time (sec)	114.8
Action time (sec)	126.8
Maximum measured headend pressure (psia)	887.3
Time at maximum headend pressure (sec)	0.638
Maximum thrust corrected to vacuum (lbf)	3,192,000
Maximum nozzle stagnation pressure (psia)	812.0
Web time average headend chamber pressure (psia)	643.0
Action time average headend chamber pressure (psia)	597.1
Web time average nozzle stagnation pressure (psia)	626.3
Action time average nozzle stagnation pressure (psia)	581.9
Web time average thrust corrected to vacuum (lbf)	2,516,000
Action time average thrust corrected to vacuum (lbf)	2,338,000

H. Impulse Data

Total impulse corrected to vacuum (Mlbf-sec)	296.62
20-sec impulse corrected to vacuum (Mlbf-sec)	61.97
60-sec impulse corrected to vacuum (Mlbf-sec)	167.50
Web time impulse corrected to vacuum (Mlbf-sec)	288.91
Action time impulse corrected to vacuum (Mlbf-sec)	296.40
I_{sp} corrected to vacuum (sec)	266.08
Web time I_{sp} corrected to vacuum (sec)	266.37
Action time I_{sp} corrected to vacuum (sec)	266.08
Propellant I_{sp} corrected to vacuum (sec)	267.60

Table 6-8. Summary of Measured Ballistic and Nozzle Performance Data (Cont)

Corrected to 60°F

I. Time and Ballistic Data

Time and first indication of headend pressure (sec)	0.030
Time when headend chamber pressure achieves 563.5 psia during ignition (sec)	0.236
Time at last indication of headend pressure (sec)	125.0
Time at web bisector (sec)	112.5
Web time (sec)	112.2
Action time (sec)	124.0
Maximum measured headend pressure (psia)	908.5
Time at maximum headend pressure (sec)	0.624
Maximum thrust corrected to vacuum (lbf)	3,268,000
Maximum nozzle stagnation pressure (psia)	831.4
Web time average headend chamber pressure (psia)	658.5
Action time average headend chamber pressure (psia)	611.2
Web time average nozzle stagnation pressure (psia)	641.3
Action time average nozzle stagnation pressure (psia)	595.6
Web time average thrust corrected to vacuum (lbf)	2,577,000
Action time average thrust corrected to vacuum (lbf)	2,392,000

J. Impulse Data

Total impulse corrected to vacuum (Mlbf-sec)	296.99
20-sec impulse corrected to vacuum (Mlbf-sec)	63.50
60-sec impulse corrected to vacuum (Mlbf-sec)	170.91
Web time impulse corrected to vacuum (Mlbf-sec)	289.21
Action time impulse corrected to vacuum (Mlbf-sec)	296.77
I_{sp} corrected to vacuum (sec)	266.41
Web time I_{sp} corrected to vacuum (sec)	266.70
Action time I_{sp} corrected to vacuum (sec)	266.41
Propellant I_{sp} corrected to vacuum (sec)	267.93

Table 6-8. Summary of Measured Ballistic and Nozzle Performance Data (Cont)

Corrected to 90°F

K. Time and Ballistic Data

Time and first indication of headend pressure (sec)	0.028
Time when headend chamber pressure achieves 563.5 psia during ignition (sec)	0.222
Time at last indication of headend pressure (sec)	120.9
Time at web bisector (sec)	108.7
Web time (sec)	108.5
Action time (sec)	120.0
Maximum measured headend pressure (psia)	941.2
Time at maximum headend pressure (sec)	0.604
Maximum thrust corrected to vacuum (lbf)	3,386,000
Maximum nozzle stagnation pressure (psia)	861.3
Web time average headend chamber pressure (psia)	682.4
Action time average headend chamber pressure (psia)	632.8
Web time average nozzle stagnation pressure (psia)	664.6
Action time average nozzle stagnation pressure (psia)	616.7
Web time average thrust corrected to vacuum (lbf)	2,670,000
Action time average thrust corrected to vacuum (lbf)	2,477,000

L. Impulse Data

Total impulse corrected to vacuum (Mlbf-sec)	297.53
20-sec impulse corrected to vacuum (Mlbf-sec)	65.85
60-sec impulse corrected to vacuum (Mlbf-sec)	176.22
Web time impulse corrected to vacuum (Mlbf-sec)	289.69
Action time impulse corrected to vacuum (Mlbf-sec)	297.33
I_{sp} corrected to vacuum (sec)	266.90
Web time I_{sp} corrected to vacuum (sec)	267.19
Action time I_{sp} corrected to vacuum (sec)	266.90
Propellant I_{sp} corrected to vacuum (sec)	268.43

A026340a

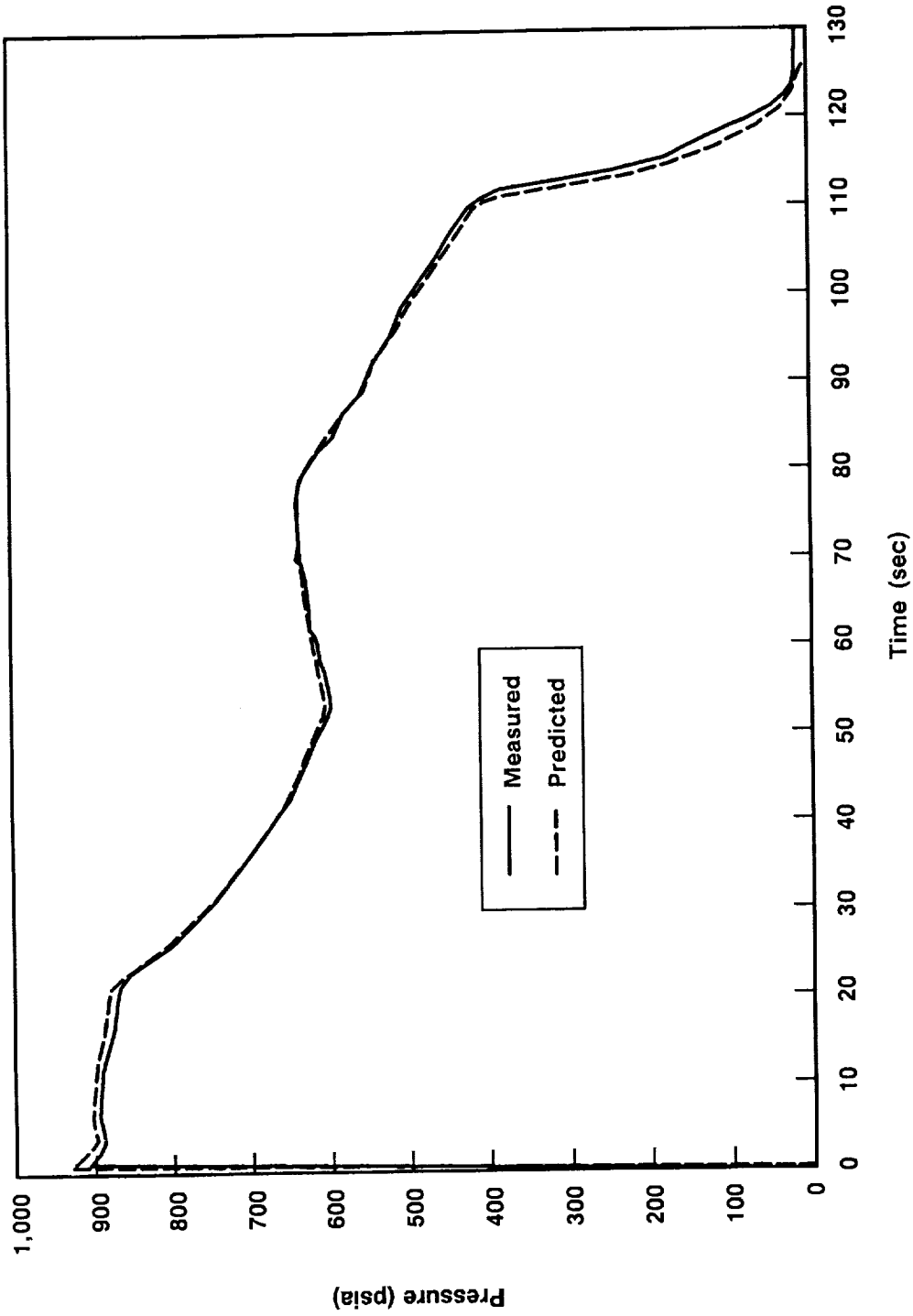

Figure 6-8. TEM-5 Predicted and Measured Pressure at 72°F

A026341a

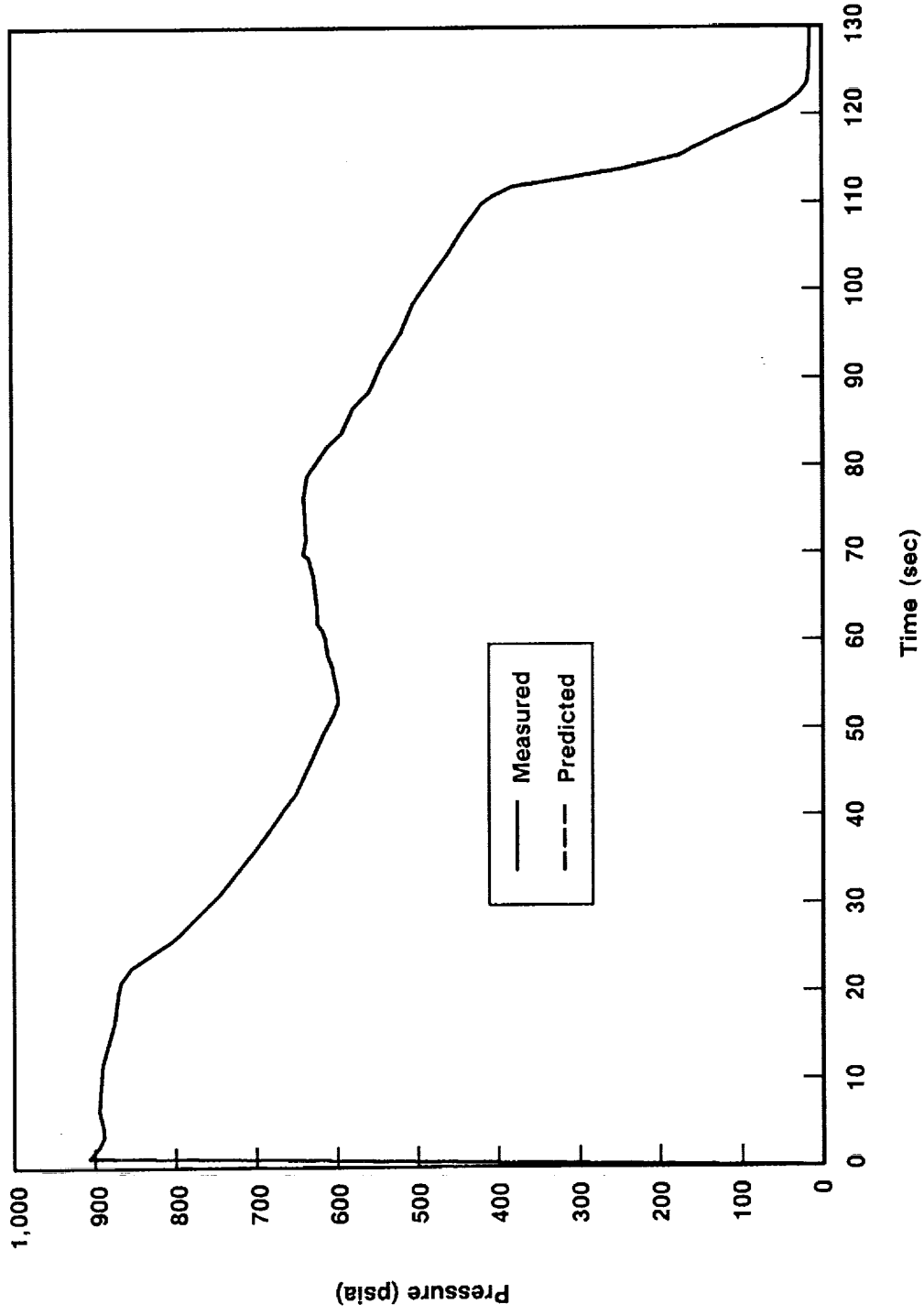

Figure 6-9. TEM-5 Reconstructed and Measured Pressure at 72°F

A026342a

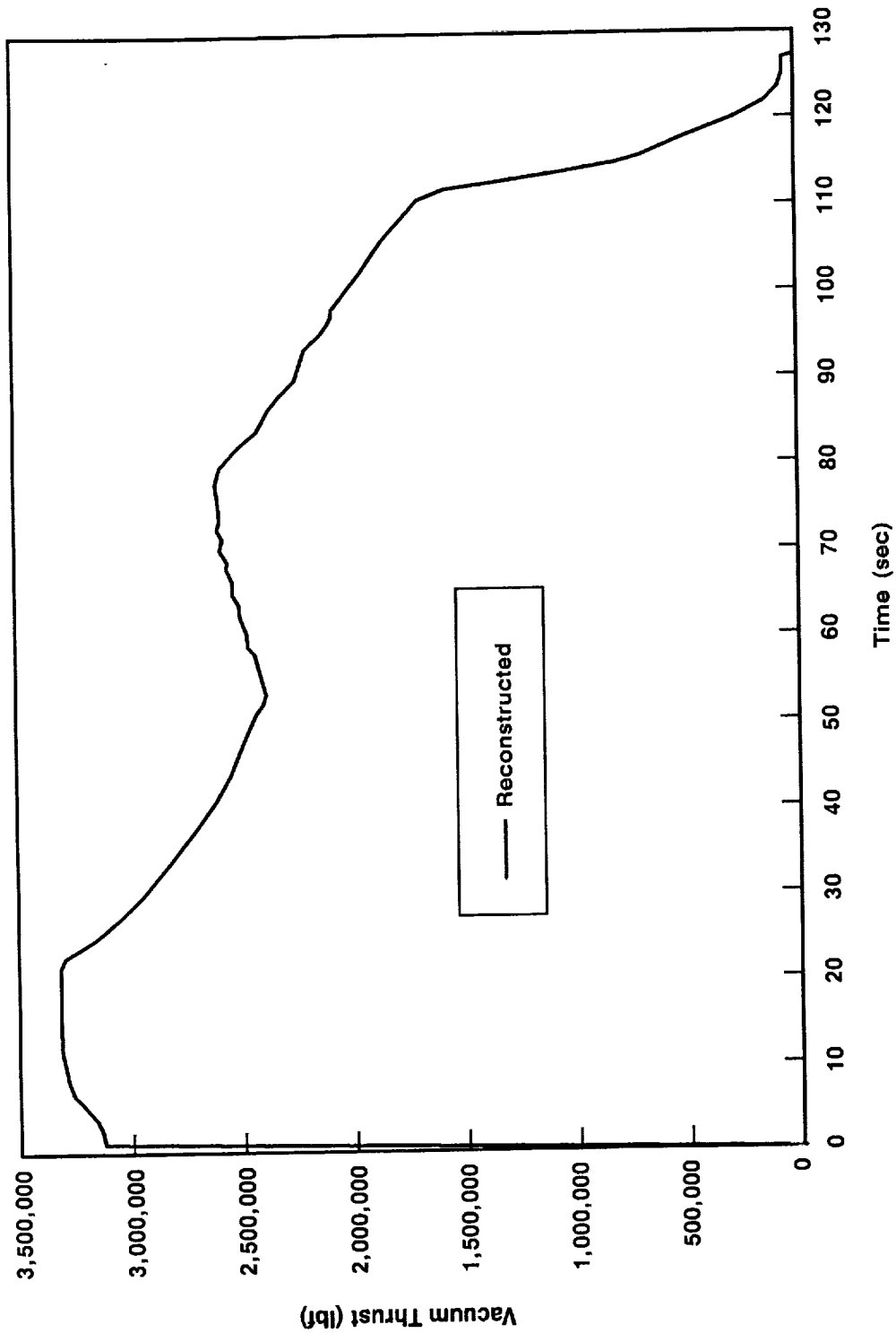

Figure 6-10. TEM-5 Reconstructed Vacuum Thrust at 72°F

Table 6-9. Burn Rate Data Comparison Subscale to Full-Scale at 625 psia, 60°F

Motor	Burn Rate: SRM Target	Burn Rate: 5-in. CP Standard	Burn Rate: SRM Predicted	Burn Rate: SRM Delivered	Scale Factor: 5-in. CP Standard
SRM-15A	0.368	0.366	0.370	0.3701	1.0112
SRM-15B	0.368	0.366	0.370	0.3709	1.0134
SRM-16A	0.368	0.365	0.369	0.3684	1.0093
SRM-16B	0.368	0.365	0.369	0.3688	1.1040
SRM-17A	0.368	0.363	0.367	0.3680	1.0138
SRM-17B	0.368	0.362	0.366	0.3694	1.0204
SRM-18A	0.368	0.362	0.367	0.3693	1.0202
SRM-18B	0.368	0.363	0.368	0.3690	1.0165
SRM-19A	0.368	0.364	0.369	0.3703	1.0173
SRM-19B	0.368	0.364	0.369	0.3704	1.0176
SRM-20A	0.368	0.368	0.373	0.3742	1.0168
SRM-20B	0.368	0.366	0.371	0.3744	1.0230
SRM-21A	0.368	0.367	0.370	0.3737	1.0183
SRM-21B	0.368	0.365	0.368	0.3744	1.0258
SRM-22A	0.368	0.362	0.365	0.3675	1.0152
SRM-22B	0.368	0.362	0.365	0.3697	1.0213
SRM-23A	0.368	0.364	0.367	0.3713	1.0201
SRM-23B	0.368	0.364	0.367	0.3721	1.0223
SRM-24A	0.368	0.360	0.365	0.3678	1.0217
SRM-24B	0.368	0.361	0.366	0.3674	1.0177
Average scale factor = 1.0175, σ = 0.00440, % CV = 0.432					
ETM-1	0.368	0.365	0.372	0.3681	1.0085
DM-8	0.368	0.360	0.366	0.3677	1.0214
DM-9	0.368	0.362	0.368	0.3691	1.0196
QM-6	0.368	0.360	0.366	0.3665	1.0181
QM-7	0.368	0.358	0.364	0.3657	1.0215
PVM-1	0.368	0.360	0.366	0.3677	1.0214
TEM-1	0.368	0.362	0.368	0.3659	1.0116
TEM-2	0.368	0.362	0.368	0.3664	1.0122
TEM-3	0.368	0.362	0.368	0.3672	1.0155
TEM-4	0.368	0.362	0.369	0.3681	1.0160
TEM-5	0.368	0.362	0.368	0.3654	1.0105

A026343a

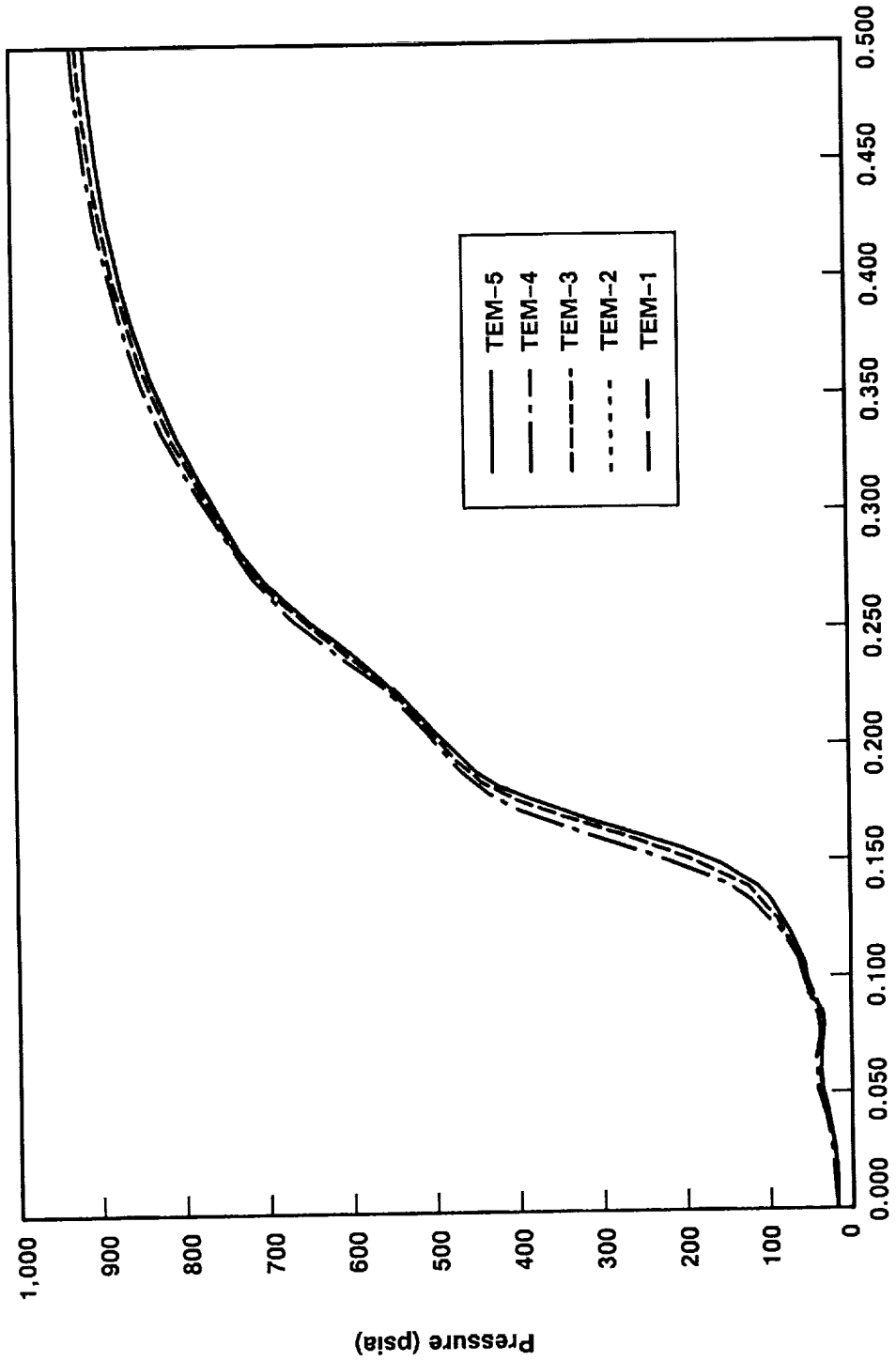

Figure 6-11. Measured Headend Pressure Transients

Table 6-10. Historical 3-point Average Thrust and Pressure Rise Rate Data

Motor	Occurrence Time	Pressure Rise Rate	Occurrence Time	Thrust Rise Rate	Ignition Interval
Static Test					
DM-2	0.1480	85.30	0.1480	245,380	0.2330
QM-1	0.1560	86.38	0.1560	246,128	0.2362
QM-2	0.1640	93.58	0.1720	234,950	0.2391
QM-3	0.1560	94.45	0.1520	245,615	0.2287
QM-4	0.1505	91.96	0.2225	234,438	0.2192
ETM-1A	0.1520	86.72	0.1560	230,023	0.2279
DM-8	0.1680	77.00	0.1760	257,272	0.2424
DM-9	0.1640	81.00	0.1720	275,525	0.2436
QM-6	0.1480	87.40	0.1520	211,476	0.2321
QM-7	0.1480	99.60	NA	NA	0.2230
PVM-1	0.1520	92.80	0.1520	294,664	0.2338
TEM-1	0.1520	85.13	0.1520	238,583	0.2255
QM-8	0.1720	72.30	NA	NA	0.2517
Flight Motors					
SRM-1A	0.1530	87.58			0.2373
SRM-1B	0.1500	91.57			0.2358
SRM-2A	0.1530	90.74			0.2348
SRM-2B	0.1660	90.27			0.2345
SRM-3A	0.1500	91.05			0.2308
SRM-3B	0.1500	89.68			0.2271
SRM-5A	0.1530	95.10			0.2361
SRM-5B	0.1660	84.43			0.2380
SRM-6A	0.1530	92.72			0.2342
SRM-6B	0.1470	88.22			0.2329
SRM-7A	0.1500	99.90			0.2282
SRM-7B	0.1500	99.32			0.2276
SRM-8A	0.1530	106.29			0.2224
SRM-8B	0.1500	91.06			0.2196
SRM-9A	0.1530	92.31			0.2303
SRM-10A	0.1530	92.89			0.2373
SRM-10B	0.1500	84.56			0.2342
SRM-13B	0.1410	98.85			0.2115
RSRM-1A	0.1501	99.0			0.2296
RSRM-1B	0.1596	80.5			0.2310
RSRM-2A	0.1564	87.3			0.2390
RSRM-2B	0.1501	100.2			0.2342
Number		35		11	35
Average		90.49		246,732	0.2321
Standard Deviation		7.07		22,627	0.0076
Coefficient of Variation (%)		7.82		9.17	3.27
TEM-2	0.1520	94.40	0.1520	288,772	0.2280
TEM-3	0.1520	88.51	NA	NA	0.2272
TEM-4	0.1480	81.52	0.1520	279,764	0.2283
TEM-5	0.1560	87.12	NA	NA	0.2299

A026344a

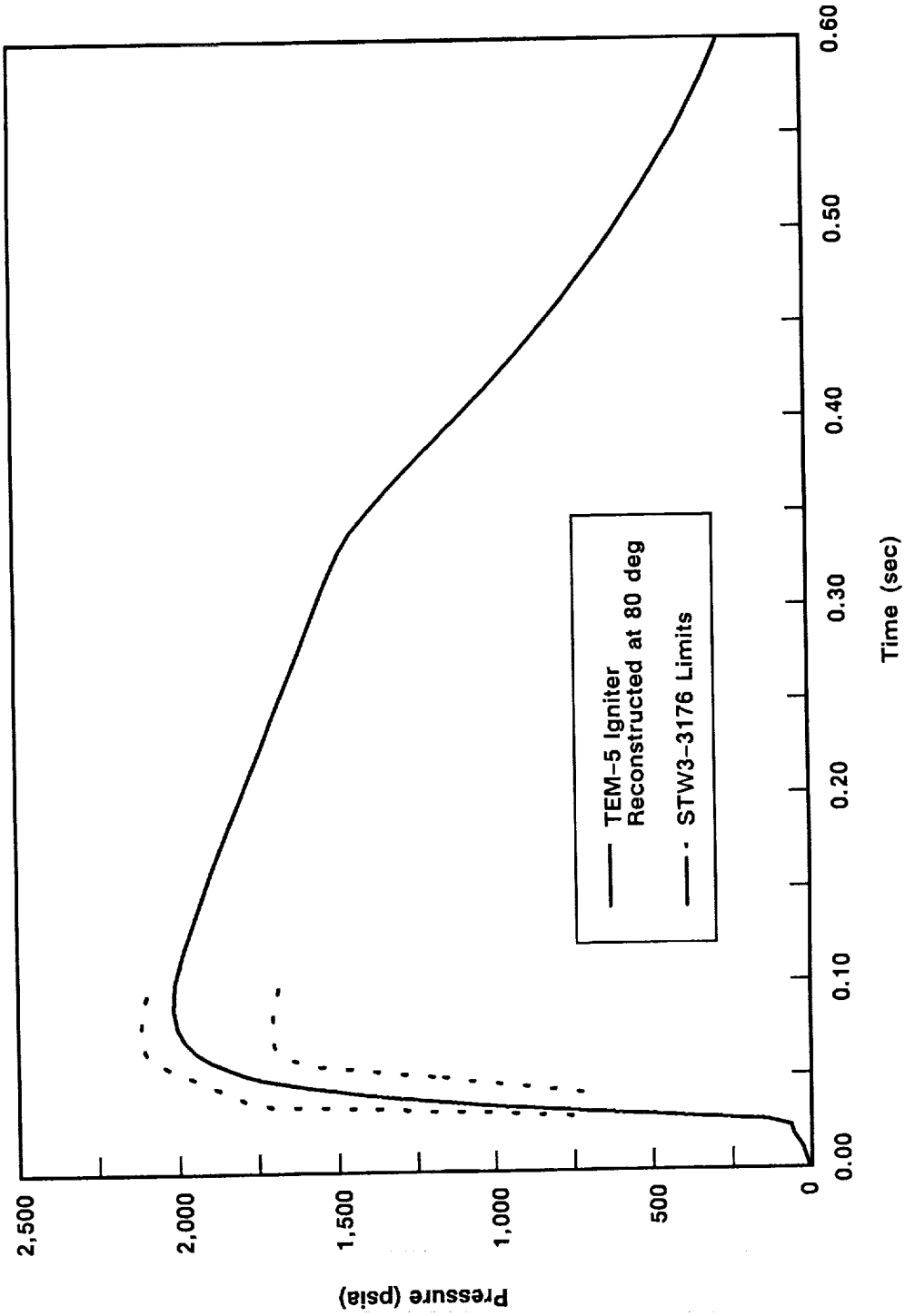

Figure 6-12. Comparison of Igniter Performance to Igniter Limits

Table 6-11. Measured SRM Ignition Performance Data At 72°F

Parameter	TEM-5	Specification Requirement
Maximum Igniter Mass Flow Rate (lbm/sec)	357.5	NA
Ignition Transient (sec) (0 to 563.5 psia)	0.230	0.170 to 0.340
Maximum Pressure Rise Rate (psi/10 ms)	87.1	109
Pressure Level at Start of Maximum Rise Rate (psia)	224	NA
Time Span of Maximum Pressure Rise (ms)	156 to 166	NA
Equilibrium Pressure 0.6 sec (ignition end) (psia)	919	NA
Time to First Ignition (sec) (begin pressure rise)	0.029	NA

A comparison of the igniter pressure versus motor headend and nozzle stagnation pressure for the first 1.4 sec of motor operation is shown in Figure 6-13. A plot of headend and nozzle stagnation pressure for the full duration of the static test is shown on Figure 6-14. These curves are characteristic of the ratio of the headend-to-nozzle stagnation pressures from previous SRM static test motors.

The OPT data channel was ac coupled and processed through special signal conditioning systems for both headend chamber mean pressure (data channel PNCAC001) and headend chamber pressure oscillation measurements. A CEC (Minuteman) pressure gage (data channel PNCAC005) was installed for a pressure oscillation data comparison with the OPT. The Minuteman gage, used on all previous TEMs for pressure oscillation measurements, was used to obtain baseline data to develop a database for replacing the CEC gage with the OPT. The Minuteman gage is considered obsolete and its use has been discontinued after TEM-5. The acoustic signatures for each gage were identical, except that the magnitudes from the OPT were consistently lower than the magnitudes from the Minuteman gage. The 1-L mode magnitudes from the OPT were 6.5 percent lower than those from the Minuteman gage, and second-longitudinal (2-L) magnitudes were 17.5 percent lower. The data acquired from the OPT compared much better to the Minuteman gage data on TEM-5 than for TEM-4.

A026335a

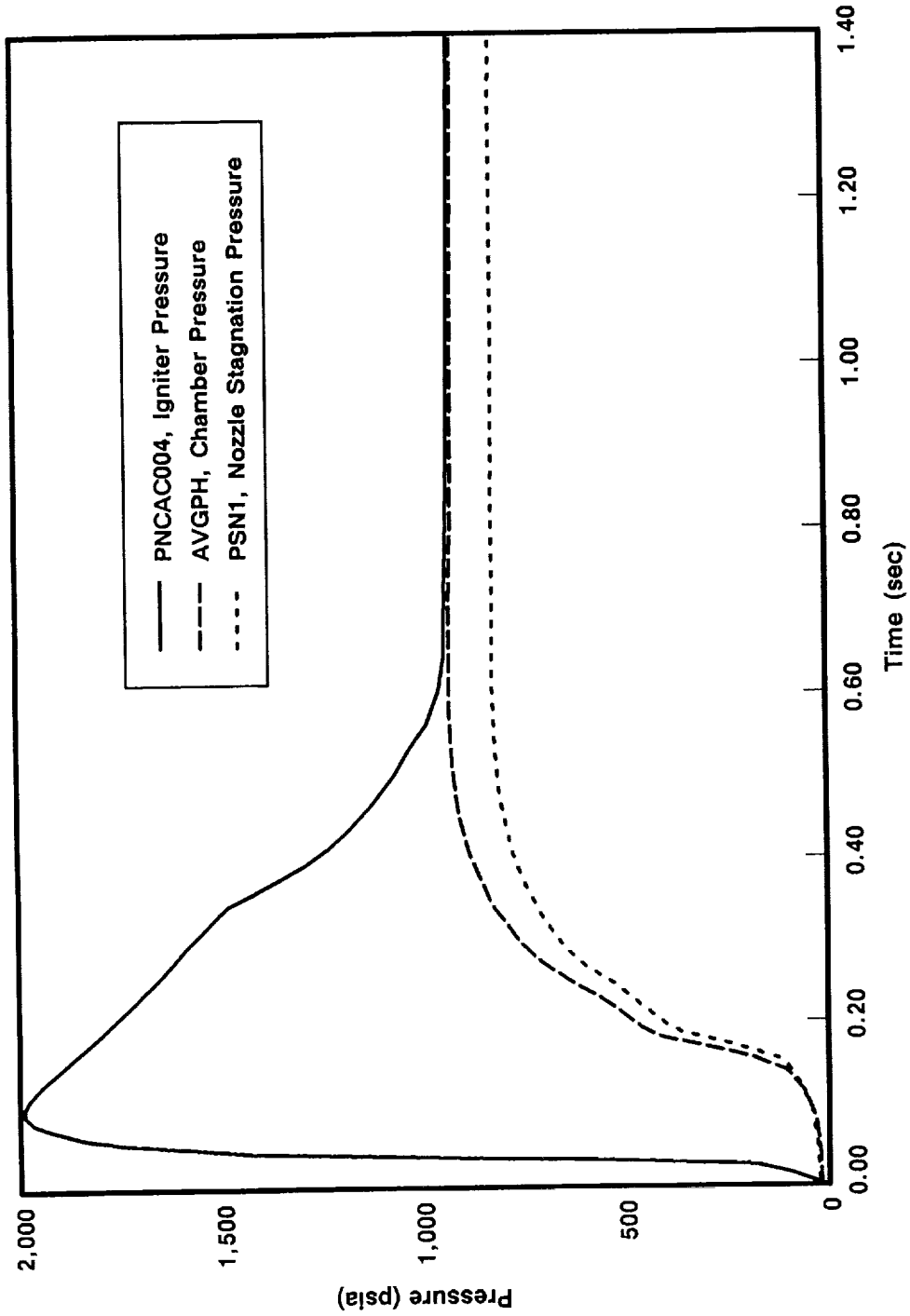

Figure 6-13. TEM-5 Igniter Pressure Versus Headend and Nozzle Stagnation Pressure

A026336a

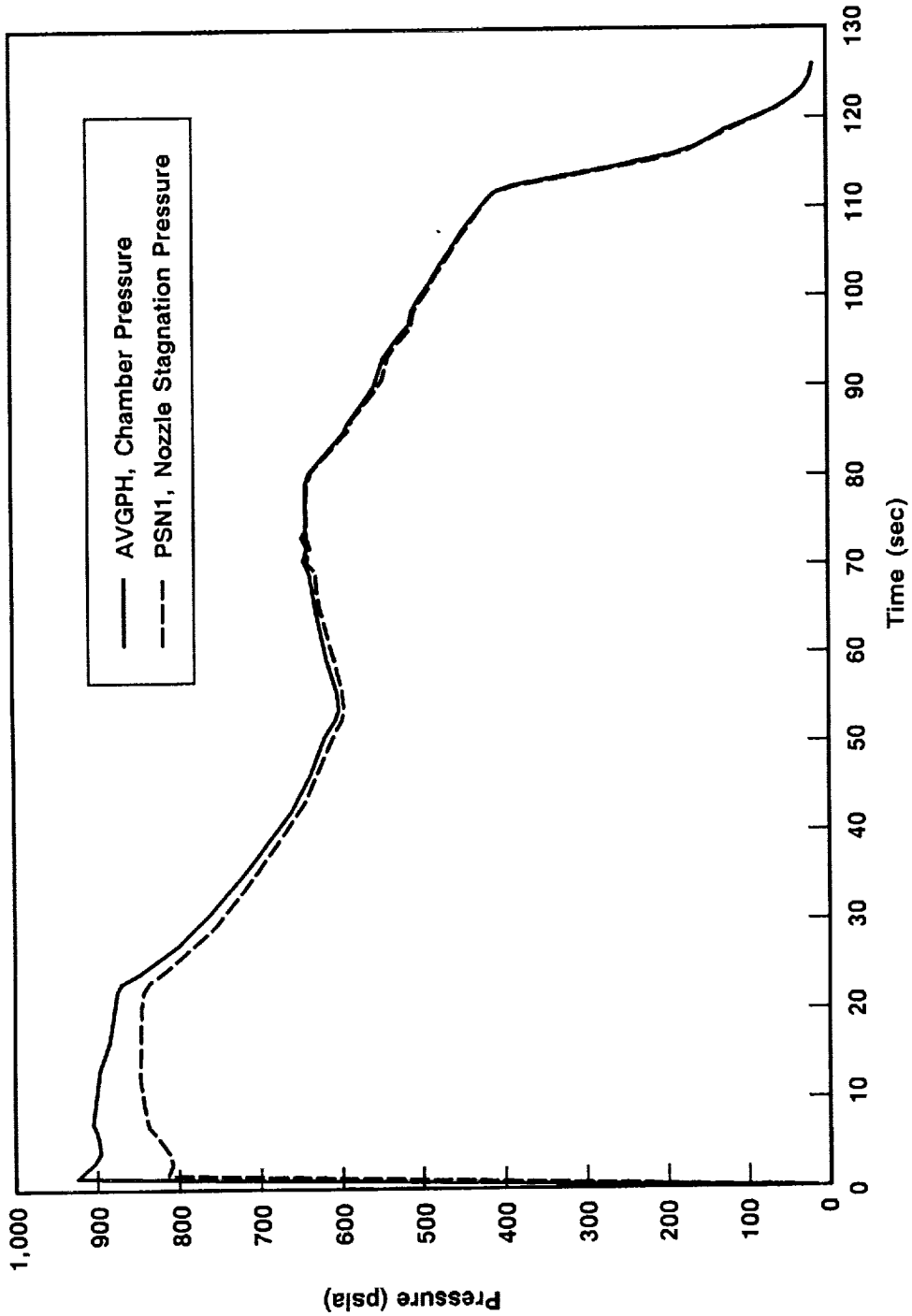

Figure 6-14. TEM-5 Measured Headend and Nozzle Stagnation Pressure Time Histories

Data acquired from gage PNCAC005 are displayed in a waterfall plot format in Figure 6-15. The 1-L and 2-L acoustic modes can be observed at about 15 and 30 Hz, respectively. This waterfall plot is fairly typical of HPM designs. Figures 6-16 and 6-17 describe the running, instantaneous, peak-to-peak oscillation amplitudes of the 1-L and 2-L acoustic modes, respectively, for the TEM-5 motor. This type of analysis is more representative of instantaneous oscillations than are the time-averaged oscillations presented in a waterfall plot.

Figures 6-18 and 6-19 show the waterfall plots of corrected P000016 (P000016 is the old instrumentation designation for PNCAC005) data acquired from the last HPM static test motor, TEM-4. These figures are provided for comparison purposes, and three observations regarding the two motors can be made:

a. Both motors have similar acoustic signatures.

b. TEM-4 experienced stronger 2-L mode oscillations than any other TEM. The 2-L mode of TEM-5 was lower and typical of an HPM.

c. Both motors have acoustic behavior typical of HPM designs. HPM 1-L mode amplitudes are low compared to those for RSRM static test motors.

When using waterfall plots to compare static test motor oscillation amplitudes, it is important to remember that this format uses an averaging method of analysis. This presents no difficulty for steady state signals but has an attenuating effect on transient signals. Since most of the data obtained from a SRM are transient, any oscillation magnitudes referred to as maxima are, in fact, not true but averaged values over a given time slice. These numbers are, nonetheless, very useful for comparison. Table 6-12 shows such a comparison for recent static test motors and the flight motors. This table contains the most recent data (errors have been found in previously measured data). DM-6 and DM-7 were filament wound case (FWC) motors.

A comparison of TEM-5 thrust data at 60°F and a burn rate of 0.368 ips at 625 psia and 60°F with the CEI Specification CPW1-3300 (dated 15 Jan 1986) thrust-time limits at 0.368 ips is shown on Figure 6-20. The TEM-5 performance was within average population limits except around time 105 sec. Note that the limits are for the average of the historical SRM population, not an individual motor. The historical motor population is well within the limits. None of the individual

ORIGINAL PAGE IS
OF POOR QUALITY

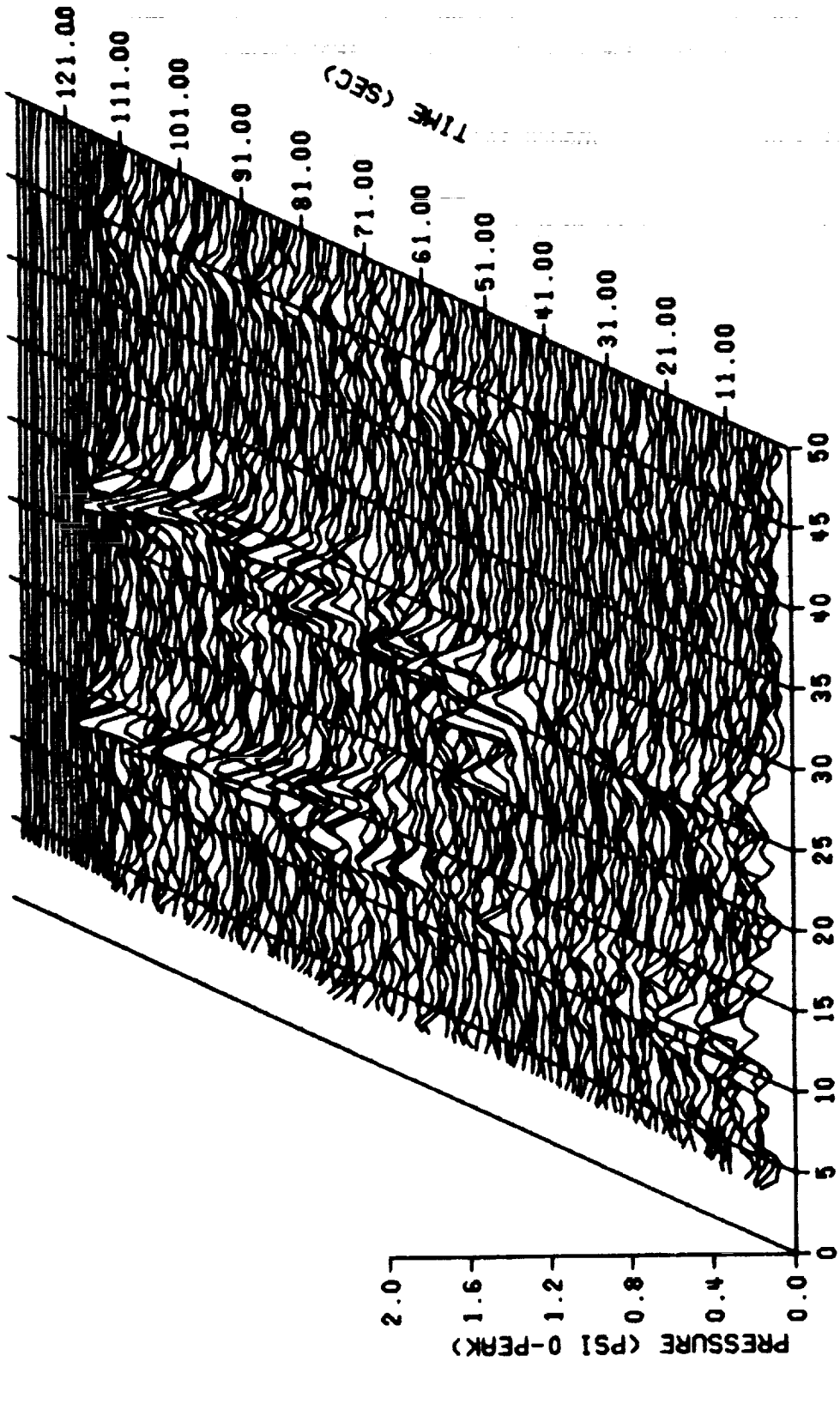

Figure 6-15. TEM-5 Dynamic Pressure Gage Data (PNCAC005)

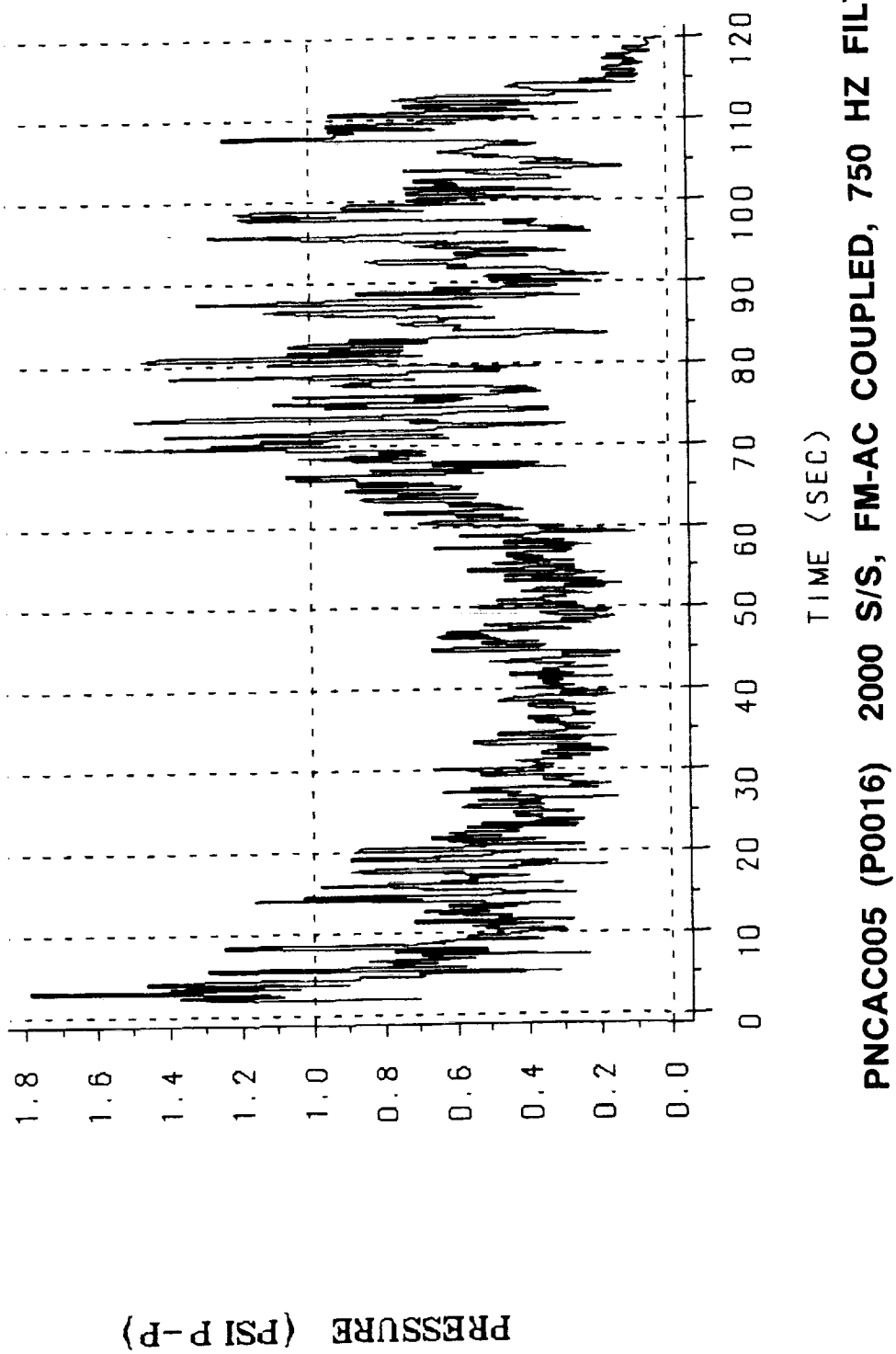

Figure 6-16. Maximum Oscillation Amplitudes--1-L Acoustic Mode 2,000 sps

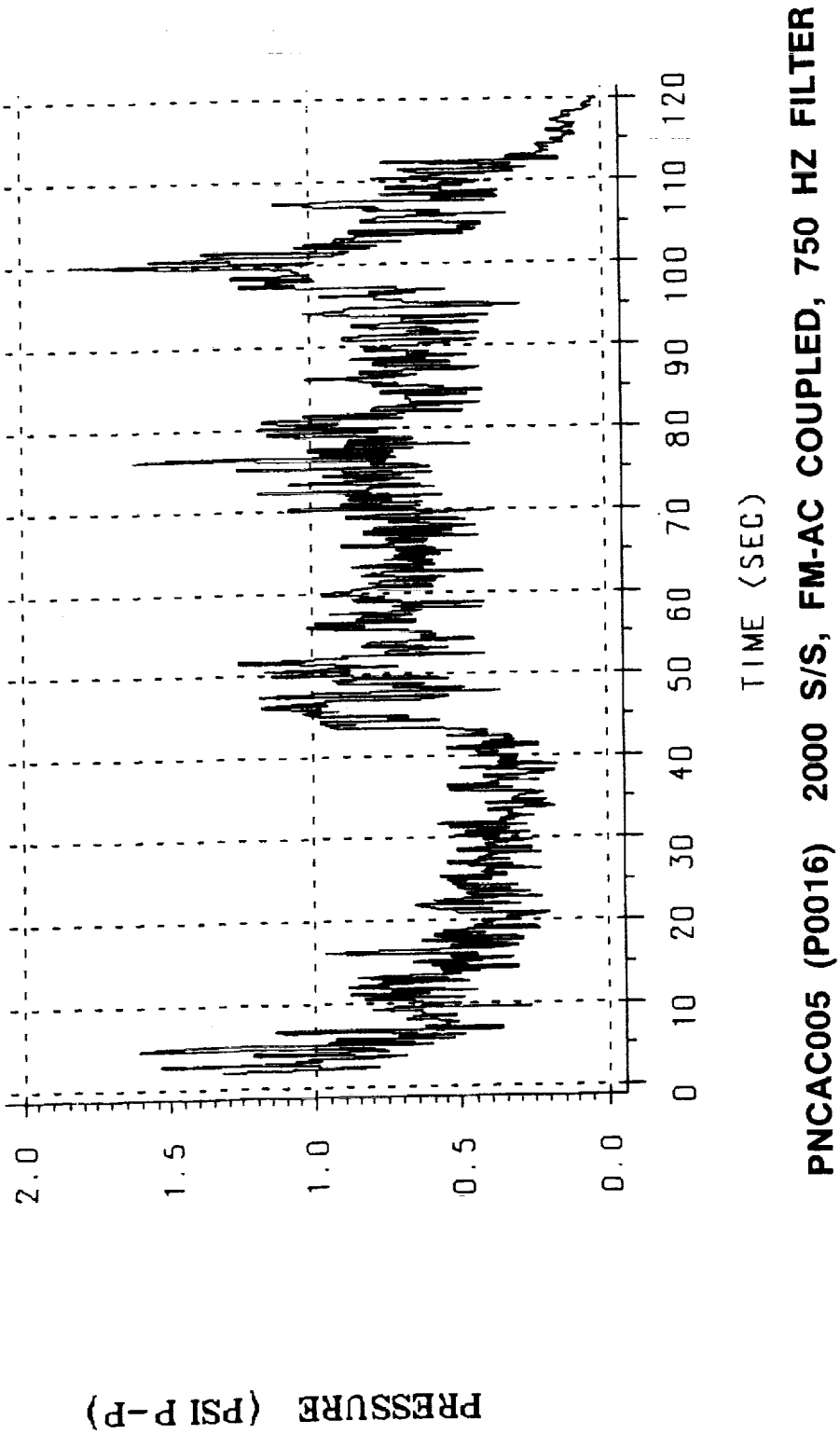

Figure 6-17. Maximum Oscillation Amplitudes--2-L Acoustic Mode 2,000 sps

ORIGINAL PAGE IS
OF POOR QUALITY

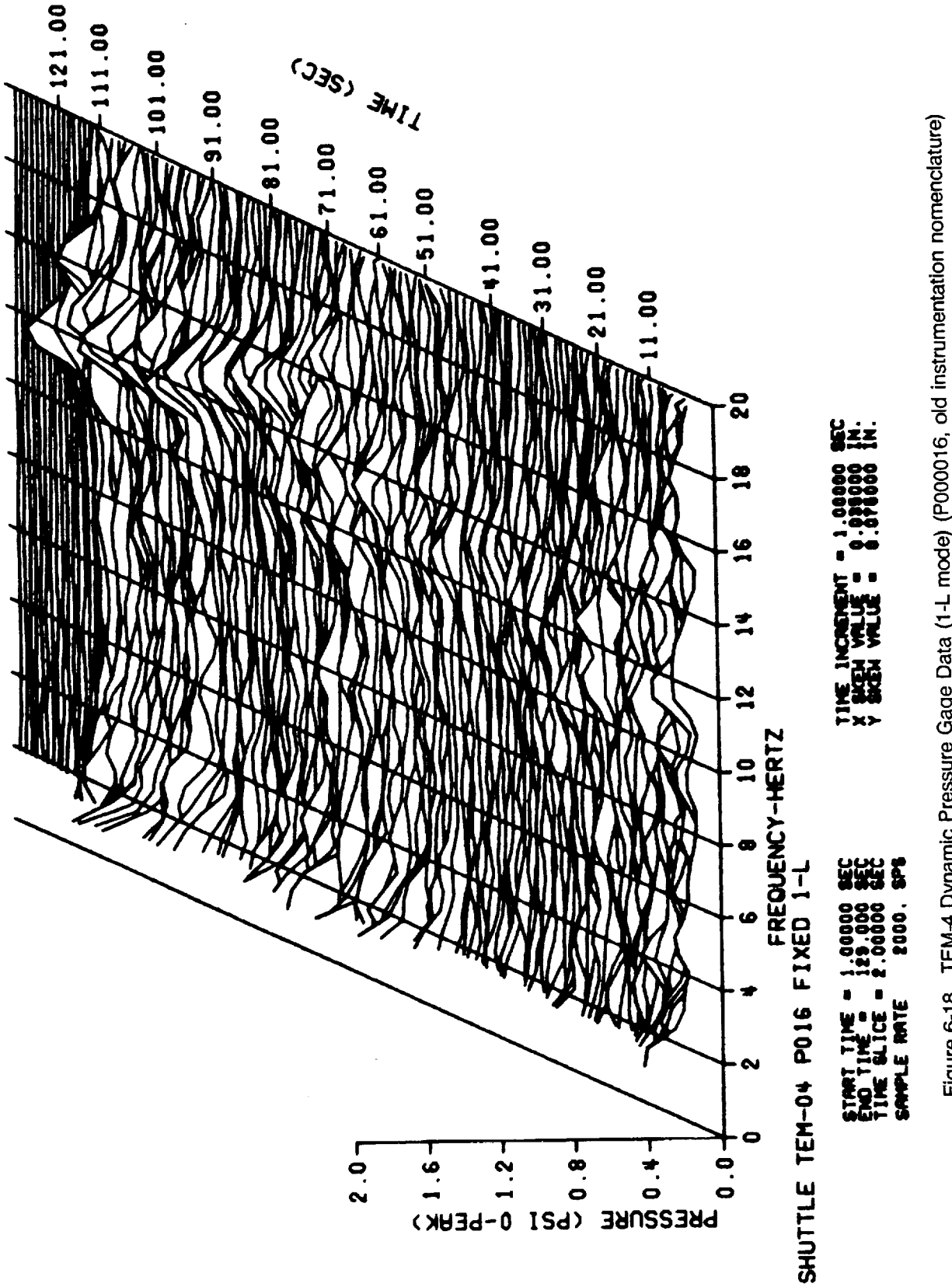

Figure 6-18. TEM-4 Dynamic Pressure Gage Data (1-L mode) (P000016, old instrumentation nomenclature)

ORIGINAL PAGE IS
OF POOR QUALITY

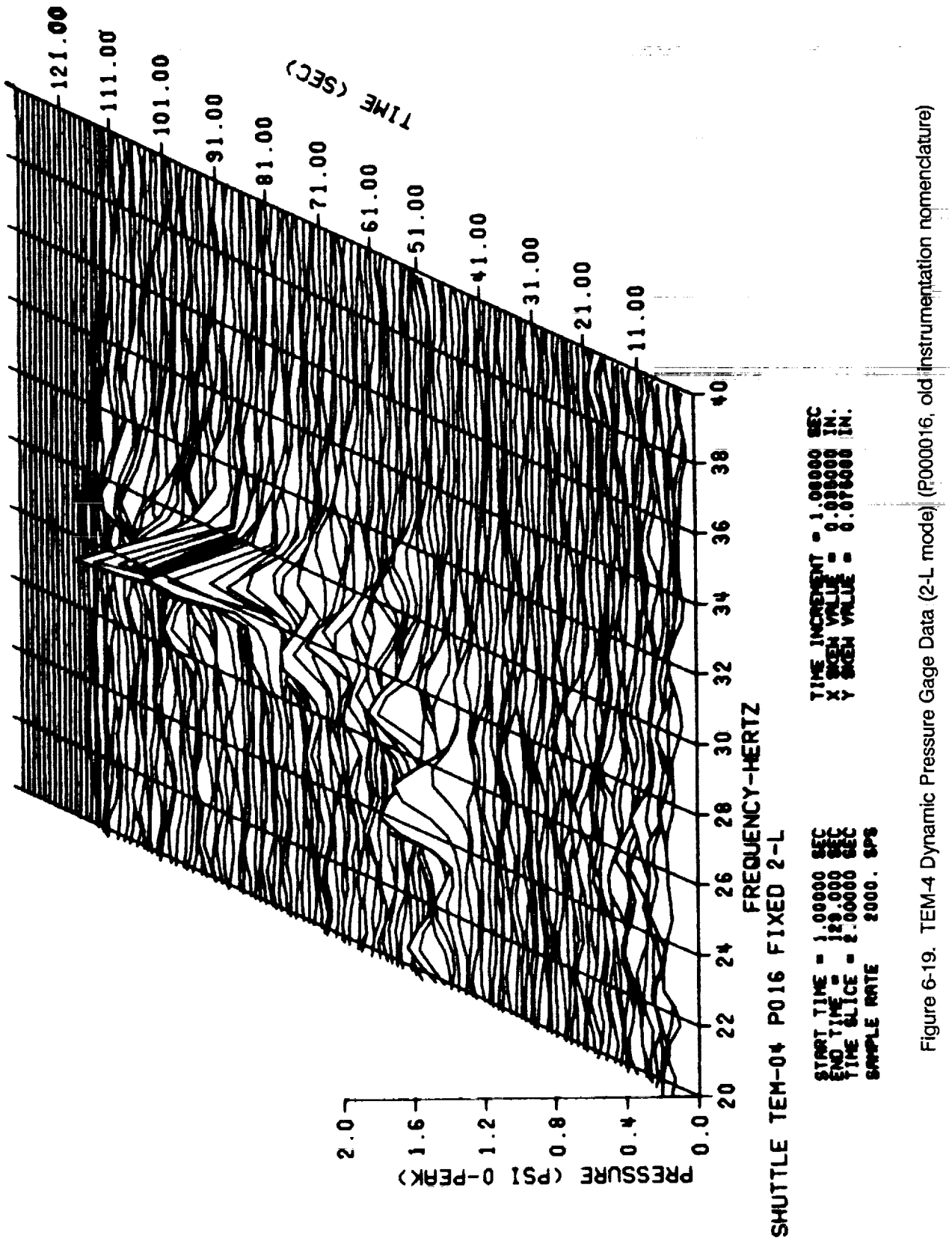

Figure 6-19. TEM-4 Dynamic Pressure Gage Data (2-L mode) (P000016, old instrumentation nomenclature)

Table 6-12. Maximum Pressure Oscillation Amplitude Comparison

Motor	Source of Measurement	Mode	Time of Measurement	Frequency (Hz)	Maximum Pressure (psi 0 to peak)
TEM-5	Waterfall	1-L	81	16.0	0.46
		2-L	100	29.5	0.57
TEM-4	Waterfall	1-L	115	14.5	0.37
		2-L	87	29.5	0.96
TEM-3	Waterfall	1-L	106	15.0	0.36
		2-L	102	30.0	0.58
TEM-2	Waterfall	1-L	78	16.0	0.43
		2-L	100	29.5	0.68
QM-8	Waterfall	1-L	104	14.5	
		2-L	55	27.5	
TEM-1	Waterfall	1-L	79	15.5	0.37
		2-L	95	29.5	0.78
STS-27 (left)	Waterfall ac OPT	1-L	82	15.5	0.37
		2-L	82	29.5	0.60
STS-27 (right)	Waterfall ac OPT	1-L	82	15.5	0.57
		2-L	83	29.5	0.72
STS-26 (left)	Waterfall ac OPT	1-L	79	16.0	0.70
		2-L	95	29.5	0.87
STS-26 (right)	Waterfall ac OPT	1-L	83	15.0	0.54
		2-L	94	30.0	0.47
PVM-1	Waterfall	1-L	99	14.5	1.23
		2-L	79	29.5	0.77
QM-7	Waterfall P000001	1-L	93	14.5	1.40
		2-L	79	29.5	0.95
QM-6	Waterfall	1-L	107	14.5	1.05
		2-L	85	29.5	0.53
DM-9	Waterfall	1-L	107	14.5	1.05
		2-L	96	30.0	0.64
DM-8	Waterfall	1-L	78	16.0	0.58
		2-L	97	29.5	0.62
ETM-1A	Waterfall	1-L	84	15.5	0.45
		2-L	101	29.5	0.61
DM-7	Waterfall	1-L	77	15.5	0.45
		2-L	96	29.0	0.62
DM-6	Waterfall	1-L	76	15.5	0.51
		2-L	86	29.0	0.78
QM-4	Waterfall	1-L	81	15.5	0.31
		2-L	80	29.5	0.30

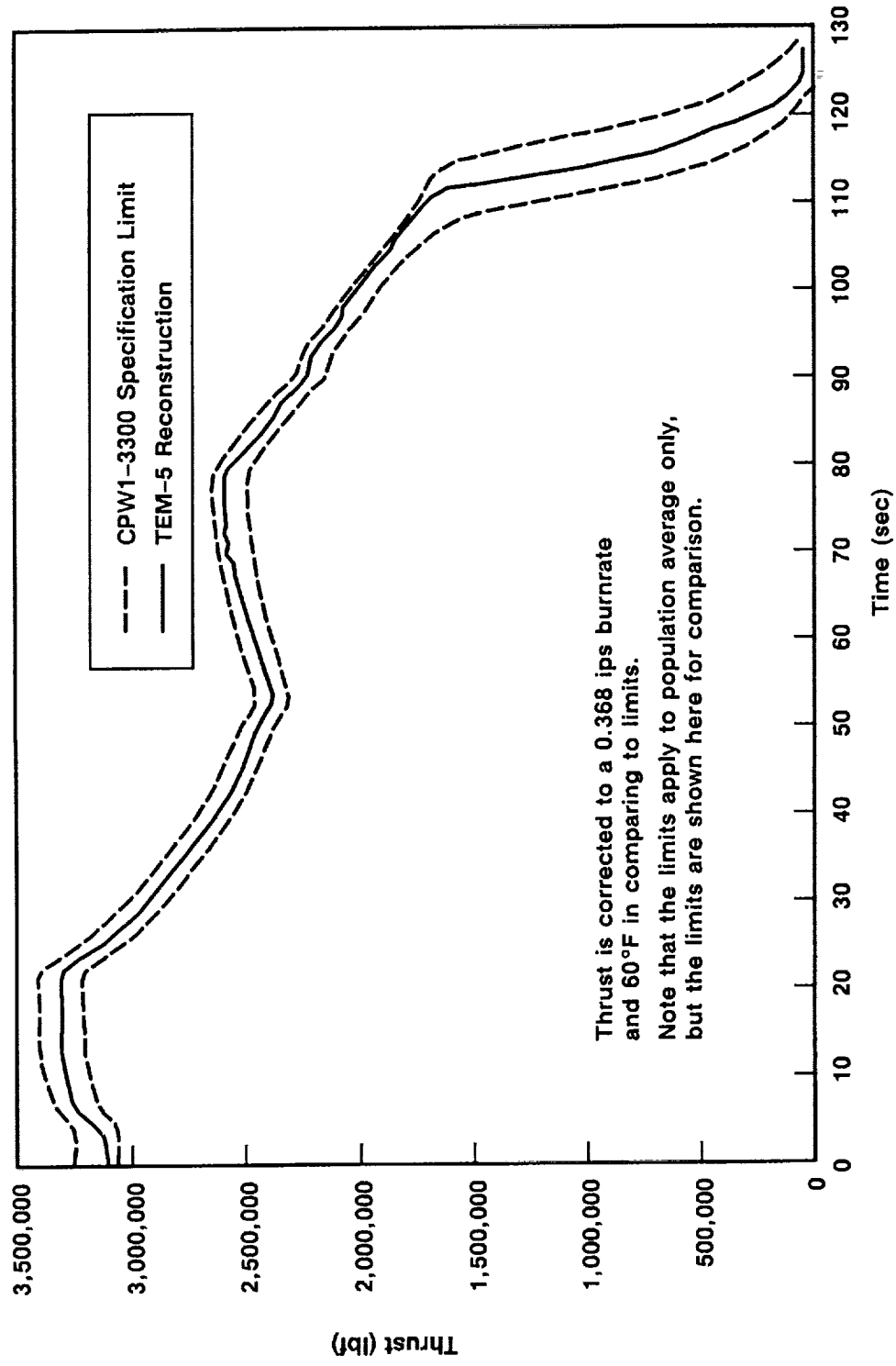

A026337a

Figure 6-20. TEM-5 Reconstructed Thrust Compared to CEI Specification Limits

motor performance tolerances or limit parameters were exceeded. The TEM-5 ignition performance satisfied the ignition interval and the maximum pressure rise rate requirements shown in Table 6-11.

6.8 STATIC TEST SUPPORT EQUIPMENT

6.8.1 Introduction

The TEM-5 deluge system and related instrumentation was similar to previous TEMs except for two additional thermocouples and a pressure transducer on the end of the deluge spray plumbing.

6.8.2 Objectives

None of the test objectives from Section 2 addressed the static test support equipment.

6.8.3 Conclusions/Recommendations

The deluge system including the CO_2 quench performed adequately, and there was no indication of excessive case heating.

On future TEMs, it is recommended that a pressure transducer continue to be installed on the end of the water deluge system plumbing. This transducer can be used to verify the pressure during steady state conditions with the boost pump running. Results from this transducer can be used to determine if additional nozzles can be added to the system to further insure the proper cooling of the motor case aft end.

6.8.4 Results/Discussion

Overall operation of the deluge system was satisfactory.

Case Temperature--Figure 6-21 shows the peak initial case temperatures versus slag weights for the previously static tested motors since the redesign of the deluge system. The initial case temperature for TEM-5 was approximately 48°F, and the peak case temperature was approximately 222°F (shown on the plot of data channel TNJAK001, included in the appendix). The peak case temperature occurred in the ET attach ring area. Case temperatures were well below 500°F, the temperature at which the paint browns; and 1,000°F, the temperature at which the steel is damaged. The two thermocouples added at the aft end of the motor case (data channels

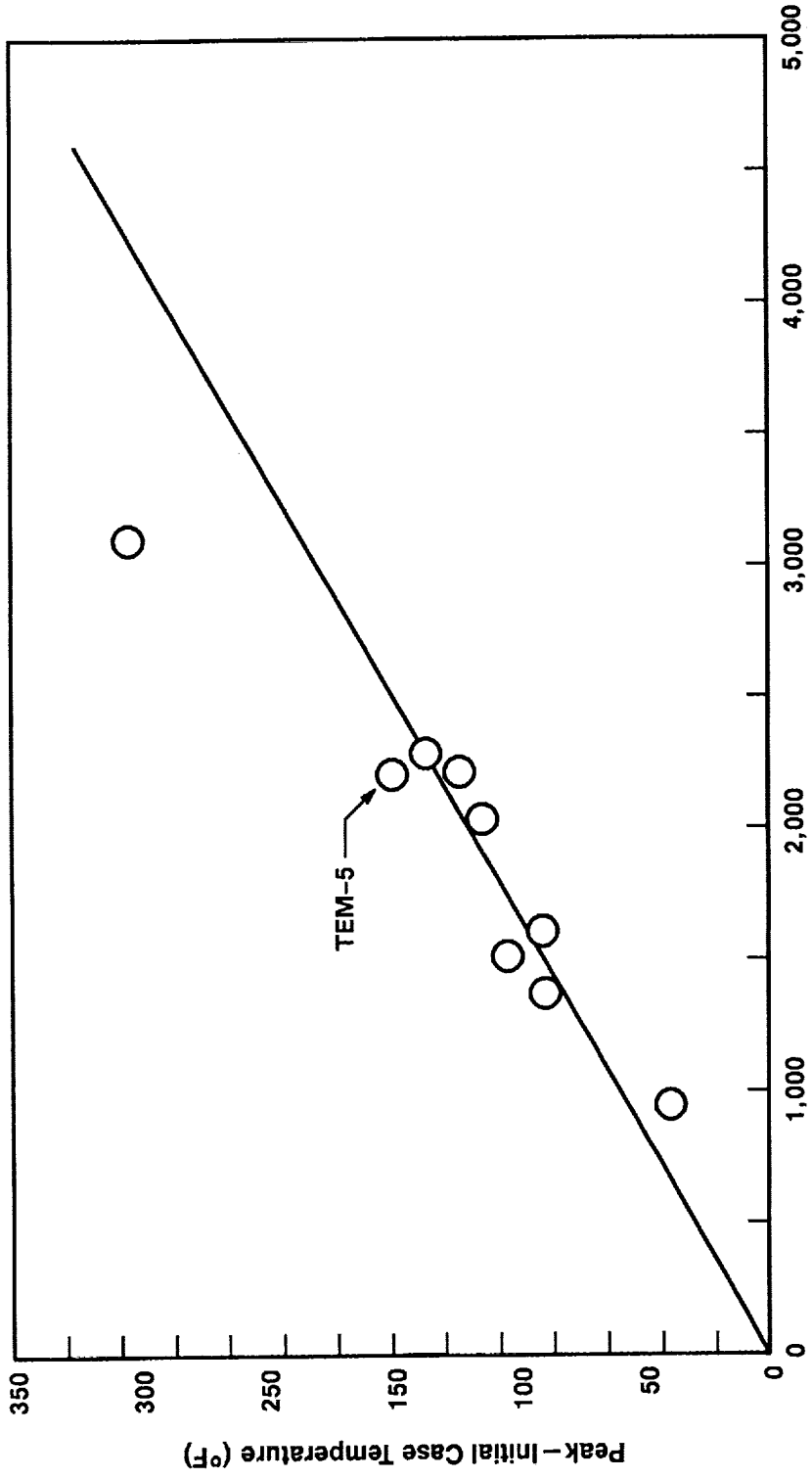

Figure 6-21. Maximum Delta Case Temperature Obtained Versus Amount of Slag

TNLAM003 and TNLAM004, plots included in the appendix) showed peak temperatures right after firing of approximately 81°F.

An interesting observation is that when the deluge system is shut off, the aft thermocouples rise in temperature nearly at the same rate as the thermocouple near the ET attach ring area; thus showing the vital need to have the thermal curtain placed correctly (as far aft as possible).

Boost Pump Performance--The boost pump performance or water flow within the deluge system lines did not perform as expected. On previous TEMs, the main manifold water pressure would immediately rise to approximately 84 psi and remain there. The pressure trace for the TEM-5 main manifold (data channel PNPAX002, plot shown in the appendix) started at approximately 70 psi and then gradually rose. The slower pressure rise rate for TEM-5 resulted in a slightly higher peak case temperature than expected. The pressure in the main manifold was monitored and was approximately 74 psi at 175 sec. Normally the main manifold system would have been 84 psi at around 175 sec. The lower pressure was primarily due to problems with the operation of the boost pump.

Deluge System Pressure--A water pressure transducer (data channel PNPAX003, plot shown in the appendix) was installed at the end of the deluge spray plumbing to gather data for possible expansion of the deluge system. This transducer gave good data until T+175 sec, when the data channel became noisy and erratic. The pressure transducer data were steadily increasing (as was the pressure in the main manifold) before the transducer failed. The maximum measured pressure was approximately 68 psi. The most likely cause of the noisy and erratic data was moisture penetration into the electrical connector. Data from this transducer could not be used to determine if additional nozzles could be added to the deluge system.

7

APPLICABLE DOCUMENTS

Document No.	Title
5613-FY90-M82	TEM-4 Pressure Oscillation Study (Memo)
CPW1-3600	Prime Equipment Contract End Item Detail Specification (CEI)
CPW1-3300	Prime Equipment Contract End Item Detail Specification Part I of Two Parts; Performance, Design and Verification Requirements Space Shuttle High Performance, Solid Rocket Motor Lightweight CPW1-3300 for Space Shuttle Solid Rocket Motor Project Operational Flight (Change Log J, 15 Jan 1986)
CTP-0105	Space Shuttle Technical Evaluation Motor #5 (TEM-5) Static Fire Test Plan
CTP-0138	Qualification Test Plan for the Improved Joint Heaters
CTP-0153	Qualification Test Plan for the Improved Joint Protection (JPS) Power Cables
ETP-0600	Thiokol/Wasatch FJPS Short Stack Demonstration Test Plan
ETP-0620	Evaluation of the New FJPS Closeout Concept Test Plan
MIL-F-18240	Fastener, Externally Threaded, 250°F Self Locking Element for
NAS 1283	Fasteners, Male Threaded, Self-Locking
STW7-2632	Space Shuttle SRM Supplier Configuration Management Requirements (Chemical Raw Materials)
STW4-2679	Silicon Dioxide, Microfine
STW4-2700	Cork, Sheet
STW7-2744	Acceptance Criteria, Refurbished Case, Space Shuttle SRM
STW7-2790	Ignition System Gaskets, Reusable, Acceptance Criteria for
STW7-2787	Leak Testing, Igniter Assembly Seal Space Shuttle Project Solid Rocket Motor

STW7-2831 Rev NC	Inspection and Process Finalization Criteria, Insulated Components, Space Shuttle Solid Propellant Rocket Motor
STW7-2853	Leak Test, Pressure Transducer Assemblies, Space Shuttle Project Solid Rocket Motor
STW7-2913	Procedure, Leak Test of Barrier-Booster Redundant Seals
STW7-3133	Barrier-Booster Assembly, Refurbishment and Acceptance Criteria for
STW4-3183	Ablation Compound, Cork-Filled
STW4-3218	Epoxy Resin Adhesive, Non-Asbestos, Structural Bonding
STW7-3633	Leak Testing, Safe and Arm Joint, Space Shuttle Project Redesigned Solid Rocket Motor
STW7-3682	Leak Testing, Case-Field and Nozzle-to-Case Joint, Test Evaluation Motor (TEM) Program
STW7-3688	Grease Application and O-ring Installation for Field and Case-to-Nozzle Joints Space Shuttle TEM Program
STW7-3745	Putty, Aft Segment and Nozzle Assembly Joint, Application of
STW7-3746	Putty Vacuum Seal, Field Joint Assembly, Application of
TWR-15723 Rev C	Development and Verification Plan (D&V Plan)
TWR-16474 Vol I-IX	Technical Evaluation Motor Postfire Engineering Evaluation Plan
TWR-19941	Qualification of the RSRM Field Joint Heater and Igniter-to-Case Joint Heater Improved Power Cables Final Test Report
TWR-19899	Qualification of Improved Joint Heaters Final Test Report
TWR-50138	Thiokol/Wasatch Installation Evaluation of the Redesigned Field Joint Protection System (Concepts 1 and 3) Final Test Report
TWR-50290	Thiokol/Wasatch Installation Evaluation of the Field Joint Protection System (Concepts 1 and 1C) Final Test Report

Drawing No.	Title
1U51926	Gasket - Inner
1U51927	Gasket - Outer

1U75150	Packing, Preformed Fluorocarbon
1U52293	Barrier-Booster Assembly S/A Device
1U52295	S/A Device
2U65686	Transducer Leak Test Fixture
2U65848	Leak Test Assy - Barrier Boost Assy, S/A Device
1U75801	Packing, Lubricated
8U75902	Leak Check System, Installation
8U76500	Leak Check System, Safe & Arm Device, Installation
8U75902	Leak Check System, Installation
7U76879	Test Assy - SRM, TEM
1U77114	Retainer Strap Assy - Heater
1U82837	Strap, Moisture Seal Retainer
1U100269	Plug, Machine Thread
2U129714	Assembly, RSRM Joint Leak Check System
2U129760	Static Test Arrangement
2U132222	Putty Tamping Tool

Appendix A

Drawing Trees

REVISION

DRAWING TREES

TEM-5

REV R DATE 10-27-89

PREPARED BY: Hilde Beutler 10-30-89

H. BEUTLER
CCB PROJECT ENGINEER

APPROVED BY: J F Rittenhouse

J. F. RITTENHOUSE
PROJECT ENGINEER

AUTOMATED BY: Stephanie Pierson

T. PIERSON
SYSTEM INTEGRATION

Thiokol CORPORATION
SPACE OPERATIONS

DOC NO. TWR-17649
SEC
PAGE A-2
VOL

Thiokol CORPORATION
SPACE OPERATIONS

REV R TEM-5 SHEET 1 OF 1

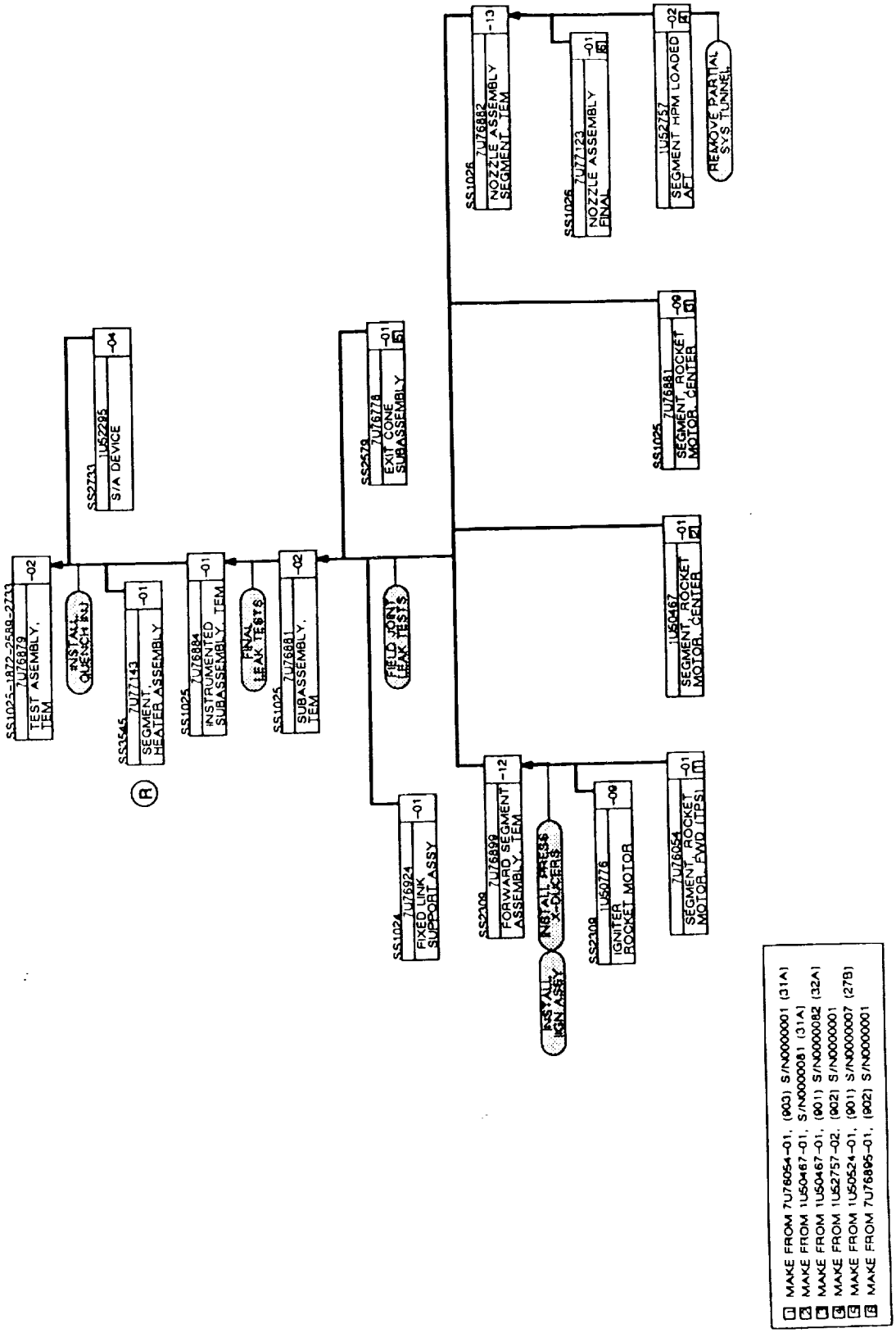

Appendix B

Instrumentation List

TABLE A --TEM-C5 INSTRUMENTATION LIST
(SEE LAST PAGE FOR NOTES AND DEFINITIONS)

OLD INST. NO.	NEW INST. NO.	(ANG LOC)	STATION	MEAS DIR	EXPECTED RANGE	REQ ACC	FM (Hz)	DIG (SPS)	REMARKS	PRIORITY NOTES	INSTALLED DRAWING
D000230	DANAU001	0.0	1867.41	AXIAL	+/- 2IN	+/-1%		250	NOZZLE AXIAL DISPLACEMENT	R	
D000231	DANAU002	90.0	1867.41	AXIAL	+/- 2IN	+/-1%		250	NOZZLE AXIAL DISPLACEMENT	R	
D000232	DANAU003	180.0	1867.41	AXIAL	+/- 2IN	+/-1%		250	NOZZLE AXIAL DISPLACEMENT	R	
D000233	DANAU004	270.0	1867.41	AXIAL	+/- 2IN	+/-1%		250	NOZZLE AXIAL DISPLACEMENT	R	
P000001	PNCAC001	40.0	487.00		0-1,000 PSI	+/-2%	2K	2K	CHAMBER PRESSURE/OSCILLATION (OPT)	M,1,3,5	1U76899
P000002	PNCAC002	270.0	487.00		0-1,000 PSI	+/-1%		2K	CHAMBER PRESSURE	M,5,9	1U76899
P000003	PNCAC003	180.0	487.00		0-1,000 PSI	+/-1%		2K	CHAMBER PRESSURE	M,5,9	1U76899
P000005	PNCAC004	115.0	487.00		0-3,000 PSI	+/-2%	2K	2K	IGNITER PRESSURE	R,1,5	1U76899
P000016	PNCAC005	100.0	487.00		+/-10 PSI	+/-2%	100	1K	CHAMBER OSCILLATION	M,1,5,12	1U76899
P000020	PNPAX002	N/A	N/A		0-500 PSIG	+/-5%		250	WATER DELUGE MANIFOLD, INLET	M,4,7	
	PNPAX003	N/A	N/A		0-500 PSIG	+/-5%		250	WATER DELUGE MANIFOLD, CTR. LINE, AFT	R,4	
P000024	PNNAR001	90.0	1875.05		0-1,000 PSIA	+/-2%		125	NOZZLE CASE JT LEAK CHK	R	
T000638	TNJAK001	0.0	1511.00		0-1200 DEG F	+/-5%			SLAG TEMP,AFT SEGMENT	M,8,10	
T000830	TNEAI002	0.0	772.00		0-1200 DEG F	+/-5%			SLAG TEMP,FORWARD SEGMENT	M,8,9	
T000831	TNHAI002	0.0	1091.00		0-1200 DEG F	+/-5%			SLAG TEMP,CENTER/FWD SEG	M,8,9	
T000832	TNIAI001	0.0	1411.00		0-1200 DEG F	+/-5%			SLAG TEMP,CENTER/AFT SEG	M,8,9	
T000833	TNJAK003	17.3	1511.00		0-1200 DEG F	+/-5%			SLAG TEMP,AFT SEGMENT	M,8,10	
T000834	TNJAK004	28.3	1511.00		0-1200 DEG F	+/-5%			SLAG TEMP,AFT SEGMENT	M,8,10	
T000835	TNJAK005	334.9	1511.00		0-1200 DEG F	+/-5%			SLAG TEMP,AFT SEGMENT	M,8,10	
T000836	TNJAK006	349.8	1511.00		0-1200 DEG F	+/-5%			SLAG TEMP,AFT SEGMENT	M,8,10	
T000837	TNJAK007	0.0	1529.00		0-1200 DEG F	+/-5%			SLAG TEMP,AFT SEGMENT	M,8,10	
T000838	TNJAI003	0.0	1547.00		0-1200 DEG F	+/-5%			SLAG TEMP,AFT SEGMENT	M,8,10	
T000839	TNKAL001	0.0	1598.00		0-1200 DEG F	+/-5%			SLAG TEMP,AFT SEGMENT	M,8,9	
T000840	TNKAM001	0.0	1652.00		0-1200 DEG F	+/-5%			SLAG TEMP,AFT SEGMENT	M,8,9	
T000841	TNKAM003	0.0	1727.00		0-1200 DEG F	+/-5%			SLAG TEMP,AFT SEGMENT	M,8,9	
T000842	TNJAI004	344.0	1563.00		0-1200 DEG F	+/-5%			SLAG TEMP,AFT SEGMENT	M,8,9	
T000843	TNJAI005	13.3	1566.00		0-1200 DEG F	+/-5%			SLAG TEMP,AFT SEGMENT	M,8,9	
T000844	TNJAI006	354.9	1538.00		0-1200 DEG F	+/-5%			SLAG TEMP,AFT SEGMENT	M,8,10	
T000845	TNJAK008	27.0	1535.00		0-1200 DEG F	+/-5%			SLAG TEMP,AFT SEGMENT	M,8,10	

TABLE A --TEM-05 INSTRUMENTATION LIST
(SEE LAST PAGE FOR NOTES AND DEFINITIONS)

OLD INST. NO.	NEW INST. NO.	(ANG LOC)	STATION	MEAS DIR	EXPECTED RANGE	REQ ACC	FM (Hz)	DIG (SPS)	REMARKS	PRIORITY NOTES	INSTALLED DRAWING
T000845	TNJAK009	339.2	1533.00		0-1200 DEG F	+/-5%			SLAG TEMP,AFT SEGMENT	M,8,10	
	TNLAM003	0.0	1735.50		0-1200 DEG F	+/-5%			SLAG TEMP,AFT SEGMENT	M,8,9	
	TNLAM004	0.0	1797.50		0-1200 DEG F	+/-5%			SLAG TEMP,AFT SEGMENT	M,8,9	
T000875	TNCAC001	94.5	487.00		0-200 DEG F	+/-5%			IGNITER HEATER TEMP	M,6,8,9	
T000878	TNCAC006	274.5	487.00		0-200 DEG F	+/-5%			IGNITER HEATER TEMP	M,6,8,9	
T001001	TNEAJ011	15.0	848.00		0-200 DEG F	+/-5%			FWD FIELD JOINT HEATER TEMP	M,5,6,8,9	7U76997
T001002	TNEAJ012	135.0	848.00		0-200 DEG F	+/-5%			FWD FIELD JOINT HEATER TEMP	M,5,6,8,9	7U76997
T001003	TNEAJ013	195.0	848.00		0-200 DEG F	+/-5%			FWD FIELD JOINT HEATER TEMP	M,5,6,8,9	7U76997
T001004	TNEAJ014	285.0	848.00		0-200 DEG F	+/-5%			FWD FIELD JOINT HEATER TEMP	M,5,6,8,9	7U76997
T001005	TNGAJ010	15.0	1168.00		0-200 DEG F	+/-5%			CTR FIELD JOINT HEATER TEMP	M,5,6,8,9	7U76997
T001006	TNGAJ011	135.0	1168.00		0-200 DEG F	+/-5%			CTR FIELD JOINT HEATER TEMP	M,5,6,8,9	7U76997
T001007	TNGAJ012	195.0	1168.00		0-200 DEG F	+/-5%			CTR FIELD JOINT HEATER TEMP	M,5,6,8,9	7U76997
T001008	TNGAJ013	285.0	1168.00		0-200 DEG F	+/-5%			CTR FIELD JOINT HEATER TEMP	M,5,6,8,9	7U76997
T001009	TNIAJ013	15.0	1488.00		0-200 DEG F	+/-5%			AFT FIELD JOINT HEATER TEMP	M,5,6,8,9	7U76997
T001010	TNIAJ014	135.0	1488.00		0-200 DEG F	+/-5%			AFT FIELD JOINT HEATER TEMP	M,5,6,8,9	7U76997
T001011	TNIAJ015	195.0	1488.00		0-200 DEG F	+/-5%			AFT FIELD JOINT HEATER TEMP	M,5,6,8,9	7U76997
T001012	TNIAJ016	285.0	1488.00		0-200 DEG F	+/-5%			AFT FIELD JOINT HEATER TEMP	M,5,6,8,9	7U76997
T001300	TNNAR001	270.0	1875.00		0-200 DEG F	+/-5%			NOZZLE-CASE JOINT HEATER TEMP	M,5,6,8,9	7U76997
T001301	TNNAR002	275.0	1875.00		0-200 DEG F	+/-5%			NOZZLE-CASE JOINT HEATER TEMP	M,5,6,8,9	7U76997
X000001	XNPAX001	N/A	N/A		+/-0.1 SEC			32	PRIMARY IGNITION (T-0)	M,4	
X000026	XNPAX004	N/A	N/A		+/-0.1 SEC				(T-0) FM1	M,4	

TABLE A --TEM-05 INSTRUMENTATION LIST
(SEE LAST PAGE FOR NOTES AND DEFINITIONS)

OLD INST. NO.	NEW INST. NO.	(ANG LOC)	STATION	MEAS DIR	EXPECTED RANGE	REQ ACC	FM (Hz)	DIG (SPS)	REMARKS	PRIORITY NOTES	INSTALLED DRAWING

PRIORITY:

M - MANDATORY, APPROVAL BY VP SPACE PROGRAMS, VP SPACE ENGINEERING, AND NASA SRM PROJECT MANAGER REQUIRED FOR ELIMINATION.

R - REQUIRED, APPROVAL BY PROGRAM MANAGER AND PROJECT ENGINEER REQUIRED FOR ELIMINATION OF MEASUREMENT.

FIRST LETTER OF INSTRUMENT DESIGNATION - SEE TWR-19910 FOR A COMPLETE DESCRIPTION:
D - DISPLACEMENT P - PRESSURE S - STRAIN T - TEMPERATURE X - EVENT

NOTES:

1. THE NOTED INSTRUMENTS WILL BE RECORDED REDUNDANTLY ON FM WITH AN ACCURACY OF +/- 5%.
2. THE NOTED INSTRUMENT IS PART OF THE THRUST STAND.
3. THE REDUNDANT SIGNAL SHALL BE AC COUPLED TO REMOVE THE DC COMPONENT.
4. THE NOTED MEASUREMENT IS PART OF THE TEST BAY FACILITY.
5. THE NOTED INSTRUMENTS ARE REFERENCED ON THE FIELD OF THE DRAWING, BUT WERE INSTALLED ON A PREVIOUS DRAWING.
6. THE NOTED INSTRUMENT SHALL BE MONITORED DURING HEATER OPERATION AS WELL AS DURING MOTOR FIRING.
7. THE NOTED INSTRUMENT SHALL BE MONITORED ON ENGINEERING UNITS DISPLAY (EUD).

TABLE A --TEM-05 INSTRUMENTATION LIST
(SEE LAST PAGE FOR NOTES AND DEFINITIONS)

OLD INST. NO.	NEW INST. NO.	(ANG LOC)	STATION	MEAS DIR	EXPECTED RANGE	REQ ACC	FM (Hz)	DIG (SPS)	REMARKS	PRIORITY NOTES	INSTALLED DRAWING

8. THE NOTED INSTRUMENT SHALL BE MONITORED WITH TEST AREA SOLARTRON SYSTEM AND RECORDED FROM T-15 MIN TO AT LEAST T + 6 MIN.

9. ONE SENSOR FROM EACH OF THE FOLLOWING COLUMNS MUST BE OPERATIONAL TO MEET THE MANDATORY REQUIREMENT:

PNCAC002	TNEAI002	TNKAL001	TNCAC001	TNEAJ011	TNGAJ010	TNIAJ013	TNMA0001	TNLAM003
PNCAC003	TNHAI002	TNKAM001	TNCAC006	TNEAJ012	TNGAJ011	TNIAJ014	TNMA0002	TNLAM004
	TNIAI001	TNKAM003		TNEAJ013	TNGAJ012	TNIAJ015		
		TNJAI004		TNEAJ014	TNGAJ013	TNIAJ016		
		TNJAI005						

10. THREE SENSORS FROM EACH OF THE FOLLOWING COLUMNS MUST BE OPERATIONAL TO MEET THE MANDATORY REQUIREMENT:

TNJAK001	TNJAK007
TNJAK003	TNJAI003
TNJAK004	TNJAI006
TNJAK005	TNJAK008
TNJAK006	TNJAK009

11. THE OLD INSTRUMENT NUMBERS ARE FOR REFERENCE ONLY. THE INSTRUMENTS SHALL BE IDENTIFIED BY THE NEW NUMBERS.

12. THE NOTED INSTRUMENT SHALL BE AC COUPLED TO REMOVE THE DC COMPONENT.

Appendix C

Data Plots (listed in the order presented in the instrumentation list)

7.4.2.1.A

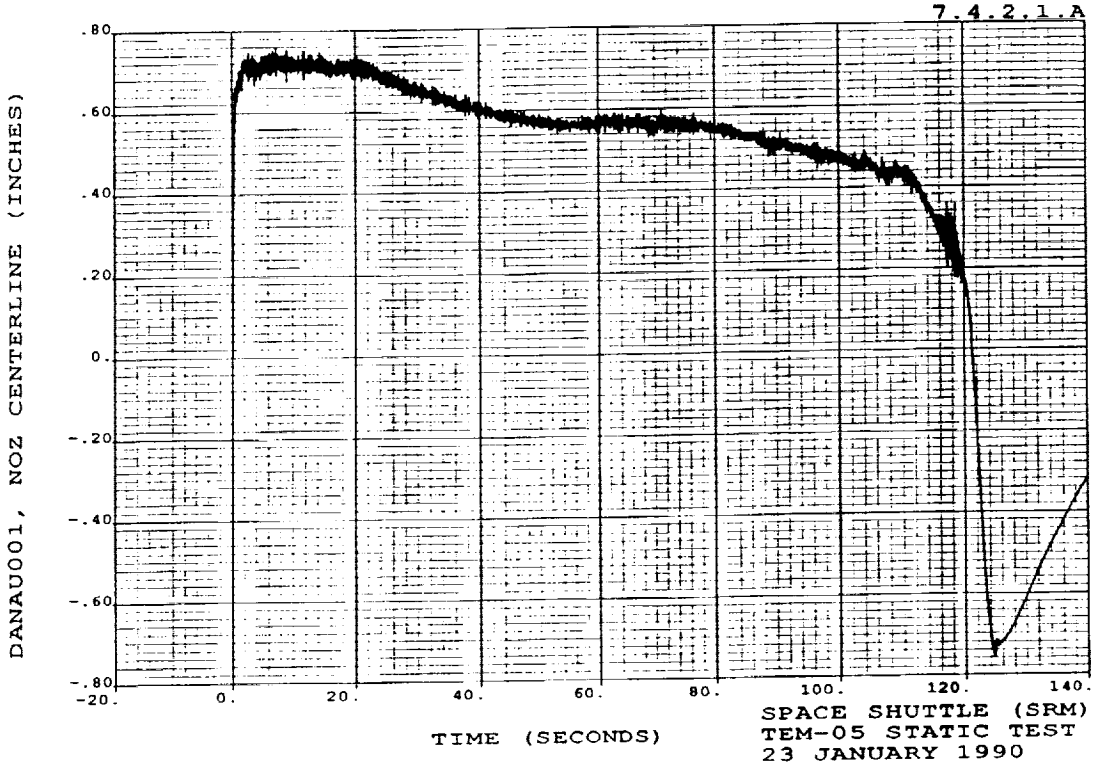
DANAU001, NOZ CENTERLINE (INCHES)
.80
.60
.40
.20
0.
-.20
-.40
-.60
-.80
-20.
0.
20.
40.
60.
80.
100.
120.
140.
TIME (SECONDS)
SPACE SHUTTLE (SRM)
TEM-05 STATIC TEST
23 JANUARY 1990

7.4.2.1.A

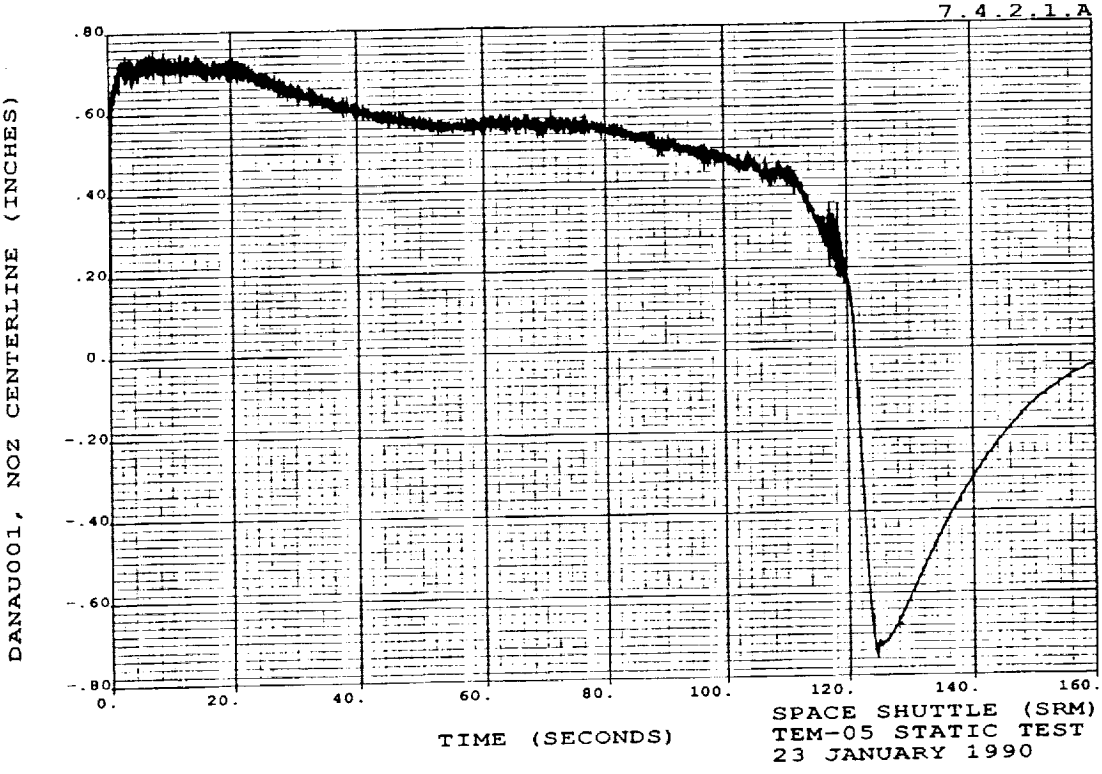
DANAU001, NOZ CENTERLINE (INCHES)
.80
.60
.40
.20
0.
-.20
-.40
-.60
-.80
0.
20.
40.
60.
80.
100.
120.
140.
160.
TIME (SECONDS)
SPACE SHUTTLE (SRM)
TEM-05 STATIC TEST
23 JANUARY 1990

7.4.2.1.A

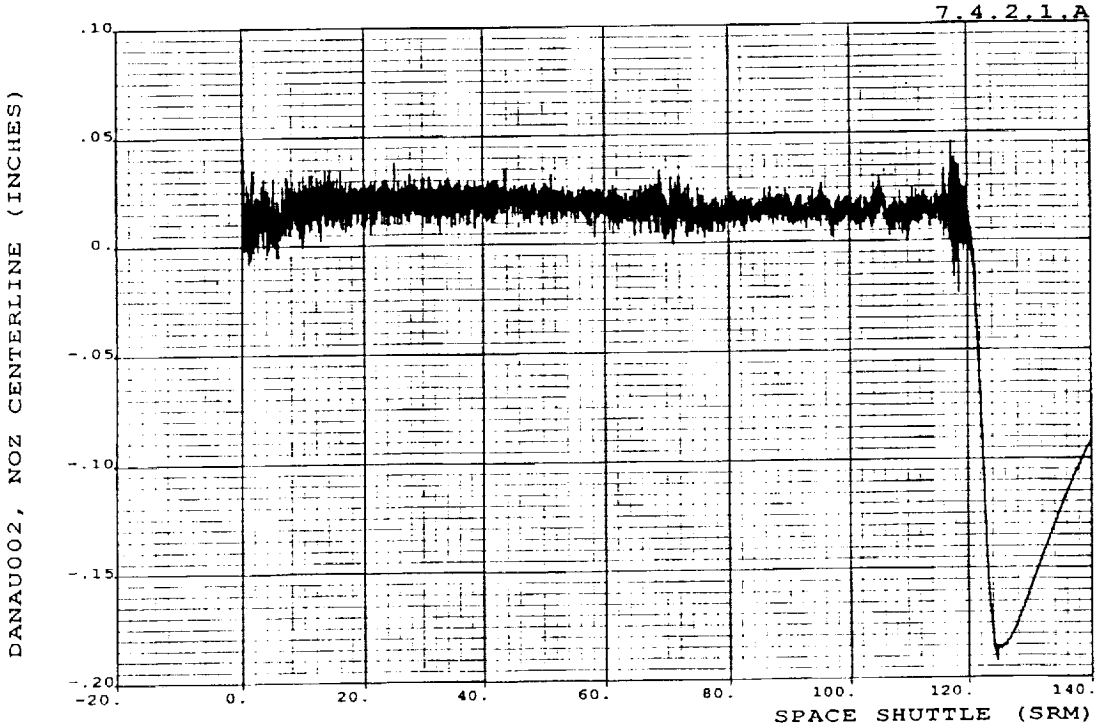

SPACE SHUTTLE (SRM)
TEM-05 STATIC TEST
23 JANUARY 1990

7.4.2.1.A

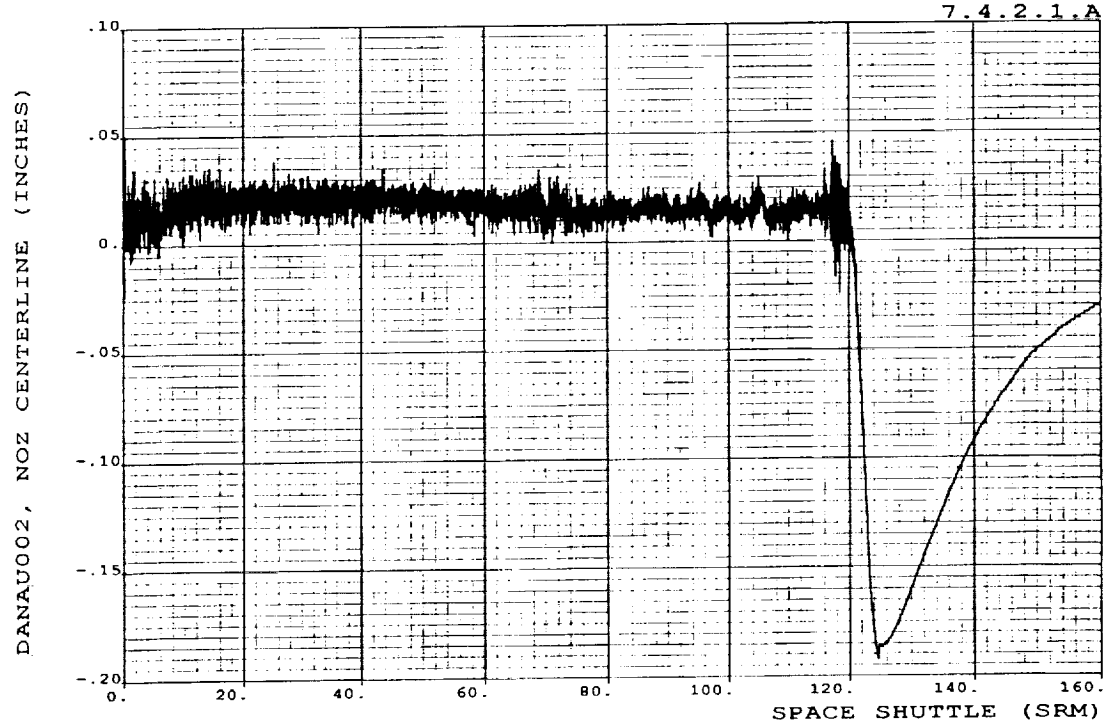

SPACE SHUTTLE (SRM)
TEM-05 STATIC TEST
23 JANUARY 1990

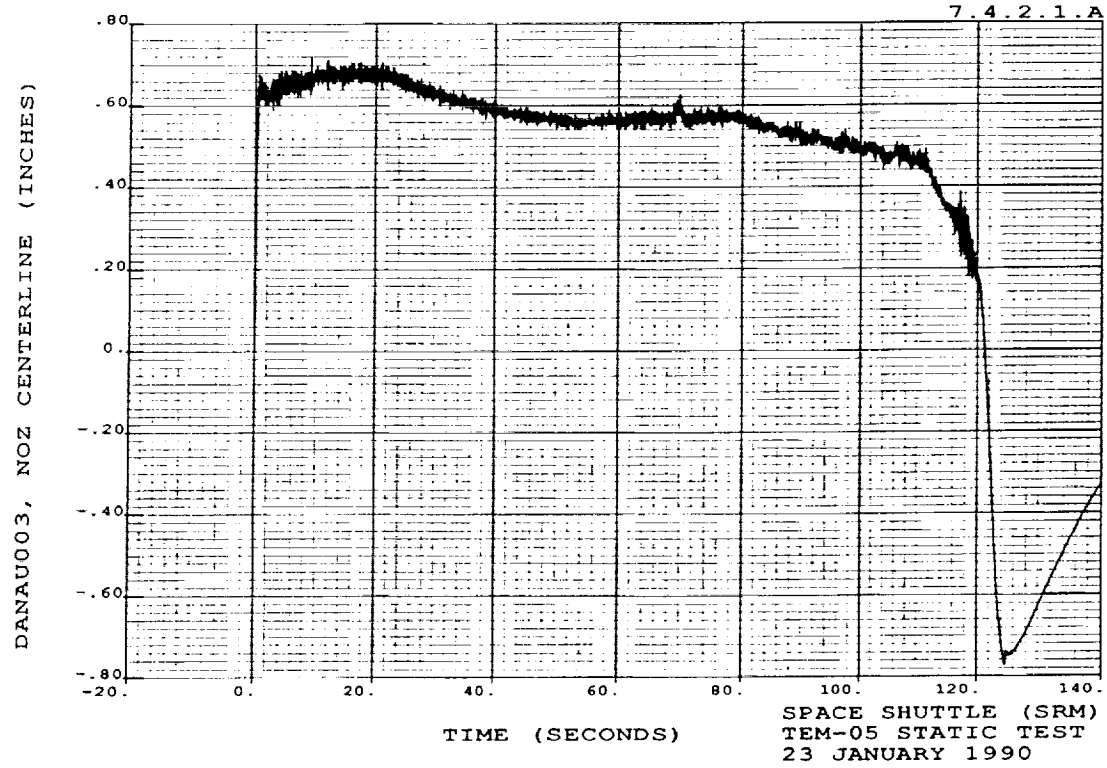
7.4.2.1.A
DANAU003, NOZ CENTERLINE (INCHES)
.80
.60
.40
.20
0.
-.20
-.40
-.60
-.80
-20.
0.
20.
40.
60.
80.
100.
120.
140.
TIME (SECONDS)
SPACE SHUTTLE (SRM)
TEM-05 STATIC TEST
23 JANUARY 1990

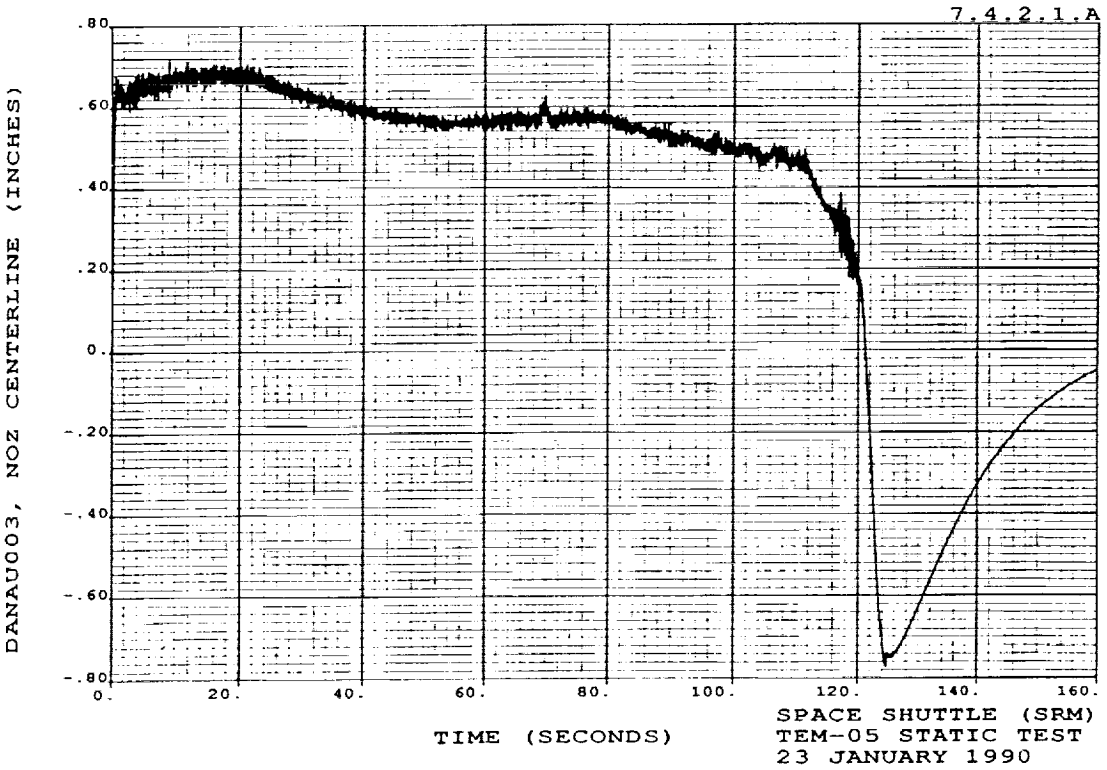
7.4.2.1.A
DANAU003, NOZ CENTERLINE (INCHES)
.80
.60
.40
.20
0.
-.20
-.40
-.60
-.80
0.
20.
40.
60.
80.
100.
120.
140.
160.
TIME (SECONDS)
SPACE SHUTTLE (SRM)
TEM-05 STATIC TEST
23 JANUARY 1990

7.4.2.1.A

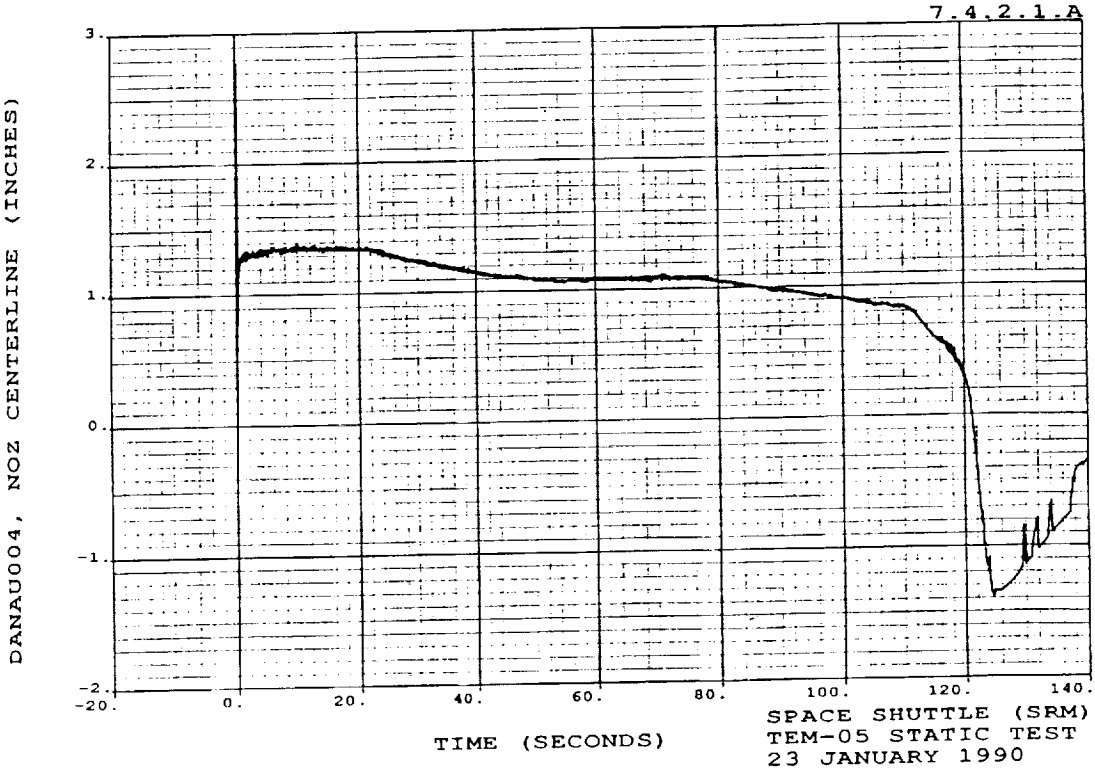

7.4.2.1.A

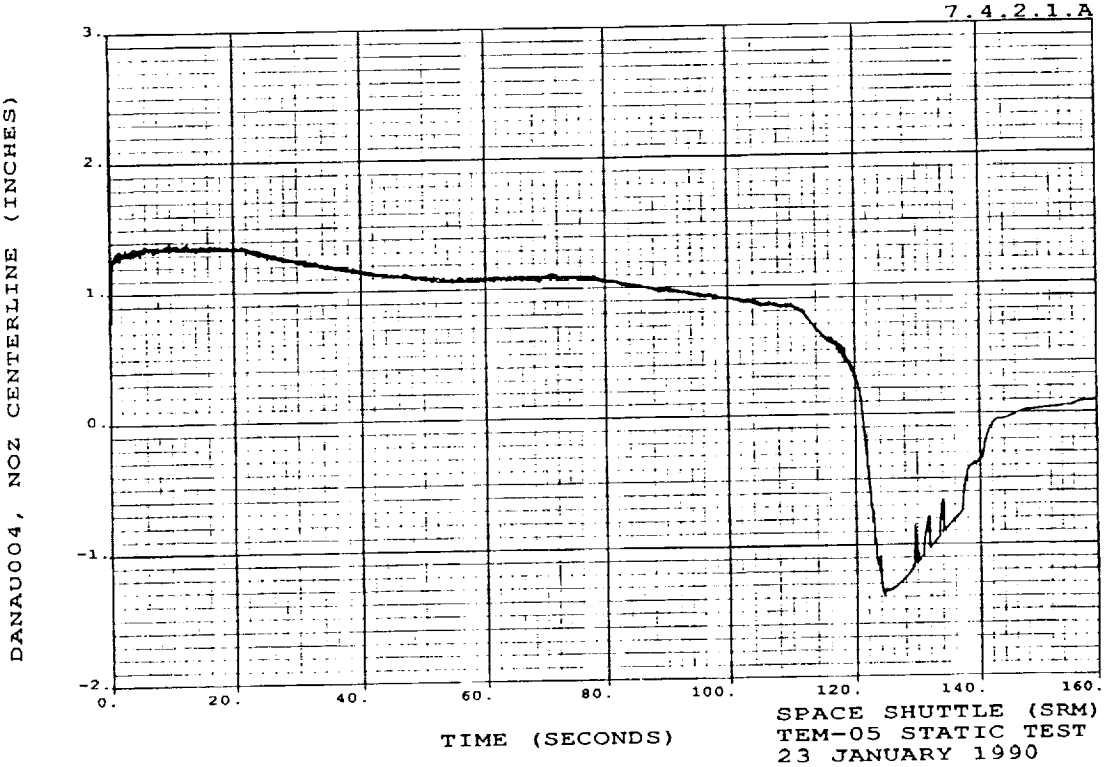

7.4.1.1.A

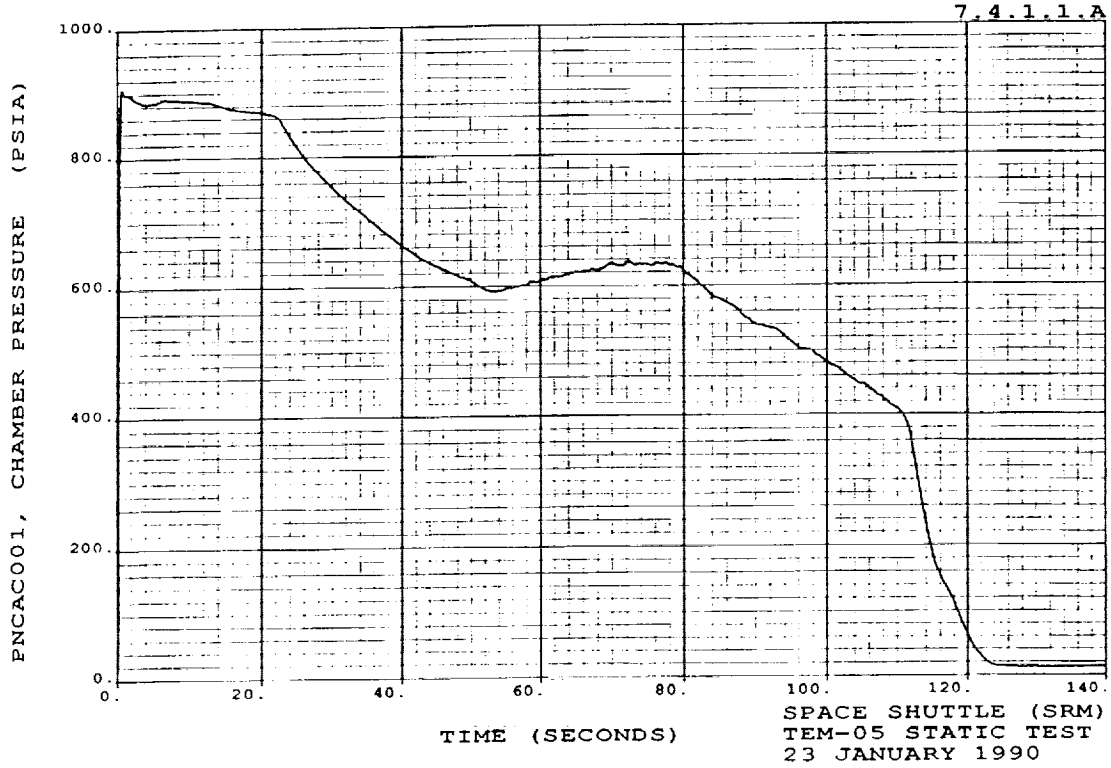

SPACE SHUTTLE (SRM)
TEM-05 STATIC TEST
23 JANUARY 1990

7.4.1.1.A

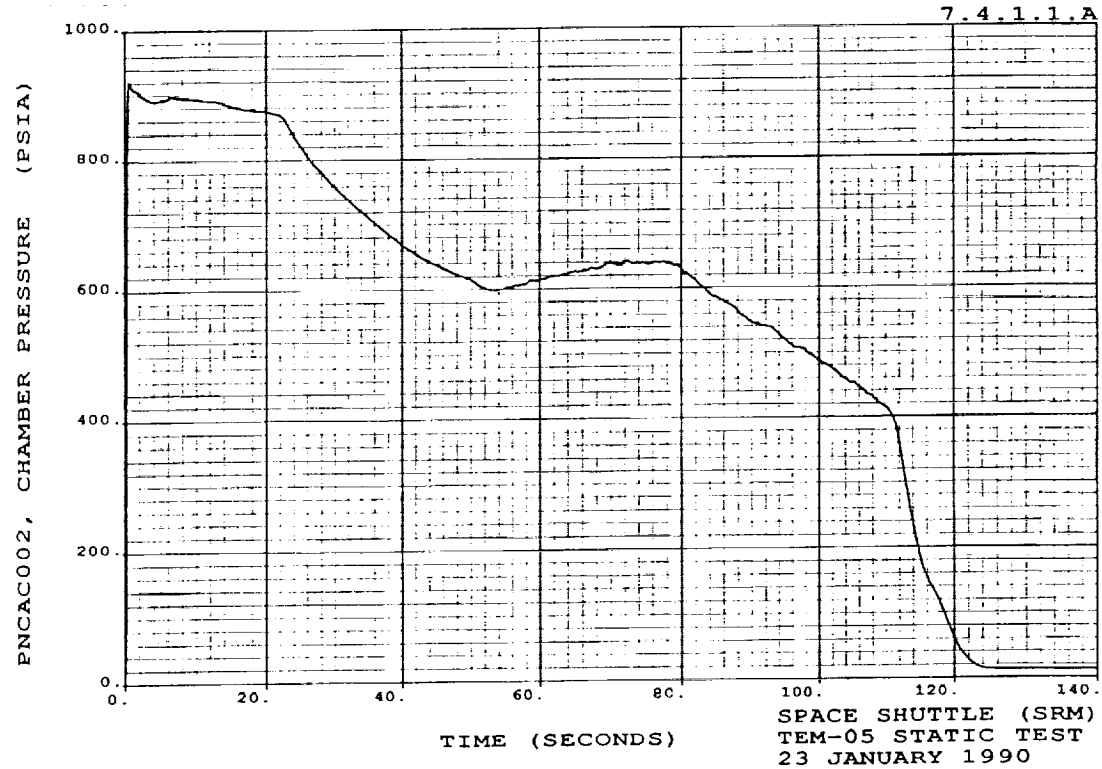

SPACE SHUTTLE (SRM)
TEM-05 STATIC TEST
23 JANUARY 1990

ORIGINAL PAGE IS
OF POOR QUALITY

7.4.1.1.A

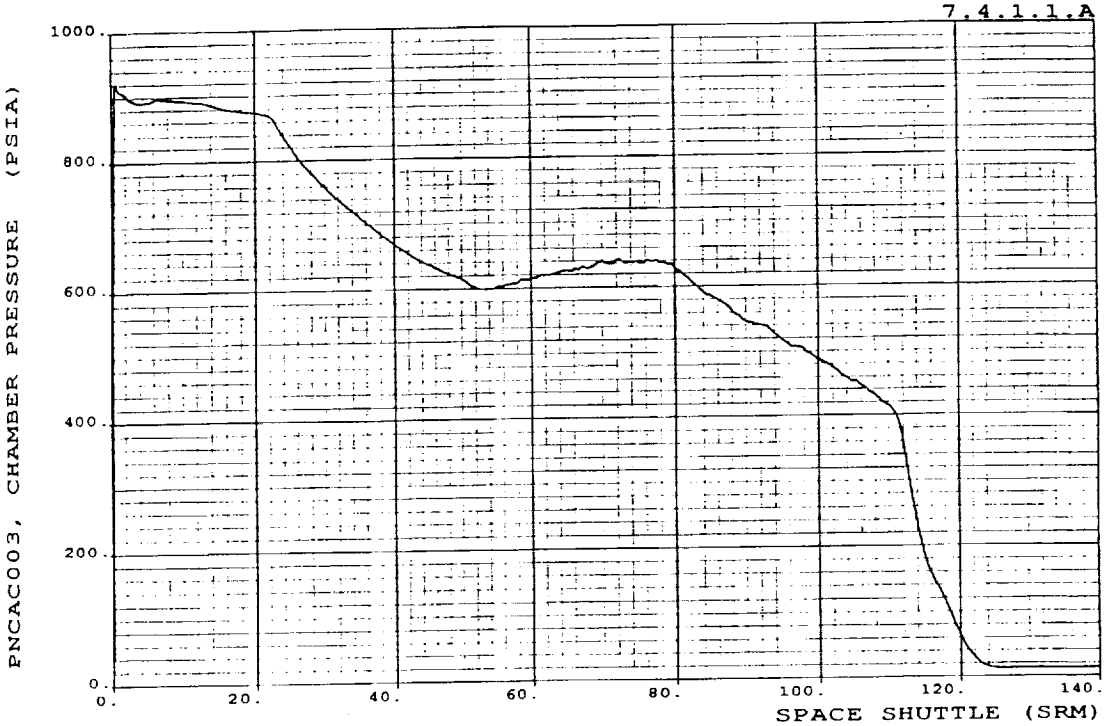

SPACE SHUTTLE (SRM)
TEM-05 STATIC TEST
23 JANUARY 1990

7.4.1.1.D

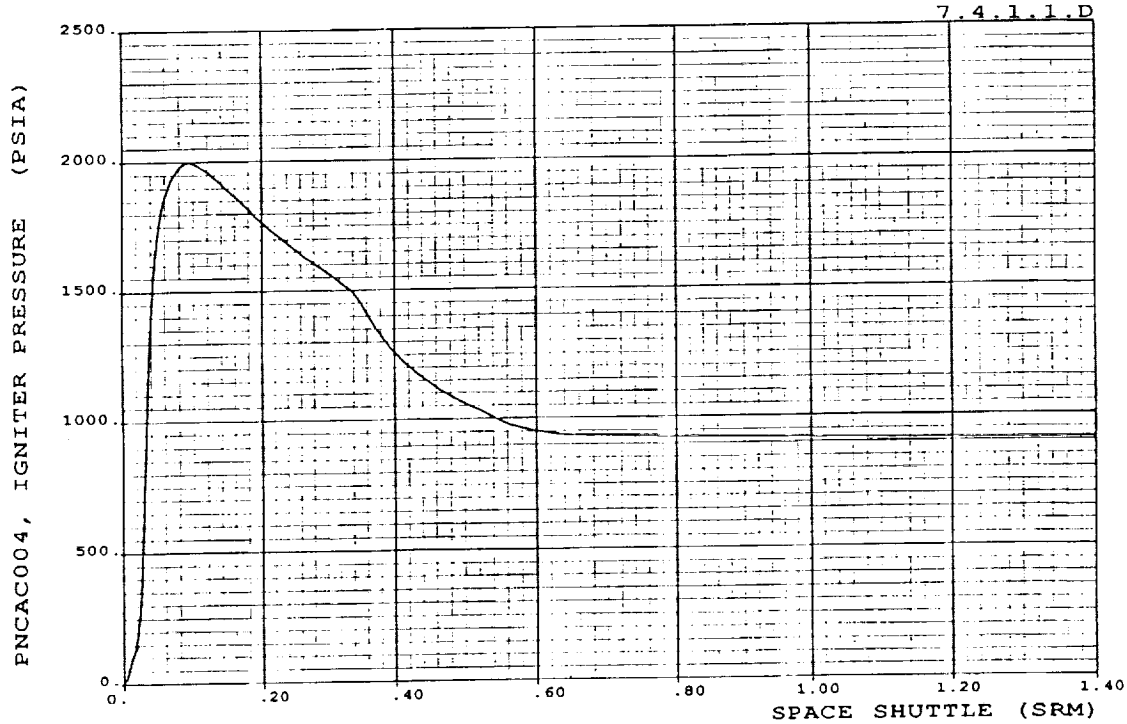

SPACE SHUTTLE (SRM)
TEM-05 STATIC TEST
23 JANUARY 1990

7.4.1.1.E

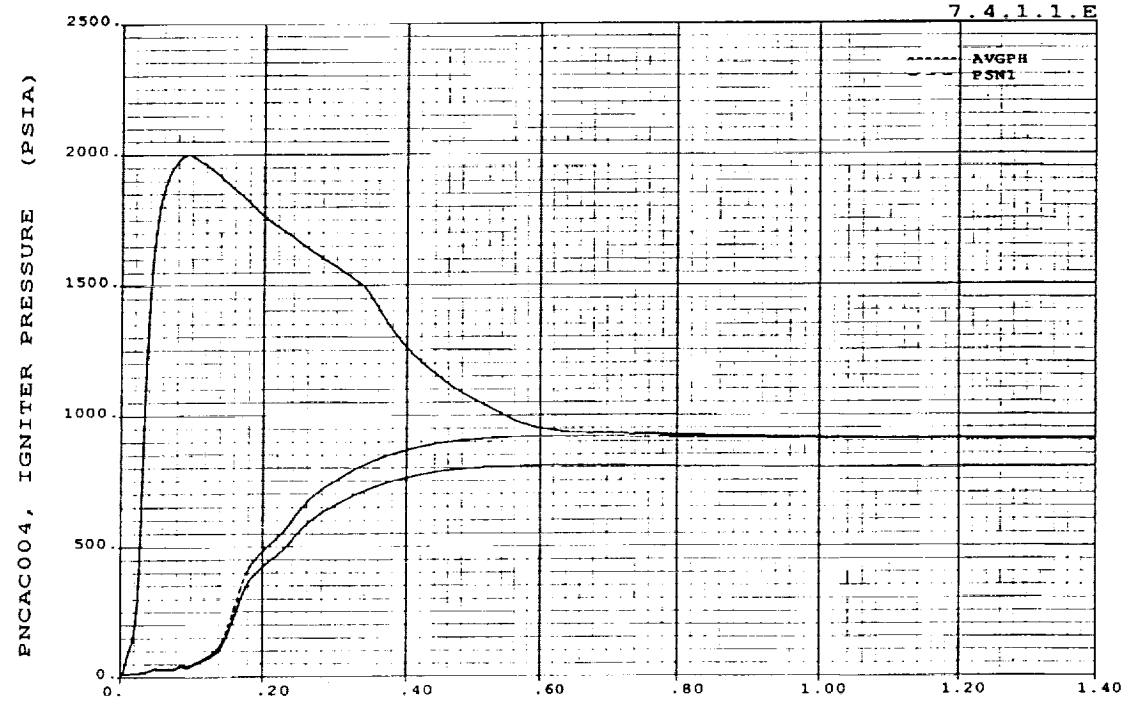

SPACE SHUTTLE (SRM)
TEM-05 STATIC TEST
23 JANUARY 1990

7.4.1.1.A

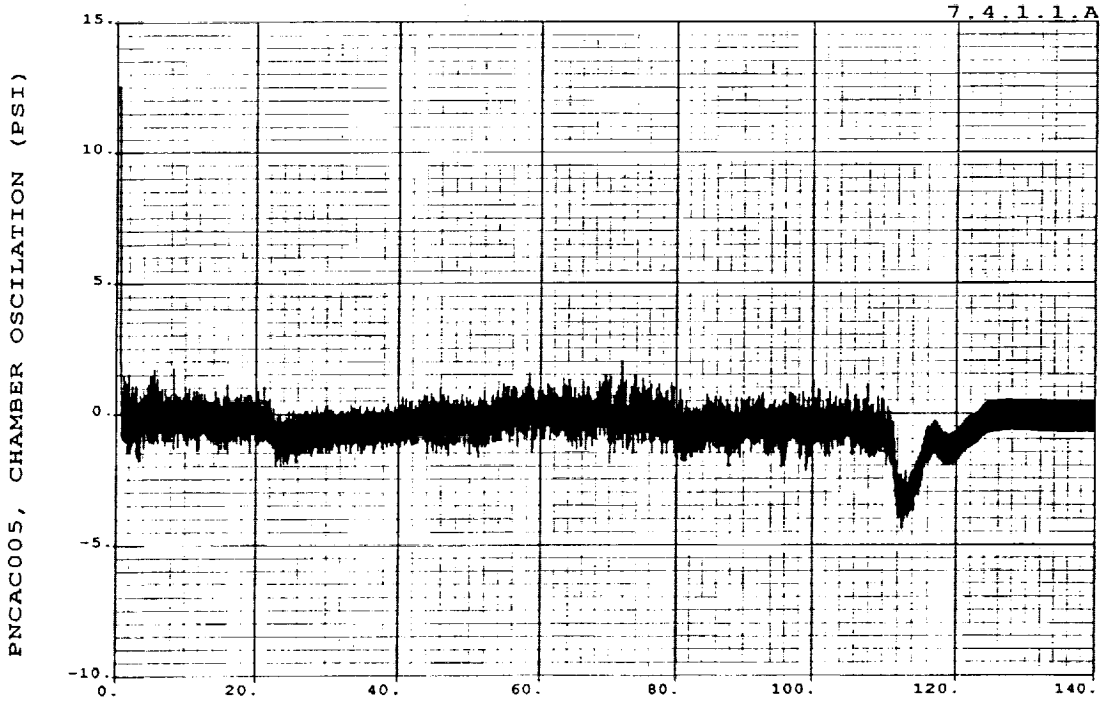

SPACE SHUTTLE (SRM)
TEM-05 STATIC TEST
23 JANUARY 1990

PRELIMINARY

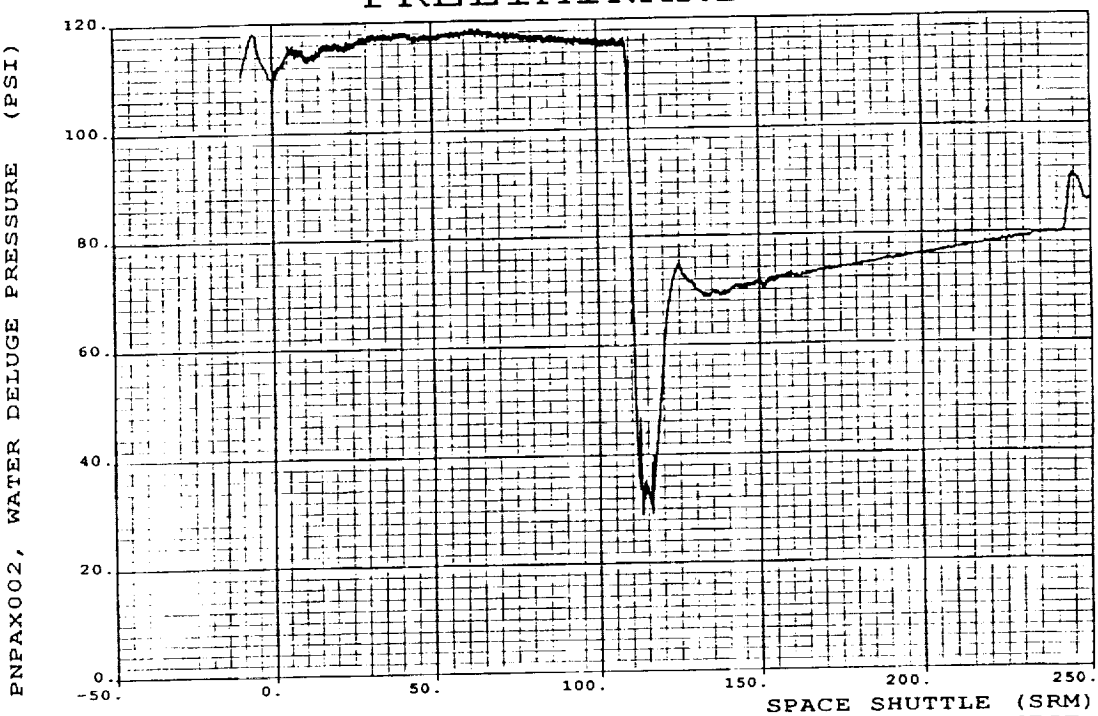

SPACE SHUTTLE (SRM)
TEM-05 STATIC TEST
23 JANUARY 1990
(QUICKLOOK)

PRELIMINARY

PRELIMINARY

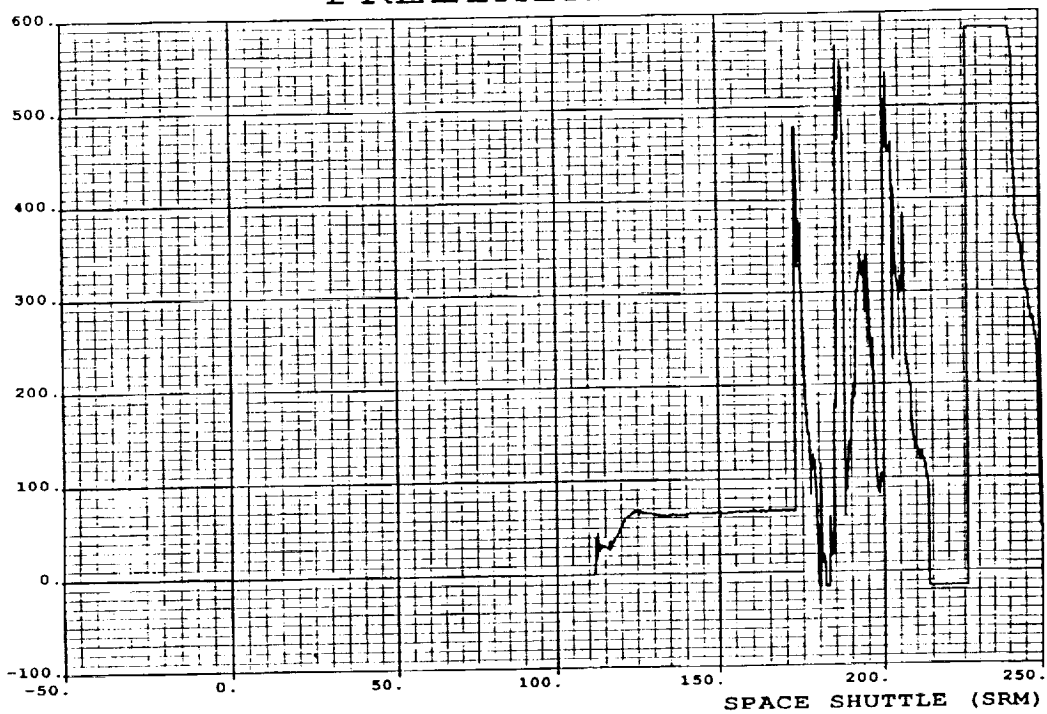

SPACE SHUTTLE (SRM)
TEM-05 STATIC TEST
23 JANUARY 1990
(QUICKLOOK)

PRELIMINARY

PRELIMINARY

7.3.1.F

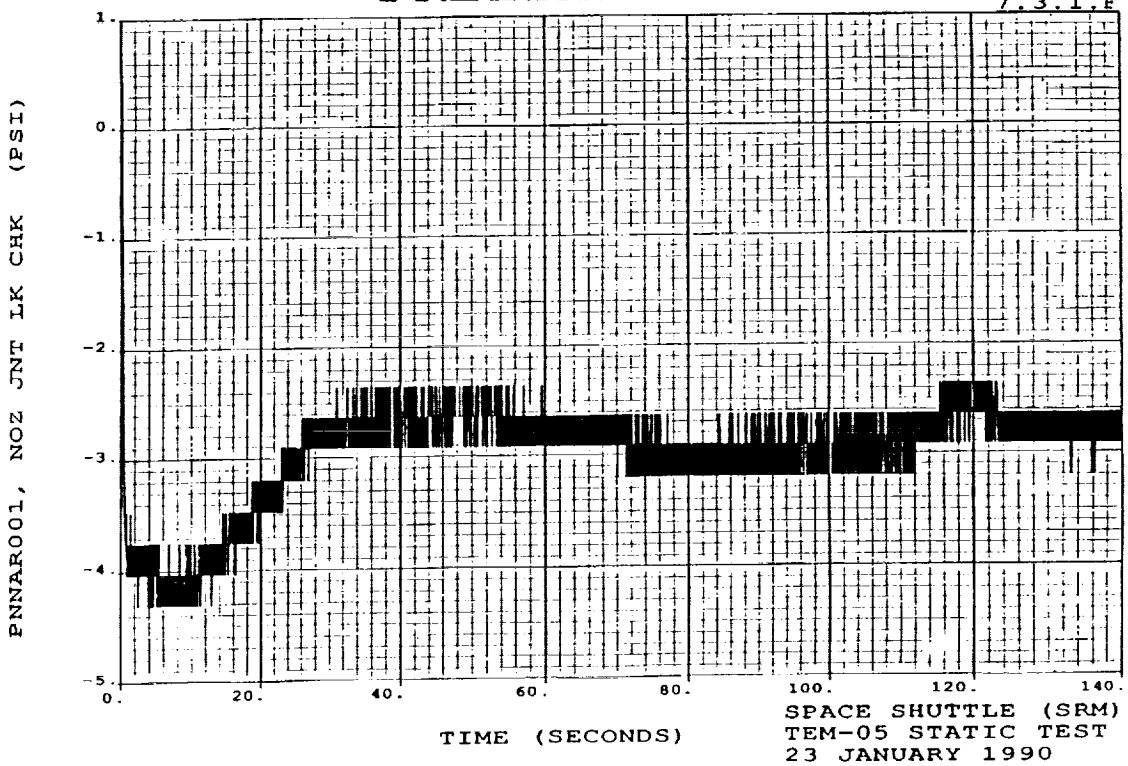

SPACE SHUTTLE (SRM)
TEM-05 STATIC TEST
23 JANUARY 1990
(QUICKLOOK)

PRELIMINARY

7.4.3.A

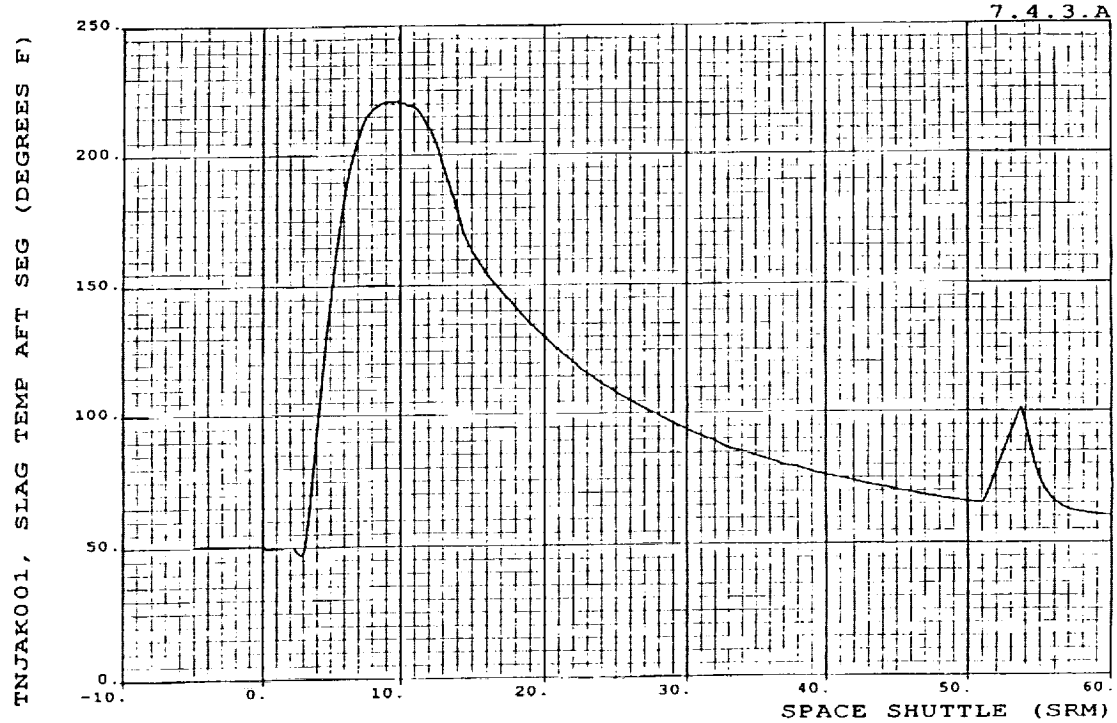

SPACE SHUTTLE (SRM)
TEM-05 STATIC TEST
23 JANUARY 1990

7.4.3.A

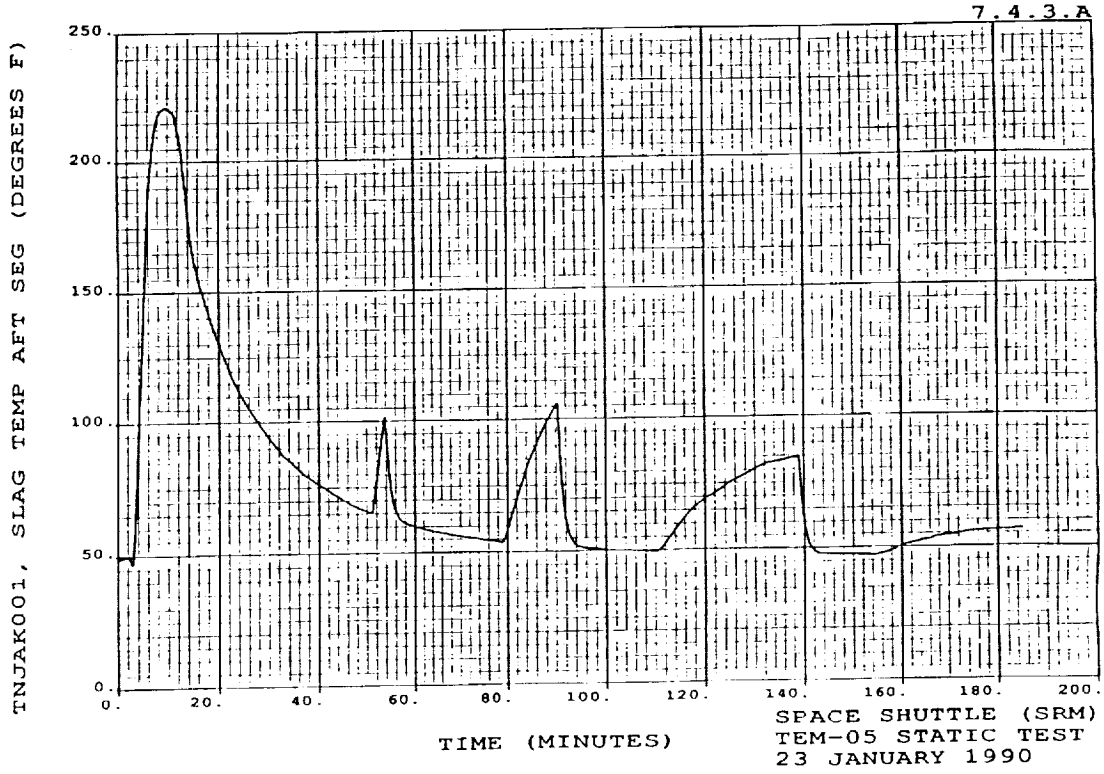
TNJAK001, SLAG TEMP AFT SEG (DEGREES F)
250.
200.
150.
100.
50.
0.
0.
20.
40.
60.
80.
100.
120.
140.
160.
180.
200.
TIME (MINUTES)
SPACE SHUTTLE (SRM)
TEM-05 STATIC TEST
23 JANUARY 1990

7.4.3.A

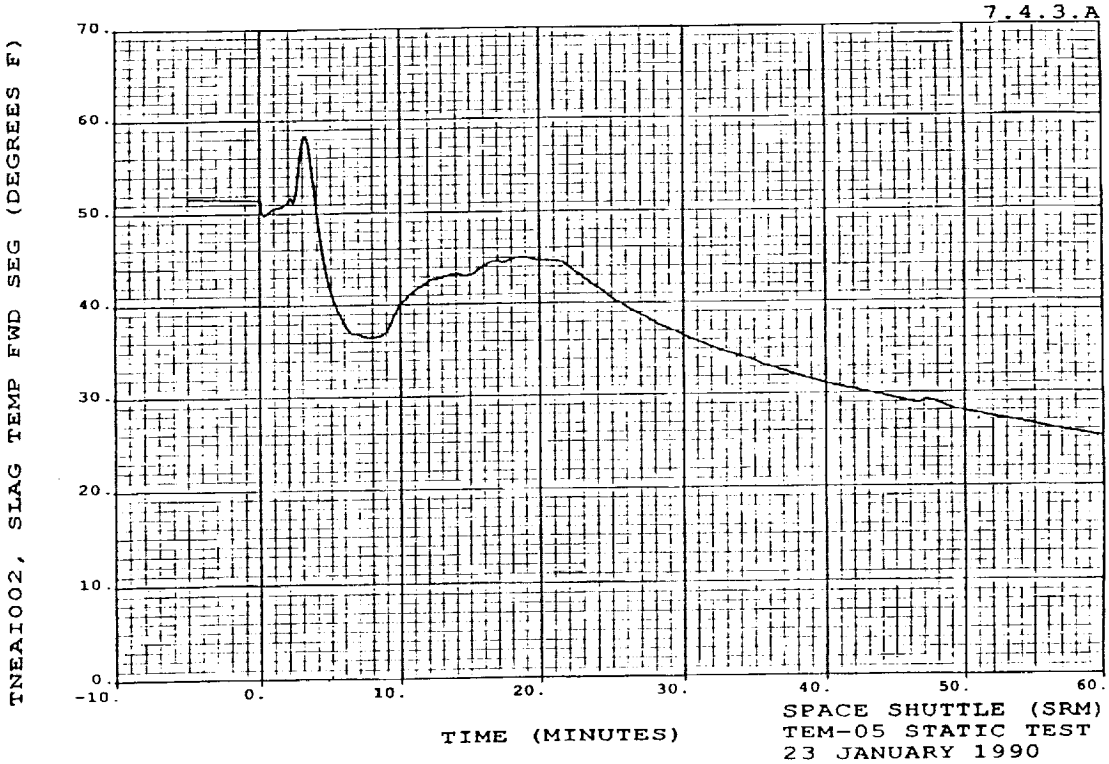
TNEAI002, SLAG TEMP FWD SEG (DEGREES F)
70.
60.
50.
40.
30.
20.
10.
0.
-10.
0.
10.
20.
30.
40.
50.
60.
TIME (MINUTES)
SPACE SHUTTLE (SRM)
TEM-05 STATIC TEST
23 JANUARY 1990

ORIGINAL PAGE IS
OF POOR QUALITY

7.4.3.A

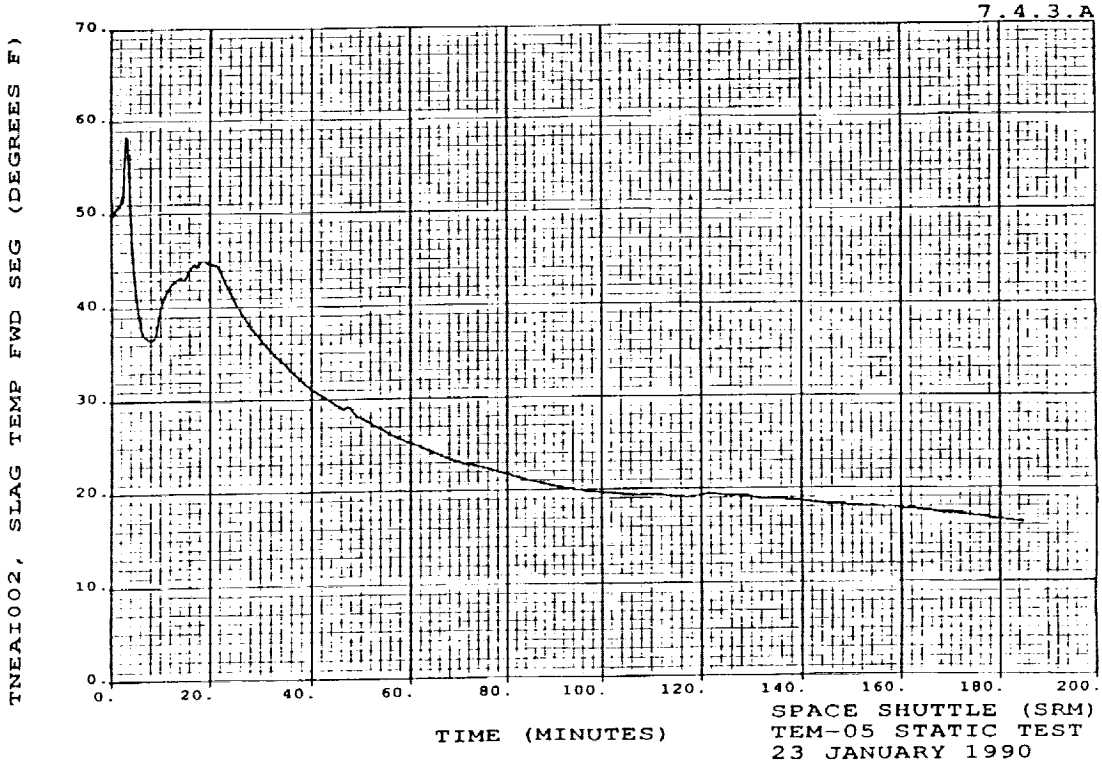

SPACE SHUTTLE (SRM)
TEM-05 STATIC TEST
23 JANUARY 1990

7.4.3.A

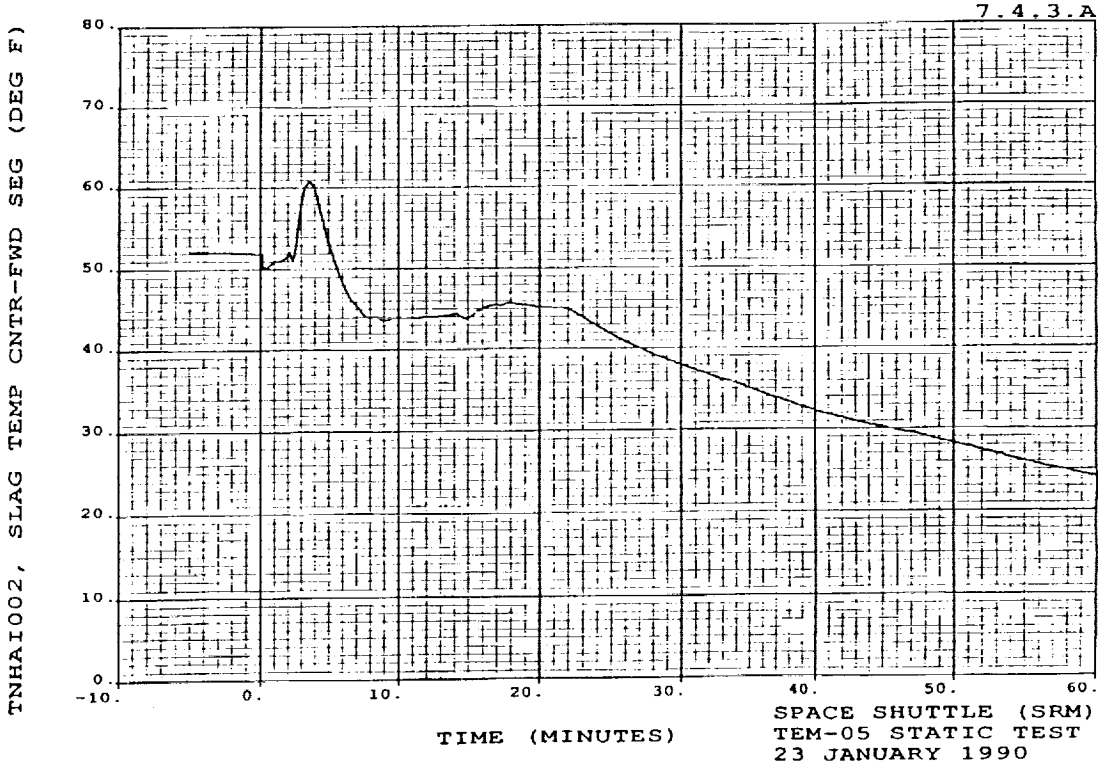

SPACE SHUTTLE (SRM)
TEM-05 STATIC TEST
23 JANUARY 1990

7.4.3.A

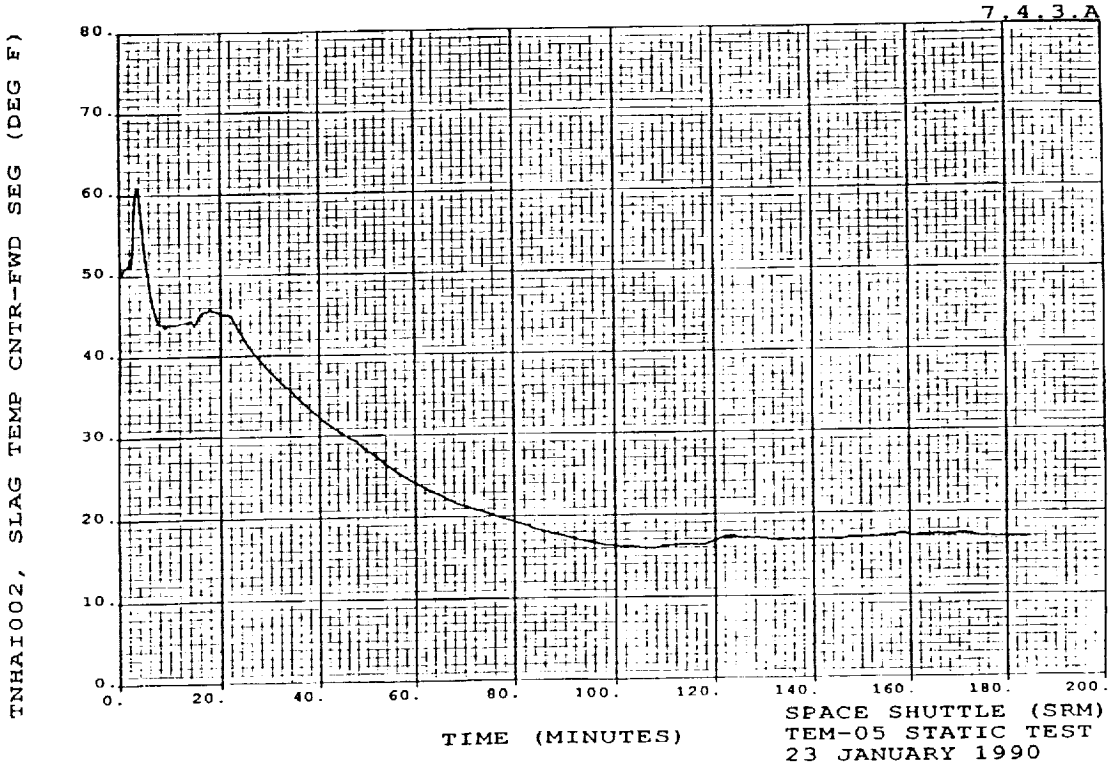

SPACE SHUTTLE (SRM)
TEM-05 STATIC TEST
23 JANUARY 1990

7.4.3.A

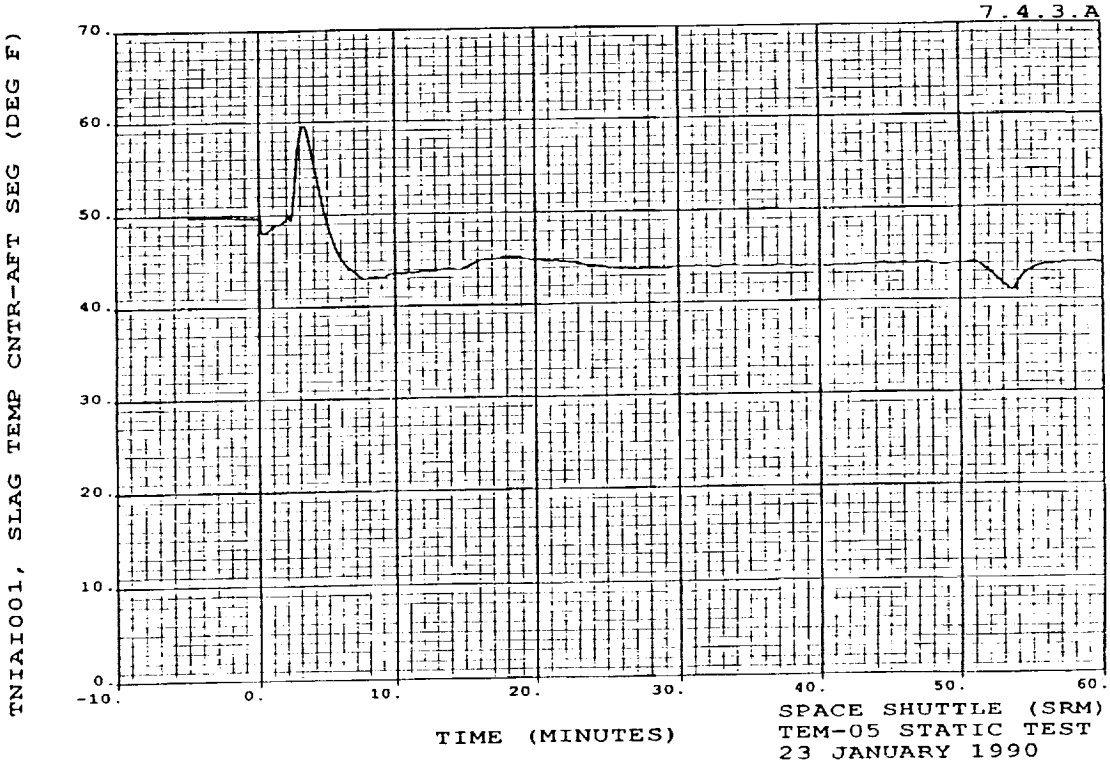

SPACE SHUTTLE (SRM)
TEM-05 STATIC TEST
23 JANUARY 1990

7.4.3.A

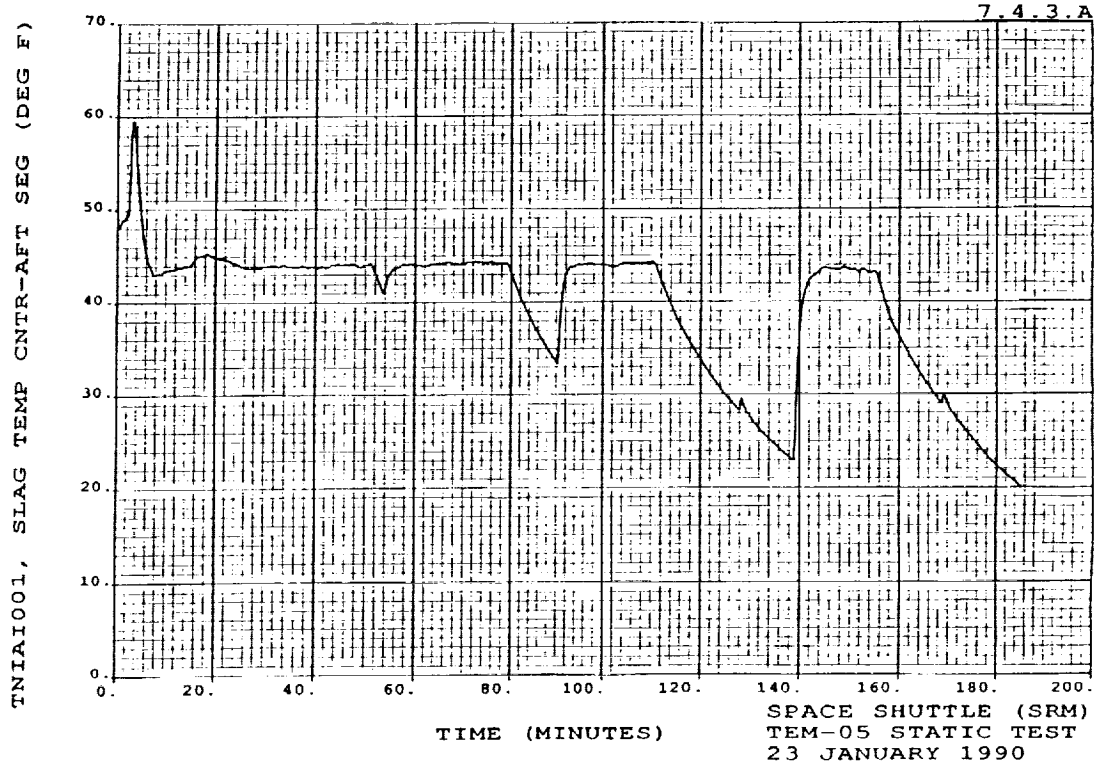

SPACE SHUTTLE (SRM)
TEM-05 STATIC TEST
23 JANUARY 1990

7.4.3.A

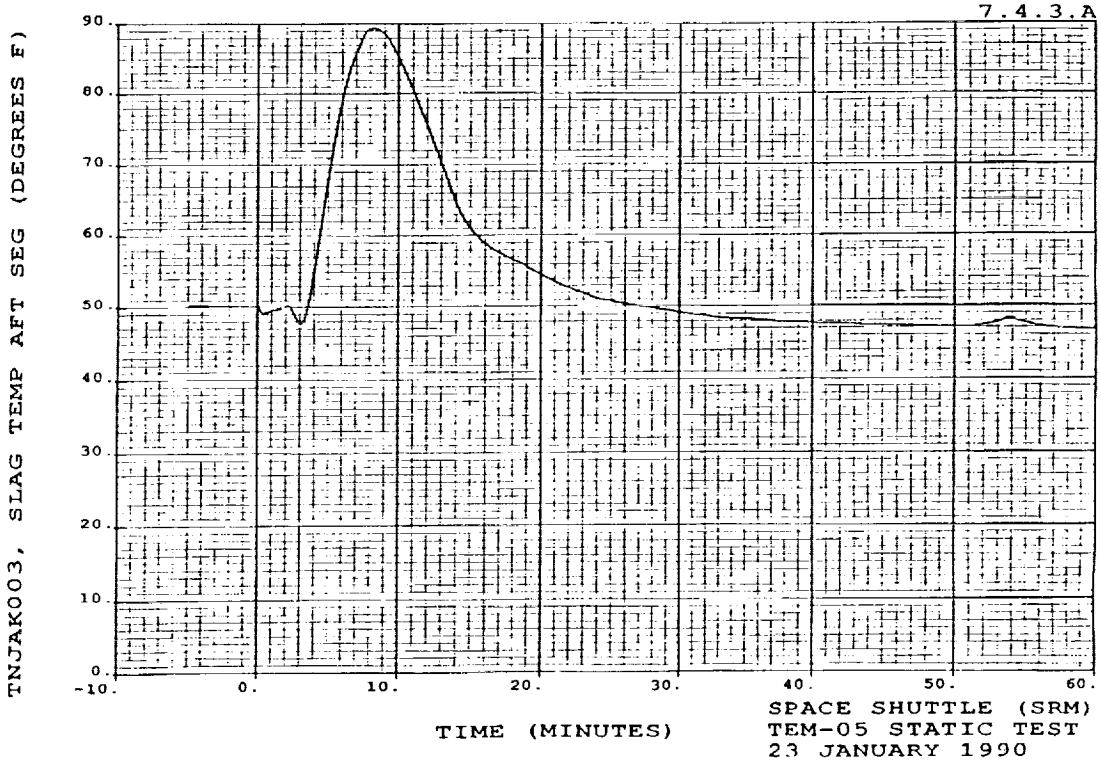

SPACE SHUTTLE (SRM)
TEM-05 STATIC TEST
23 JANUARY 1990

7.4.3.A

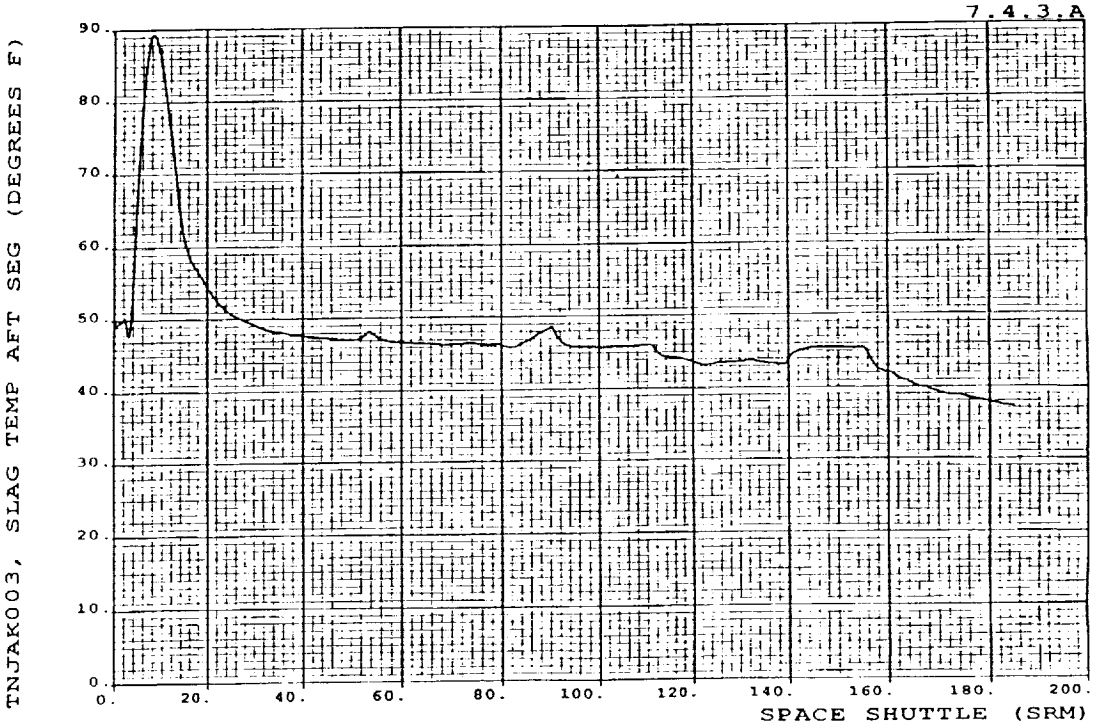

SPACE SHUTTLE (SRM)
TEM-05 STATIC TEST
23 JANUARY 1990

7.4.3.A

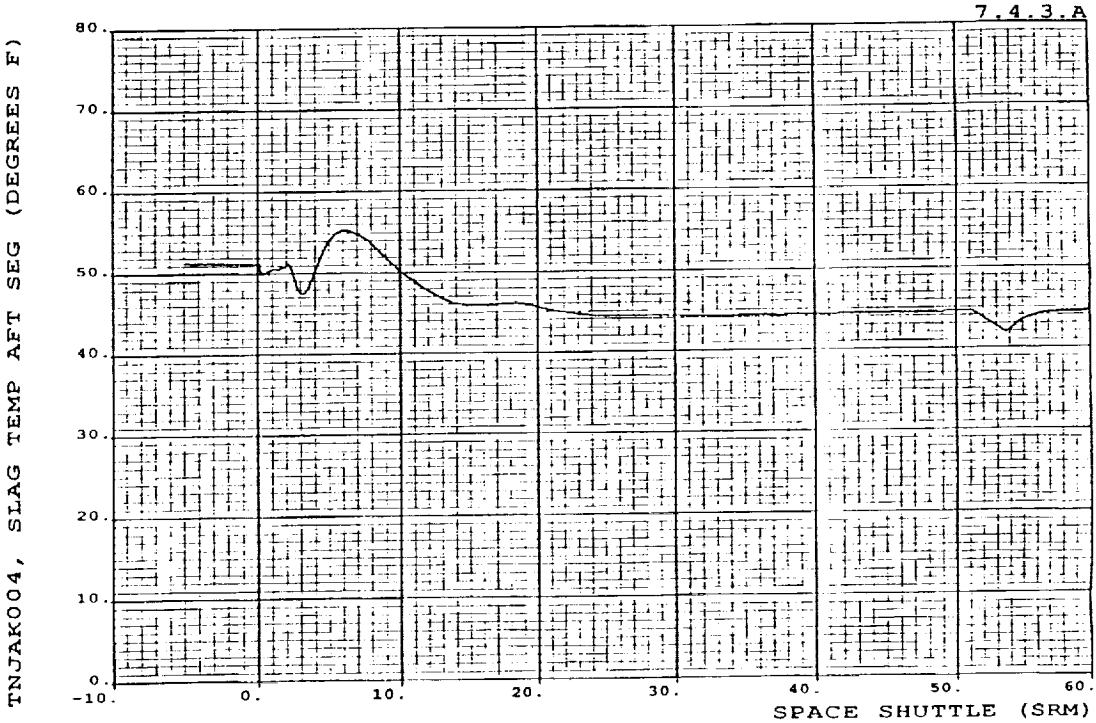

SPACE SHUTTLE (SRM)
TEM-05 STATIC TEST
23 JANUARY 1990

7.4.3.A

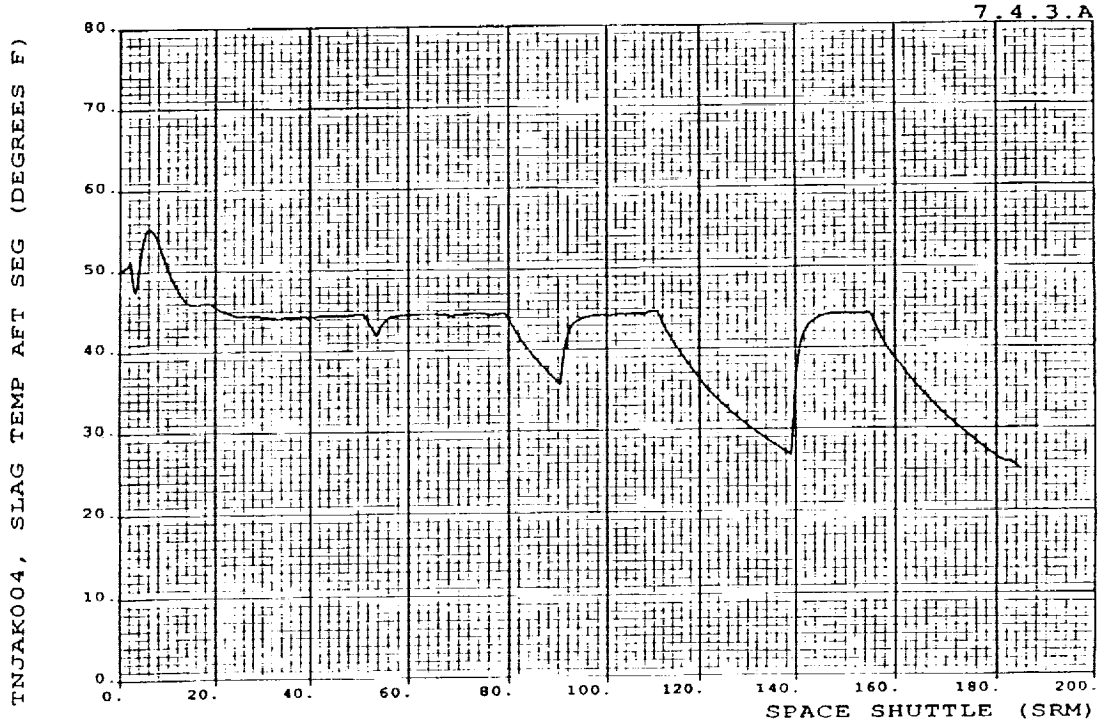

SPACE SHUTTLE (SRM)
TEM-05 STATIC TEST
23 JANUARY 1990

7.4.3.A

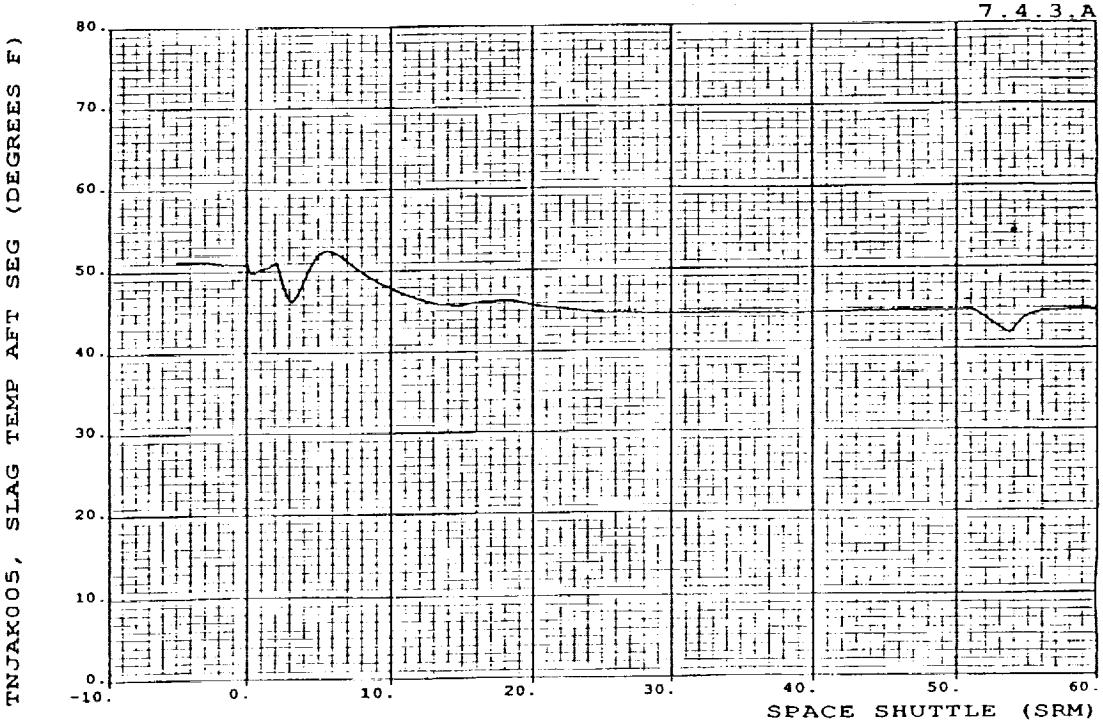

SPACE SHUTTLE (SRM)
TEM-05 STATIC TEST
23 JANUARY 1990

7.4.3.A

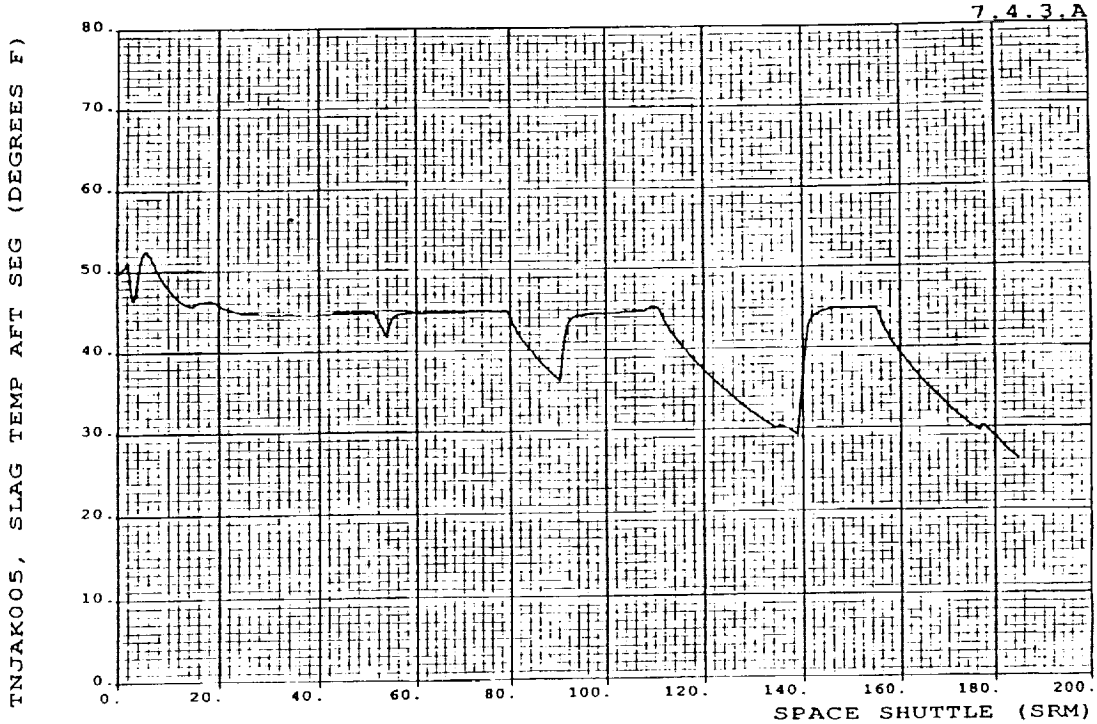

SPACE SHUTTLE (SRM)
TEM-05 STATIC TEST
23 JANUARY 1990

7.4.3.A

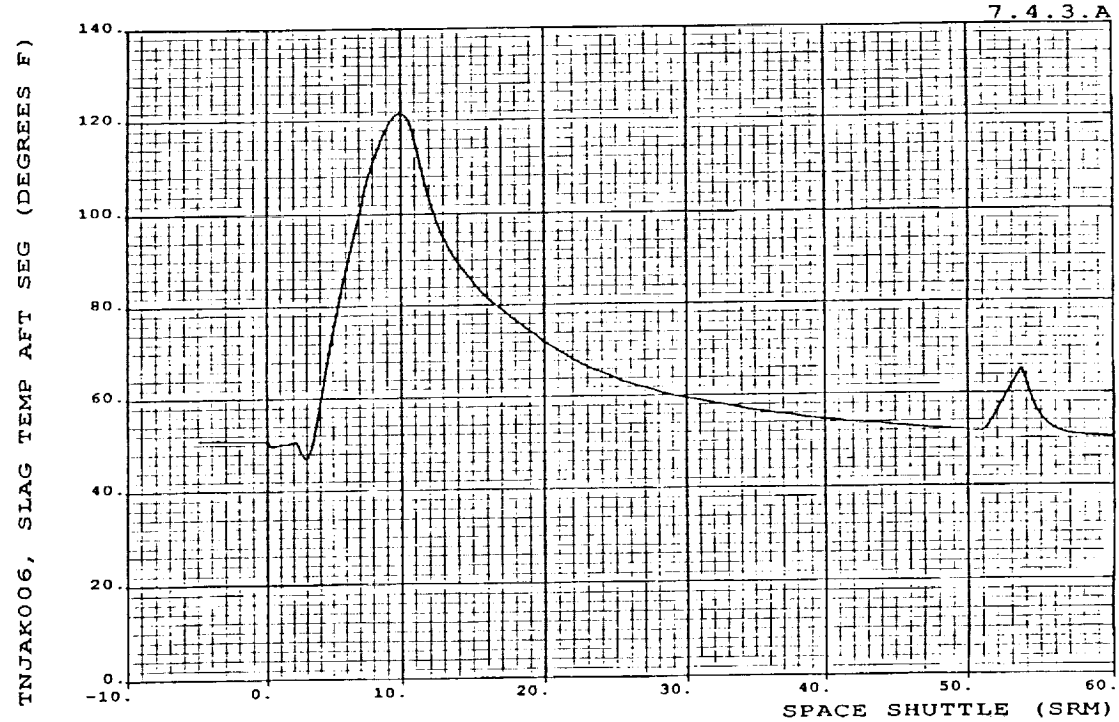

SPACE SHUTTLE (SRM)
TEM-05 STATIC TEST
23 JANUARY 1990

7.4.3.A

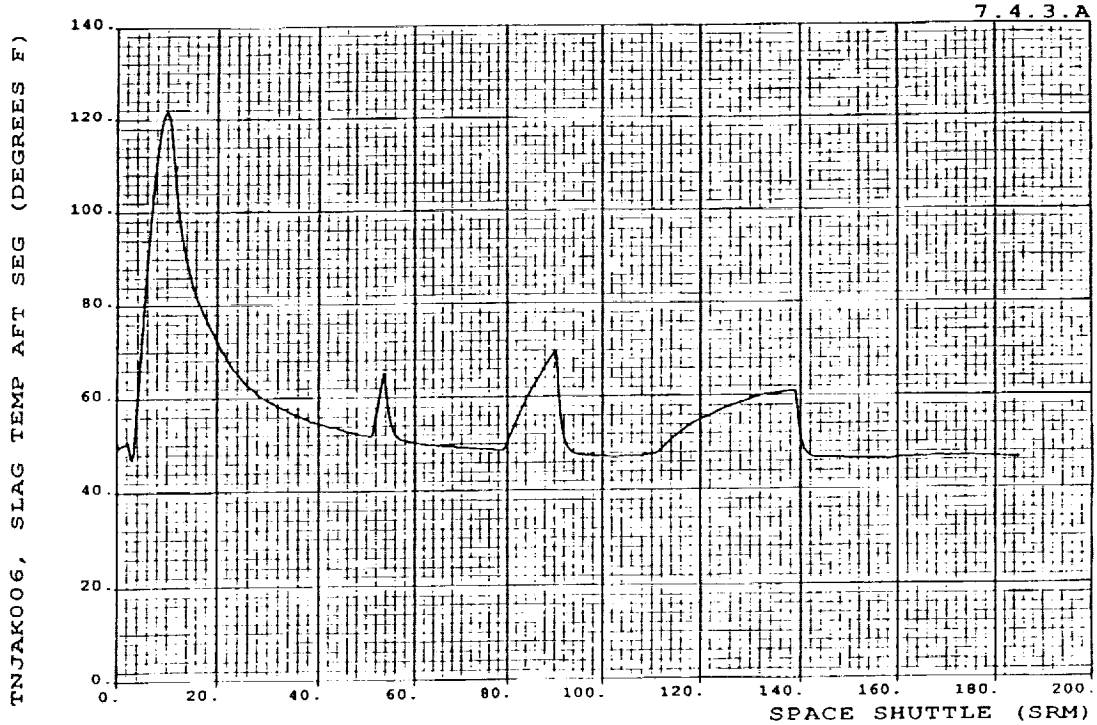
TNJAK006, SLAG TEMP AFT SEG (DEGREES F)
140.
120.
100.
80.
60.
40.
20.
0.
0.
20.
40.
60.
80.
100.
120.
140.
160.
180.
200.
TIME (MINUTES)
SPACE SHUTTLE (SRM)
TEM-05 STATIC TEST
23 JANUARY 1990

7.4.3.A

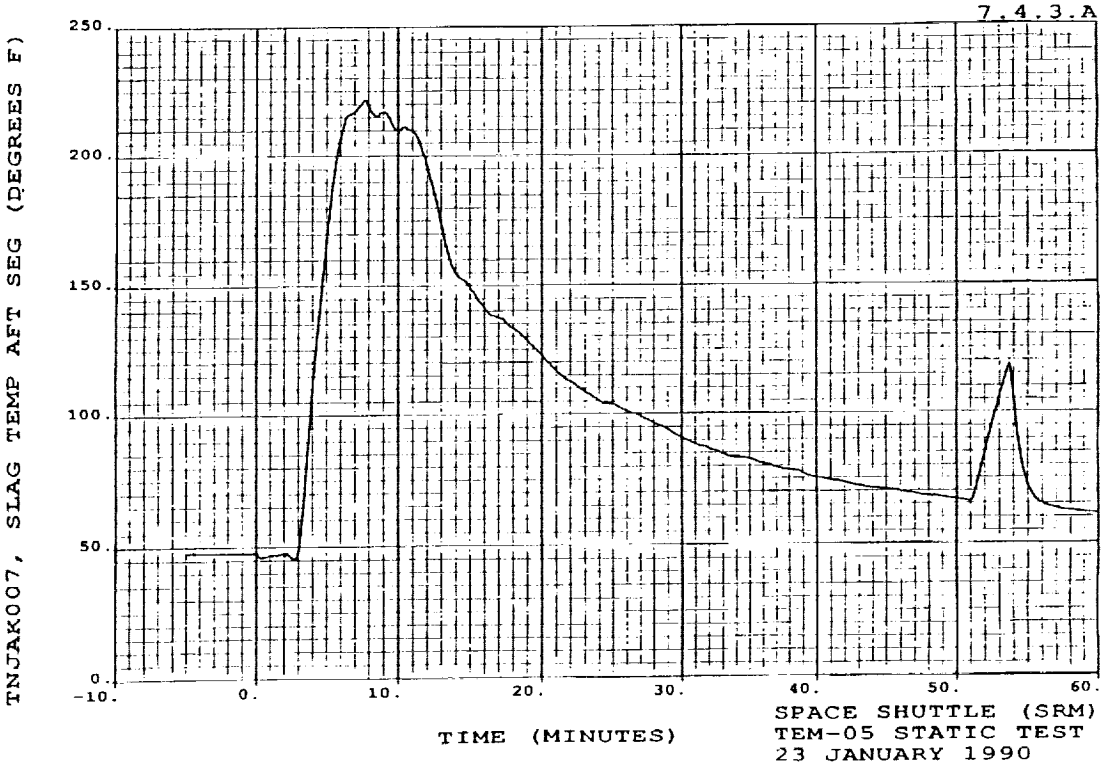
TNJAK007, SLAG TEMP AFT SEG (DEGREES F)
250.
200.
150.
100.
50.
0.
-10.
0.
10.
20.
30.
40.
50.
60.
TIME (MINUTES)
SPACE SHUTTLE (SRM)
TEM-05 STATIC TEST
23 JANUARY 1990

7.4.3.A

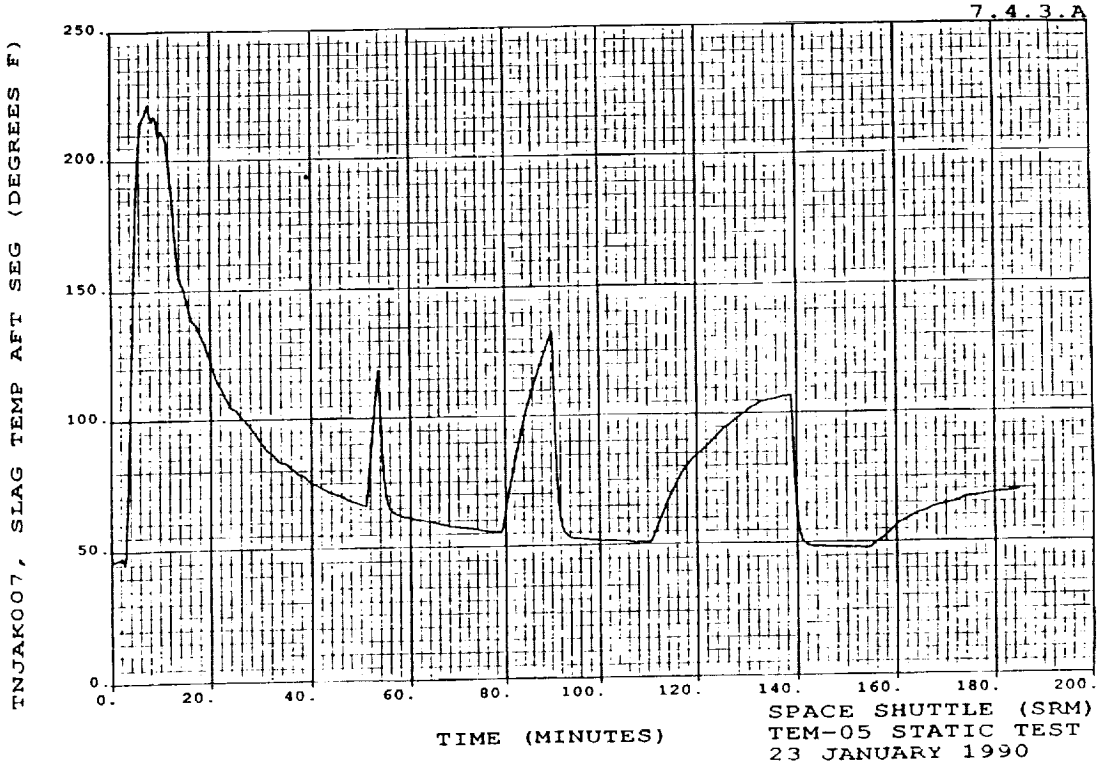

SPACE SHUTTLE (SRM)
TEM-05 STATIC TEST
23 JANUARY 1990

7.4.3.A

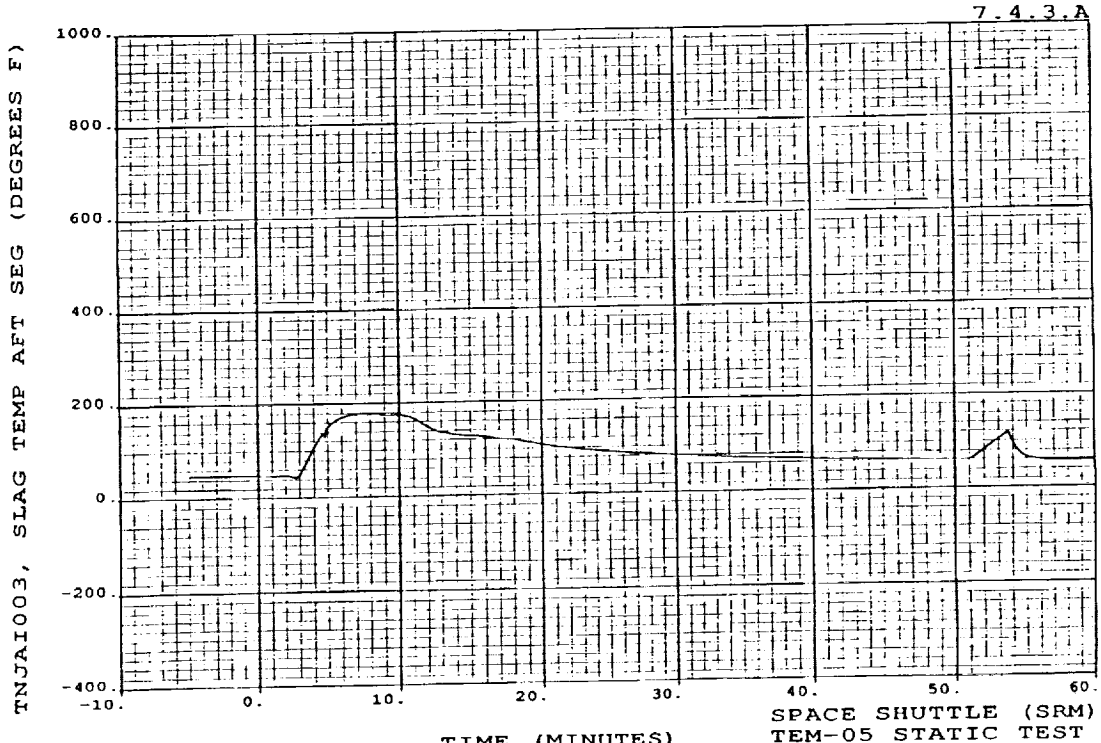

SPACE SHUTTLE (SRM)
TEM-05 STATIC TEST
23 JANUARY 1990

7.4.3.A

SPACE SHUTTLE (SRM)
TEM-05 STATIC TEST
23 JANUARY 1990

7.4.3.A

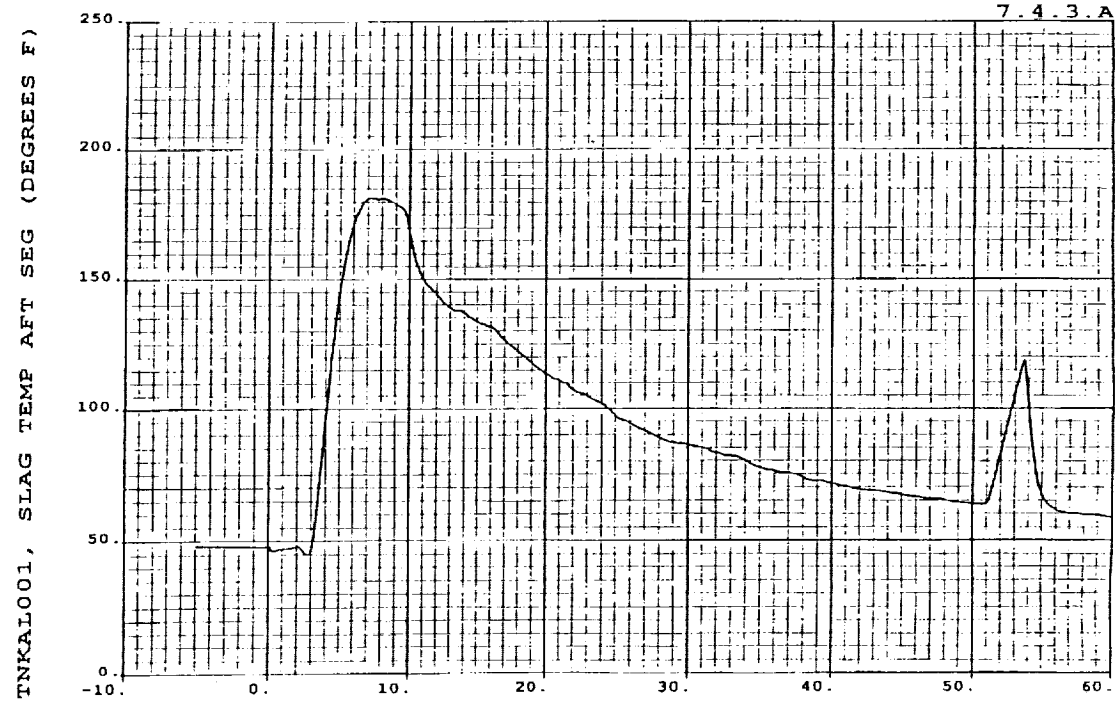

SPACE SHUTTLE (SRM)
TEM-05 STATIC TEST
23 JANUARY 1990

7.4.3.A

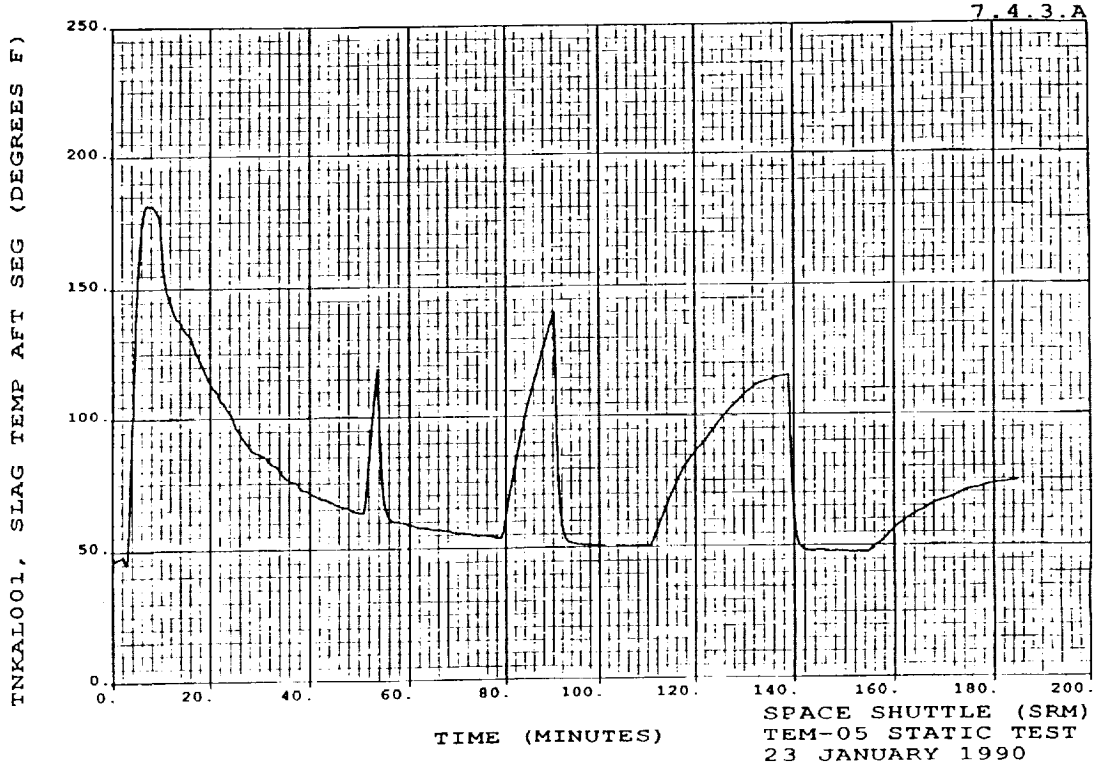

SPACE SHUTTLE (SRM)
TEM-05 STATIC TEST
23 JANUARY 1990

7.4.3.A

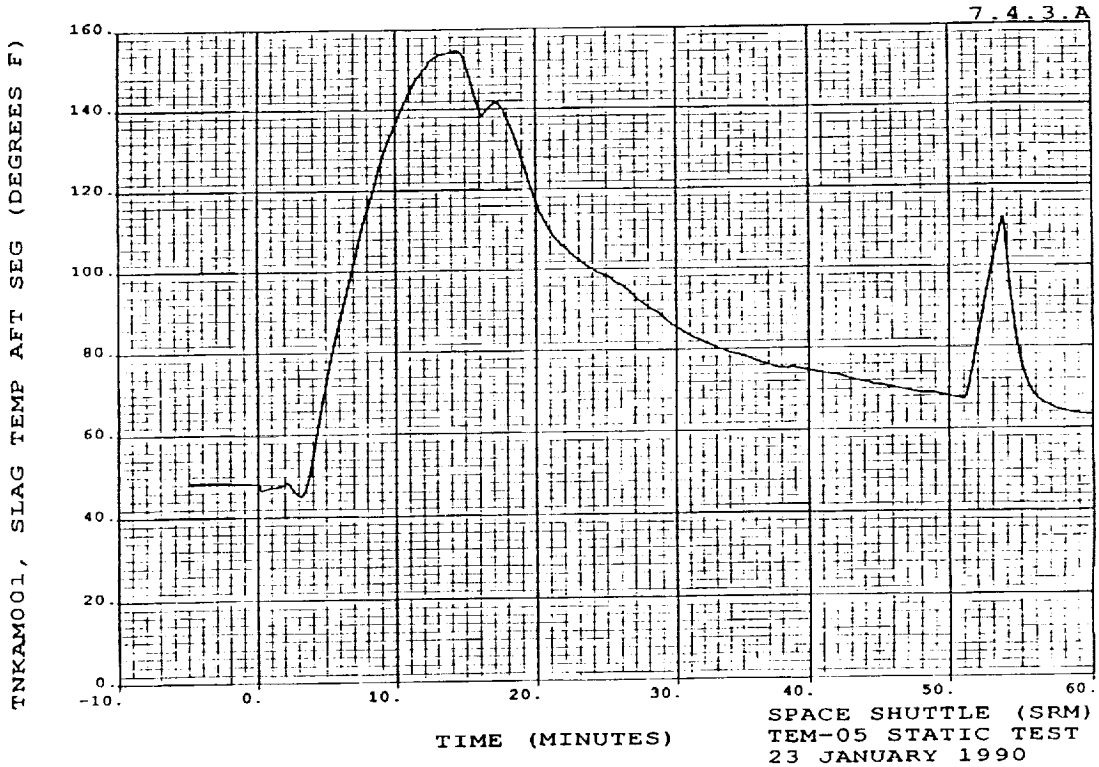

SPACE SHUTTLE (SRM)
TEM-05 STATIC TEST
23 JANUARY 1990

7.4.3.A

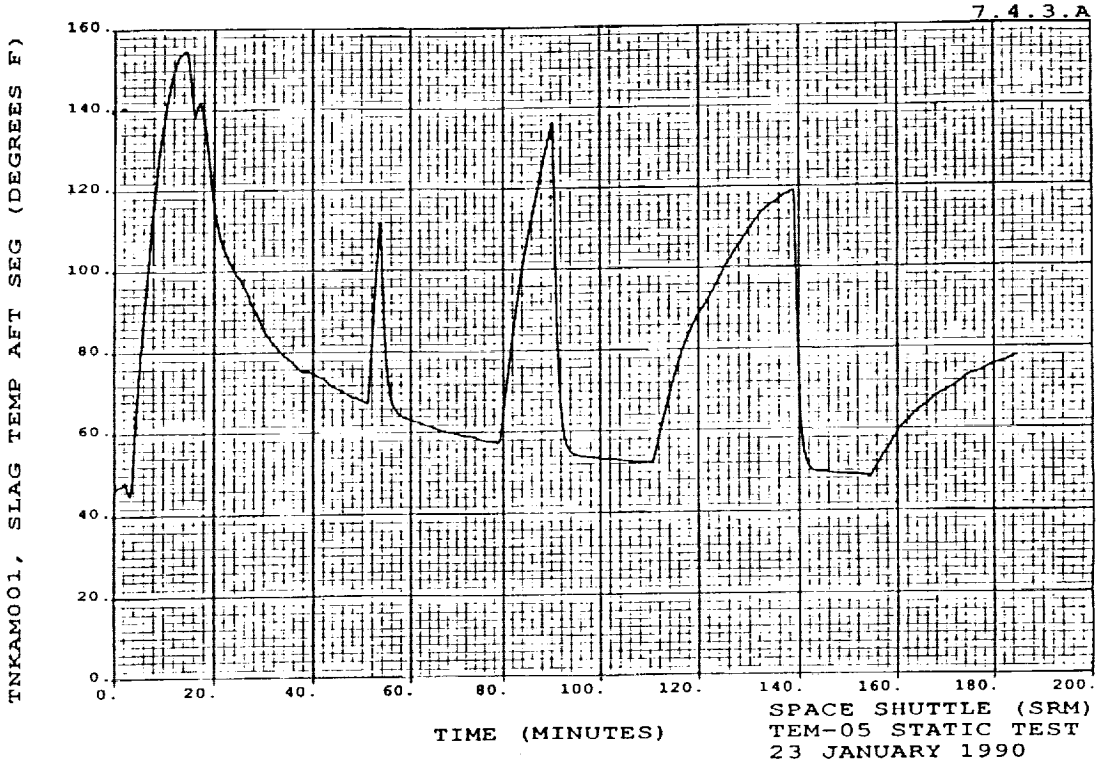
TNKAM001, SLAG TEMP AFT SEG (DEGREES F)
160.
140.
120.
100.
80.
60.
40.
20.
0.
0.
20.
40.
60.
80.
100.
120.
140.
160.
180.
200.
TIME (MINUTES)
SPACE SHUTTLE (SRM)
TEM-05 STATIC TEST
23 JANUARY 1990

7.4.3.A

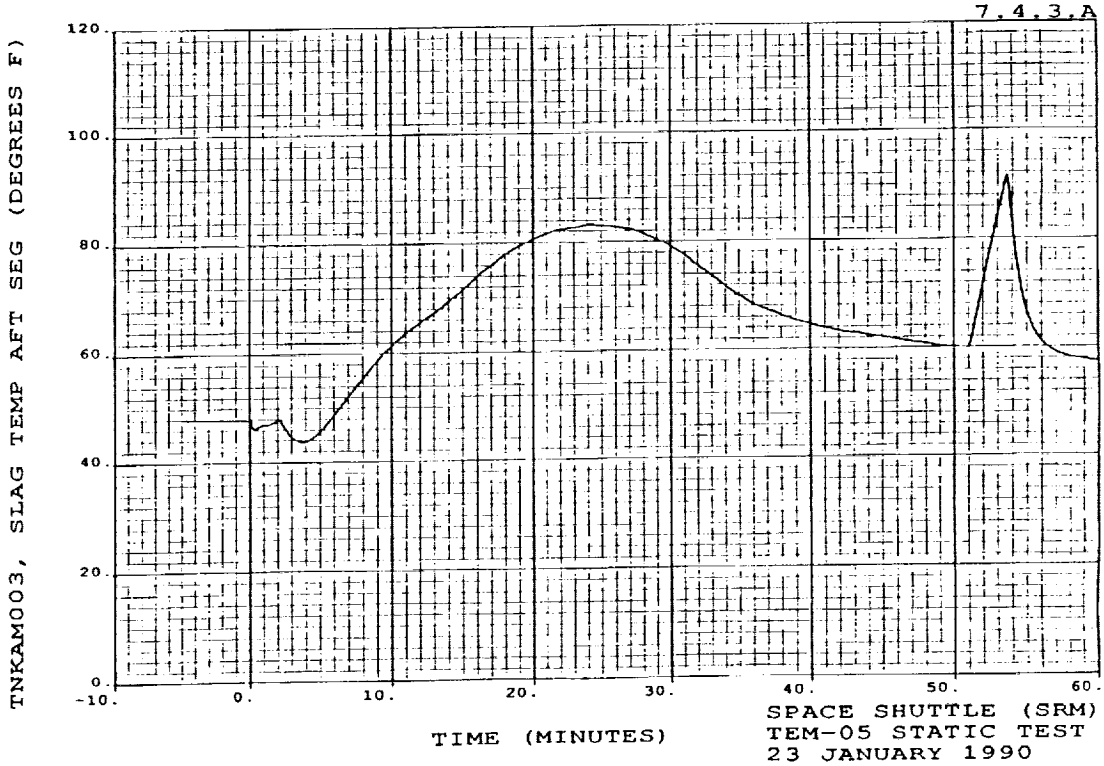
TNKAM003, SLAG TEMP AFT SEG (DEGREES F)
120.
100.
80.
60.
40.
20.
0.
-10.
0.
10.
20.
30.
40.
50.
60.
TIME (MINUTES)
SPACE SHUTTLE (SRM)
TEM-05 STATIC TEST
23 JANUARY 1990

7.4.3.A

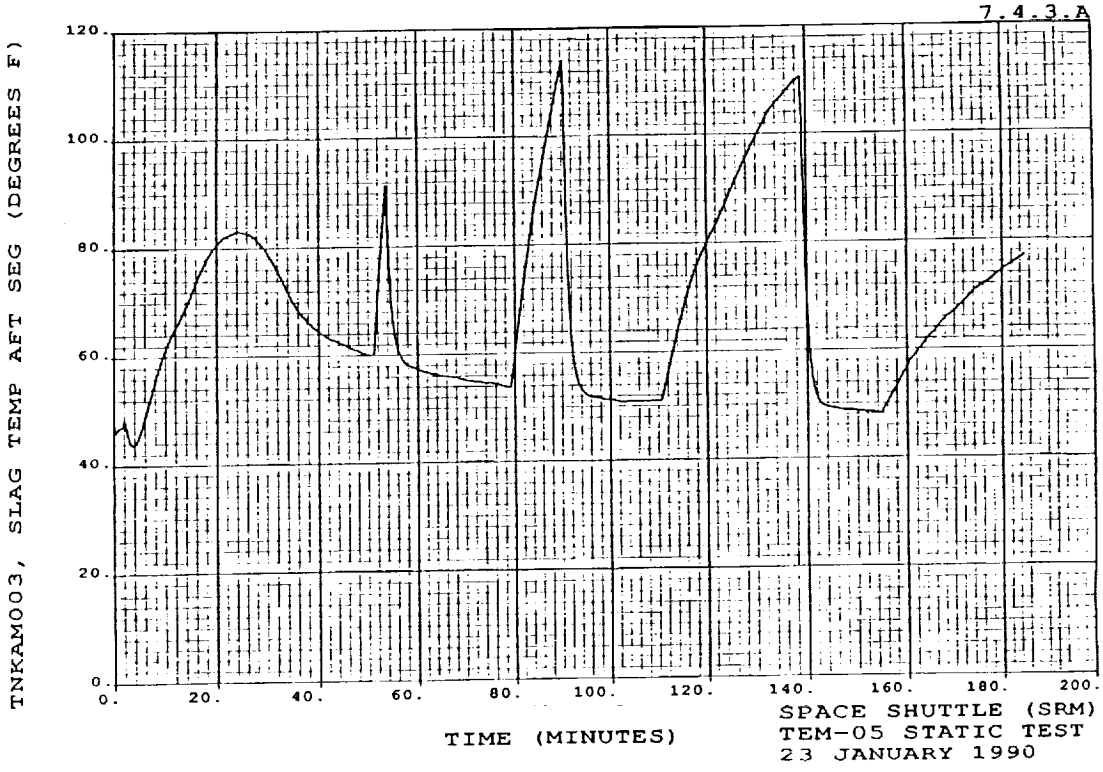
TNKAM003, SLAG TEMP AFT SEG (DEGREES F)
120.
100.
80.
60.
40.
20.
0.
0.
20.
40.
60.
80.
100.
120.
140.
160.
180.
200.
TIME (MINUTES)
SPACE SHUTTLE (SRM)
TEM-05 STATIC TEST
23 JANUARY 1990

7.4.3.A

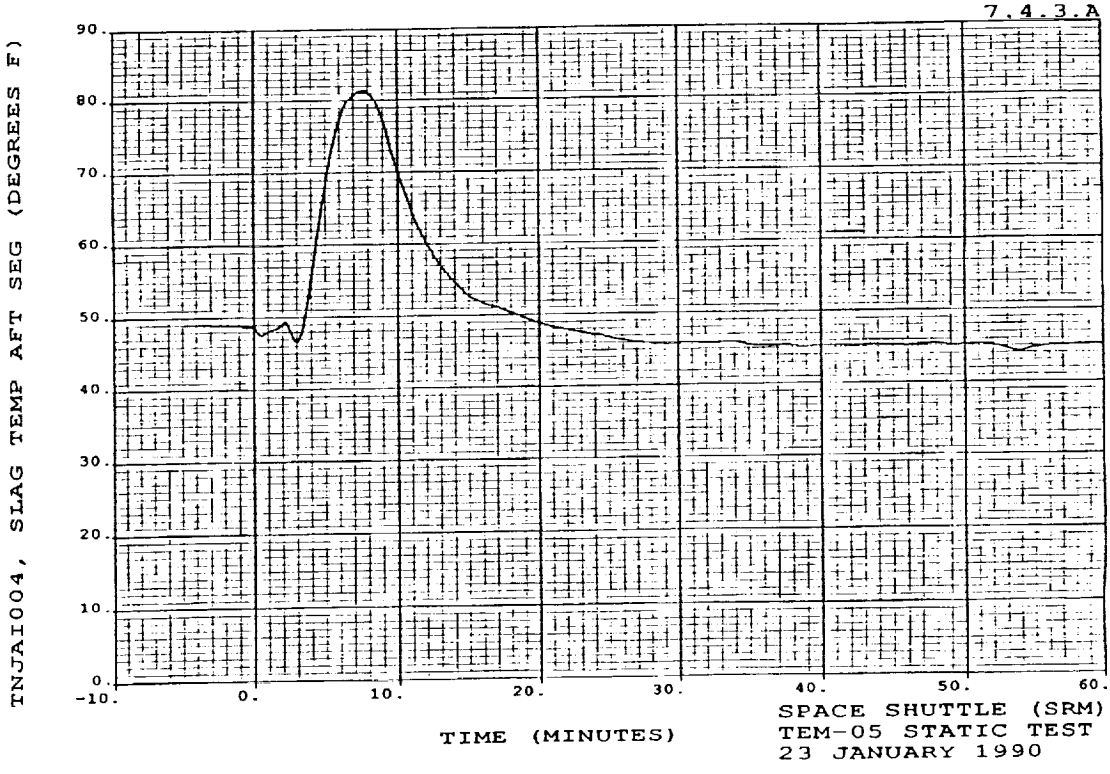
TNJAI004, SLAG TEMP AFT SEG (DEGREES F)
90.
80.
70.
60.
50.
40.
30.
20.
10.
0.
-10.
0.
10.
20.
30.
40.
50.
60.
TIME (MINUTES)
SPACE SHUTTLE (SRM)
TEM-05 STATIC TEST
23 JANUARY 1990

7.4.3.A

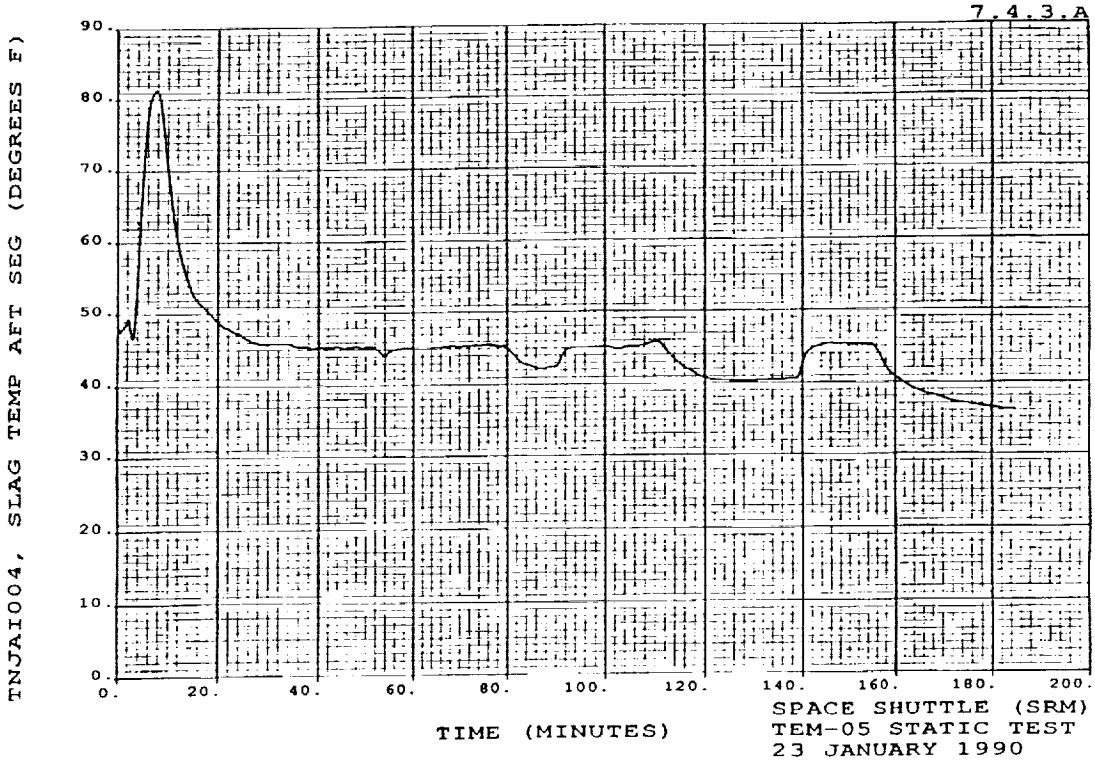
TNJAI004, SLAG TEMP AFT SEG (DEGREES F)
90.
80.
70.
60.
50.
40.
30.
20.
10.
0.
0.
20.
40.
60.
80.
100.
120.
140.
160.
180.
200.
TIME (MINUTES)
SPACE SHUTTLE (SRM)
TEM-05 STATIC TEST
23 JANUARY 1990

7.4.3.A

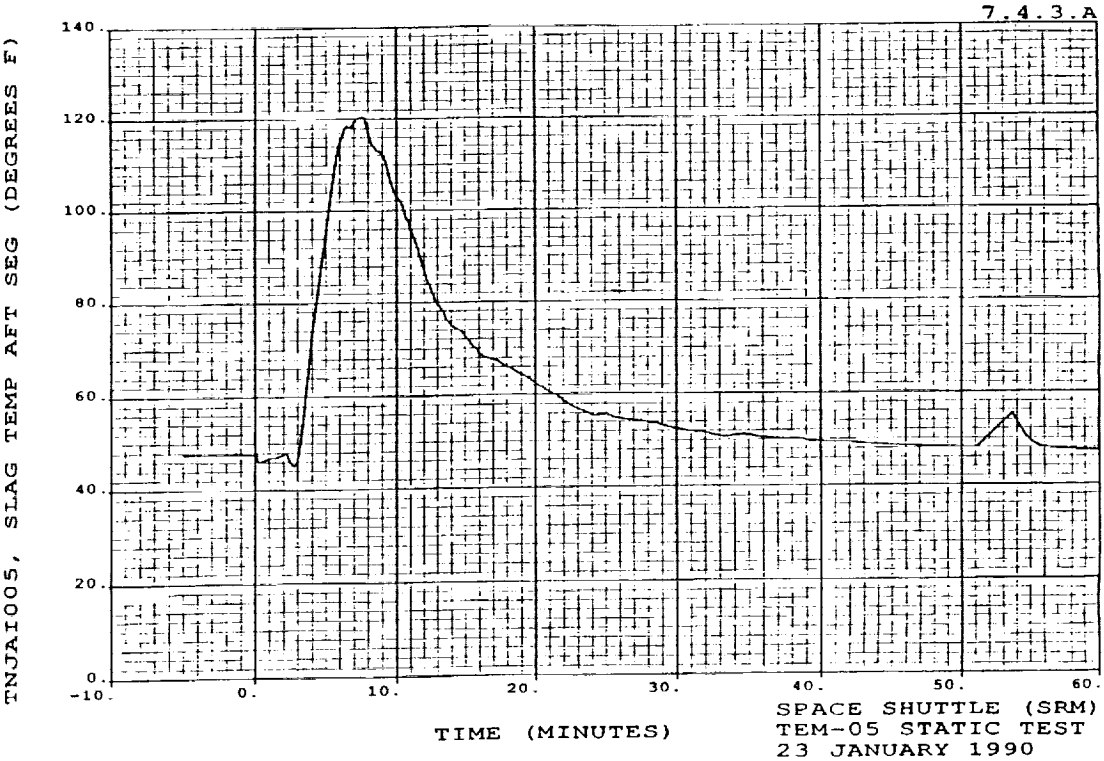
TNJAI005, SLAG TEMP AFT SEG (DEGREES F)
140.
120.
100.
80.
60.
40.
20.
0.
-10.
0.
10.
20.
30.
40.
50.
60.
TIME (MINUTES)
SPACE SHUTTLE (SRM)
TEM-05 STATIC TEST
23 JANUARY 1990

7.4.3.A

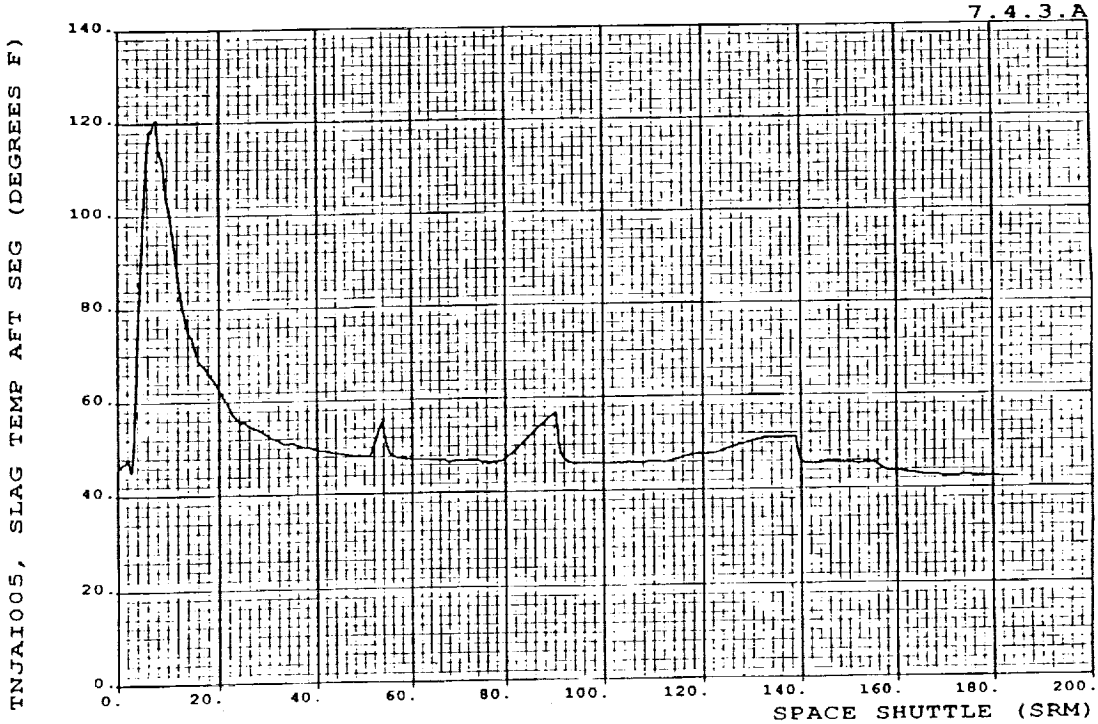

SPACE SHUTTLE (SRM)
TEM-05 STATIC TEST
23 JANUARY 1990

7.4.3.A

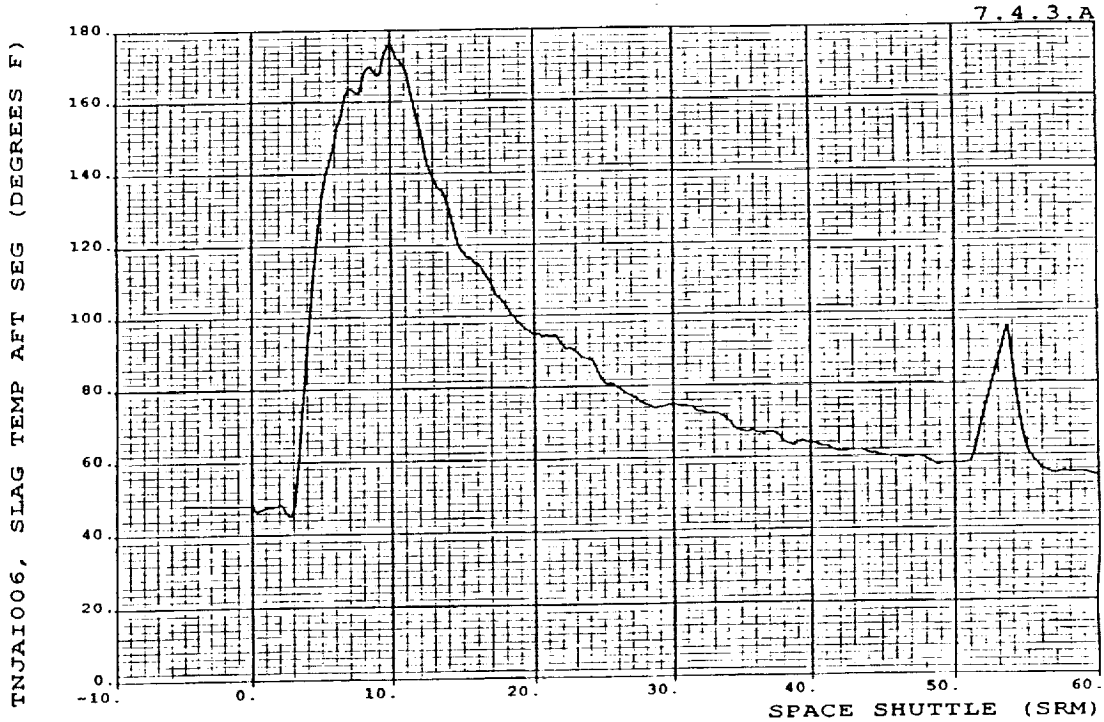

SPACE SHUTTLE (SRM)
TEM-05 STATIC TEST
23 JANUARY 1990

7.4.3.A

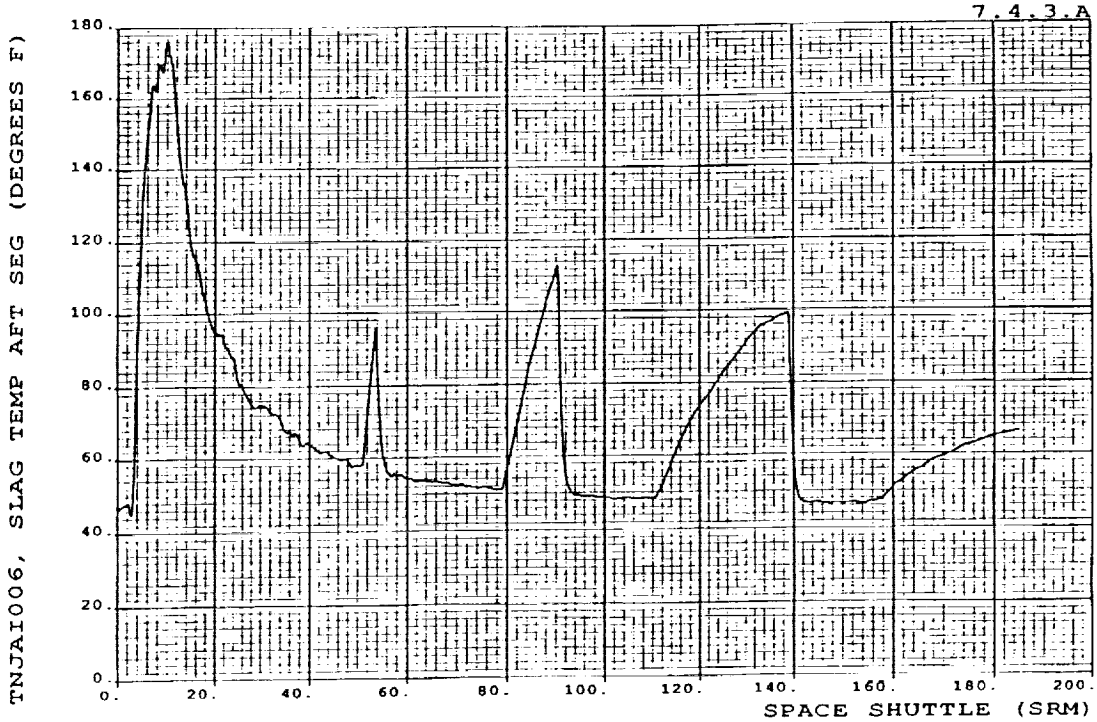

SPACE SHUTTLE (SRM)
TEM-05 STATIC TEST
23 JANUARY 1990

7.4.3.A

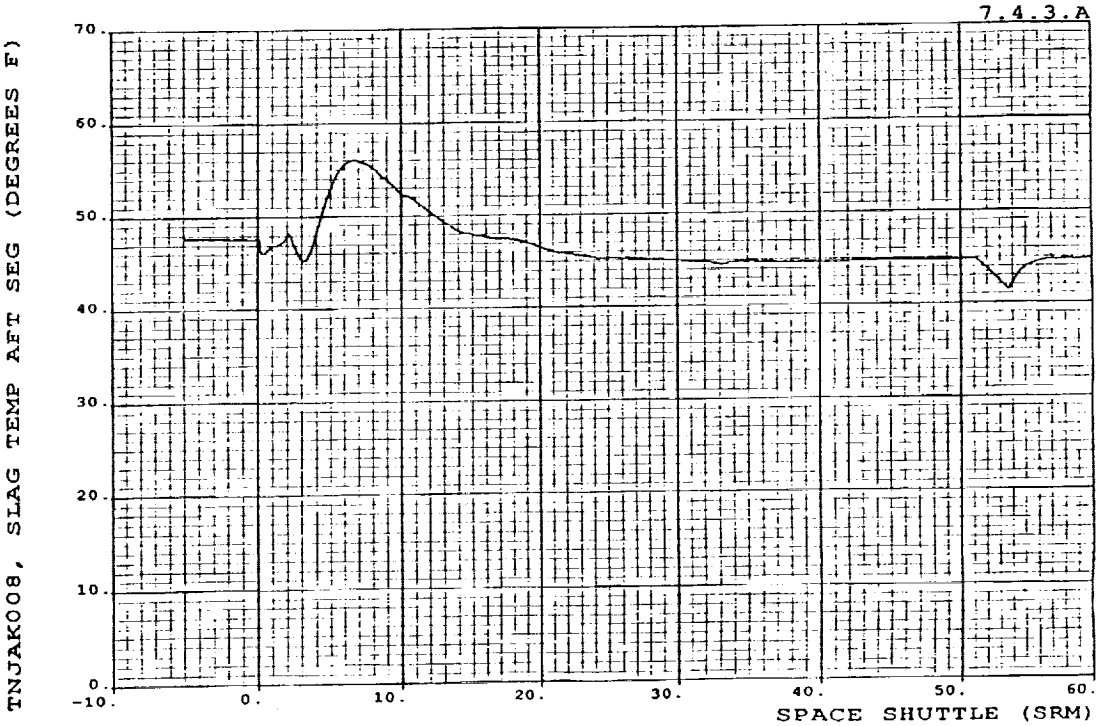

SPACE SHUTTLE (SRM)
TEM-05 STATIC TEST
23 JANUARY 1990

7.4.3.A

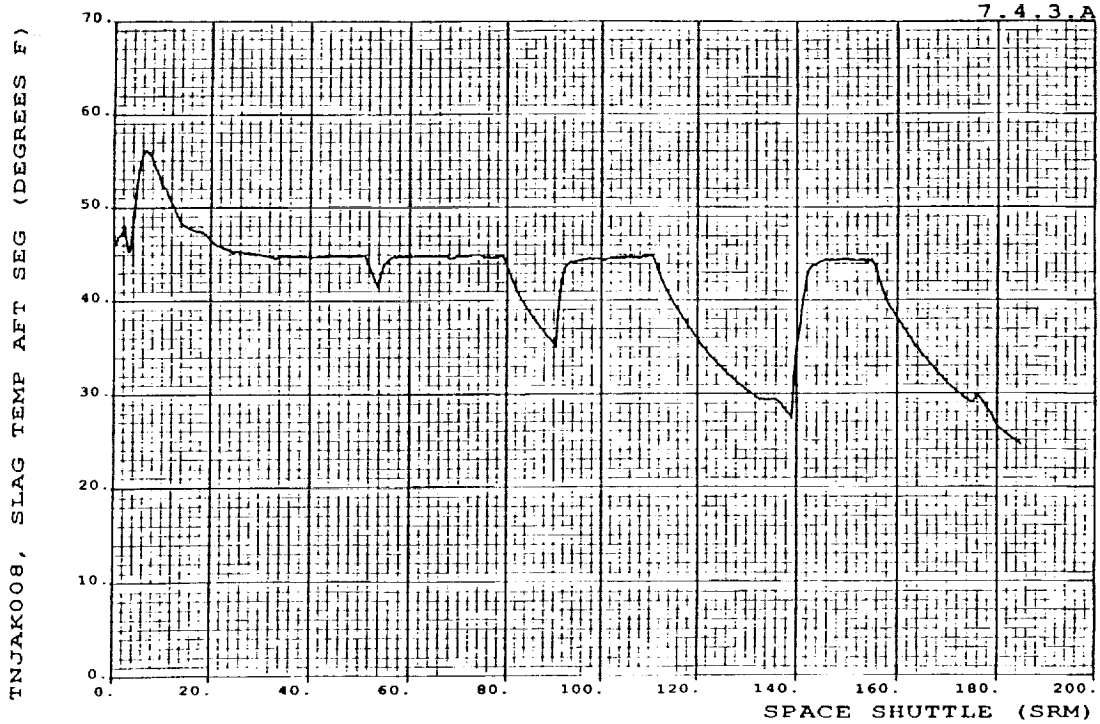

SPACE SHUTTLE (SRM)
TEM-05 STATIC TEST
23 JANUARY 1990

7.4.3.A

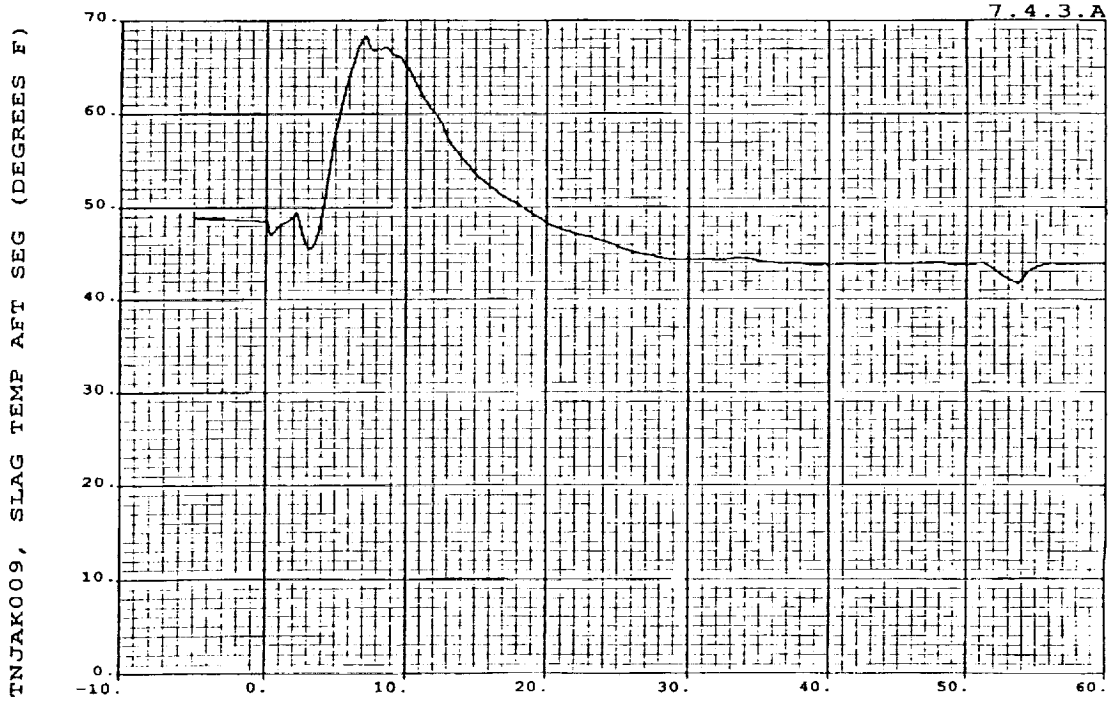

SPACE SHUTTLE (SRM)
TEM-05 STATIC TEST
23 JANUARY 1990

7.4.3.A

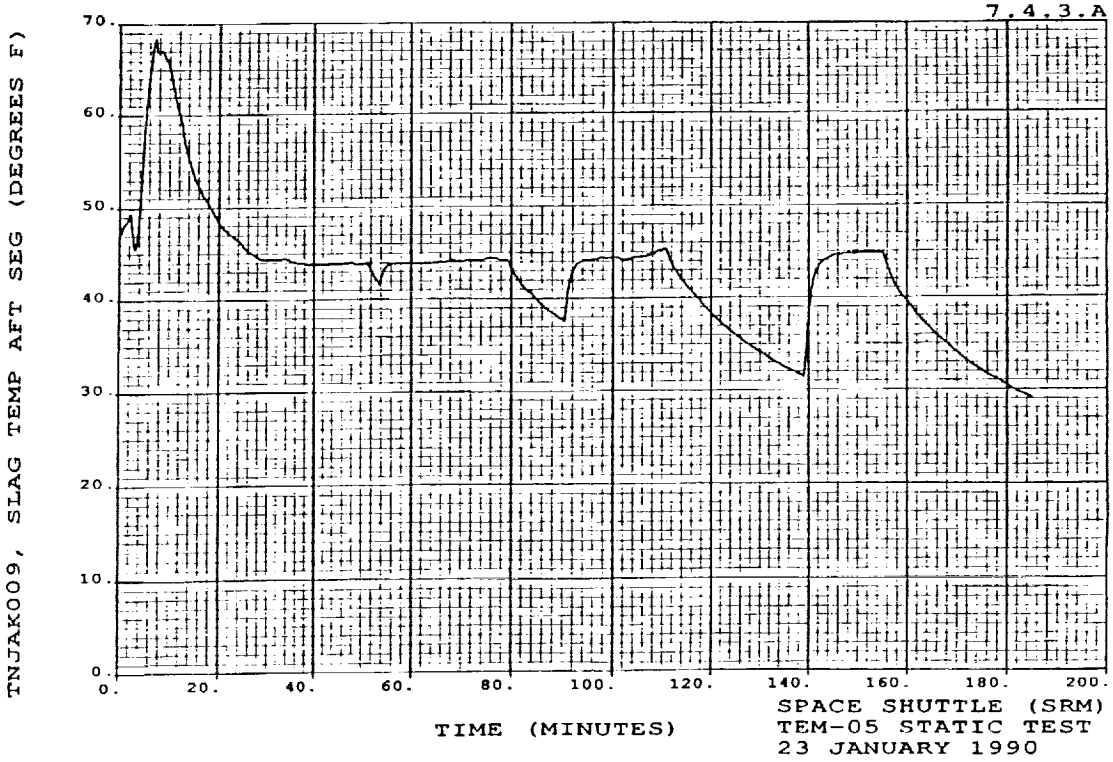
TNJAK009, SLAG TEMP AFT SEG (DEGREES F)
70.
60.
50.
40.
30.
20.
10.
0.
0.
20.
40.
60.
80.
100.
120.
140.
160.
180.
200.
TIME (MINUTES)
SPACE SHUTTLE (SRM)
TEM-05 STATIC TEST
23 JANUARY 1990

7.4.3.A

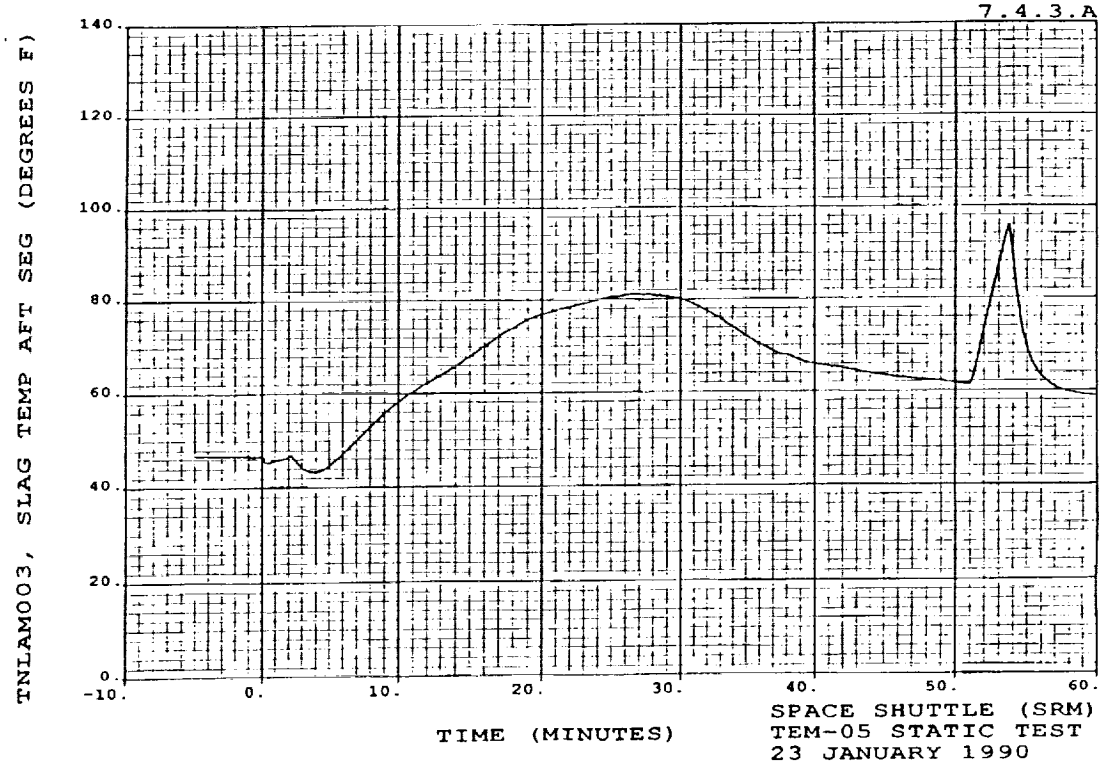
TNLAM003, SLAG TEMP AFT SEG (DEGREES F)
140.
120.
100.
80.
60.
40.
20.
0.
-10.
0.
10.
20.
30.
40.
50.
60.
TIME (MINUTES)
SPACE SHUTTLE (SRM)
TEM-05 STATIC TEST
23 JANUARY 1990

7.4.3.A

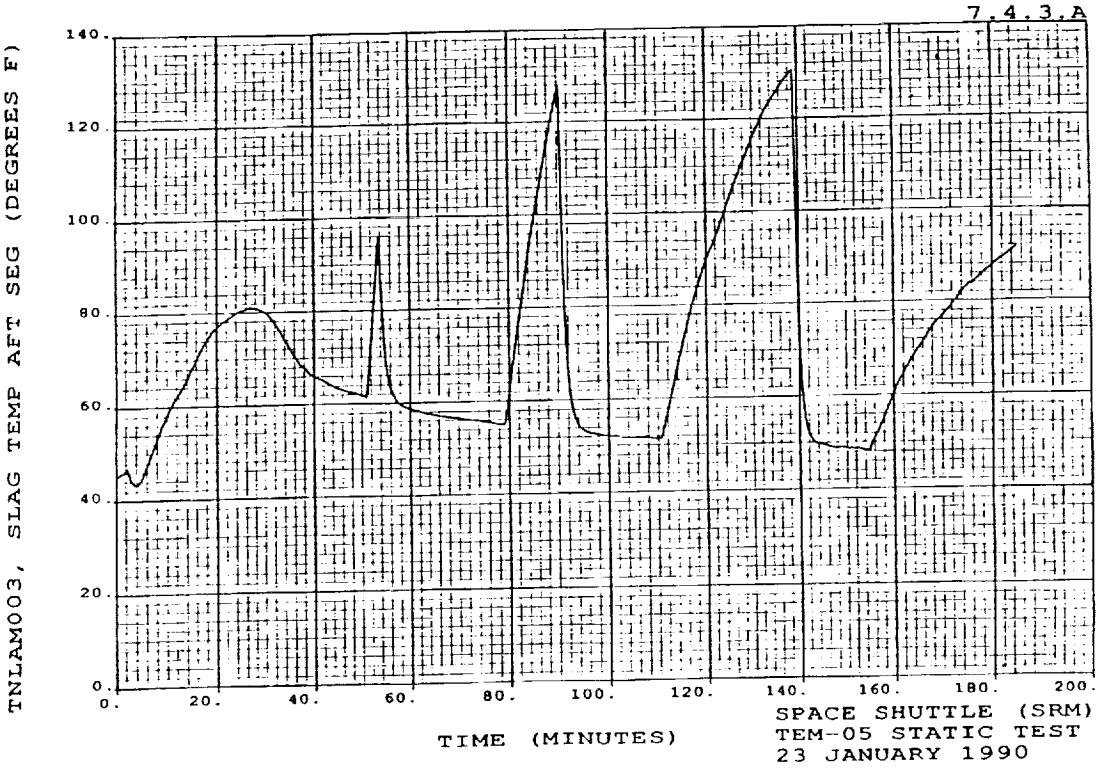

SPACE SHUTTLE (SRM)
TEM-05 STATIC TEST
23 JANUARY 1990

7.4.3.A

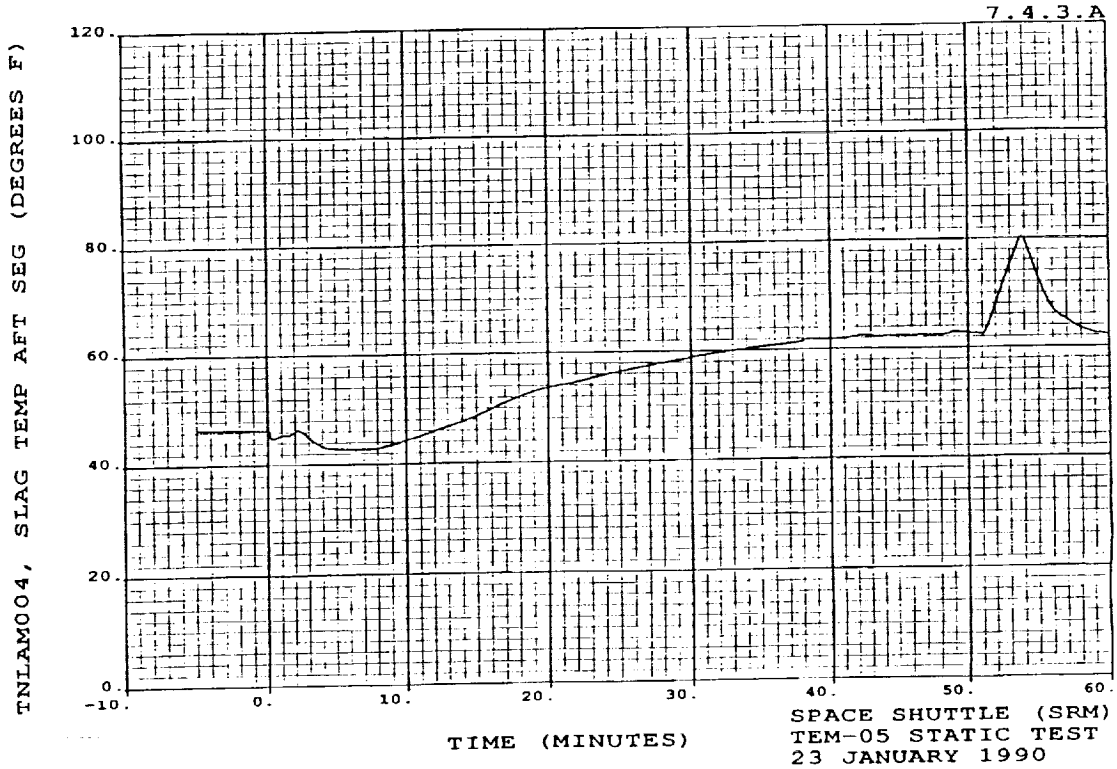

SPACE SHUTTLE (SRM)
TEM-05 STATIC TEST
23 JANUARY 1990

7.4.3.A

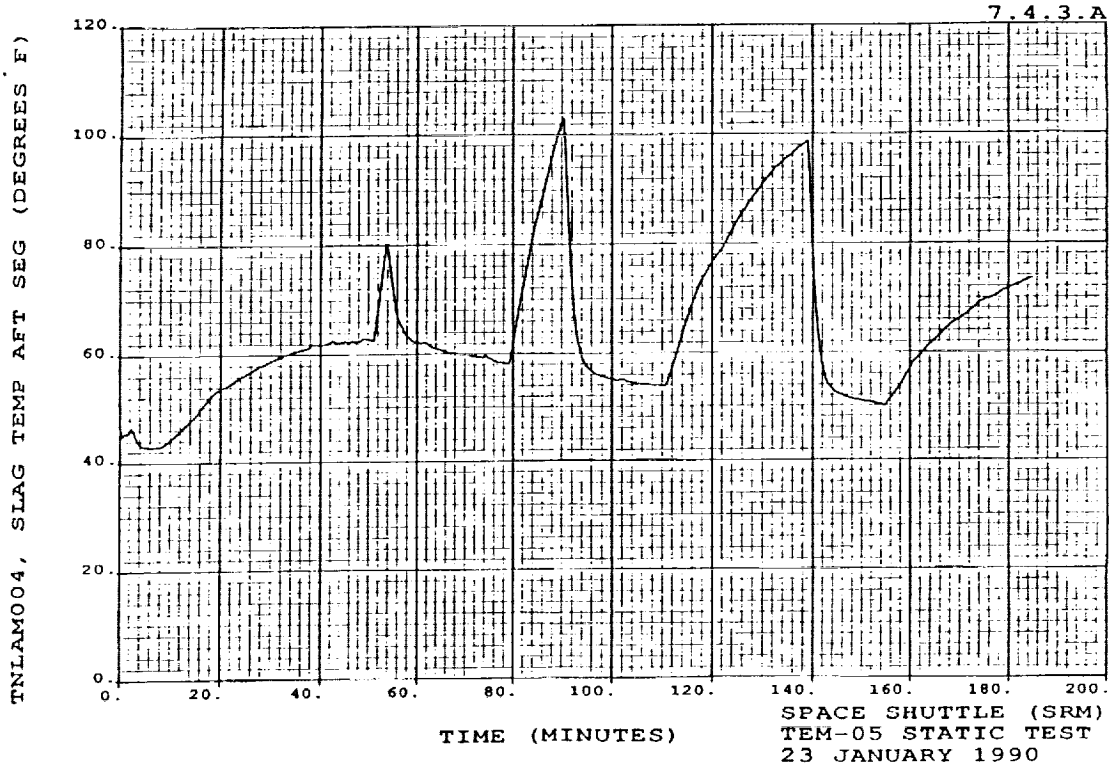
TNLAM004, SLAG TEMP AFT SEG (DEGREES F)
120.
100.
80.
60.
40.
20.
0.
0.
20.
40.
60.
80.
100.
120.
140.
160.
180.
200.
TIME (MINUTES)
SPACE SHUTTLE (SRM)
TEM-05 STATIC TEST
23 JANUARY 1990

7.4.3.B

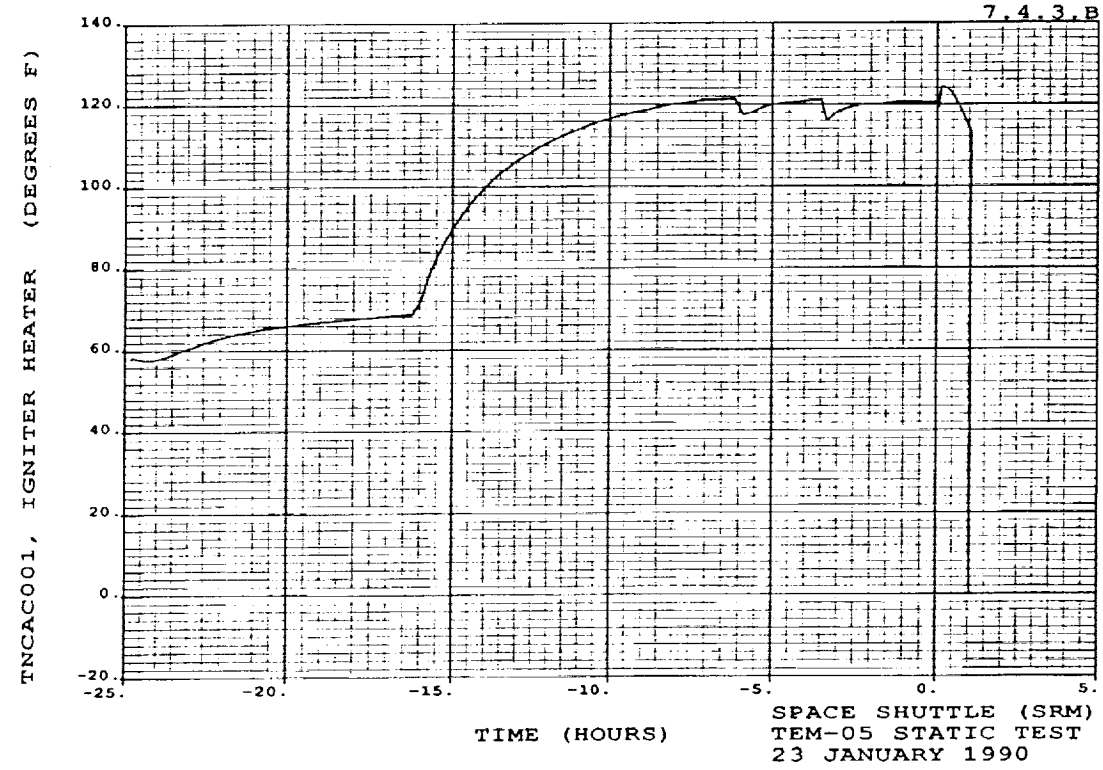
TNCAC001, IGNITER HEATER (DEGREES F)
140.
120.
100.
80.
60.
40.
20.
0.
-20.
-25.
-20.
-15.
-10.
-5.
0.
5.
TIME (HOURS)
SPACE SHUTTLE (SRM)
TEM-05 STATIC TEST
23 JANUARY 1990

7.4.3.B

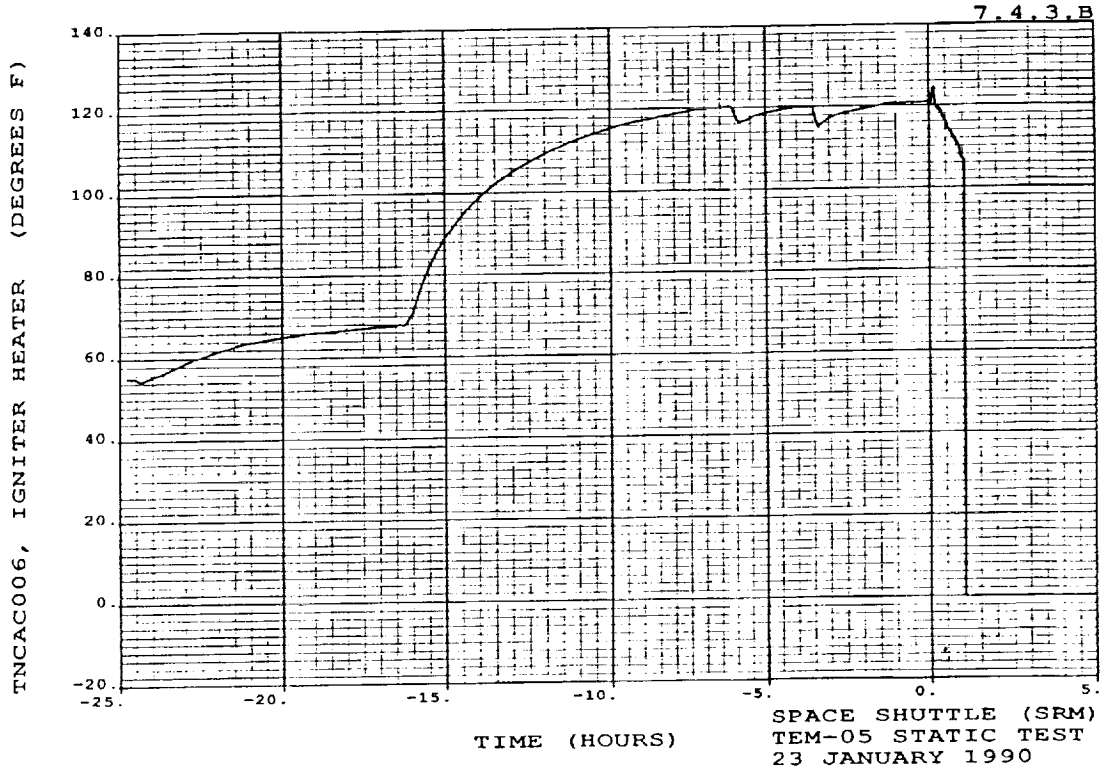

SPACE SHUTTLE (SRM)
TEM-05 STATIC TEST
23 JANUARY 1990

7.4.3.B

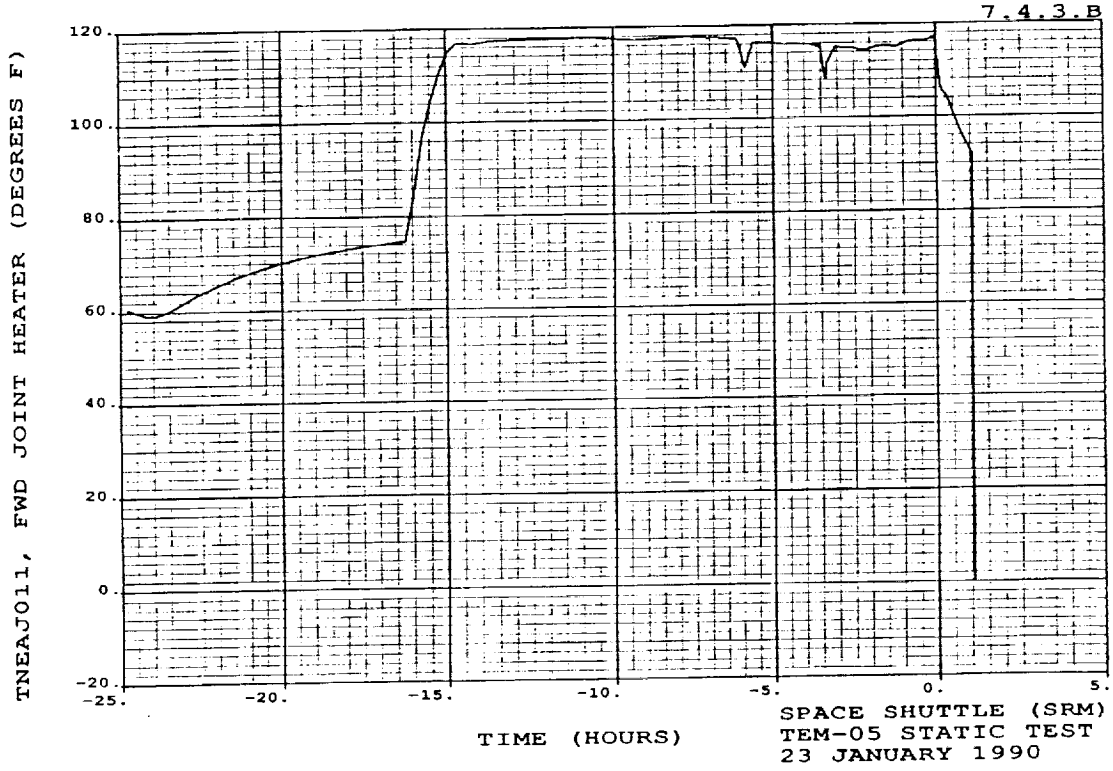

SPACE SHUTTLE (SRM)
TEM-05 STATIC TEST
23 JANUARY 1990

7.4.3.B

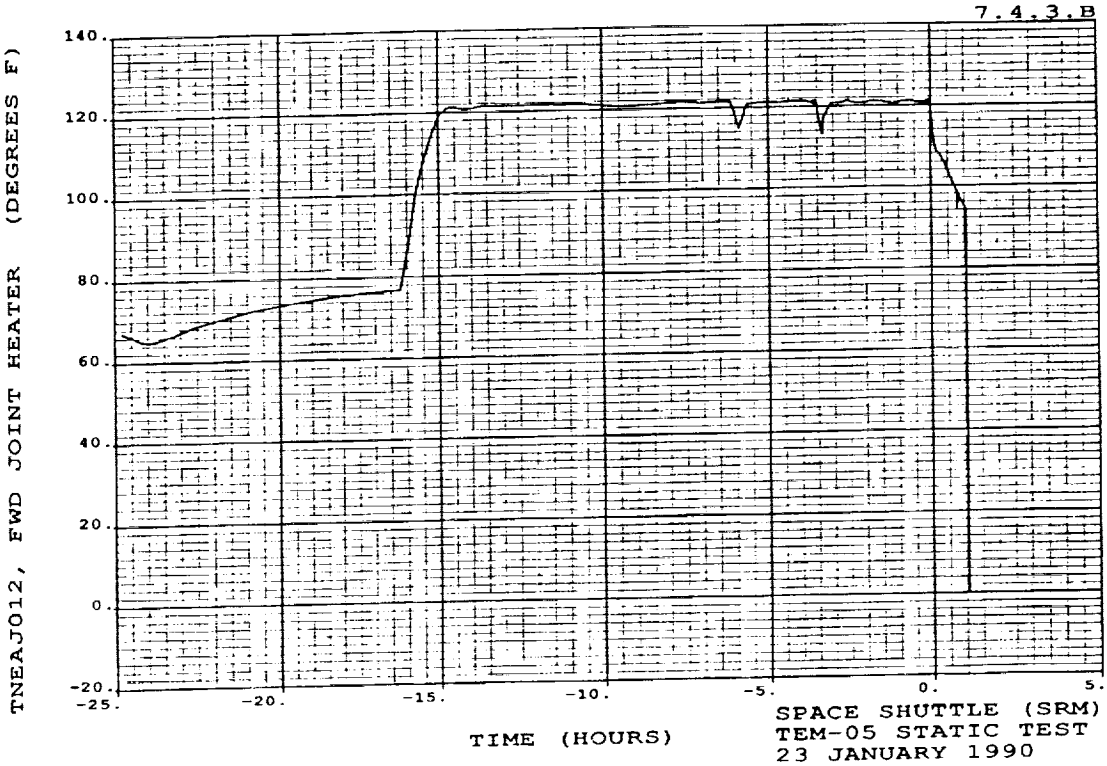
TNEAJ012, FWD JOINT HEATER (DEGREES F)
140.
120.
100.
80.
60.
40.
20.
0.
-20.
-25.
-20.
-15.
-10.
-5.
0.
5.
TIME (HOURS)
SPACE SHUTTLE (SRM)
TEM-05 STATIC TEST
23 JANUARY 1990

7.4.3.B

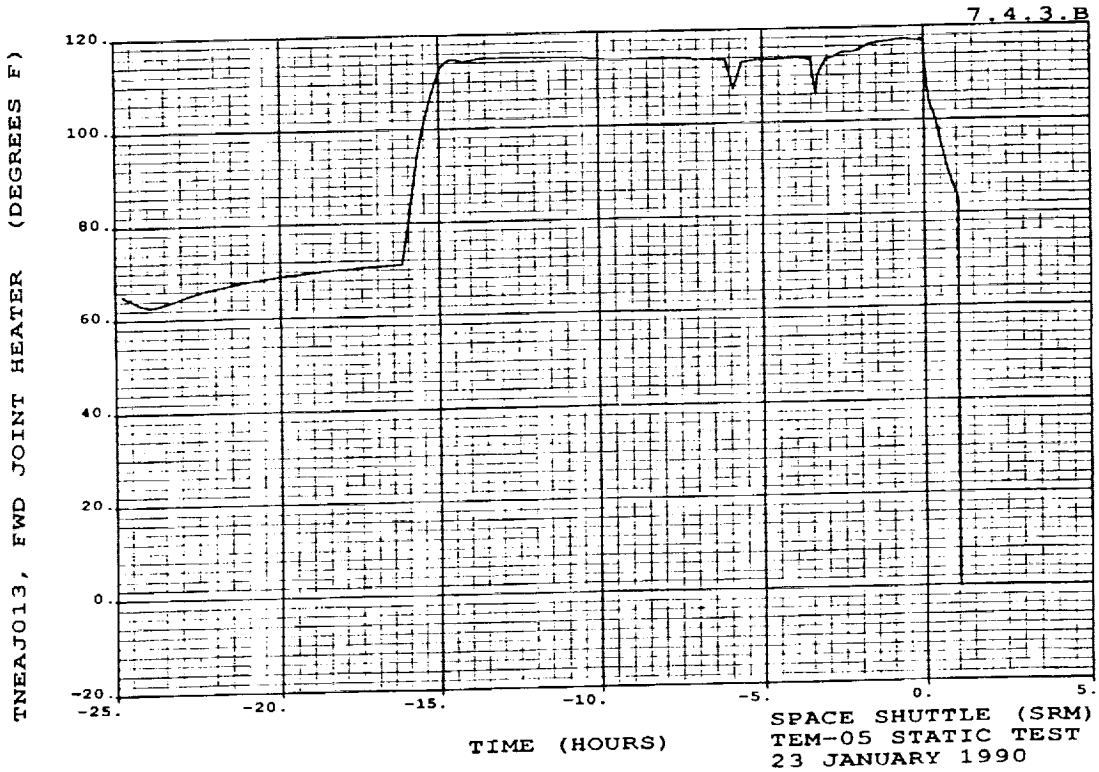
TNEAJ013, FWD JOINT HEATER (DEGREES F)
120.
100.
80.
60.
40.
20.
0.
-20.
-25.
-20.
-15.
-10.
-5.
0.
5.
TIME (HOURS)
SPACE SHUTTLE (SRM)
TEM-05 STATIC TEST
23 JANUARY 1990

7.4.3.B

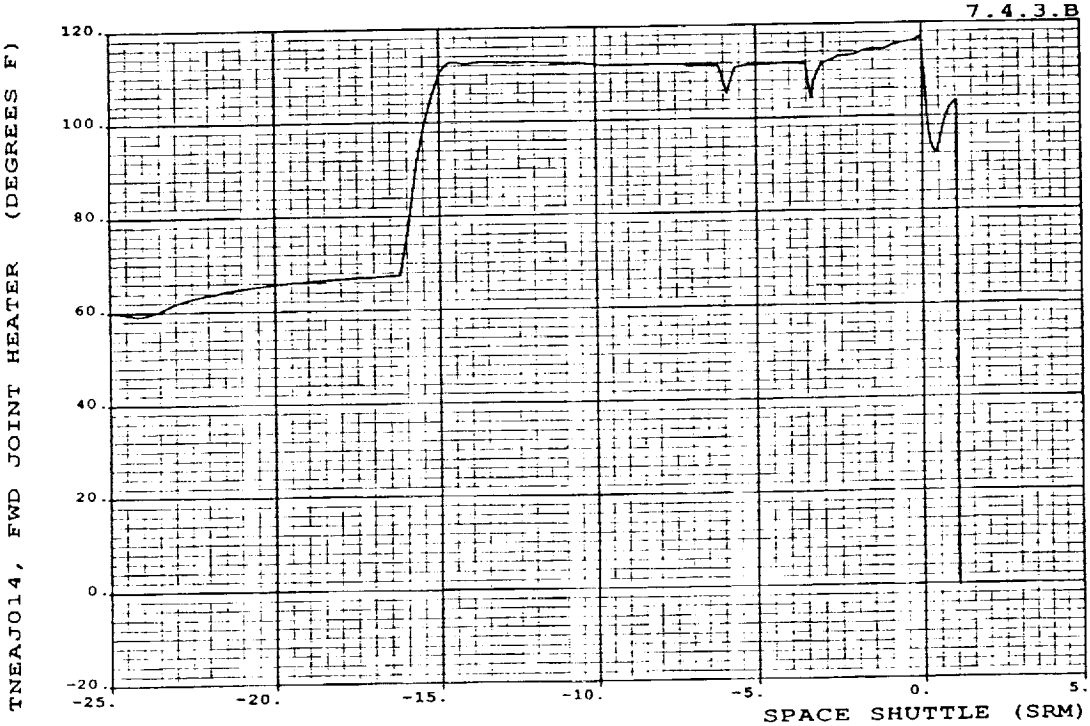

SPACE SHUTTLE (SRM)
TEM-05 STATIC TEST
23 JANUARY 1990

7.4.3.B

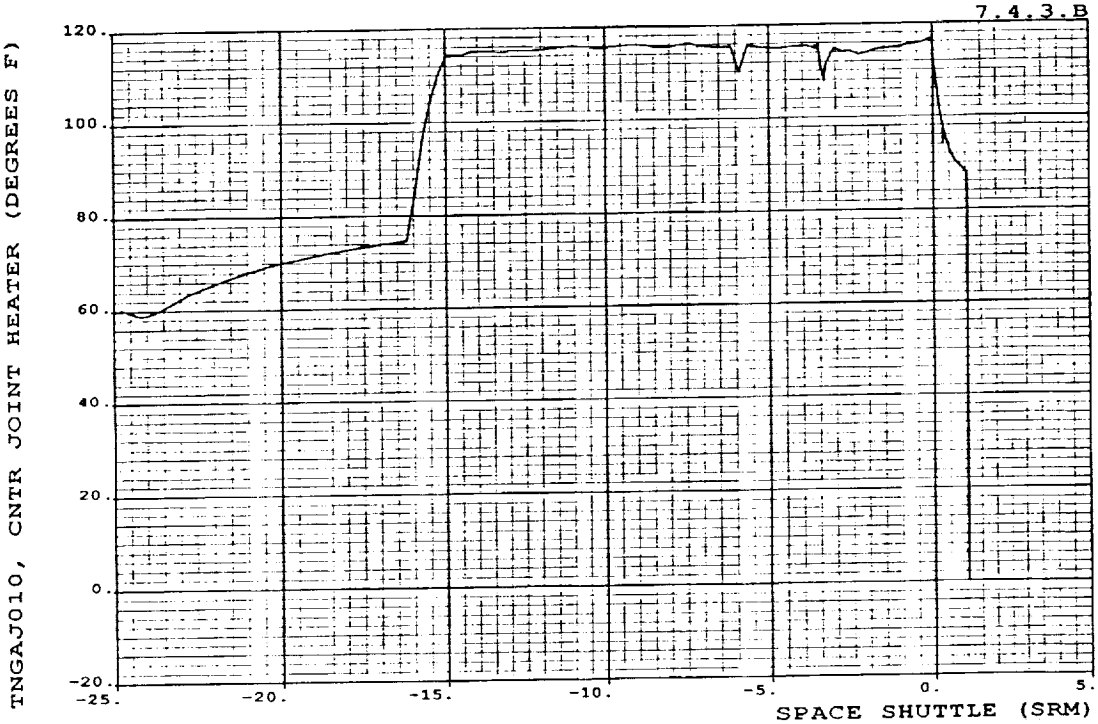

SPACE SHUTTLE (SRM)
TEM-05 STATIC TEST
23 JANUARY 1990

7.4.3.B

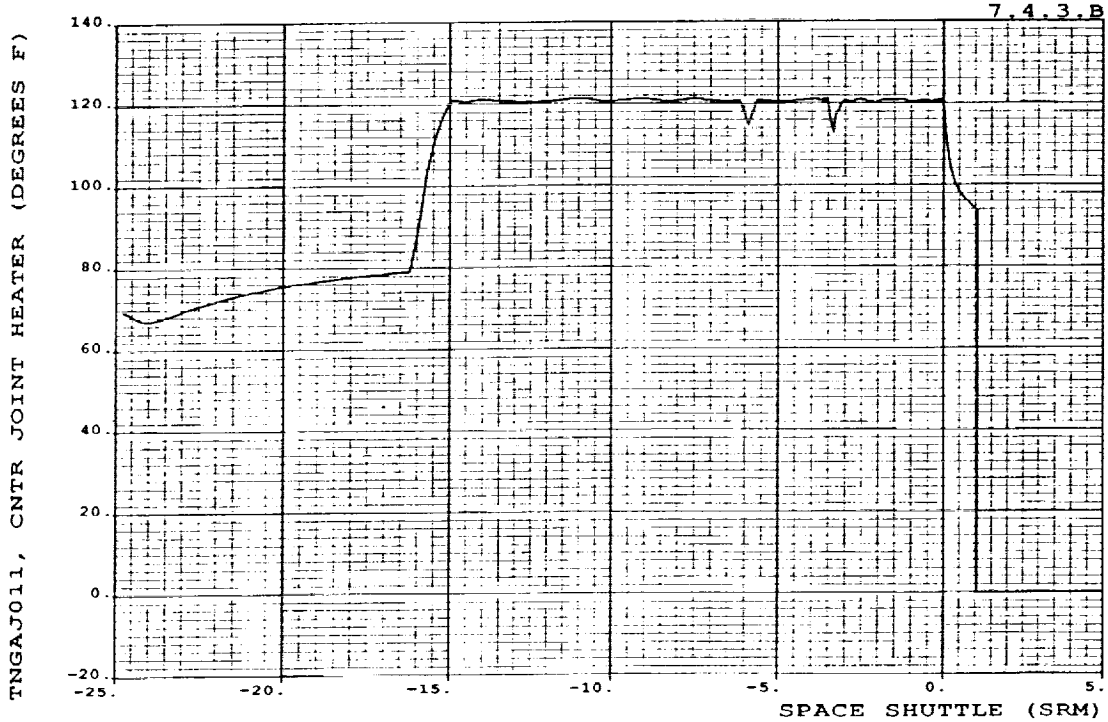

SPACE SHUTTLE (SRM)
TEM-05 STATIC TEST
23 JANUARY 1990

7.4.3.B

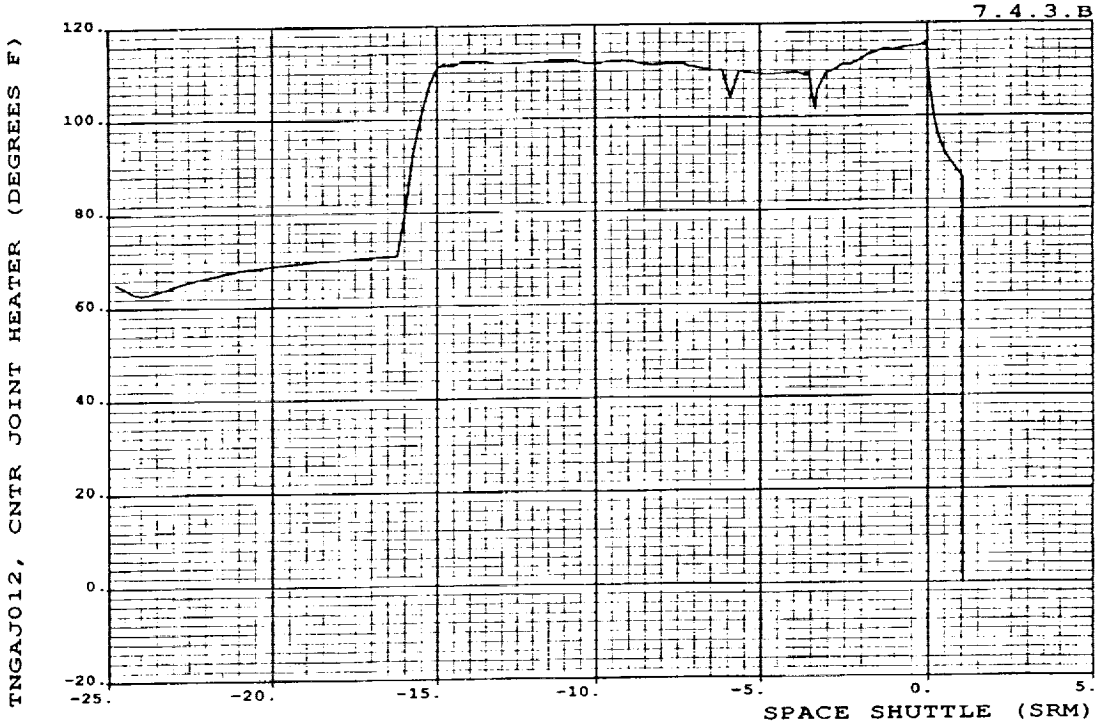

SPACE SHUTTLE (SRM)
TEM-05 STATIC TEST
23 JANUARY 1990

7.4.3.B

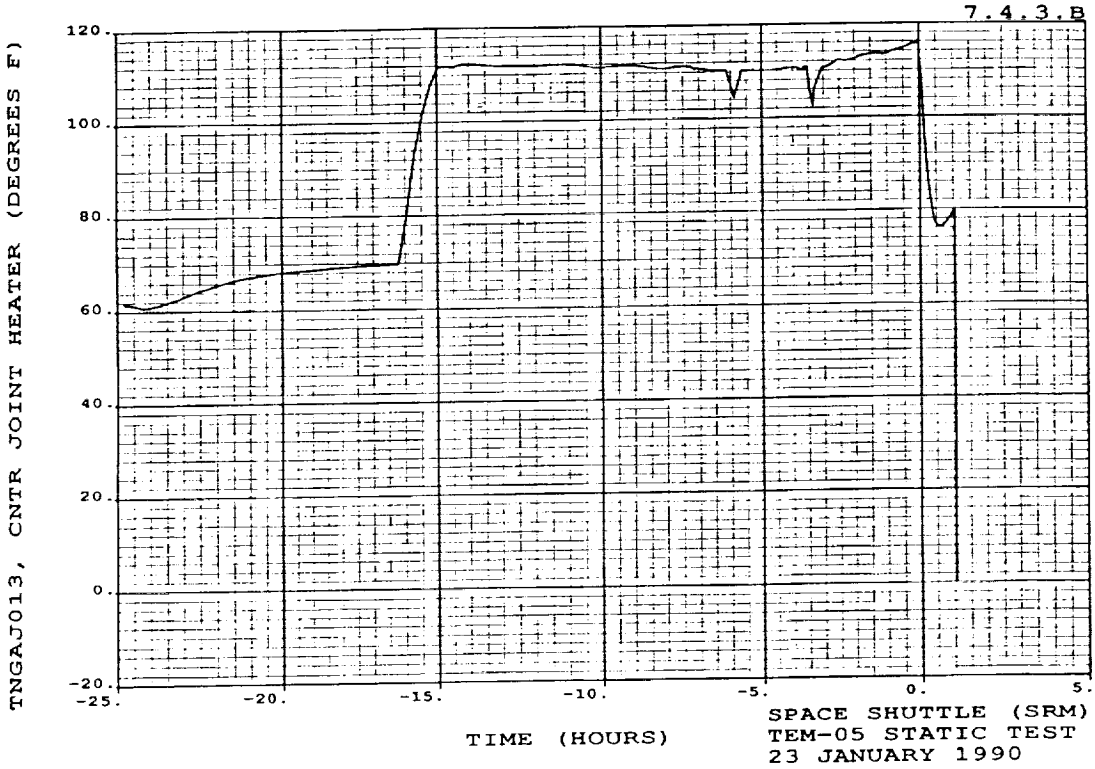
TNGAJ013, CNTR JOINT HEATER (DEGREES F)
120.
100.
80.
60.
40.
20.
0.
-20.
-25.
-20.
-15.
-10.
-5.
0.
5.
TIME (HOURS)
SPACE SHUTTLE (SRM)
TEM-05 STATIC TEST
23 JANUARY 1990

7.4.3.B

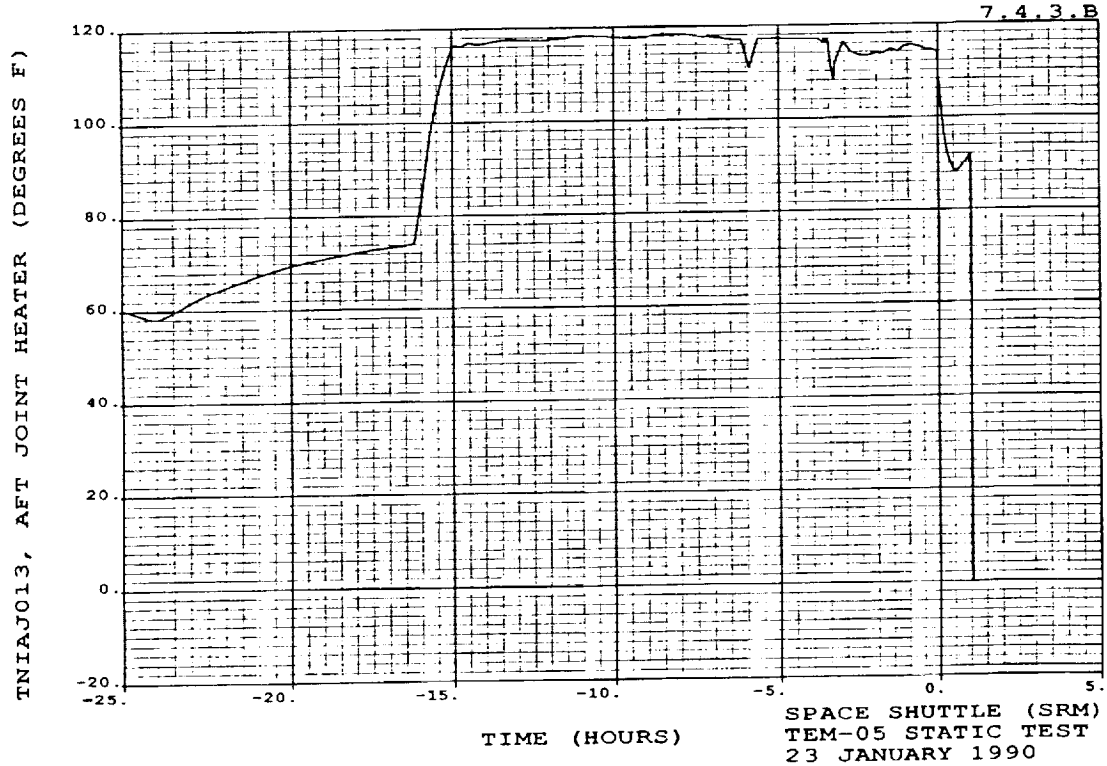
TNIAJ013, AFT JOINT HEATER (DEGREES F)
120.
100.
80.
60.
40.
20.
0.
-20.
-25.
-20.
-15.
-10.
-5.
0.
5.
TIME (HOURS)
SPACE SHUTTLE (SRM)
TEM-05 STATIC TEST
23 JANUARY 1990

7.4.3.B

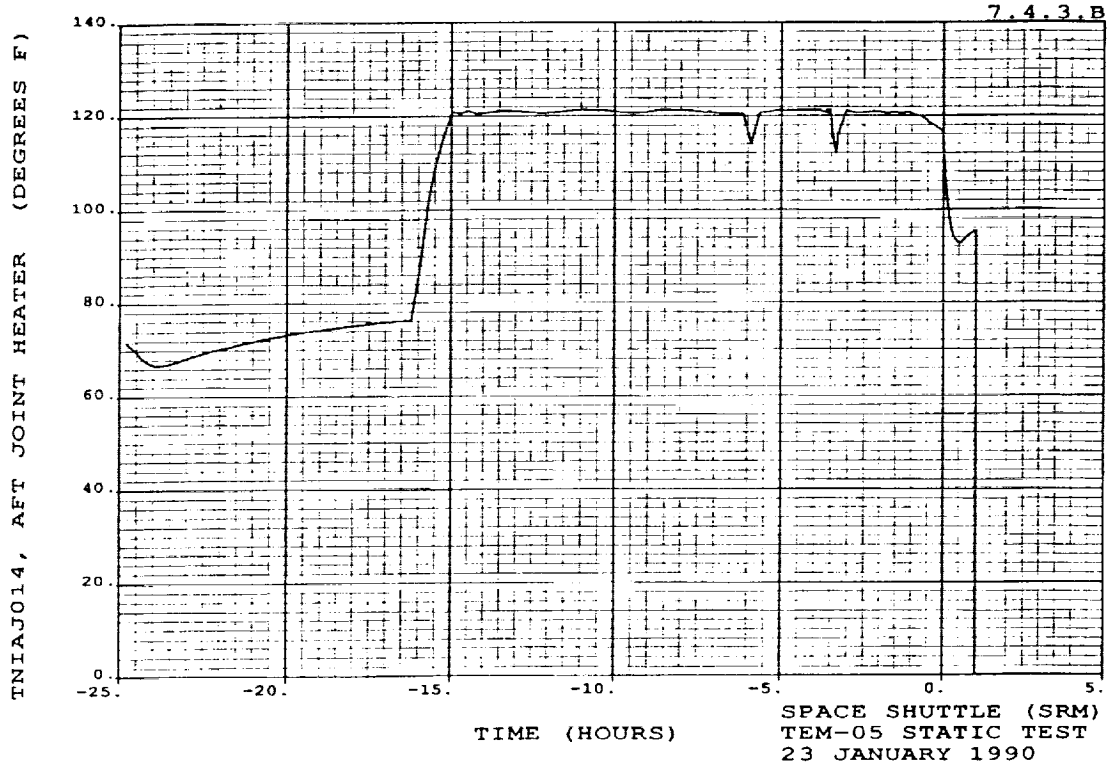

SPACE SHUTTLE (SRM)
TEM-05 STATIC TEST
23 JANUARY 1990

7.4.3.B

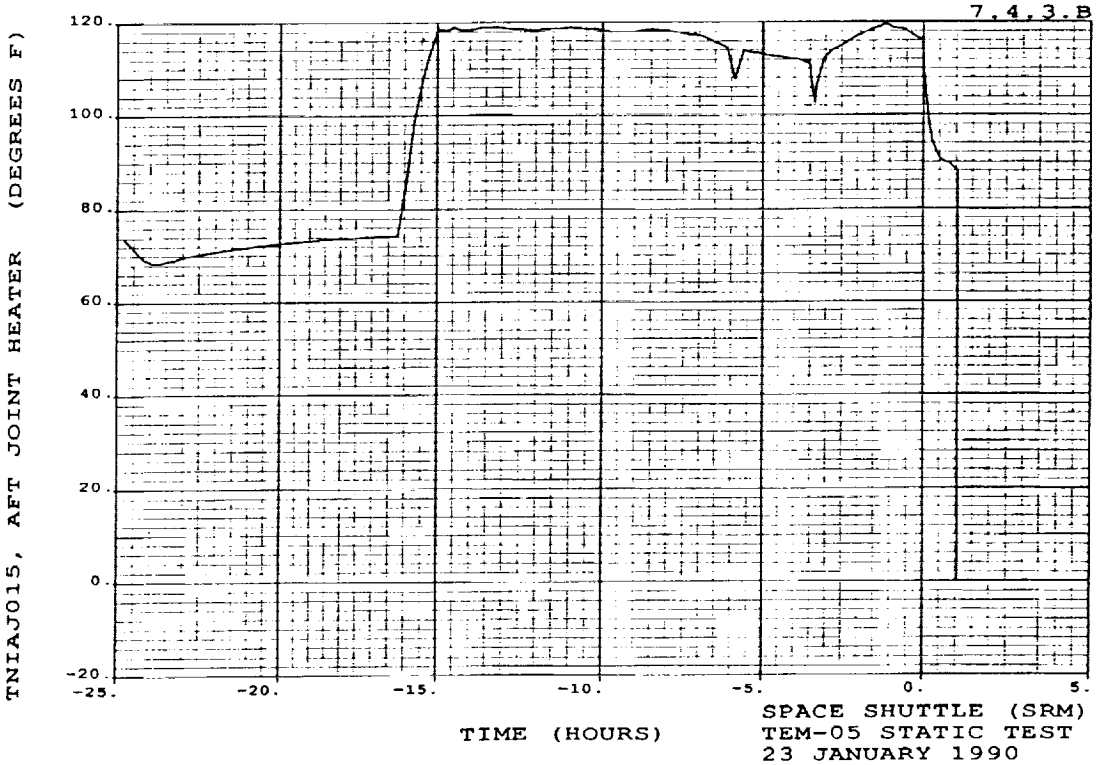

SPACE SHUTTLE (SRM)
TEM-05 STATIC TEST
23 JANUARY 1990

7.4.3.B

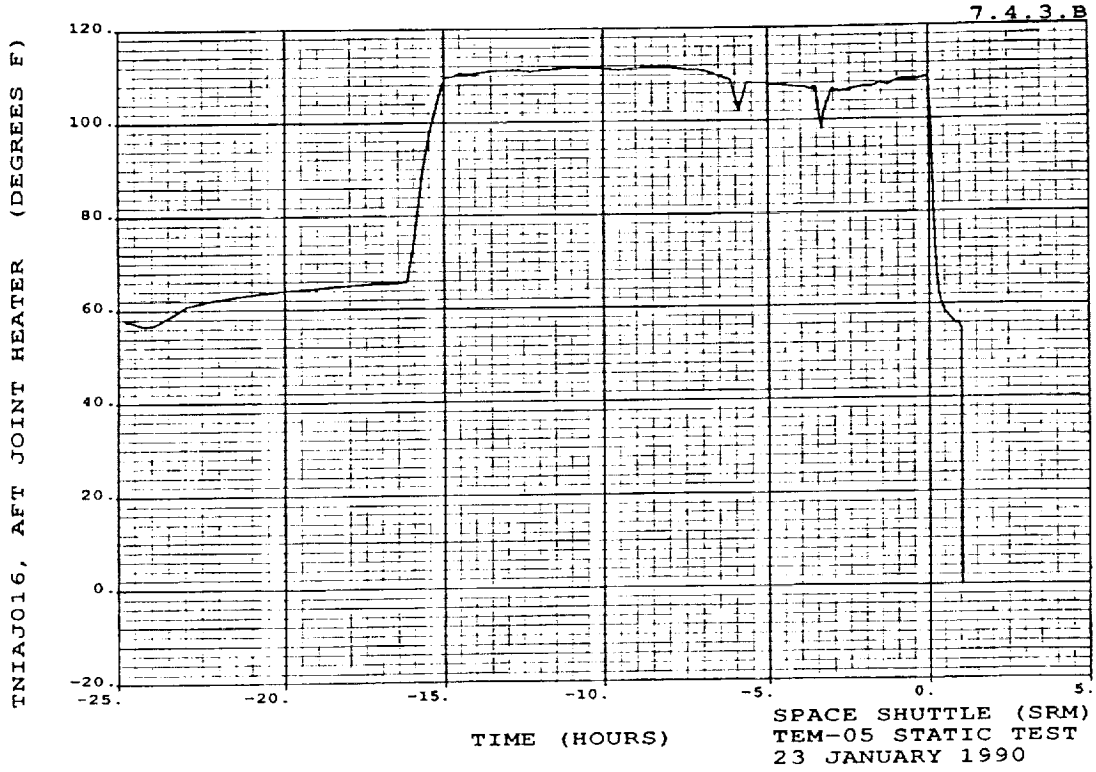

SPACE SHUTTLE (SRM)
TEM-05 STATIC TEST
23 JANUARY 1990

7.4.3.B

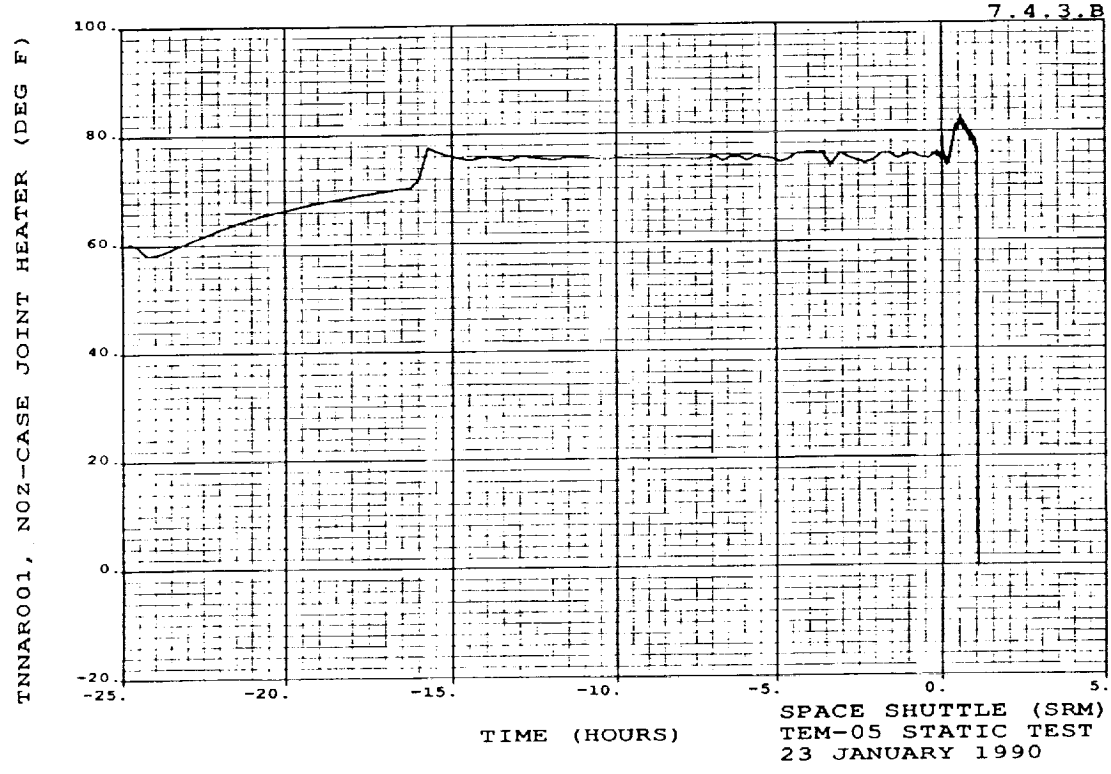

SPACE SHUTTLE (SRM)
TEM-05 STATIC TEST
23 JANUARY 1990

7.4.3.B

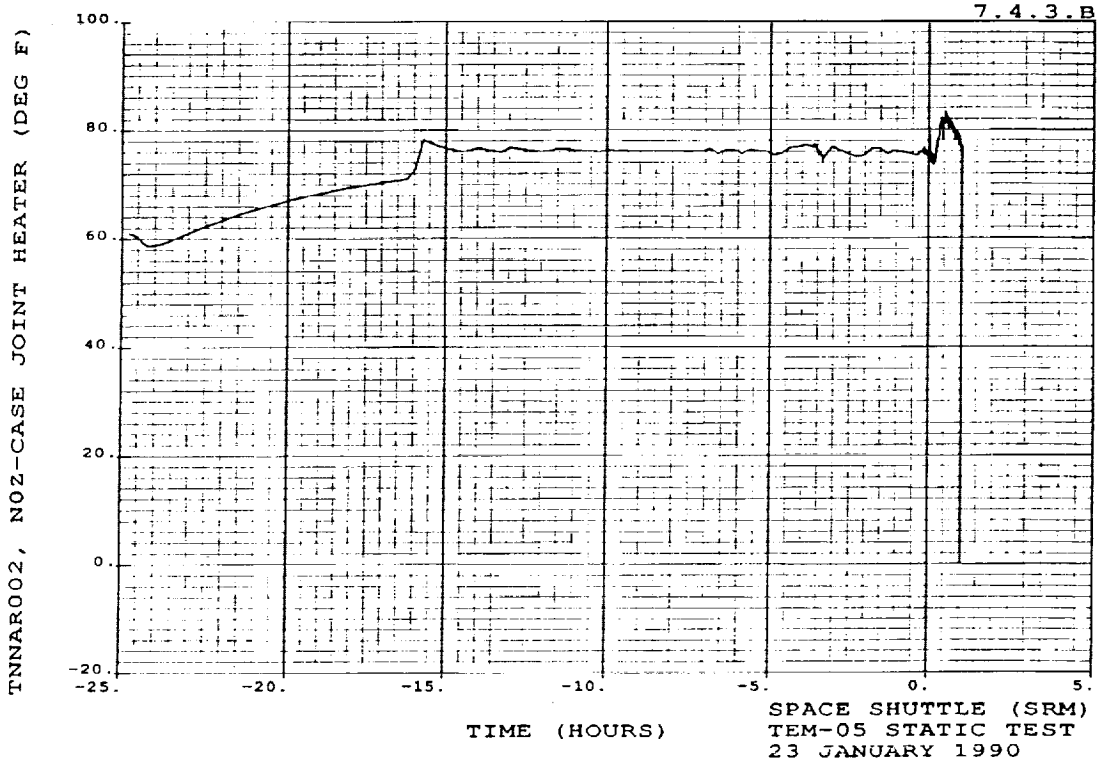
TNNAR002, NOZ-CASE JOINT HEATER (DEG F)
100.
80.
60.
40.
20.
0.
-20.
-25.
-20.
-15.
-10.
-5.
0.
5.
TIME (HOURS)
SPACE SHUTTLE (SRM)
TEM-05 STATIC TEST
23 JANUARY 1990

7.4.1.1.F

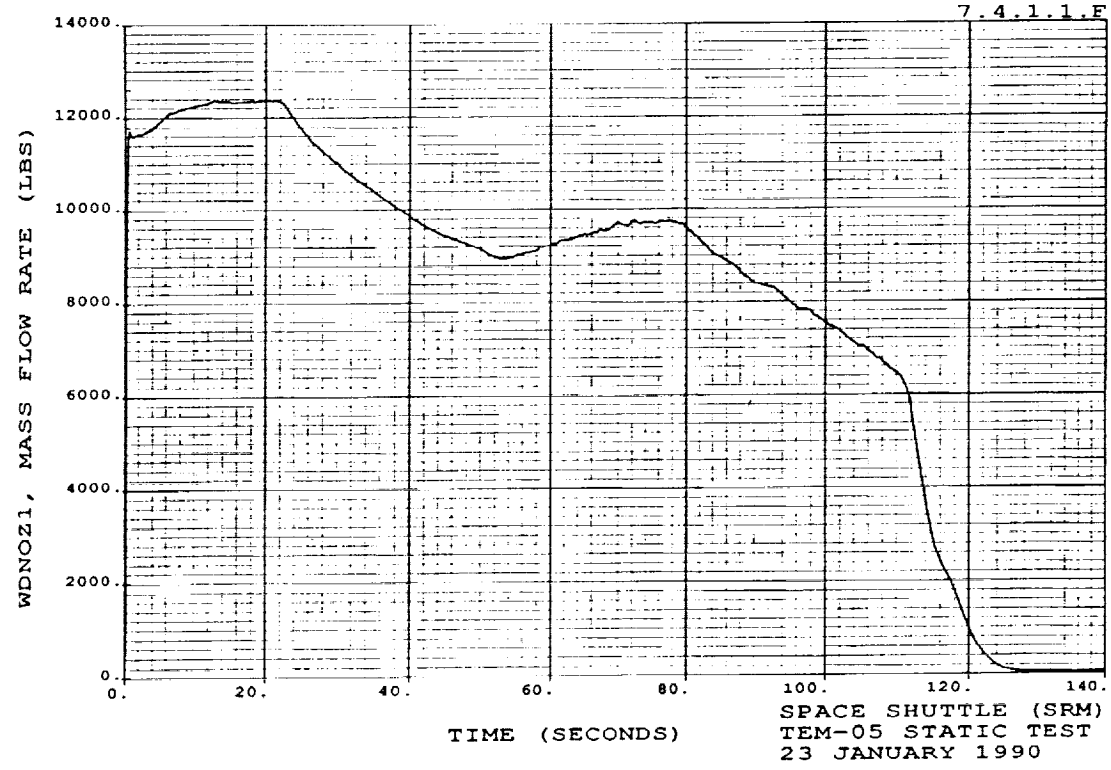
WDNOZ1, MASS FLOW RATE (LBS)
14000.
12000.
10000.
8000.
6000.
4000.
2000.
0.
0.
20.
40.
60.
80.
100.
120.
140.
TIME (SECONDS)
SPACE SHUTTLE (SRM)
TEM-05 STATIC TEST
23 JANUARY 1990

7.4.1.1.C

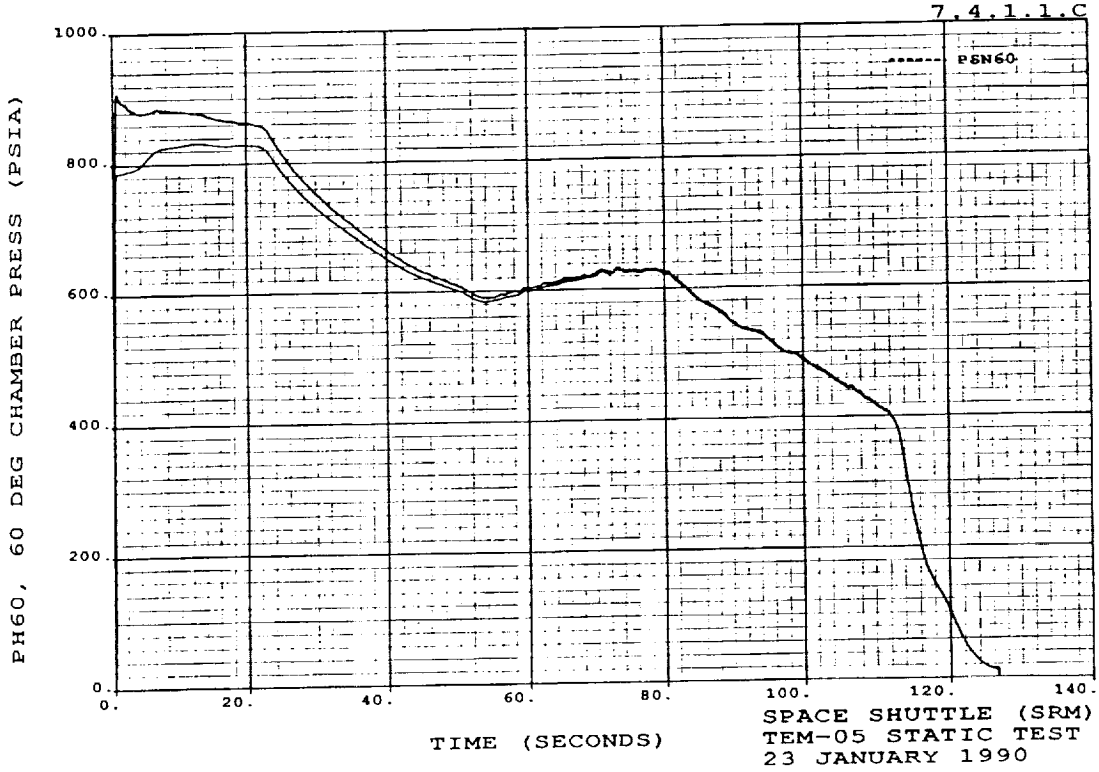
PSN60
PH60, 60 DEG CHAMBER PRESS (PSIA)
1000.
800.
600.
400.
200.
0.
0.
20.
40.
60.
80.
100.
120.
140.
TIME (SECONDS)
SPACE SHUTTLE (SRM)
TEM-05 STATIC TEST
23 JANUARY 1990

7.4.1.1.B

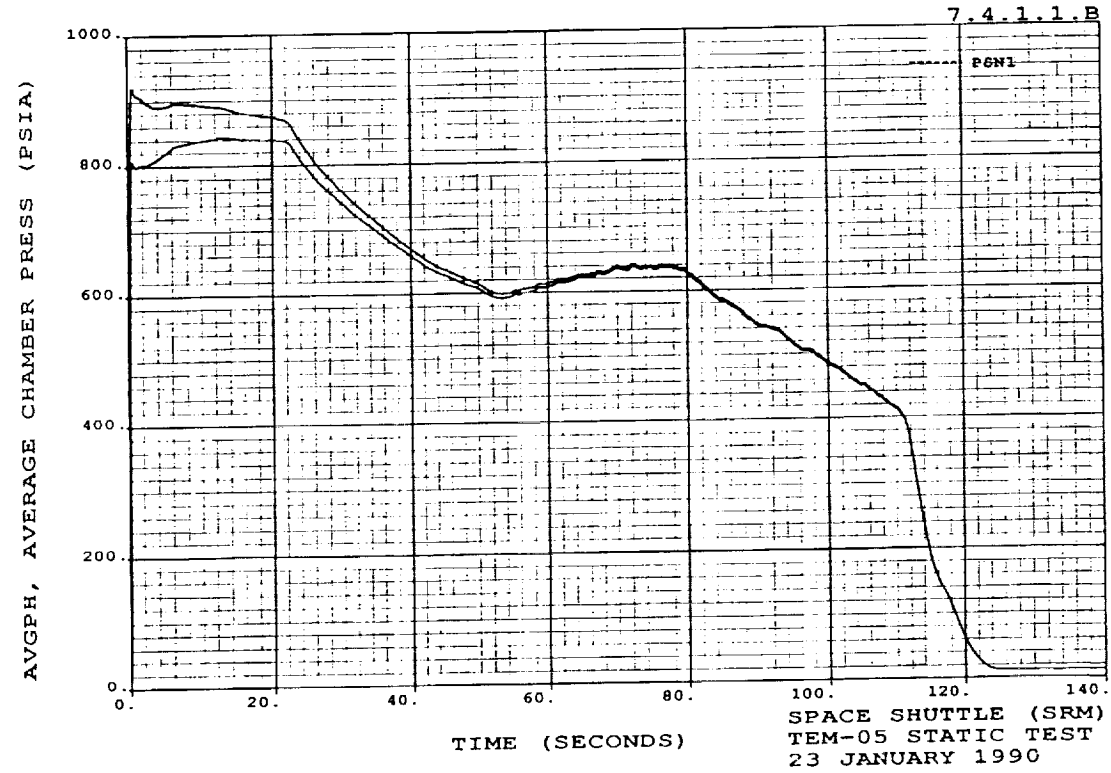
PSN1
AVGPH, AVERAGE CHAMBER PRESS (PSIA)
1000.
800.
600.
400.
200.
0.
0.
20.
40.
60.
80.
100.
120.
140.
TIME (SECONDS)
SPACE SHUTTLE (SRM)
TEM-05 STATIC TEST
23 JANUARY 1990

Appendix D

TEM-5 Case-to-Nozzle Joint Pressure Measurement Analysis

TEM-5 Case-to-Nozzle Joint Pressure Measurement Analysis

Action:

Determine if predicted case-to-nozzle joint opening correlates with negative pressure measurements on TEM-5.

Analysis:

A hand analysis was completed using nominal hardware dimensions, gap openings from the NJES 1A hot fire test, and the assumption that primary O-ring was in the upstream position (post-leak-test position) and stayed there throughout motor pressurization. The last assumption is valid where no blowholes were found in the joint.

Calculations:

Initial Volume Calculation (nominal) O-rings in Post-Leak-Test Position

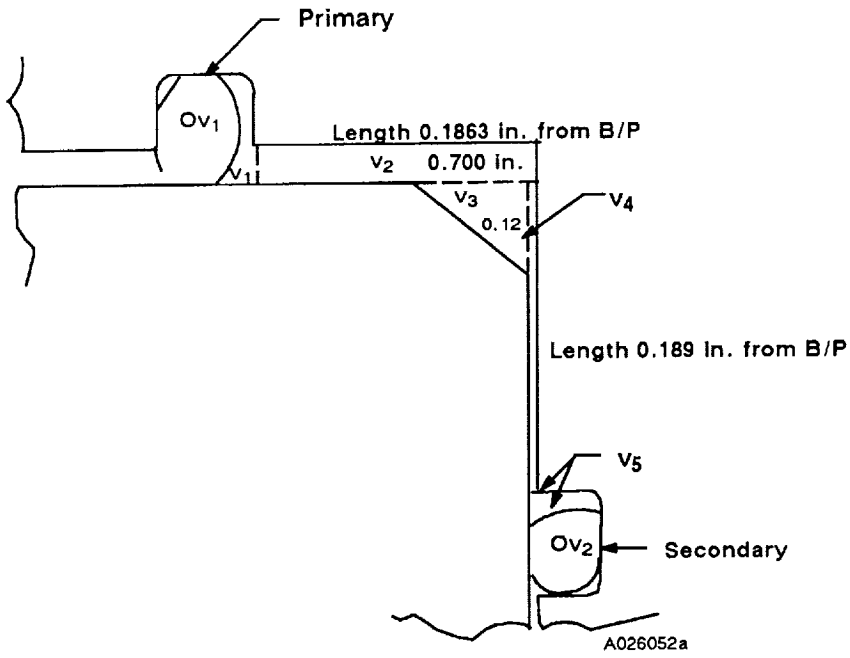

Used standard circular torus equation to calculate volumes.

$2\pi R$ (area) where R is the distance to the center of the axis of rotation

Ov_1 = O-ring volume in Gland No. 1
Ov_2 = O-ring volume in Gland No. 2

O-ring volumes calculated per squeeze formula (TWR-15771) on squeeze program on computer.

Ov_1 = 81% (Table 1)
Ov_2 = 91.8% (Table 2)

$v_1 = 2\pi R_1$ (Gland Area$_1$ (1-Ov_1))
$v_5 = 2\pi R_5$ (Gland Areas$_5$ (1-Ov_2))
$v_2 = 2\pi R_2$ (initial gap x area length)
$v_3 = 2\pi R_3$ (chamfer area)
$v_4 = 2\pi R_4$ (initial gap x area length)
$v_T = v_1 + v_5 + v_2 + v_3 + v_4$

$v_1 = 2\pi R_1$ (Gland Area$_1$ (1 - Ov_1))

Gland Area$_1$ = 0.199 in. nominal groove depth
+ 0.020 in. assumed initial gap
x 0.378 in. nominal groove width

Gland Area$_1$ = (0.199 + 0.020 in.) (0.378 in.) = 0.082782 in.^{2}

R_1 = 51.6535 in. from B/P (nominal)

$v_1 = 2\pi$ (51.6535 in.) (0.082782 in.^{2}) = <u>5.1047 in.^{3}</u> (1 - 0.81 in.)

$v_5 = 2\pi R_5$ (Gland Area$_5$ (1 - Ov_2))

Gland Area$_5$ = 0.214 in. nominal groove depth
+ 0.0 in. initial gap
x 0.308 in. nominal groove width

Gland Area$_5$ = (0.214 + 0.0 in.) (0.308 in.) = 0.065912 in.^{2}

R_5 = 51.952 in. from B/P (nominal)

$v_5 = 2\pi$ (51.952 in.) (0.065912 in.^{2}) (1 - 0.918 in.) = <u>1.7643 in.^{3}</u>

$v_2 = 2\pi R_2$ (initial gap x area length)

Initial gap = 0.020 in. (assumed)

Area length = 0.8163 in. (from B/P)

R_2 = 51.753 in. from B/P (nominal)

Table 1

TEM N/C Primary With 1U75150-26 O-ring — Assembled Results

	Minimum	Maximum	Units
Stretch	1.6906	1.6906	%
Stretch Red	1.5162	1.5162	%
Temperature Adjusted Diameter	0.2898	0.2898	inches
Total Adjusted Diameter	0.2898	0.2898	inches
Squeeze	0.0708	0.0708	inches
Squeeze	24.4236	24.4236	%
Fill	81.0868	81.0868	%

TEM N/C Primary With 1U75150-26 O-ring — Input Parameters

	Minimum	Maximum	Units
O-ring Diameter	0.2940	0.2940	inches
O-ring ID	101.3000	101.3000	inches
Groove OD	103.5260	103.5260	inches
Groove Depth	0.2190	0.2190	inches
Groove Width	0.3780	0.3780	inches
Temperature	75.0000	75.0000	°F
Initial Gap	0.0000	0.0000	inches

Ambient Temperature	68.0°F
Comp Set	0.0%
Coefficient Expansion O-ring	0.11E-03 in./in./°F
Coefficient Expansion Case	0.74E-05 in./in./°F

Table 2

TEM N/C Secondary With 1U75150-28 O-ring — Assembled Results

	Minimum	Maximum	Units
Stretch	0.6475	0.6475	%
Stretch Red	0.6544	0.6544	%
Temperature Adjusted Diameter	0.2764	0.2764	inches
Total Adjusted Diameter	0.2764	0.2764	inches
Squeeze	0.0624	0.0624	inches
Squeeze	22.5756	22.5756	%
Fill	91.9819	91.8433	%

TEM N/C Secondary With 1U75150-28 O-ring — Input Parameters

	Minimum	Maximum	Units
O-ring Diameter	0.2780	0.2780	inches
O-ring ID	103.1600	103.1600	inches
Groove OD	104.5200	104.5200	inches
Groove Depth	0.2140	0.2140	inches
Groove Width	0.3080	0.3080	inches
Temperature	75.0000	75.0000	°F
Initial Gap	0.0000	0.0000	inches

Ambient Temperature	68.0°F
Comp Set	0.0%
Coefficient Expansion O-ring	0.11E-03 in./in./°F
Coefficient Expansion Case	0.74E-05 in./in./°F

v_2 = 2π (51.753 in.) (0.020 x 0.8163 in.) = 5.3088 in.^{3}

v_3 = $2\pi R_3$ (chamfer area)

chamfer area = $\frac{0.120 \times 0.700 \text{ in.}}{2}$ (from B/P)

R_3 = 51.823 in. from B/P (nominal)

v_3 = 2π (51.823 in.) ((0.120 x 0.700 in.)/2) = 13.6758 in.^{3}

v_4 = $2\pi R_4$ (initial gap x area length)

Initial gap = 0.0 (assumed)

Area length = 0.189 in. (from B/P)

R_4 = 51.8575 in. from B/P (nominal)

v_4 = 2π (51.8575 in.) (0.0 x 0.189 in.) = 0.0 in.^{3}

$v_T = v_1 + v_5 + v_2 + v_3 + v_4$

v_T = 5.1047 in.^{3} + 1.7643 in.^{3} + 5.3088 in.^{3} + 13.6758 in.^{3} + 0.0 in.^{3}

v_T = 25.8536 in.^{3} (initial volume before pressurization)

Volume Calculation During Motor Pressurization Assumed Primary O-ring Not Pressurized

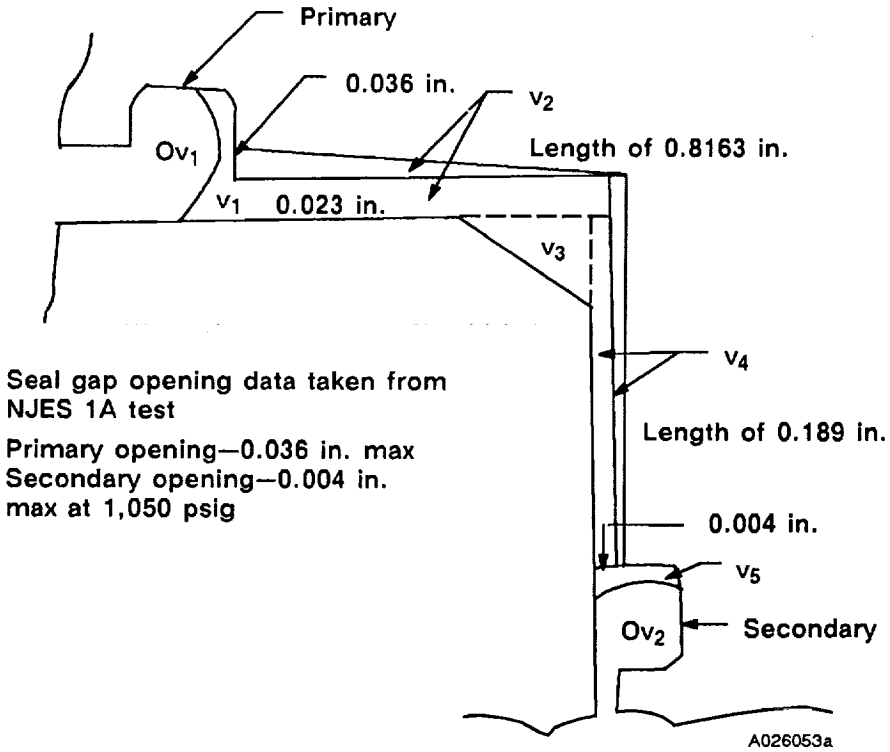

Seal gap opening data taken from NJES 1A test

Primary opening—0.036 in. max
Secondary opening—0.004 in. max at 1,050 psig

By use of similar triangles, taking into account the 0.004 in. deflection at the secondary, it was determined that the corner would experience a 0.00481 in. deflection. Zero deflection was assumed at the axial bolt centerline. An assumed linear opening of 0.003 in. was added to the initial gap opening of 0.020 in. aft of the primary O-ring groove making the pressurized initial gap equal 0.023 in. Deflection of 0.036 in. at primary O-ring groove assumed.

Pressurized squeeze calculations allowed new O-ring volume calculations.

Ov_1 = 69.6% (Table 3)

Ov_2 = 90.1% (Table 4)

$v_1 = 2\pi R_1$ (Gland Area$_1$ (1 - Ov_1))

Gland Area$_1$ = 0.199 in. nominal groove depth
+ 0.020 in. assumed initial gap
+ 0.036 in. gap opening (NJES 1A primary deflection)
x 0.378 in. nominal groove width

Gland Area$_1$ = (0.199 + 0.02 + 0.036 in.) (0.378 in.) = 0.096390 in.^{2}

R_1 = 51.6355 in. (rotation adjusted)

$v_1 = 2\pi$ (51.6355 in.) (0.096390 in.^{2}) (1 - 0.696 in.) = <u>9.5068 in.^{3}</u>

$v_5 = 2\pi R_5$ (Gland Area$_5$ (1-Ov_5))

Gland Area$_5$ = 0.214 in. nominal groove depth
+ 0.004 in. deflection (NJES 1A secondary deflection)
x 0.308 in. nominal groove width

Gland Area$_5$ = (0.214 + 0.004 in.) (0.308 in.) = 0.067144 in.^{2}

R_5 51.952 in. from B/P (nominal)

$v_5 = 2\pi$ (51.952 in.) (0.067144 in.^{2}) (1 - 0.901 in.) = <u>2.1698 in.^{3}</u>

$v_2 = 2\pi R2_A$ [(initial gap x area length)]
+ $2\pi R2_B$[(deflection-linear opening) (area length)]/2

Initial gap = 0.023 in. (linear opening of 3 mil added to original assumed gap)

Area length = 0.8163 in. + 0.004 in. (deflection)

Deflection = 0.036 in. (NJES 1A primary deflection)

Linear opening = 0.003 in. (assumed)

R_{2A} = 51.7415 in. (rotation adjusted) R_{2B} = 51.735 in. (rotation adjusted)

Table 3

TEM N/C Primary With 1U75150-26 O-ring — Assembled Results

	Minimum	Maximum	Units
Stretch	1.6906	1.6906	%
Stretch Red	1.5162	1.5162	%
Temperature Adjusted Diameter	0.2898	0.2898	inches
Total Adjusted Diameter	0.2898	0.2898	inches
Squeeze	0.0348	0.0348	inches
Squeeze	12.0000	12.0000	%
Fill	69.5831	69.5831	%

TEM N/C Primary With 1U75150-26 O-ring — Input Parameters

	Minimum	Maximum	Units
O-ring Diameter	0.2940	0.2940	inches
O-ring ID	101.3000	101.3000	inches
Groove OD	103.5980	103.5980	inches
Groove Depth	0.2550	0.2550	inches
Groove Width	0.3780	0.3780	inches
Temperature	75.0000	75.0000	°F
Initial Gap	0.0000	0.0000	inches

Ambient Temperature	68.0°F
Comp Set	0.0%
Coefficient Expansion O-ring	0.11E-03 in./in./°F
Coefficient Expansion Case	0.74E-05 in./in./°F

Table 4

TEM N/C Secondary With 1U75150-28 O-ring — Assembled Results

	Minimum	Maximum	Units
Stretch	0.6475	0.6475	%
Stretch Red	0.6544	0.6544	%
Temperature Adjusted Diameter	0.2764	0.2764	inches
Total Adjusted Diameter	0.2764	0.2764	inches
Squeeze	0.0584	0.0584	inches
Squeeze	21.1284	21.1284	%
Fill	90.2874	90.1513	%

TEM N/C Secondary With 1U75150-28 O-ring — Input Parameters

	Minimum	Maximum	Units
O-ring Diameter	0.2780	0.2780	inches
O-ring ID	103.1600	103.1600	inches
Groove OD	104.5200	104.5200	inches
Groove Depth	0.2180	0.2180	inches
Groove Width	0.3080	0.3080	inches
Temperature	75.0000	75.0000	°F
Initial Gap	0.0000	0.0000	inches

Ambient Temperature	68.0°F
Comp Set	0.0%
Coefficient Expansion O-ring	0.11E-03 in./in./°F
Coefficient Expansion Case	0.74E-05 in./in./°F

v_2 = 2π (51.7415 in.) (0.023 x 0.8203 in.) + 2π (51.735)
([0.036 - 0.003 in.] (0.8211 in.)/2
v_2 = 10.5376 in.^{3}

v_3 = Same as initial no change due to pressurization

v_3 = 13.6758 in.^{3}

v_4 = $2\pi R_4$ [(deflection x area length) + (corner deflection x area length)/2]
Deflection = 0.004 in. (NJES 1A secondary deflection)
Area length = 0.189 in.(from B/P)
Corner deflection = 0.00081 in. (calculated from secondary deflection experienced)
R_4 = 51.8575 in. (from B/P)

v_4 = 2π (51.8575 in.)[(0.004 x 0.189 in.) + (0.00081 x 0.0212 in.)/2]
v_4 = 0.2743 in.^{3}

$v_T = v_1 + v_5 + v_2 + v_3 + v_4$

v_T = 9.5068 in.^{3} + 2.1698 in.^{3} + 10.5376 in.^{3} + 13.6758 in.^{3} + 0.2743 in.^{3}

v_T = 36.1643 in.^{3} (volume during motor pressurization)

Pressure Calculation

$P_1v_1 = P_2v_2$ (pressure volume relation equation)
P_1 = 12.5 psia
v_1 = 25.8536 in.^{3} (initial volume)
v_2 = 36.1643 in.^{3} (pressurized volume)
12.5 (25.8536 in.) = P_2 (36.1643 in.)
P_2 = 8.9 psia
Therefore the TEM-5 gage should have read:
12.5 - 8.9 = 3.6 or -3.6 psig

TEM-5 gage read: -4.2 psig (Figure 1)

Conclusion:

The results of the analysis show a negative pressure of 3.6 psig is possible. The results of the TEM-5 static test was a negative pressure of 4.2 psig. Engineering feels the gage reading is accurate.

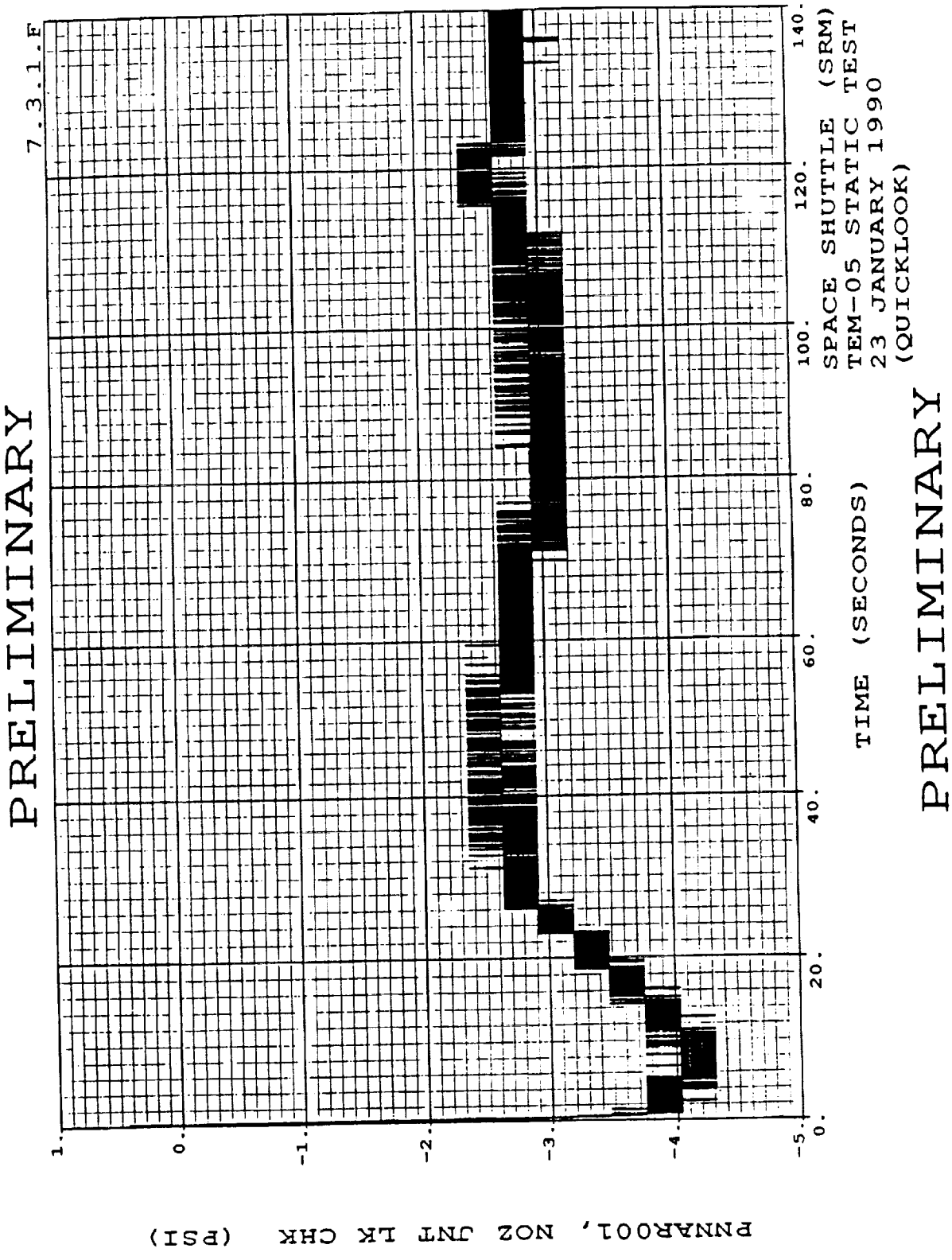

Figure 1. TEM-5 Gage

Appendix E

Flash Report

TEM-05 FLASH REPORT 24 JANUARY 1990

TWR-17646

CONTRACT NO. NAS8-30490

DR NO. 5-2

WBS NO. HQ601-20-10

TEST DATE: 23 January 1990

TEST TITLE: Technical Evaluation Motor No. 5 (TEM-05)

TEST LOCATION: Thiokol Corp., Space Operations
Brigham City, Utah
Static Test Bay T-97

I. TEM-05 TEST ARTICLE CONFIGURATION

A. Ignition System
- o HPM S&A using Krytox grease
- o SRM igniter modified for CO_2 quench port
- o Improved Igniter joint strip heater installed
  - o Set point at 122°F, with a minimum of 87°F at sensors
- o All pressure transducers lockwired
- o 180 ksi bolts (A-286) torqued to 275 to 295 ft (65 to 135 ksi stress)
- o New configuration inner and outer igniter gaskets installed

B. Propellant/Liner
- o HPM configuration

C. Systems Tunnel
- o N/A

D. Case-to-case factory joints
- o HPM tang and clevis hardware design joint
- o Insulation overlaid and cured over interior of the joint (HPM configuration)
- o HPM-type short pins and HPM-type pin retainer consisting of a steel band which is installed on each joint
- o Standard SRM shim clips

I. TEST ARTICLE CONFIGURATION (cont.)

E. Case-to-case field joints
- o RSRM-type long pins and RSRM-type hat band pin retainers
- o Improved joint heaters installed
  - o Set point at 121°F, with a minimum of 87°F at sensors
- o Standard-fit shims
- o Seals are 1U75150-11-RSRM
- o O-ring squeeze was calculated for each assembly (minimum 15% squeeze for each seal)
- o Standard HPM insulation configuration with putty joint filler (STW4-3266)
- o Redesigned FJPS installed on forward and center field joints

F. Case-to-nozzle joint
- o Standard HPM nozzle joint insulation configuration with putty joint filler (STW4-3266)
- o Fluorocarbon O-rings (primary, secondary)
  - o New 0.290 in. RSRM O-ring used for primary
  - o HPM groove will accommodate larger diameter RSRM sizes
- o Joint heater-set point at 76°F, with sensor readings to be between 71°F to 81°F
- o One hundred axial bolts installed and ultrasonically torqued to 120 ±9 kips
- o Four vent ports provided in fixed housing forward of primary O-ring; vents then plugged using adjustable vent port plugs

G. Internal Nozzle Joints
- o RSRM O-rings used for forward-to-aft exit cone

H. ET Attach Ring
- o No ET Attach Ring

I. Stiffener Rings
- o None installed

J. Aft skirt ring
- o Aft skirt ring/actuator support ring assembly installed in place of the aft skirt. This ring provides mounting provisions for the fixed links which will be used in place of the TVC actuators
- o No nozzle vectoring

I. TEST ARTICLE CONFIGURATION (cont.)

K. Instrumentation
- o Limited

L. Nozzle assembly
- o Pre-51-L design
- o Linear shaped charge removed
- o Snubbers removed from forward exit cone

M. Heaters
- o New redesigned igniter-to-case joint and case-to-case field joint heaters and heater power cables
- o New, higher capacity case-to-nozzle joint heater

II. TEM-05 TEST OBJECTIVES:

The TEM-05 test objectives were derived from the objectives of TWR-15723 Rev C, Development and Verification Plan, to satisfy the requirements of Contract End Item (CEI) Specification CPW1-3600A, dated 3 August 1987.

A. Recover case, nozzle and igniter hardware for RSRM flight and static test programs.

B. Obtain additional data on the effect of three-year storage of loaded SRM case segments upon motor ignition and performance.

C. Obtain data on the performance of the new flight configuration joint heaters on the igniter-to-case joint and field joints and the new higher output heater for the nozzle-to-case joint, which is used on static test motors only.

D. Obtain additional data on the low frequency chamber pressure oscillations in the motor forward end.

E. Obtain additional breakaway and removal torque data for the leak check port plug Nylok® thread locking device.

F. Demonstrate the fit, operation, and similarity of the new JPS heater power cables to the old power cables.

II. TEM-05 TEST OBJECTIVES (cont.)

G. Obtain additional data on the performance of Krytox grease on the Barrier-Booster shaft O-rings.

H. Obtain additional data on nozzle axial deflection during motor pressurization.

I. Demonstrate and evaluate processing and installation of new Field Joint Protection System (FJPS) designs.

J. Evaluate structural integrity of new FJPS designs through full scale, full duration static firing.

III. TEM-05 PRE-TEST PREDICTIONS

A. General Ballistics Performance Predictions

No thrust measurement

TEM-05 Predicted Individual Motor Ballistics Performance Summary (vacuum, 60°F)*:

	Prediction**
Web time (sec)	111.5
Action time (sec)	122.9
MOP Headend (psia)	920.0
Maximum sea level thrust (Mlb_f)	3.07
Web time average headend pressure (psia)	663.9
Web time average vacuum thrust (Mlb_f)	2.606
Web time total impulse(Mlb_f-sec)	290.6
Action time impulse (Mlb_f-sec)	297.7
I_{sp} average delivered (lb_f-sec/lb_m)	268.2
Ignition Interval (sec), Time 563.5 psia	0.232
Maximum pressure rise rate (psi/10-ms)	90.5
Loaded propellant weight (lb)	1,109,928***

* TEM-05 prediction based on the following motor segments: Forward: SRM-31A Forward (cast on 19 Dec 85); CF: SRM-31A CF (cast on 20 Jan 86); CA: SRM-32A CA (cast on 23 Jan 86); Aft: SRM-26B Aft (cast on 31 Jul 85)

** Based on burn rate of 0.368 at 60°F, 625 psia

*** Based on nominal propellant weights. No actual weights available for these segments

III. TEM-05 PRE-TEST PREDICTIONS (cont)

B. Pre-Test Predictions:

- All joints will function within the HPM experience base
  - Pressure and/or gas jetting may reach the primary O-ring of nozzle joint
  - Low probability that gas paths may occur through the putty to the primary O-ring of field and nozzle joints
  - Experience indicates primary O-ring may allow blowby if exposed to pressure
    - Narrow seal gland
    - Large seal gap deflection
  - Secondary O-ring expected to maintain seal
    - low probability of metal hardware damage

IV. INITIAL ENGINEERING ASSESSMENT

The TEM-05 static test was successfully conducted at T-97 on 23 January 1990. The motor performed well with no apparent anomalies. All comments presented here are based on preliminary data and external observations. The final test report (TWR-17649) will include a detailed assessment of the test data and physical inspection information gathered from the test and during disassembly.

BALLISTICS

Preliminary ballistic performance data is shown in Table I. Chamber pressure was measured, and is plotted in Figures 1 and 2.

NOZZLE

Initial observations indicate no anomalous conditions. Nozzle erosion was typical. No heat affected areas on the paint or cork on the outside of the aft exit cone were detected. Plots of the nozzle-to-case joint pressure, monitored between the primary and secondary O-rings, are shown in Figures 3 and 4. The negative pressure between the O-rings indicates that the joint expanded, which resulted in an increased volume between the O-rings. The negative pressure also indicates that pressure did not reach the primary O-ring. Nozzle axial deflection plots are shown in Figures 5 through 8.

IV. INITIAL ENGINEERING ASSESSMENT (cont.):

CASE

There was no evidence of slag damage to the case.

IGNITER

Preliminary data verifies that the igniter performed within the specified requirements. Historical data on S&A cycle times is shown in Table II.

TEMPERATURE SPECIFICATIONS

Field joints. During the test firing, all field joint temperature sensors registered between 106°F and 115°F, well over the minimum of 87°F.

Igniter joint temperature. During the test firing, the igniter joint temperature sensors registered between 119°F and 120°F, well over the minimum of 87°F.

Case-to-nozzle joint. During the test firing, the case-to-nozzle joint temperature sensors registered between 75°F and 80°F, within the specified range of 71°F to 81°F.

Plots of the joint temperatures during the test firing are shown in Figures 9 through 13.

INSTRUMENTATION

All instrumentation performed as expected.

FIELD JOINT PROTECTION SYSTEM

Initial observations indicate that both the redesigned field joint protection system configurations remained intact and did not degrade.

STATIC TEST SUPPORT EQUIPMENT

The water deluge system, CO_2 quench, and other test support equipment performed as expected during all required test operations.

FINAL REPORT DUE (TWR-17649): 24 March 1990

NEXT TEST: TEM-06 - Approximate Test Date: 8 March 1990

M. L. Cook
Test Planning and Reporting

I. N. Black, Supervisor
Test Planning and Reporting

S. Vigil
Program Manager

N. Milsap
System Integration Engineer

TABLE I
TEM-05 PERFORMANCE SUMMARY *
2 HOUR QUICK LOOK

	SPEC LIMITS ADJUSTED FROM 60 °F TO 77 °F (VACUUM CONDITIONS)	PREDICTED** (VACUUM) . (77 °F) .	DELIVERED (VACUUM) . (77 °F).
WEB TIME (SEC)	104.1 - 115.1	109.5	111.1
ACTION TIME (SEC)	113.2 - 129.0	120.8	122.2
MOP HEAD-END (PSIA)	874.9 - 996.6	937.3	922
MOF (VACUUM MLBF) ***	3.17 - 3.59	3.39	N/A
WEB TIME AVERAGE HEAD-END PRESSURE (PSIA)	637.6 - 709.0	676.5	667.4
WEB TIME AVERAGE THRUST (MLBF)	2.50 - 2.78	2.66	2.62*
WEB TIME PRESSURE INTEGRAL (PSIA-SEC)	N/A	74100	74100
WEB TIME TOTAL IMPULSE (MLBF*SEC)	286.2 - 292.0	290.7	290.4*
ACTION TIME AVERAGE HEAD-END PRESSURE (PSIA)	N/A	627.6	620.5
ACTION TIME AVERAGE THRUST (MLBF)	N/A	2.47	2.43*
ACTION TIME PRESSURE INTEGRAL (PSIA-SEC)	N/A	75800	75900
ACTION TIME IMPULSE (MLBF*SEC)	293.6 - 299.5	297.9	297.5*
ISP AVERAGE DELIVERED (LBF*SEC/LBM)	265.4 - 269.2	268.4	268.2*
IGNITION INTERVAL (SEC), TIME TO 563.5 PSIA	0.170 - 0.340	0.232	0.230
MAXIMUM PRESSURE RISE RATE (PSI/10-MSEC)	X < 109.0	90.5	87.1
BURN RATE (IN/SEC)	N/A	0.372	0.369
IGNITER MAXIMUM PRESSURE	N/A	1965	1997
LOADED PROPELLANT WEIGHT (INCLUDING IGNITER) (LB)	X > 1,104,714	1,109,928****	

* ALL THRUST AND IMPULSE VALUES BASED ON AN AVERAGE THRUST/PRESSURE OF 3919 LBF/PSI
** BASED ON BURN RATE OF 0.368 IN/SEC AT 60 DEG F, 625 PSIA
*** SPEC. LIMIT ADJUSTED FROM SEA LEVEL THRUST (14.7 PSIA) AND 60 ° F
**** BASED ON NOMINAL PROPELLANT WEIGHTS

TEM-04 PREDICTION BASED ON THE FOLLOWING AS CAST MOTOR SEGMENTS:
FWD: SRM-31A FWD, CF: SRM-31A C/F, CA: SRM-32A C/A, AFT: SRM-26B AFT

Test Article	Off Motor Test Safe to Arm (Sec)	On Motor Test Safe to Arm (Sec)	Firing Safe to Arm (Sec)	Off Motor Test Voltage to Arm (Volts)
QM-7	0.60			
PVM-1	0.73	0.79		
QM-8		0.90		
TEM-01	0.79	0.68		
TEM-02	0.67	0.65	0.66	
TEM-03	0.60	0.70	0.70	30.5
TEM-04	0.67	TEST #1: 0.64 TEST #2: 0.65	0.66	28.5
TEM-05	0.50	0.60	0.60	31.0

Table II. Historical Data on S&A Cycle Times

PRELIMINARY

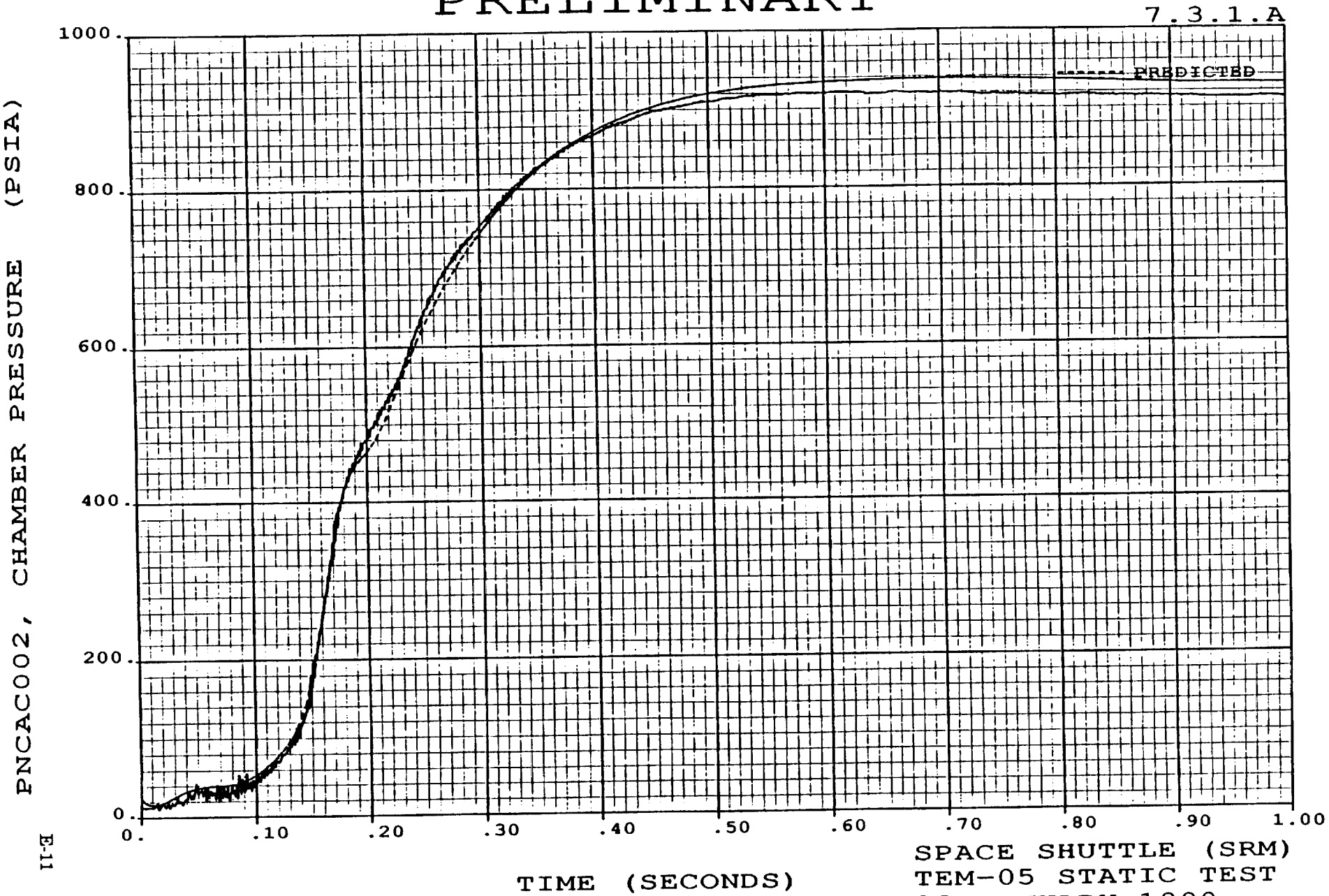

Figure 1. Chamber Pressure vs Time

PRELIMINARY

PRELIMINARY

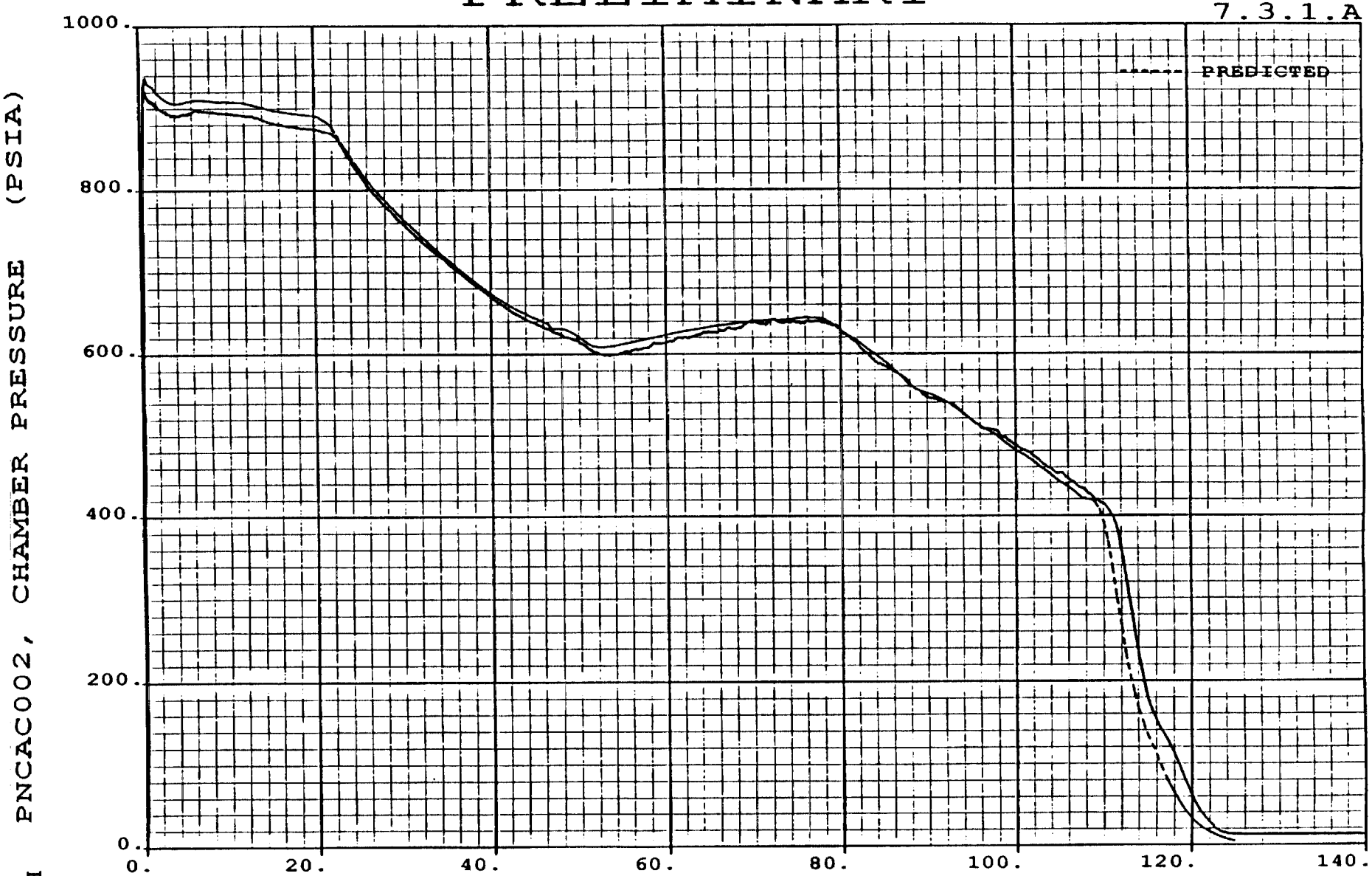

Figure 2. Chamber Pressure vs Time

PRELIMINARY

PRELIMINARY

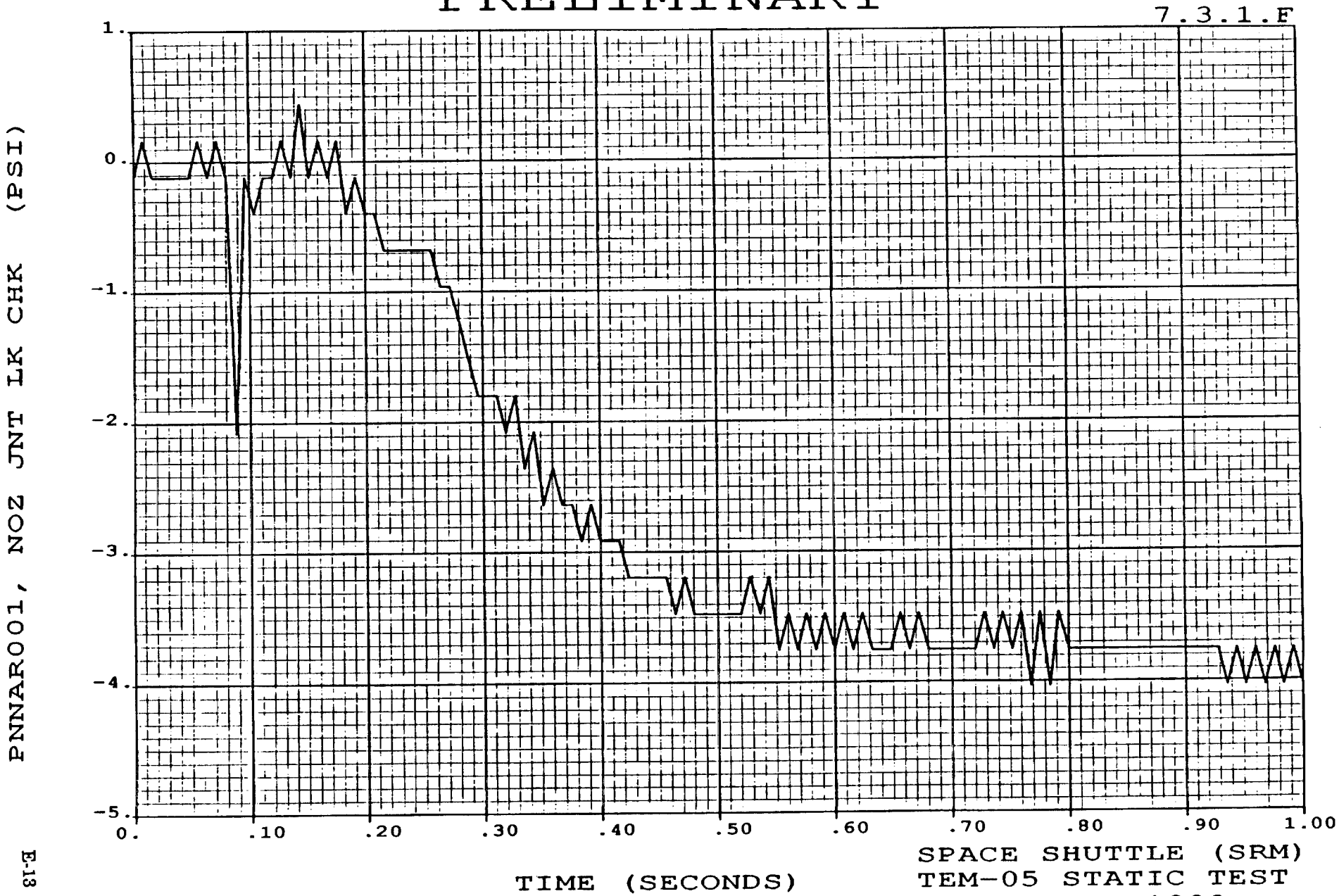

Figure 3. Nozzle-to-Case Joint Pressure

PRELIMINARY

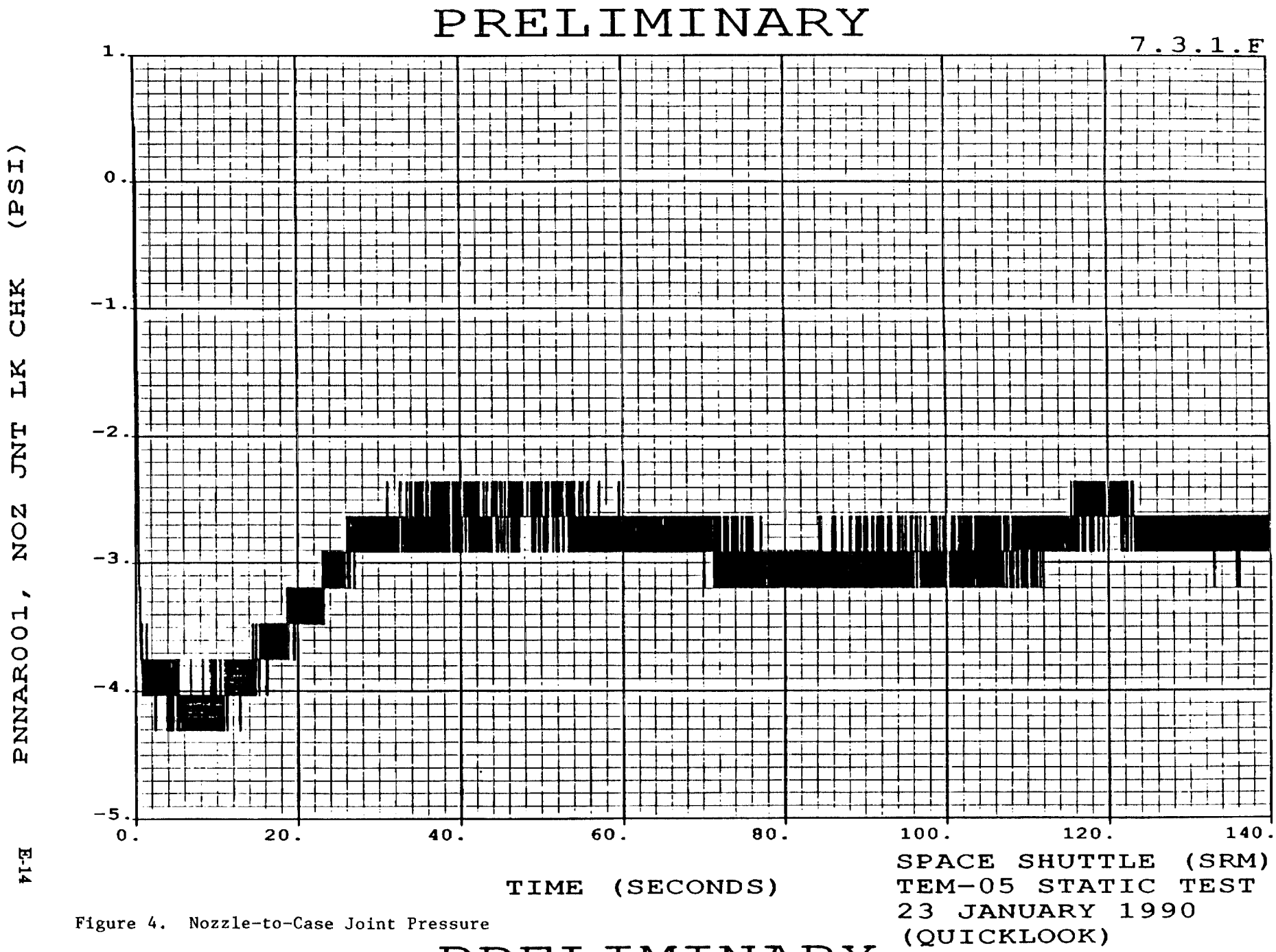

Figure 4. Nozzle-to-Case Joint Pressure

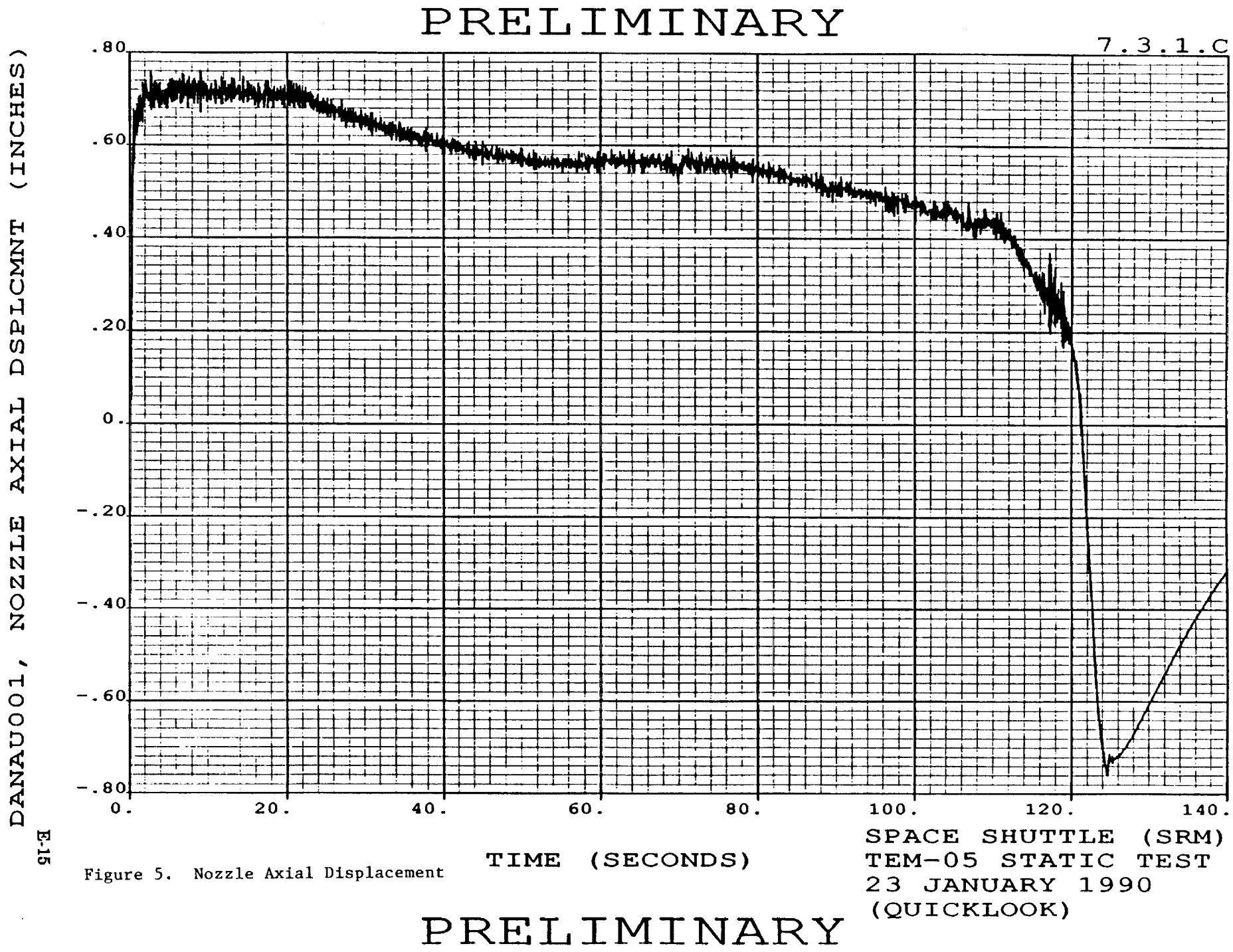

Figure 5. Nozzle Axial Displacement

PRELIMINARY

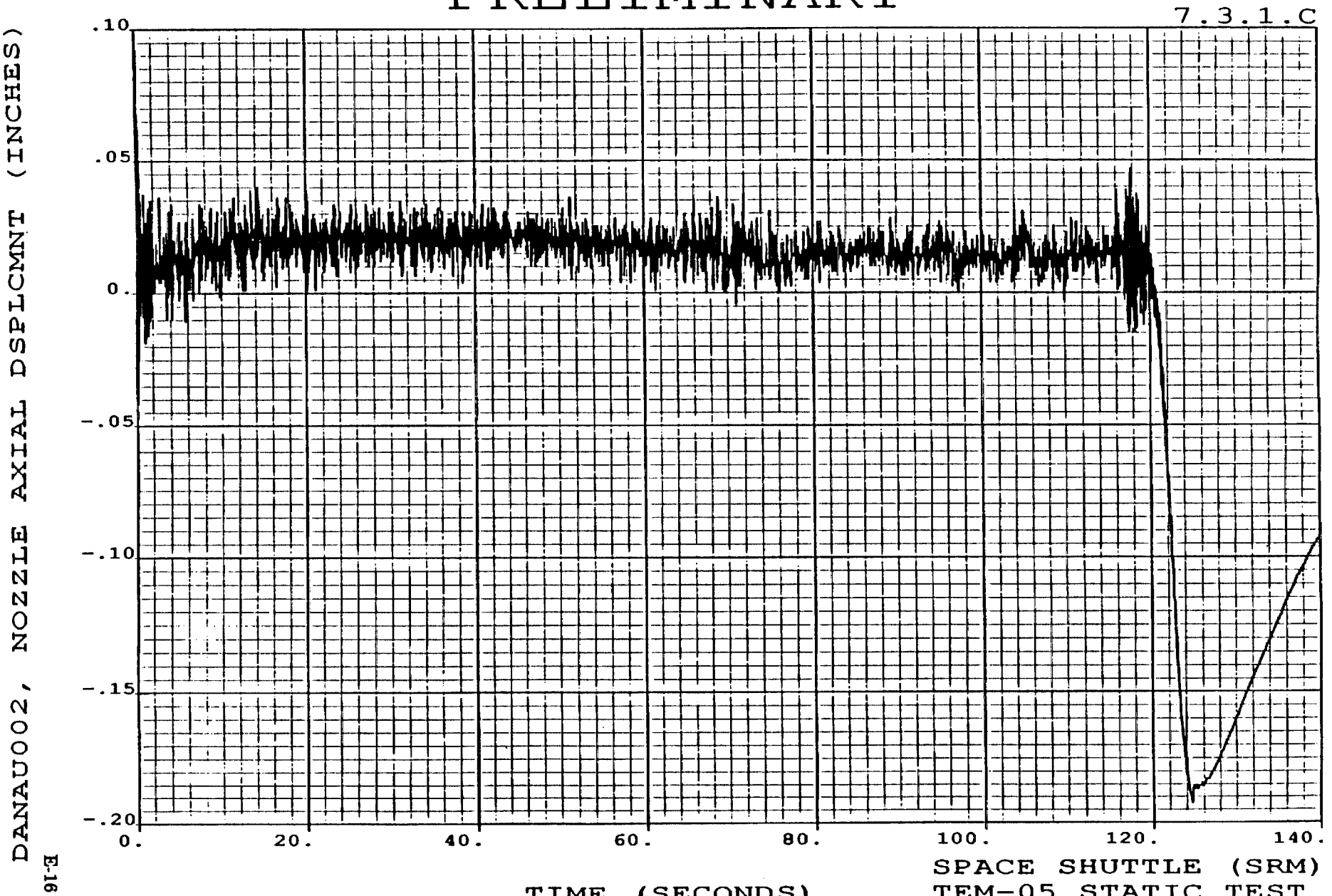

Figure 6. Nozzle Axial Displacement

PRELIMINARY

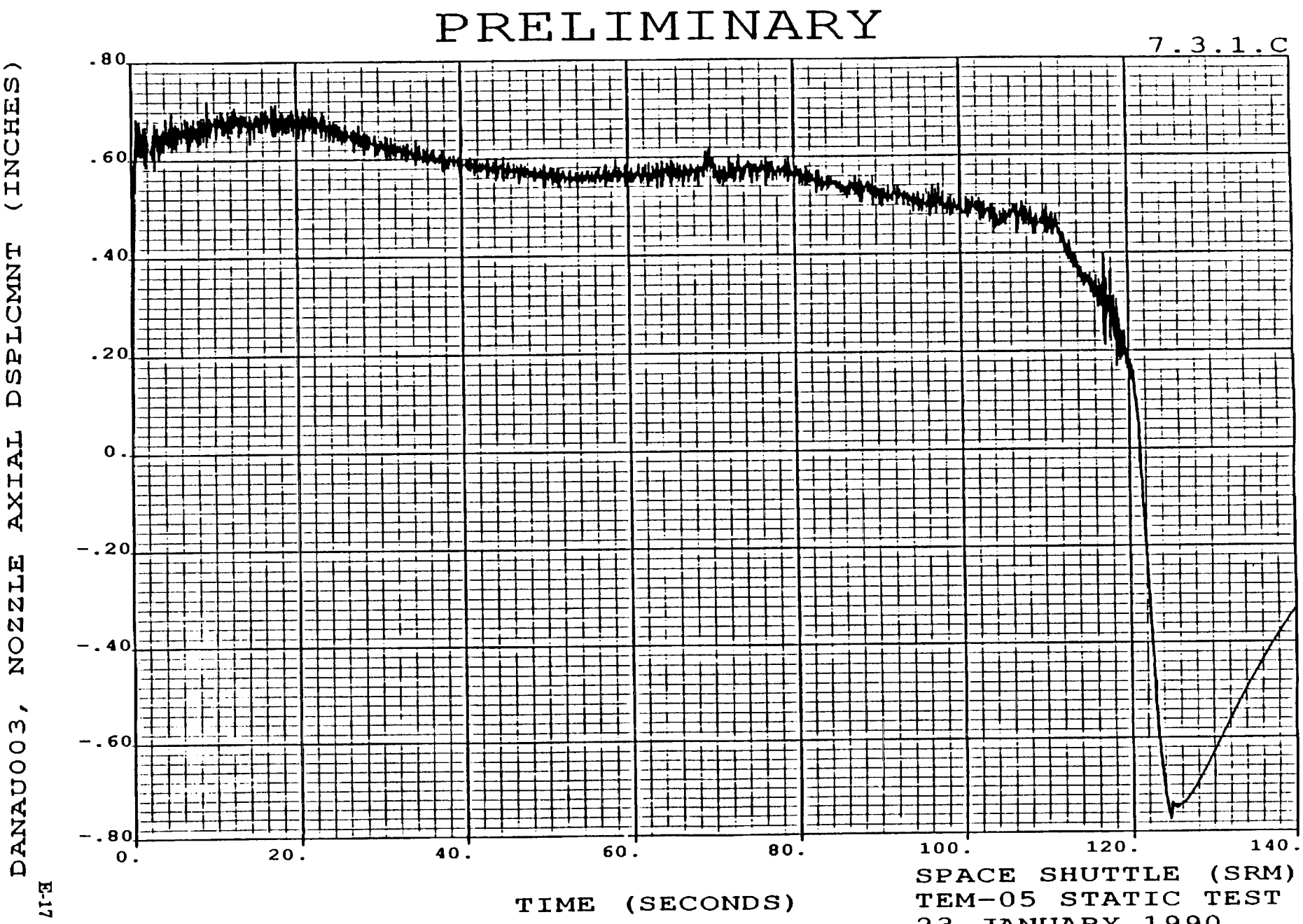

Figure 7. Nozzle Axial Displacement

PRELIMINARY

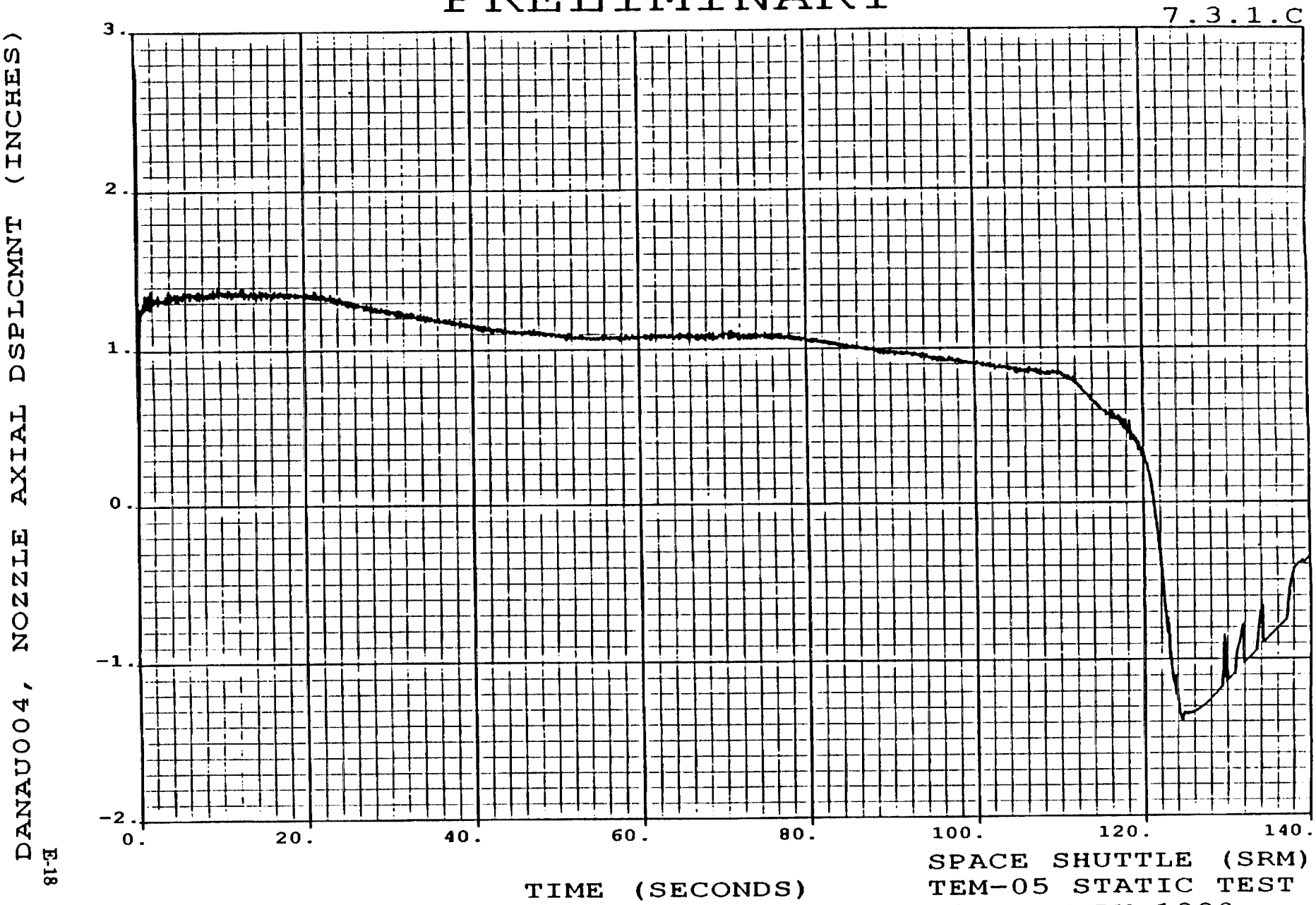

Figure 8. Nozzle Axial Displacement

PRELIMINARY

PRELIMINARY

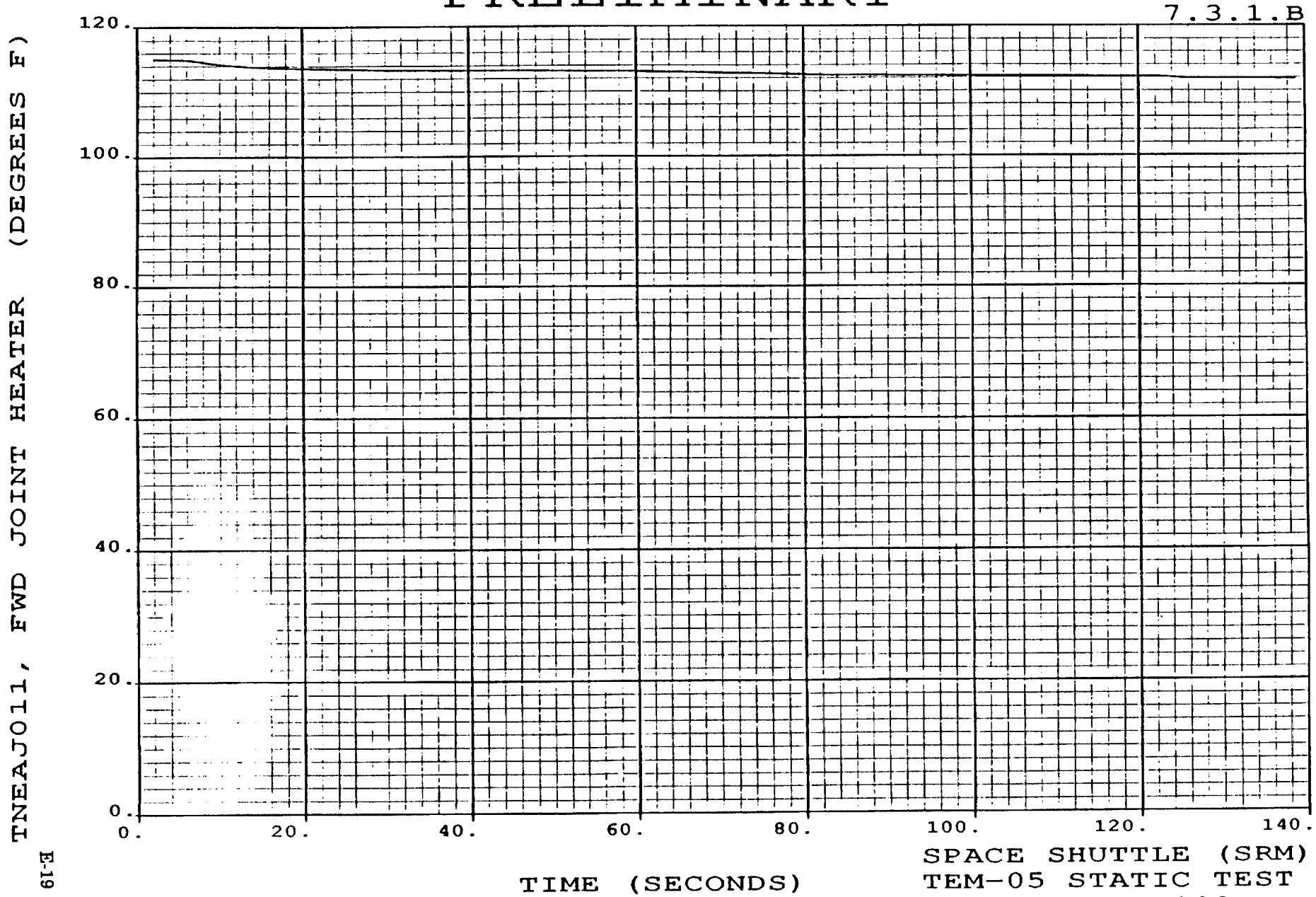

Figure 9. Forward Field Joint Temperature

PRELIMINARY

PRELIMINARY

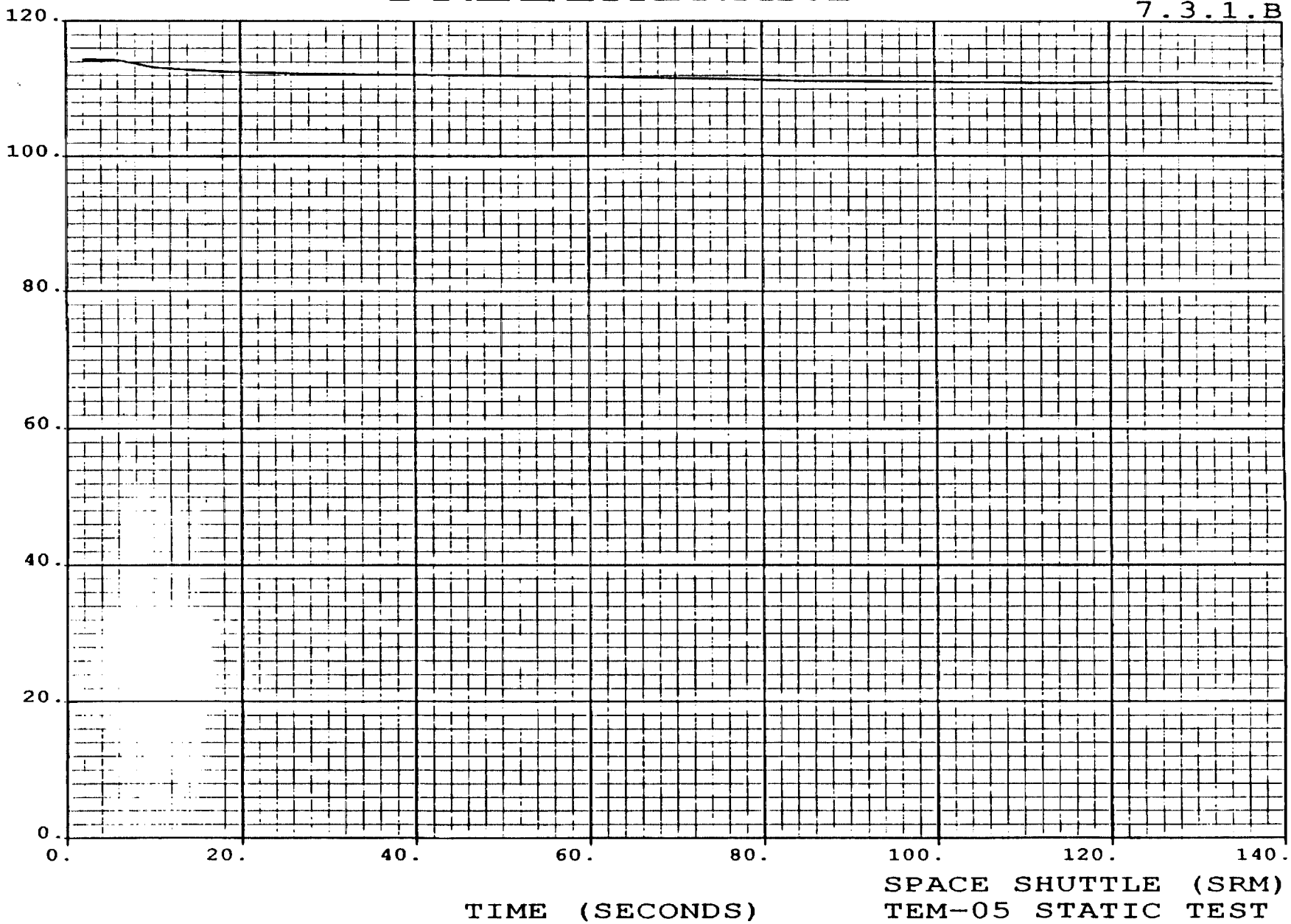

Figure 10. Center Field Joint Temperature

PRELIMINARY

PRELIMINARY

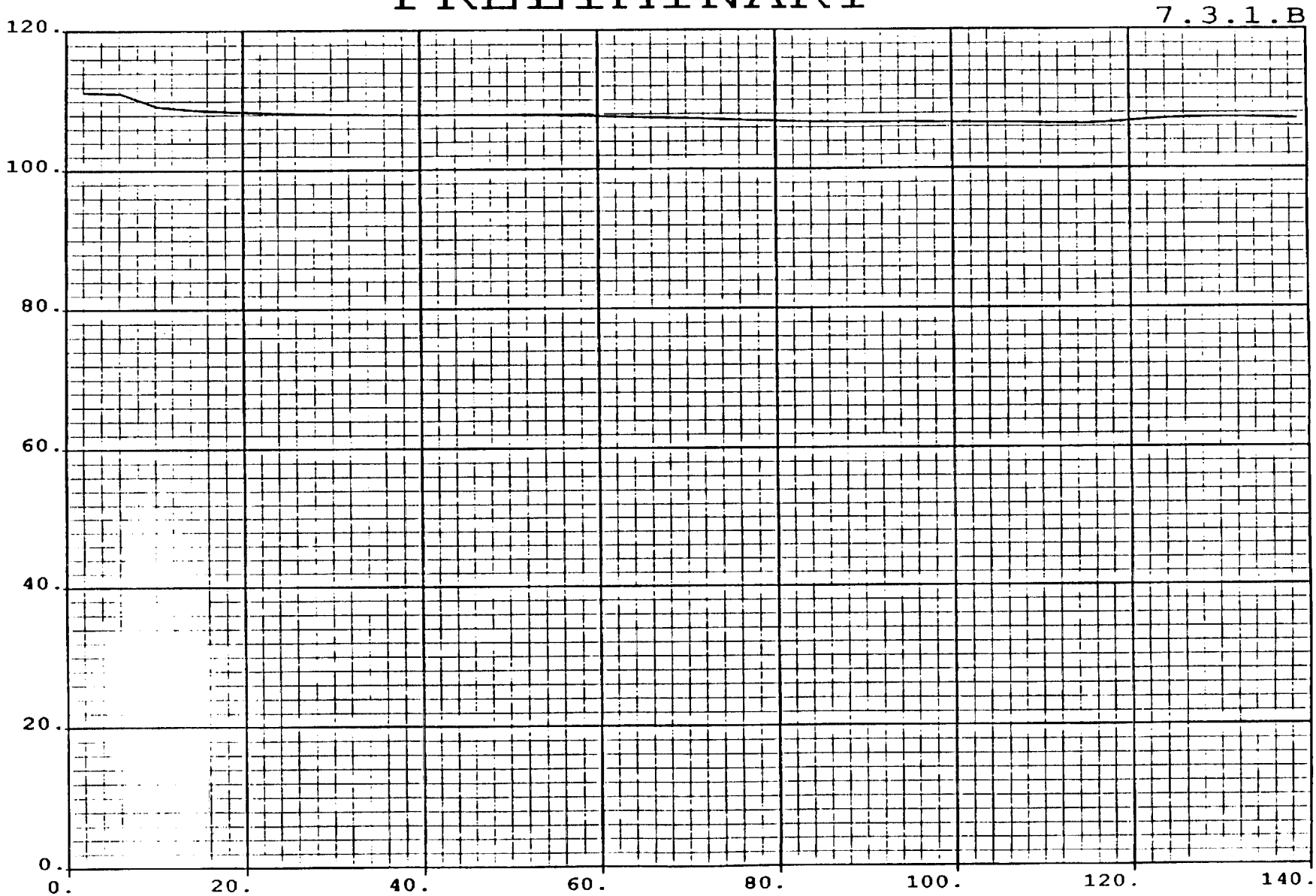

Figure 11. Aft Field Joint Temperature

PRELIMINARY

PRELIMINARY

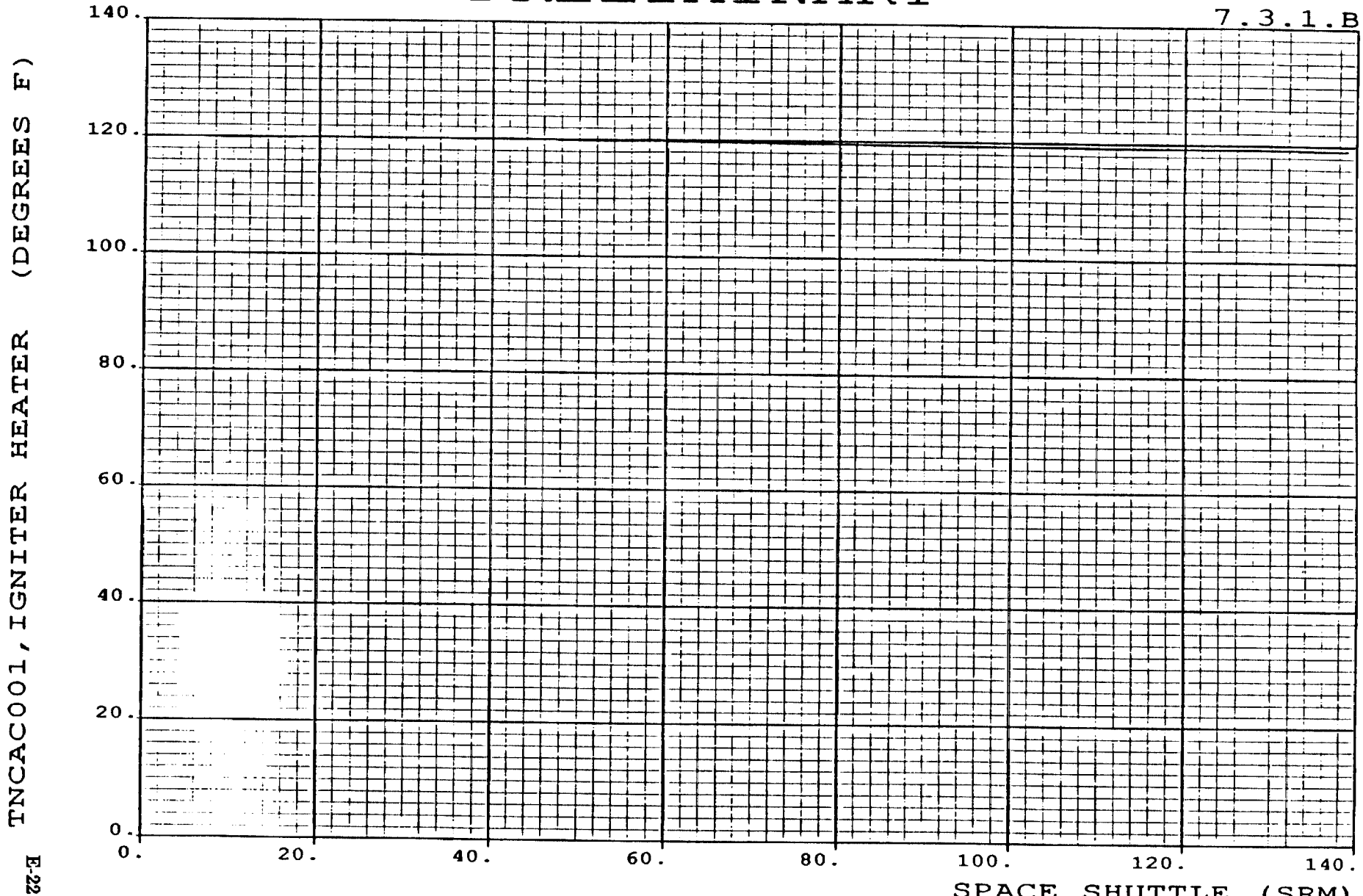

Figure 12. Igniter Joint Temperature

PRELIMINARY

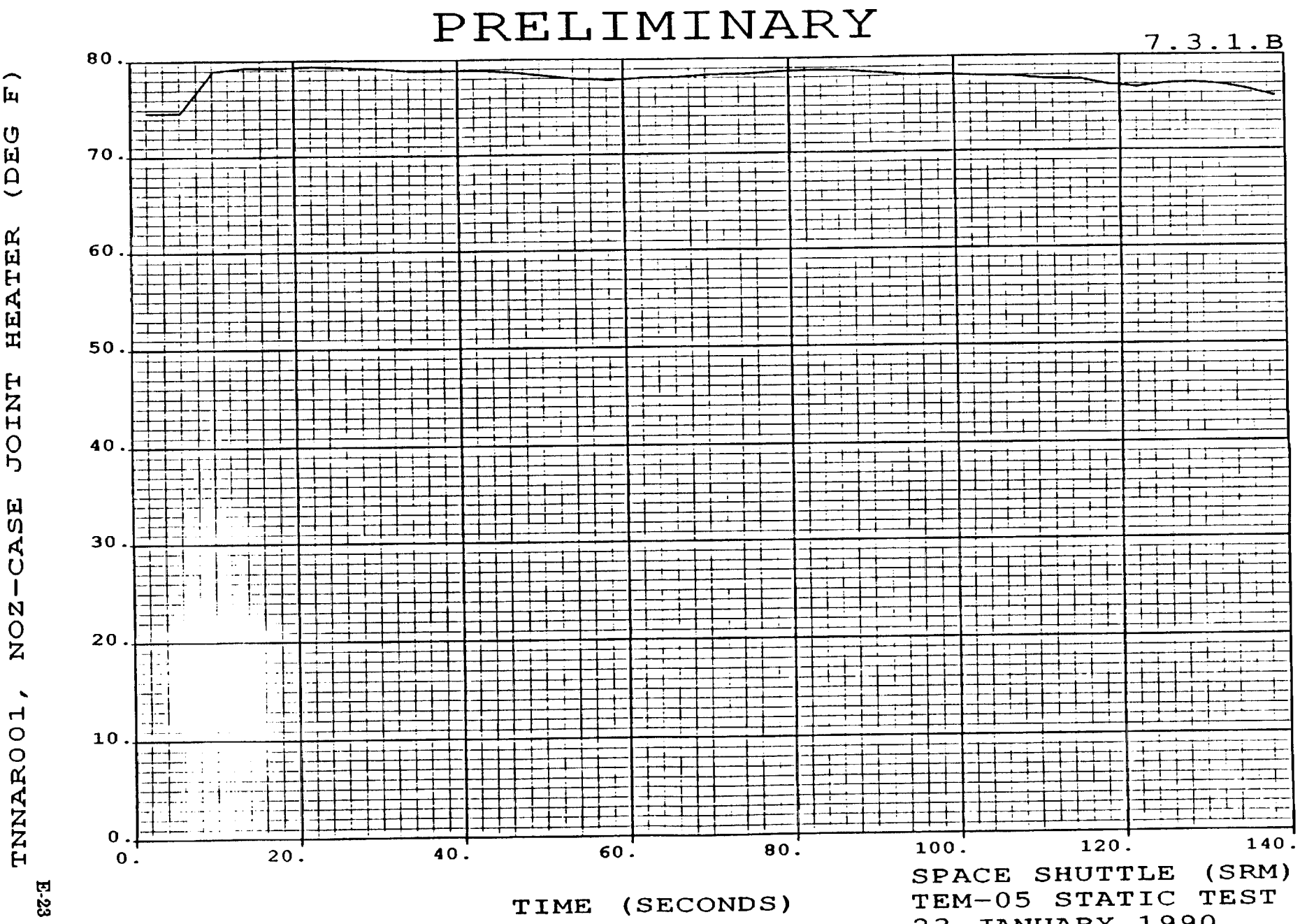

Figure 13. Nozzle-to-Case Joint Temperature

DISTRIBUTION

Recipient	No. of Copies	Mail Stop
M. Cook	3	L71
N. Black	1	L71
S. Vigil	1	E62C
S. Harris	1	E62C
N. Millsap	1	L72
D. Smith	1	L72
L. MacCauley	1	L52
K. Sanofsky	1	851
F. Duersch	1	851
J. Passman	1	L62B
L. Nelsen	1	L61C
R. Jensen	1	L72
G. Stephens	1	E66
M. Williams	1	L62B
C. Prokop	1	L62B
C. Greatwood	1	L62A
D. South	1	L62A
D. Smith Jr.	1	L62A
M. Perry	1	L84
A. Drendal	1	L63
E. Mathias	1	L63
T. Dougherty	1	Z20
D. Burton	1	K68
A. Braxton	1	K68
R. Papasian	45	E05
Print Crib	5	K23B1
Data Management	5	L23E